GDAŃSK UNIVERSITY OF TECHNOLOGY

The author of the doctoral dissertation: Katarzyna Kłosowska
Scientific discipline: Chemical sciences

DOCTORAL DISSERTATION

Title of doctoral dissertation: The effect of phospholipids on the intestinal lipolysis and proteolysis

Title of doctoral dissertation (in Polish): Wpływ fosfolipidów na lipolizę i proteolizę w warunkach jelita cienkiego

Supervisor	Second supervisor
signature	*signature*
PhD Adam Macierzanka	PhD Jens Brockmeyer

Gdańsk, year 2025

GDAŃSK UNIVERSITY OF TECHNOLOGY

STATEMENT

The author of the doctoral dissertation: Katarzyna Kłosowska

I, the undersigned, declare that I am aware that in accordance with the provisions of Art. 27 (1) and (2) of the Act of 4th February 1994 on Copyright and Related Rights (Journal of Laws of 2021, item 1062), the university may use my doctoral dissertation entitled:

The effect of phospholipids on the intestinal lipolysis and proteolysis

for scientific or didactic purposes.[1]

Gdańsk,..... .....

signature of the PhD student

Aware of criminal liability for violations of the Act of 4th February 1994 on Copyright and Related Rights and disciplinary actions set out in the Law on Higher Education and Science (Journal of Laws 2021, item 478), as well as civil liability, I declare, that the submitted doctoral dissertation is my own work.

I declare, that the submitted doctoral dissertation is my own work performed under and in cooperation with the supervision of prof. Adam Macierzanka and the second supervision of prof. Jens Brockmeyer.

This submitted doctoral dissertation has never before been the basis of an official procedure associated with the awarding of a PhD degree.

All the information contained in the above thesis which is derived from written and electronic sources is documented in a list of relevant literature in accordance with Art. 34 of the Copyright and Related Rights Act.

I confirm that this doctoral dissertation is identical to the attached electronic version.

Gdańsk,..... .....

signature of the PhD student

I, the undersigned, agree/do not agree* to include an electronic version of the above doctoral dissertation in the open, institutional, digital repository of Gdańsk University of Technology.

Gdańsk,..... .....

signature of the PhD student

[1] Art 27. 1. Educational institutions and entities referred to in art. 7 sec. 1 points 1, 2 and 4–8 of the Act of 20 July 2018 – Law on Higher Education and Science, may use the disseminated works in the original and in translation for the purposes of illustrating the content provided for didactic purposes or in order to conduct research activities, and to reproduce for this purpose disseminated minor works or fragments of larger works.

2. If the works are made available to the public in such a way that everyone can have access to them at the place and time selected by them, as referred to in para. 1, is allowed only for a limited group of people learning, teaching or conducting research, identified by the entities listed in paragraph 1.

GDAŃSK UNIVERSITY OF TECHNOLOGY

DESCRIPTION OF DOCTORAL DISSERTATION

The Author of the doctoral dissertation: Katarzyna Kłosowska
Title of doctoral dissertation: The effect of phospholipids on the intestinal lipolysis and proteolysis

Title of doctoral dissertation in Polish: Wpływ fosfolipidów na lipolizę i proteolizę w warunkach jelita cienkiego

Language of doctoral dissertation: English

Supervisor: Adam Macierzanka

Second supervisor*: Jens Brockmeyer

Date of doctoral defense:

Keywords of doctoral dissertation in Polish: fosfolipidy, sole żółciowe, proteoliza, lipoliza, trawienie żywnośći, trawienie *in vitro*

Keywords of doctoral dissertation in English: phospholipids, bile salts, proteolysis, lipolysis, bile, food digestion, *in vitro* digestion

Summary of doctoral dissertation in Polish:

W tej pracy zbadano wpływ fosfolipidów i soli żółciowych, jako głównych surfaktantów żółci, na trawienie triacylogliceroli oraz białek izolatu serwatkowego, w szczególności β-laktoglobuliny. Dotychczasowa literatura dotycząca trawienia w obecności fosfolipidów i soli żółciowych oraz ich wzajemnego oddziaływania w różnych stężeniach jest ograniczona, zwłaszcza w kontekście białek, szczególnie na poziomie peptydów. Ponadto istnieje wiele braków i kontrowersji w literaturze na temat trawienia lipidów oraz ich współdziałania z biosurfaktantami w badaniach międzyfazowych.

W badaniach wykorzystano model trawienia *in vitro* i wykazano znaczenie fosfolipidów jako surfaktantów żółciowych, które nie powinny być pomijane w procedurach protokołów *in vitro* dotyczących trawienia. Wyniki pokazują wpływ fosfolipidów na różnicowanie profilu peptydowego podczas trawienia białka modelowego – β-laktoglobuliny, w porównaniu do trawienia z użyciem samych soli żółciowych, różnych stosunków surfaktantów żółciowych oraz w ich braku. Ponadto, po raz pierwszy przeprowadzono badania na granicy faz w obecności fizjologicznych stężeń surfaktantów żółciowych, w których wykazano synergiczny efekt w trawieniu tłuszczów przy fizjologicznym stężeniu tych biosurfaktantów (sole żółciowe 9 mM i fosfolipidy 4 mM).

GDAŃSK UNIVERSITY OF TECHNOLOGY

Summary of doctoral dissertation in English:

In this study, the impact of phospholipids and bile salts, as the main biliary surfactants, on the digestion of triacylglycerols and whey protein isolate, particularly β-lactoglobulin, was investigated. The current literature on digestion in the presence of phospholipids and bile salts and their interactions at different concentrations is limited, especially in the context of proteins, particularly at the peptide level. Furthermore, there are many gaps and controversies in the literature regarding lipid digestion and their interplay with biosurfactants in interfacial studies.

In the experiments, *in vitro* digestion model was used to demonstrate the importance of phospholipids as biliary surfactants, which should not be overlooked in the procedures of *in vitro* digestion protocols. The results demonstrate the impact of phospholipids on the differentiation of the peptide profile during the digestion of the model protein – β-lactoglobulin, compared to digestion with bile salts alone, different ratios of bile surfactants, and in their absence. Moreover, for the first time, interfacial studies were conducted in simulated physiological conditions, showing a synergistic effect in fat digestion at physiologically relevant concentration of these biosurfactants (bile salts 9 mM and phospholipids 4 mM).

I would like to express my deepest gratitude to everyone who supported me throughout the process of creating this work, from the research stage to the final writing. I am profoundly grateful to everyone who believed in me, inspired me, and offered constant encouragement throughout this journey.

Table of Content

Abbreviations

ACE	Angiotensin-converting enzyme
ANOVA	Analysis of variance
BA	Bile acid
BS	Bile salt
BSEP	Bile salt export pump
BTEE	Bis(triethoxysilyl)ethane
C	Cholesterol
CE	Cholesterol ester
CID	Collision-induced dissociation
CMC	Critical micelle concentration
DAG	Diacylglycerol
DHA	Docosahexaenoic acid
DIA	Data-independent acquisition
DIAAS	Digestible indispensable amino acid score
DLS	Dynamic light scattering
DPPC	Dipalmitoylphosphocholine
DTT	Dithiothreitol
E'	Storage modulus
E''	Loss modulus
E	Dilatational modulus
ELISA	Enzyme-linked immunosorbent assay
EPA	Eicosapentaenoic acid
ESI	Electrospray ionization
ETD	Electron-transfer dissociation
FA	Fatty acid
FaS	Fasted state
FC	Fold change
FDR	False discovery rate
FeS	Fed state
FFA	Free fatty acid
FXR	Farnesoid X receptor
GC-FID	Gas chromatography -flame ionization detector
GC-MS	Gas chromatography-mass spectrometry
HCl	Hydrochloric acid
HDL	High-density lipoprotein
HGL	Human gastric lipase
HPL	Human pancreatic lipase
HPLC	High performance liquid chromatography
IFT	Interfacial tension
LC	Liquid chromatography
LDL	Low-density lipoprotein
LFQ	Label-free quantification
LTP	Lipid transfer protein
m/z	Mass-to-charge ratio
MAG	Monoacylglycerol
MALDI	Matrix-assisted laser desorption/ionization
MDR	Multidrug resistance

MES	2-(N-morpholino)ethanesulfonic acid
MFGM	Milk fat globule membrane
MS	Mass spectrometry
MUFA	Monounsaturated
MW	Molecular weight
NaC	Sodium cholate
NaCl	Sodium chloride
NaDC	Sodium deoxycholate
NaGC	Sodium glycocholate
NaGDC	Sodium glycodeoxycholate
NaOH	Sodium hydroxide
NaTC	Sodium taurocholate
NaTDC	Sodium taurodeoxycholate
NSAIDs	Nonsteroidal anti-inflammatory drugs
PC	Phosphatidylcholine
PDCAAS	Protein digestibility-corrected amino acid score
PE	Phosphatidylethanolamine
PEPT1	Peptide transporter 1
PL	Phospholipid
PLA_2	Phospholipase A2
PMSF	Phenylmethanesulfonyl fluoride
PS	Phosphatidylserine
PUFA	Polyunsaturated fatty acids
Q-TOF	Quadrupole time-of-flight
RT	Room temperature
rt	Retention time
SD	Standard deviation
SDS	Sodium dodecyl sulphate
SDS-PAGE	Sodium dodecyl sulphate polyacrylamide gel electrophoresis
SGF	Simulated gastric fluid
SIF	Simulated intestinal fluid
SM	Sphingomyelin
SPT	Skin prick test
SSF	Simulated salivary fluid
TAG	Triacylglycerol
TLC	Thin-layer chromatography
TOF	Time-of-flight
UV	Ultraviolet
VIP-HESI	Vacuum Insulated Probe Heated Electrospray Ionization
WPI	Whey protein isolate
XIC	Extracted ion chromatogram
α-La	Alpha lactalbumin
β-Lg	Beta lactoglobulin

1 Introduction

1.1 Digestion in the human gastrointestinal tract

The digestion of food is a complex, multi-step, and interdependent process occurring in the gastrointestinal tract. It involves the breakdown of larger organic compounds into smaller units that the body can absorb and utilize. This process encompasses the digestion of primary food components, such as carbohydrates, proteins, and lipids, to provide essential nutrients for the body, specifically simple sugars, amino acids, and fatty acids, respectively (Capuano and Janssen 2021). These small molecules are absorbed in the small intestine and transported throughout various parts of the human body. The human alimentary tract is composed of several compartments: the mouth, pharynx, esophagus, stomach, small intestine, large intestine, and anus. Additionally, the liver, along with the gallbladder, and the pancreas play crucial roles in digestion (Smith 2019) (Figure 1.1).

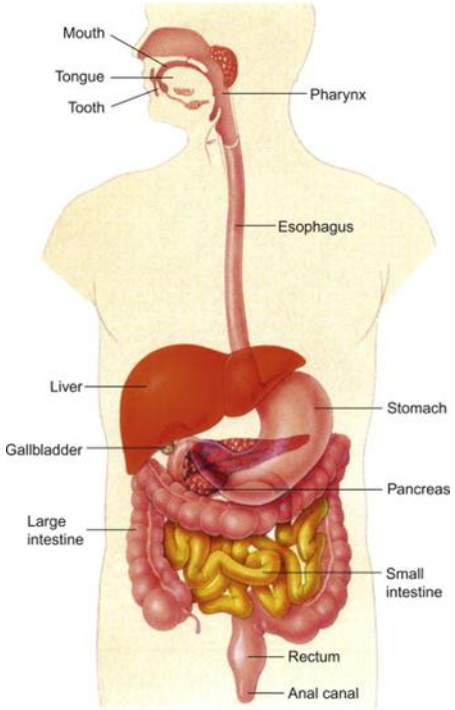

Figure 1.1 Human gastrointestinal tract (Bhagavan and Ha 2015).

The process of digestion begins in the mouth, where food is chewed and mixed with saliva. Salivary α-amylase initiates carbohydrate digestion (Sareen S. Gropper, Jack L. Smith 2022). Mastication increases the surface area of food fragments by mechanical breakdown, aiding for subsequent digestion (Boland Mike; Golding Matt 2014).

After being formed in the mouth, the food bolus travels through the esophagus to the stomach, where protein and fat digestion begins. In the stomach, food is mixed with gastric secretions and churned into a semi-liquid mixture called chyme (Smith 2019). Parietal cells secrete hydrochloric acid as separate hydrogen (H^+) and chloride (Cl^-) ions (Sareen S. Gropper, Jack L. Smith 2022). The stomach's pH is around 1–2 in the fasting state (Lairon 2009), which not only optimizes enzymatic activity but also functions as a defense mechanism, destroying most viruses and bacteria ingested with food before the chyme advances further along the gastrointestinal tract (Sareen S. Gropper, Jack L. Smith 2022).

At this acidic pH, pepsinogen, a zymogen released by chief cells, is activated to form pepsin, the primary enzyme responsible for breaking down proteins into peptides (Smith 2019). Although some lipid digestion also occurs in the stomach, the action of gastric lipase (also secreted by chief cells) is limited; most lipid digestion takes place in subsequent sections of the digestive tract. Gastric lipase hydrolyzes only up to 30% of ingested lipids (Armand 2007). The important role of the stomach in lipid digestion is to mechanically mix lipids with other food contents, breaking them down and increasing their surface area for enzymatic action in later stages (Lairon 2009).
The motility and secretion within the stomach are regulated by various peptides and hormones. The release of pepsinogen and gastric acid is stimulated by the hormone gastrin, which is secreted by G cells. In contrast, the inhibition of gastric acid secretion is regulated by secretin, peptide YY, and somatostatin. When the chyme reaches the appropriate consistency and volume, the vagus nerve stimulates an increase in gastric motility, a response is relayed to the parasympathetic nervous system. This coordination allows the partially digested chyme—a coarse emulsion of food and gastric secretions – to enter the duodenum (Sareen S. Gropper, Jack L. Smith 2022).

The duodenum, the proximal segment of the small intestine, receives the chyme at a regulated pace controlled by stomach contractions. In the duodenum, sodium bicarbonate is secreted to neutralize the chyme's acidity, raising its pH from approximately 3–3.5 to 6-6.6 (Golding and Wooster 2010; Smith 2019). In the fasted state, duodenal osmolality ranges between 140–180 mOsm/kg, increasing to 270-290 mOsm/kg in the fed state. The predominant ions in human intestinal fluid are Na^+ and Cl^-, with K^+ and Ca^{2+} present at lower concentrations. However, with the influx of bile following a meal, the concentration of calcium in the duodenum increases significantly, reaching approximately 15 mM (Golding and Wooster 2010). Calcium plays a crucial role in pancreatic enzyme activation (Alvarez and Stella 1989). Enzyme precursors are secreted into the duodenal lumen by pancreatic acinar cells (Smith 2019). Trypsinogen, activated by enterokinase, converts into trypsin, a powerful proteolytic enzyme that initiates a cascade of other enzyme activations. Here, pancreatic secretions blend with bile from the gallbladder, enhancing digestion (Smith 2019). The duodenum serves as the main site for intestinal digestion, where enzymes and bile promote further hydrolysis of carbohydrates, lipids, and proteins. Initial absorption also begins here, particularly for iron, calcium, and select vitamins (Jackson and Mclaughlin 2006). Then peristalsis, the characteristic motility of the small intestine, moves the chyme from duodenum into the jejunum (Samsom and Verhagen 2004). The jejunum's structure, abundant in microvilli that increase surface area, facilitates nutrient absorption (Samsom and Verhagen 2004). Microvilli are lined with brush border enzymes, completing digestion by releasing final products, such as single amino acids from di- or tripeptides (Ozorio et al. 2020). Disaccharides are also converted into monosaccharides (e.g., sucrose into glucose and fructose) (Goodman 2010), and nucleotides into nitrogenous bases, sugars, and phosphates (Carver 1999). The jejunum is the primary site for nutrient absorption, including amino acids, simple sugars like glucose, free fatty acids, monoglycerides, and vitamins.

The digestive mass then moves to the ileum, the last and longest part of the small intestine, where remaining nutrients are absorbed. Here, vitamin B_{12} (Samsom and Verhagen 2004) and bile salts (BSs) – released initially in the duodenum – are mostly reabsorbed, returning to the circulatory system and ultimately to the liver for storage in the gallbladder (Reshetnyak 2013). The ileum terminates with the ileocaecal sphincter, located between the small intestine and the colon. This sphincter prevents the backward flow of undigested food particles, waste, and bacteria is prevented. Meanwhile, Peyer's patches, clusters of lymphatic tissue, play an essential role in immune defense, especially as intestinal content moves toward the large intestine. The primary functions of the large intestine include several key roles. First, it regulates water and electrolyte balance

through the absorption and secretion of ions by epithelial cells in the colon (Smith 2019). It also facilitates the fermentation of residual food by gut microbiota. Additionally, it supports immune function by promoting the activity of immune cells. For example, bacteria such as *Akkermansia muciniphila* degrade mucin, which helps modulate immune responses (Flint et al. 2012). Finally, the large intestine is responsible for stool formation (Smith 2019).
Building upon the above description, the next sections will delve further into the molecular mechanisms of lipid and protein digestion and will examine bile in detail, highlighting its vital role in this context.

1.1.1 Bile and the physical-chemical properties of biliary surfactants

Bile is an exocrine secretion of the liver that is stored in the gallbladder. Its primary functions include aiding in fat digestion and absorption as well as in the excretion of waste metabolites. Bile is mainly composed of water and organic compounds, with surface-active substances such as 70% of BSs and 22% of phospholipids (PLs) comprising the majority of the latter (Vlahcevic, Bell, and Swell 1970). The remaining organic components are primarily cholesterol, bilirubin, and other organic molecules (Swell, Bell, and Vlahcevic 1971). The latest research using a multi-omics approach provided a comprehensive analysis of 50 BSs to distinguish various species in multiple biological matrices. It was found that bile acids in humans have a higher level of sulfation compared to other studied species. Sulfated BSs may play a role in detoxification, which is characteristic of humans (Sangaraju et al. 2021). Sharma et al. (2022) analyzed the bile to identify bile lipids and microbial peptides. The results showed that the lipid profile markers, and microbiome composition of bile can be used for early detection of gallbladder cancer (Sharma et al. 2022).

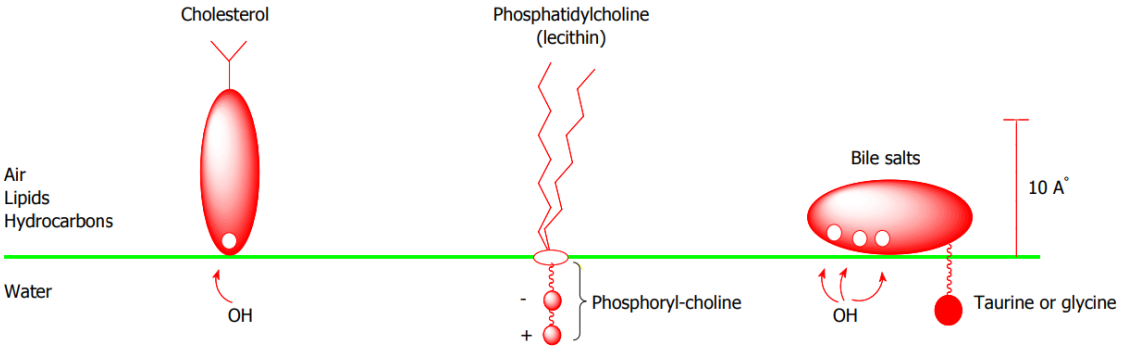

Figure 1.2 The amphiphilic character and simplified chemical formulas of cholesterol, phosphatidylcholine, and bile salts at the lipid (air, hydrocarbons)–water interface (Reshetnyak 2013).

A distinctive characteristic of BSs is their planar amphipathic structure (Carey 1972) (Figure 1.2). The defined hydrophobic and hydrophilic groups in BSs contribute to their surface-active properties (Tazuma 2017). The hydrophobic properties of BSs increase as follows: ursodeoxycholate (ursodeoxycholic acid) < cholate (cholic acid) < chenodeoxycholate (chenodeoxycholic acid) < deoxycholate (deoxycholic acid) (Reshetnyak 2013). Additionally, the stereochemistry of BSs determines the spatial orientation of polar groups, influencing the micelle formation process. However, the structure of BSs differs from the typical 'head and tail' surfactant structure, resulting in the formation of small micelles, usually involving 2-9 molecules. Over the past 60

years, theories on BS micelle structure have evolved through the description of three different models. First, in 1972, Carey and Small proposed a disk model, in which the micelle consists of one or two layers (Figure 1.3a-b). Next, in 1989, Kawamura proposed a single-layer disk model (Figure 1.3c). The third model, proposed by Giglio in 1988, was a helical model. In this model, the hydrophobic surface is exposed to the aqueous phase (Figure 1.3d). However, research by Warren et al. in 2006 presented molecular dynamics simulations of six BSs. It revealed that the micellar structure of BSs and dynamics differ from traditional literature models. The proposed micelle structures are more dynamic and less ordered than those previously described (Warren et al. 2006).

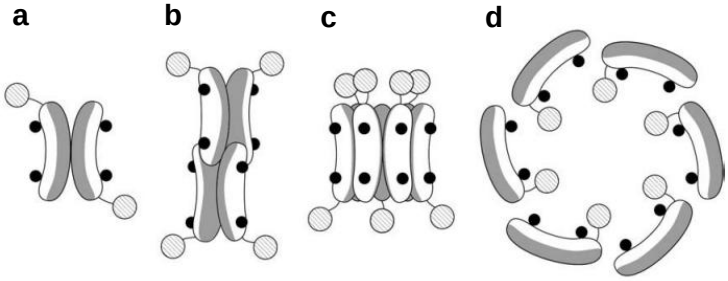

Figure 1.3 Models of BS micellar structures. (a) and (b) represent two types of primary micelles, (c) shows a disc-like micelle, and (d) presents a top view of a helical micelle (Madenci and Egelhaaf 2010).

Similarly, to BSs, PLs are amphipathic compounds (Figure 1.2). However, they have very low solubility in water (Cevc Gregor 2018). They contain a hydrophilic head, consisting of a glycerol backbone with a phosphate group at the sn-3 position. The hydrophobic portion is composed of two long-chain saturated or unsaturated fatty acids esterified to glycerol at the sn-1 and sn-2 positions. An additional group attached to the phosphate determines the type of PL; this is typically choline, ethanolamine, serine, glycerol, or inositol. These groups influence the PL's solubility in water, which also depends on the length and degree of saturation of the fatty acid hydrocarbon chains (Cevc Gregor 1993).

Due to their amphiphilic nature, PLs exhibit diverse self-assembly behaviors in different environments. In aqueous solutions, they spontaneously form bilayer structures, with their hydrophilic heads interacting with water and hydrophobic tails shielded within the bilayer's core (Pichot, Watson, and Norton 2013). Upon contact with oil, these bilayers tend to separate into two monolayers at the oil-water interface (Pichot, Watson, and Norton 2013). The behavior of PLs at this interface is further influenced by factors such as electrostatic potential. For instance, zwitterionic PLs can form stable monolayers under a negative electrostatic potential. However, an increase in potential can induce a transformation into ionic species, destabilizing the monolayer and leading to its breakdown (Pichot, Watson, and Norton 2013). The presence of PLs at the water droplet interface also impacts its physical properties, contributing to increased elasticity and viscosity (Pichot, Watson, and Norton 2013).

Each surfactant has its unique self-aggregation tendency. PLs tend to form large multilamellar vesicles composed of bilayers, while BSs form simple spherical micelles ($Ø \approx 50$ Å) (Müller 1984). X-ray scattering analysis, as illustrated in Figure 1.4, reveals how the specific micellar structures formed by BSs and PLs in aqueous solutions depend on the molar ratio of these two surfactants. Initially, globular BS micelles incorporate lecithin without significant changes in overall size. However, this incorporation creates a distinct low-electron-density zone within the micelle's core (Müller 1984). As the lecithin

proportion increases, reaching a maximum incorporation point, the structure transitions. It progresses through an oblate ellipsoid shape and eventually forms a bilayer structure characteristic of mixed disc micelles (Müller 1984). These disc micelles are then capable of further growth with the addition of more lecithin (Müller 1984). Figure 1.4. depicts these structural transformations as a function of the sodium taurodeoxycholate percentage.

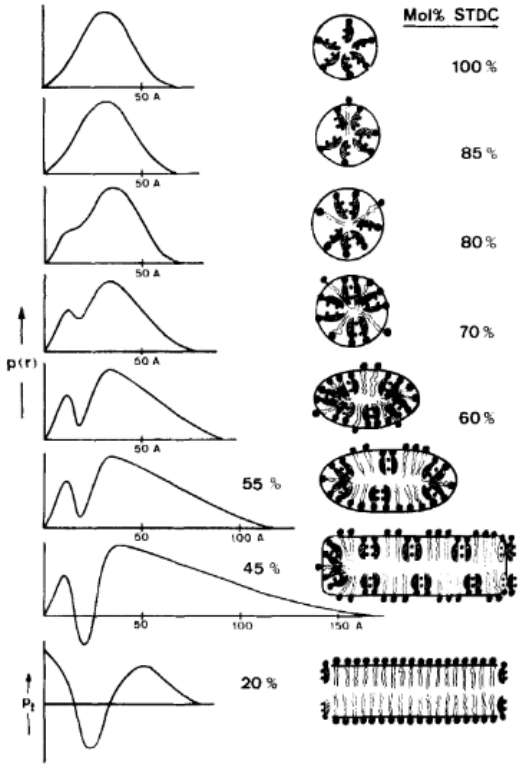

Figure 1.4. The micellar structures of BSs/PLs complexes formed in aqueous solutions depend on the ratio of both surfactants. STDC – sodium taurodeoxycholate The graphs on the left-hand side present X-ray scattering results (distance distribution function p(r)) (Müller 1984).

Bile acids synthesis occurs in liver hepatocytes. They are synthesized from cholesterol in 17-spets enzymatic reactions beginning with the formation of cholic acid, which is subsequently conjugated with taurine or glycine via an amide bond at the carboxyl group (Maldonado-Valderrama et al. 2011). The BSs synthetized in the liver are called primary BSs, however they undergo bacterial metabolism in the intestine, yielding in secondary BSs and they are also conjugated (Macierzanka et al. 2019). Conjugation lowers the pKa, enhancing ionization and increasing solubility in water at acidic pH. That helps the conjugated bile acids maintain water solubility in the postprandial pH range of the duodenum (3-5), facilitating digestion in the duodenum and upper jejunum. The pKa values of free (unconjugated) bile acids is between 5 and 6.5, while for glycine-conjugated bile acids its ~3 and for and taurine-conjugated pKa is 4. Conjugation prevents nonionic passive absorption, ensuring bile acids remain in the lumen for digestion. However, it allows bile acids to be actively absorbed in the terminal ileum after aiding digestion (Tazuma 2017; Jenkins, Gereth; Hardie 2008). Approximately 95% of BSs are reabsorbed, and the rest is excreted with the feacal mass (Macierzanka et al. 2019).

Biliary PLs are also synthesized in the liver (Reshetnyak 2013). The most abundant PL in human bile is phosphatidylcholine (PC), which differs in fatty acid chain length from that found in liver tissue or plasma. Biliary PC contains higher amounts of palmitic acid, with

the main types being 1-palmitoyl-2-oleoyl-PC and 1-palmitoyl-2-linoleoyl-PC (Cohen 1996; Reshetnyak 2013; Hay et al. 1993). The percentage of fatty acids participation in the biliary PC is as follow: palmitic acid (16:0) represents 41.40%, linoleic acid (18:2) 32.83%, and oleic acid (18:1) 12.09% (van Berge Henegouwen, van der Werf, and Ruben 1987). It is believed that the selection of the type of PC occurs in a selective manner during bile formation (Reshetnyak 2013). Newly synthetized PC is translocated from the outer to the inner membrane of hepatocytes with the involvement of the MDR3 P-glycoprotein and is finally released in vesicular form in bile canaliculi (Reshetnyak 2013). This process is closely linked to BSs secretion. The hydrophobicity of BSs plays an essential role in regulating the rate of PL secretion. More hydrophobic BSs stimulate greater PC secretion than more hydrophilic ones (Cohen 1996).

While BAs act as detergents they are toxic at high concentrations. They damage canalicular membranes, but the presence of PLs (mainly PC) and cholesterol provides a protective barrier, reducing toxic effects. Moreover, canalicular membranes are rich in sphingomyelin and cholesterol, which are less fluid than PC and more resistant to bile acid micelle formation. BSs is requiring strict regulation within cells to avoid cell damage (Jenkins, Gereth; Hardie 2008). The system of bile acid regulation is essential for maintaining safe cellular concentrations and involves complex networks of hepatobiliary transporters and receptors. The transport mechanism in hepatocytes of the bile secretion into canaliculus involves BS export pump (BSEP, ABCB11) for bile acids and MDR3 (ABCB4), MRP2 (ABCC2), ABCG5/G8 for other components such as PLs, organic anions and cholesterol, respectively (Pohl, Devaux, Herrmann 2005). This transport system is further regulated by the activation of the farnesoid X receptor (FXR, NR1H4), a nuclear receptor, and the G protein-coupled bile acid receptor (TGR5). The FXR is primarily expressed in the liver, intestine, kidney, and adrenal gland. The TGR5 is found in various tissues, including the liver, gallbladder, bile ducts, intestine, brown adipose tissue, and macrophages. These receptors initiate various physiological responses that control bile acid concentrations and metabolism (Tazuma 2017; Claudel and Trauner 2010). During the excretion various assemblages are formed in the bile, such as BSs micelles or mixed micelles with PC and cholesterol as presented in the Figure 1.5 (Morita and Terada 2014).

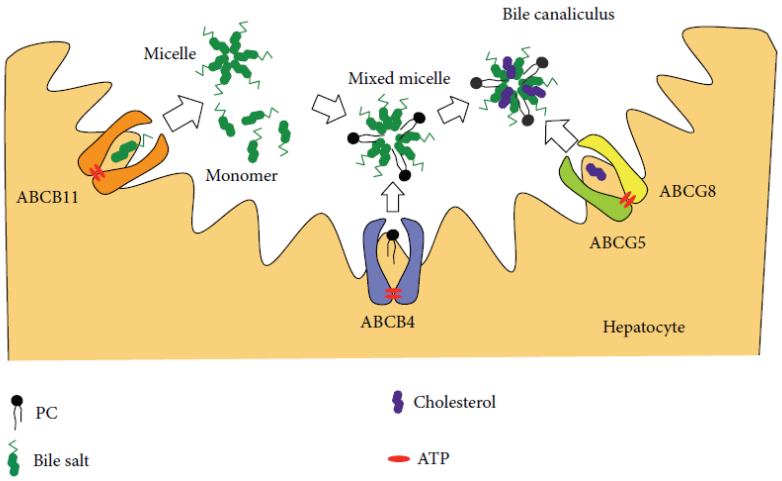

Figure 1.5 Mixed micelles containing BSs, PLs, and cholesterol are formed in the bile canaliculus. The ABCB11 protein facilitates the transport of BSs into bile. BS monomers are crucial for the PL transport mediated by ABCB4. Heterodimer ABCG5/ABCG8 mediates cholesterol transport in the presence of mixed BS/PL micelles (Morita and Terada 2014).

After bile is secreted to the intestine, mixed micelles reorganize alongside dietary and mucus PLs. PLs present in the mucus layer of the gastrointestinal tract serve a protective function against 'aggressive' substances, such as certain drugs

(e.g., nonsteroidal anti-inflammatory drugs, NSAIDs). They participate in the dynamic exchange of PLs derived from bile and/or diet. They act as a defensive barrier, reducing the availability of potent detergent effects caused by bile acid-simple micelles formed, for example, as a result of xenobiotic activity (Nervi 2000). Elvang et al. (2016) found two main types of particles with different structures and sizes in human intestinal fluid during the fed state. The first fraction is composed of mixed micelles created primarily by taurocholate and PLs (size < 70 nm). The second fraction is created primarily by small PL vesicles ranging from 90-210 nm in diameter (Elvang et al. 2016).

1.1.2 Proteins in human digestion

Proteins are one of the essential nutrients in the human diet and play many critical roles necessary for the proper functioning of the body. They provide amino acids that are required for tissue building, enzyme and hormone production, and the synthesis of other biologically active compounds. Proteins are the primary structural components that provide the body with essential amino acids for the development of muscles, as well as bones and other tissues. The recommended daily intake for adults is approximately 0.8–1.2 g of protein per kilogram of body weight, though requirements may increase for physically active individuals, children, pregnant women, and older adults. Excessive protein intake can place strain on the kidneys and liver, while a protein deficiency may lead to muscle loss - sarcopenia, weakened immunity, and other health issues (Wu 2016).

The main dietary sources of protein for humans are animal-derived proteins, including those from dairy products, and plant-based proteins. The latter are predominantly obtained from legumes as well as grains, nuts, and seeds. Animal proteins are found in meat, fish, eggs, milk, and dairy products. These are considered complete proteins as they contain all essential amino acids, the ones the body cannot produce and must obtain from food (His, Ile, Leu, Lys, Met, Phe, Thr, Trp, Val), while some plant proteins may be low in certain amino acids (Elmadfa and Meyer 2017). Protein quality is assessed based on both amino acid composition and protein digestibility. A well-known method for evaluating protein quality is PDCAAS (Protein Digestibility-Corrected Amino Acid Score). Currently, PDCAAS is gradually being replaced by DIAAS (Digestible Indispensable Amino Acid Score), which provides more accurate information on protein quality. DIAAS uses digestibility of protein and amino acid release measured at the ileum, while protein digestibility in PDCAAS is measured at the faecal level. PDCAAS is calculated by comparing the amount of amino acids in a given protein to that in a reference protein, considering the digestibility of the protein. The result is expressed on a scale from 0 to 100%, where 100% means that the protein fully meets the body's requirements. On the other hand, DIAAS allows values greater than 100%, which provides better differentiation for proteins with the highest nutritional value (Adhikari et al. 2022). Animal proteins often have a PDCAAS score close to 100%. This means they are complete and highly digestible. Whey Protein Isolate (WPI) scores 97%. Whey Protein Concentrate scores 100%. Some plant proteins also score high, such as soy flour at 93%. In contrast, wheat scores only 51% due to deficiencies in certain essential amino acids and lower digestibility (Mathai, Liu, and Stein 2017).

A broad class of proteins important for human nutrition are storage proteins. They are a type of protein whose primary function is to store and supply nutrients, particularly amino acids, at the appropriate time, such as during growth, development, or germination. Major types include prolamins (gluten), globulins (legumins), and albumins (Shewry 1995).

As previously described, protein digestion begins in the stomach and continues in the small intestine. Figure 1.6 illustrates the process of enzymatic digestion of proteins along the gastrointestinal tract. Where pepsin (EC 3.4.23.1), an enzyme released in the stomach, effectively cleaves most proteins during the initial stage of protein digestion, producing polypeptides and oligopeptides. Pepsin is an aspartic endopeptidase, with an active site formed by a catalytic dyad composed of two aspartic acid residues (Asp). The acidic environment of the stomach facilitates the protonation of these Asp residues, enabling effective proteolysis. Pepsin preferentially cleaves peptide bonds near the carboxyl ends of aromatic and acidic residues, such as tyrosine (Tyr), phenylalanine (Phe), tryptophan (Trp), methionine (Met), leucine (Leu), glutamic acid (Glu), and aspartic acid (Asp) (Sareen S. Gropper, Jack L. Smith 2022; Brix and St 2013). The results of Herrera et al. show that gastric digestion plays a key role in protein breakdown and their subsequent interaction with BSs, which may modulate lipid digestion. Pea proteins, especially after processing, may aid in better fat digestion (Herrera et al. 2024).

Moving into intestinal digestion, enzymes released in pancreatic juice into the duodenum form a complex mixture with complementary actions. The three most abundant proteolytic enzymes are trypsin (EC 3.4.21.4), chymotrypsin (EC 3.4.21.1), and elastase (EC 3.4.21.36) which are endopeptidases that cleave peptide bonds within the protein/peptide structure (Pekar, Ret, and Untersmayr 2018). These enzymes are classified as serine proteases due to their catalytic triad in the active site, composed of serine, histidine, and aspartic acid. Serine acts as a nucleophile, attacking the carbonyl group of the peptide bond, while aspartic acid stabilizes histidine, which serves as a proton acceptor, activating serine for nucleophilic attack (Polgár 2005). Trypsin cleaves peptide bonds near basic amino acids (Arg, Lys) on the carboxyl side, while chymotrypsin, the activated form of chymotrypsinogen, preferentially cleaves peptide bonds at the carboxyl end of aromatic amino acids such as Tyr, Phe, Trp, Met, Asn, and His. Elastase, released from its zymogen proelastase, targets peptide bonds near aliphatic amino acids (e.g., alanine, Ala) within fibrous connective tissue, such as elastin. Additionally, pancreatic juice contains collagenase, a robust enzyme essential for degrading the tight structure of collagen (Sareen S. Gropper, Jack L. Smith 2022; Whitcomb and Lowe 2007; Bradley and Bradley 2022). Other pancreatic proteases include carboxypeptidases A and B (EC 3.4.17.1 and EC 3.4.17.2), which are zinc-dependent exopeptidases activated from procarboxypeptidase. These enzymes specifically cleave the single, terminal amino acid at the C-terminus of peptide chains (Smith 2019). Carboxypeptidase A acts on neutral, aromatic, or acidic residues at the peptide's end, whereas carboxypeptidase B cleaves peptides terminating with basic amino acids (Whitcomb and Lowe 2007).

The brush border enzymes, as previously mentioned, break down polypeptides into smaller fragments or free amino acids, which are then transported into enterocytes through sodium-dependent active transport (symport with Na^+ ions). Peptide absorption primarily occurs via the peptide transporter PEPT1, which facilitates the uptake of di- and tripeptides. This transport process is driven by a proton (H^+) gradient, enabling efficient translocation of small peptides across enterocyte membranes. PEPT1 shows a preference for peptides composed of L-amino acids, as demonstrated by its preferential absorption of di- and tripeptides derived from milk protein digestion over certain synthetic drugs (Sina Vahdatpour et al. 2016). Interestingly, it was observed that BSs may be useful in inhibiting peptide degradation at this stage, which could help improve the bioavailability of certain peptides. Their action involves inhibiting the activity of cytosolic proteases and brush border enzymes (Bai 1994).

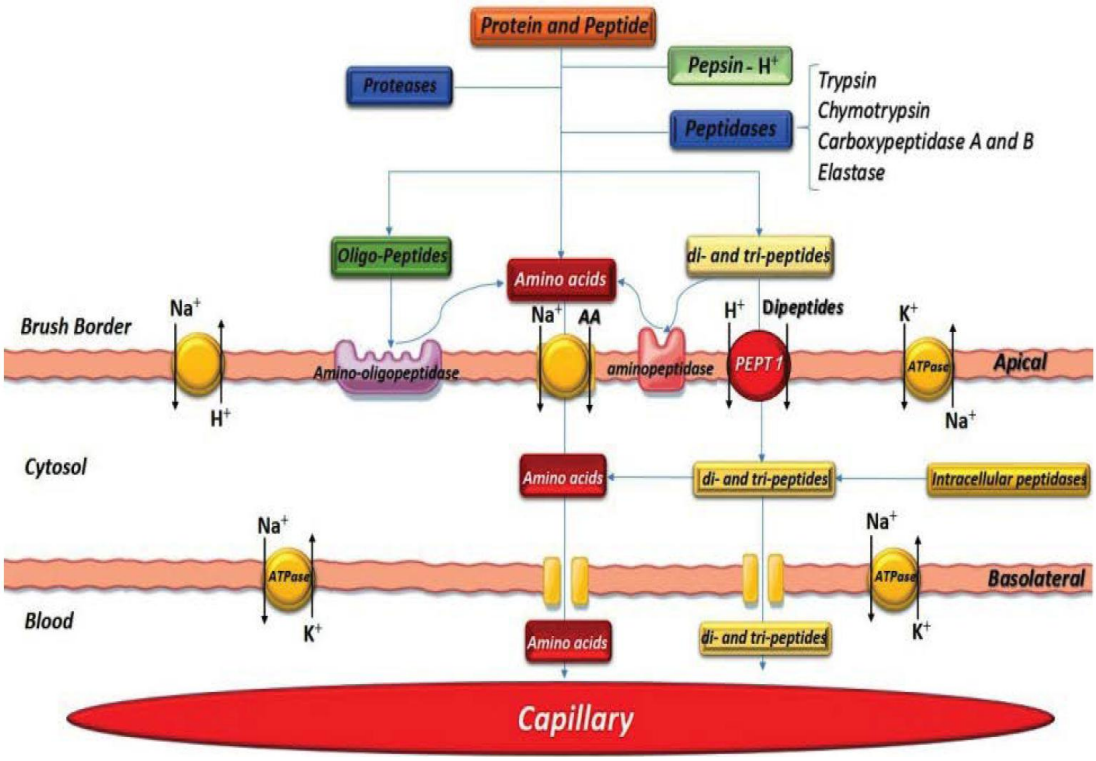

Figure 1.6 A schematic representation of protein digestion and mechanism of absorption from the intestine to the capillaries through the apical and basolateral layers. It illustrates the enzymatic actions and digestion of proteins, oligopeptides, and peptides across the compartments involved in protein digestion within the human intestinal tract: the stomach (pepsin) and the intestine (trypsin, chymotrypsin, carboxypeptidase A and B, elastase), brush border enzymes, and intracellular peptidases. Main transporters of the apical layer: from the left, Na^+/H^+ transporter, amino acid (AA) and Na^+ transporter (enabling cotransport of amino acids and sodium ions into the cell), PEPT1 (facilitating the transport of dipeptides into the cell using the proton gradient H^+), Na^+/K^+ ATPase; and basolateral layer: Na^+/K^+ ATPase, amino acid transporter, and transporter for di- and tripeptides, allowing their passage into the bloodstream (Sina Vahdatpour et al. 2016).

While most proteins are susceptible to pepsinolysis, some proteins or their fragments resist complete digestion, either in the gastric phase or even during pancreatic digestion in the intestinal phase. The survival of certain peptides in the gastrointestinal tract may increase the risk of exposure to allergens; however, it does not define allergenicity itself (Akkerdaas et al. 2018). Gliadin and glutenin are common storage proteins found in wheat that form gluten. Although gluten contains essential amino acids it is relatively low in lysine. Due to its elastic properties crucial for the texture its widely used for baking (Barak, Mudgil, and Khatkar 2015). Gluten can be hard to digest for some individuals and is harmful to those with celiac disease or gluten sensitivities, as it can trigger an immune response in the small intestine (Balakireva and Zamyatnin 2016). Legumins are storage proteins present in legumes (e.g., soybeans, lentils), they are rich in lysine, which are often limited in grains, making legumes valuable in plant-based diets (Duranti and Gius 1997). However, it has been found that legume proteins are harder to digest after cooking, mainly due to changes in their structure that make them clump together and less soluble. Although compounds like lectins and trypsin inhibitors slightly reduce digestibility, the main issue is that cooking causes proteins to form stable complexes that the body struggles to break down (Carbonaro et al. 2000). For example, studies have shown that pepsin-resistant proteins, such soybean trypsin inhibitor (STI), remain stable even in the presence of high pepsin concentrations and low pH, indicating

they are not easily degraded by this enzyme. Moreover, lipid transfer protein (LTP) resistance to pepsin degradation (R. Wang et al. 2017) may be attributed to its compact structure, consisting of four α-helices and a C-terminal arm, which is stabilized by four disulfide bridges (Perrocheau et al. 2006). Another example of a plant-based protein resistant to digestion is the 16-kDa buckwheat protein. Due to its resistance to pepsin, this protein is considered the primary allergen responsible for immediate allergic reactions. It also shows high homology with a rice allergen, suggesting the potential for cross-reactivity in individuals allergic to both grains (Tanaka et al. 2002).

When considering protein digestion, it is important to note that, aside from potential negative effects associated with exposure to epitopes, some food proteins can provide additional health benefits beyond basic nutrition. Specifically, bioactive proteins and peptides can positively impact health and reduce the risk of chronic diseases. Bioactive peptides are often generated during digestion, fermentation or chemical hydrolysis and may exhibit various effects, such as antihypertensive, anti-inflammatory, immunomodulatory, and more (Rutherfurd-Markwick 2012).

Milk proteins are another vital component of human nutrition, comprising approximately 3.5% of milk's composition. Casein constitutes the primary fraction, accounting for around 80%, while the remaining 20% consists of whey proteins, including β-lactoglobulin (β-Lg) and α-lactalbumin (α-La). Milk proteins supply essential amino acids and contain bioactive compounds, such as immunoglobulins, vitamin-binding proteins, and protein hormones (Mahony and Fox 2014). The articles by Nielsen et al. and Koirala et al. provide the comprehensive reviews of the significance of bioactive peptides derived from milk proteins. Antioxidant peptides, for instance, neutralize free radicals, thereby they protect the body from oxidative stress and reduce the risk of cardiovascular disease. Antihypertensive peptides, derived from β-casein, inhibit the angiotensin-converting enzyme (ACE), thereby lowering blood pressure and supporting cardiovascular health. Immunomodulatory peptides enhance immune function, while phosphopeptides facilitate calcium absorption and bone mineralization, contributing to osteoporosis prevention (S. D. H. Nielsen et al. 2023; Koirala et al. 2023).

These health benefits are also attributed to β-Lg, whose peptides contribute to blood pressure regulation and exhibit antioxidant activity (Nielsen et al. 2023; Koirala et al. 2023; Zhao and Joshua 2020). However, cow's milk allergy remains one of the most prevalent food allergies, particularly in children, and often persists into adulthood. Managing this allergy requires the elimination of milk from the diet, which may lead to nutritional deficiencies (Villa et al. 2018). The article by Monaci et al. (2006) highlights that, while bioactive peptides offer potential health benefits, they may also pose challenges for individuals with milk allergies, as certain fragments can retain immunogenic properties (Monaci et al. 2006). The primary allergens in milk are casein (specifically αs1-CN) and β-Lg; however, other proteins, such as lactoferrin, bovine serum albumin, and immunoglobulins, may also trigger allergic reactions (Wal 2001; Monaci et al. 2006; Villa et al. 2018).

The digestion of β-Lg leads to the formation of peptides that may exhibit allergenic properties, such as the β-Lg fragment f(127–135), which is a potential allergenic epitope that survived the proteolysis conditions (Picariello, Iacomino, et al. 2013). Studies on β-Lg digestion in complex food matrices, such as dairy products, have shown that the presence of various components, such as PLs, significantly influences the proteolysis rate of this protein. In infant digestion models, β-Lg was found to be more susceptible to digestion than in adult models, likely due to a lower presence of PLs (Dupont et al. 2010).

The stability of β-Lg plays a crucial role in its susceptibility to digestion. Research by Mandalari et al. (2009) indicates that the presence of PLs, such as PC, enhances β-Lg stability, thereby slowing its proteolysis in the intestine (Mandalari et al. 2009; Mandalari et al. 2009). Interactions between PLs and proteins or peptides can be classified according to the nature of the forces involved: hydrophobic, hydrophilic, or mixed. The nature of these interactions determines their impact on the structure and biological activity of the combined molecules (Cserhåti and Szögyi 1993). Moreover, it was observed that β-Lg digestion was slowed by the formation of complexes with polyphenols, which are present in beverages such as tea, coffee, and cocoa (Stojadinovic et al. 2013).

Additionally, studies on the peptidomic profile of kefir showed that β-Lg exhibited greater resistance to hydrolysis by microorganisms compared to other milk proteins, such as casein, which was more susceptible to kefir's proteolytic enzymes (Dallas et al. 2016). These findings align with previous research suggesting that the difficulty in breaking down β-Lg may reflect structural characteristics, such as disulfide bonds (Ferreira et al. 2010).

β-Lg is a globular protein, comprises 60% of Whey Protein Isolates (WPI) (Edwards 2014). It is frequently used as a model in digestion studies due to its availability and low production cost (Didier Dupont et al. 2010). Moreover, β-Lg is highly water-soluble and possesses excellent foaming, gelling, and emulsifying properties. Consequently, WPI is widely used in the food industry, enhancing the stability, texture, and mouthfeel of food products (Abd El-Salam, El-Shibiny, and Salem 2009). As consumer perception of the flavor and texture of processed food products is influenced by multiple factors, the structure of ingredients becomes particularly significant (Boland Mike; Golding Matt 2014). Although potential allergenicity of β-Lg, WPI is one of the most functional food ingredients, known for its high GRAS (Generally Recognized as Safe) status and nutritional value (Abd El-Salam, El-Shibiny, and Salem 2009). As a member of the lipocalin protein family, β-Lg consists of 162 amino acids and has two common structural variants, A and B, which differ by only two amino acids (Asp64Gly and Val118Ala). Due to these slight differences, variant B is less densely packed and exhibits lower thermal stability. The protein includes a binding site capable of binding small hydrophobic molecules, allowing β-Lg to function as a transport protein for retinoid compounds. Its quaternary structure is influenced by factors such as pH, pressure, ionic strength, and temperature, enabling it to form monomers, dimers, and oligomers. However, under physiological conditions, the dimer is the predominant form (Figure 1.7) (Edwards Patrick 2014).

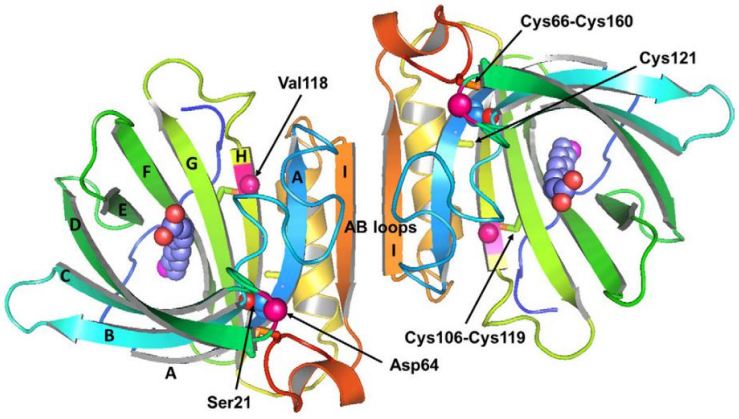

Figure 1.7 Dimeric structure of bovine β-lg with 12-bromododecanoic acid bound (Edwards Patrick 2014).

This protein has a dominant β-barrel structure composed of 9 antiparallel β-strands and one α-helix. β-Lg has a high propensity to undergo a conformational change from β-strand to α-helix, especially under specific environmental conditions, such as the presence of urea or organic solvents. The heptad repeat region (residues 14-52) plays a key role in the transition from β-structure to α-helix (Ragona et al. 1999).

The previously mentioned study by Stojadinovic et al. demonstrates that within the pH range of 6.8–7.5, deprotonation of previously hidden amino acid residues occurs, revealed by the opening of the calyx due to a protein conformational change. Polyphenols, such as negatively charged phenolic acids, form electrostatic and hydrogen bonds with the protein, influencing the formation of intermediate α-helical structures. As a result of this destabilization, there was a reduction in β-sheet content accompanied by an increase in α-helix content and random coils (Stojadinovic et al. 2013).

The above literature review highlights the importance of β-Lg protein in human nutrition but also reveals gaps in knowledge regarding its digestion in the presence of biliary surfactants (BSs and PLs). Although the digestion of this protein has been studied extensively, none of the research has provided insights into the impact of these two biosurfactants on the peptide profile resulting from β-Lg digestion at various BS/PL ratios, which are inherent components of human bile. This may be particularly important in the release of bioactive peptides or epitopes from the protein in the intestinal lumen.

1.1.3 **Lipids in human digestion**

Lipids are a diverse group of compounds, including fats (triacylglycerols), PLs, sterols, waxes, glycolipids, and fatty acids. Lipids play crucial biological roles as structural components of cell membranes, energy sources (providing over twice the energy content of carbohydrates or proteins), and signaling molecules that influence physiological functions.

Triacylglycerols (TAGs) are the primary energy reserves, found as lipid droplets in plants and animal adipose tissue. They consist of glycerol linked to three fatty acids (FAs).In the gastrointestinal tract, TAGs are hydrolyzed by lipases, enzymes within the hydrolase group that have a high affinity for interfaces (Figure 1.8). Lipases act at the water-oil interface, hydrolyzing hydrophobic substrates, such as TAGs, into more water-miscible products (Brockman 2000).

The primary lipases in the human digestive system are human gastric lipase (HGL) and human pancreatic lipase (HPL), both belonging to the α/β hydrolase family (Armand 2007). The active sites of these enzymes contain an oxyanion hole and operate through the catalytic triad mechanism, comprising serine, histidine, and aspartic acid residues (Ser-His-Asp) (Reis et al. 2009).

As previously mentioned, ingested TAGs can be emulsified in the stomach through its peristaltic movements, especially in the presence of surface-active compounds (e.g., proteins or PLs), and are partially hydrolyzed by human gastric lipase (HGL). During the gastric phase, 30% of triglycerides are hydrolyzed, releasing free fatty acids (FFAs), diacylglycerols (DAGs), and monoacylglycerols (MAGs) (Figure 1.9) (Armand 2007). The primary site for triglyceride digestion is the small intestine, where approximately 70% of ingested lipids undergo hydrolysis by HPL. HPL is released by the pancreas along with other enzymes. It has two structural domains (Figure 1.8): a smaller C-terminal domain that binds colipase, forming the HPL-colipase complex, which anchors the enzyme at the interface in the presence of BSs, and a larger N-terminal domain that includes a lid domain and two β loops (β5 and β9). The enzyme's active site is hidden beneath the lid, and HPL can adopt two conformations - open and closed - regulated by the adjacent β loops. In the open conformation, hydrophobic residues are exposed, allowing substrate access to the active site. The catalytic triad in the active site is similar to serine proteases; however, lipases and esterases structurally differ by incorporating a unique Gly-X-Ser-X-Gly sequence (Miled et al. 2000).

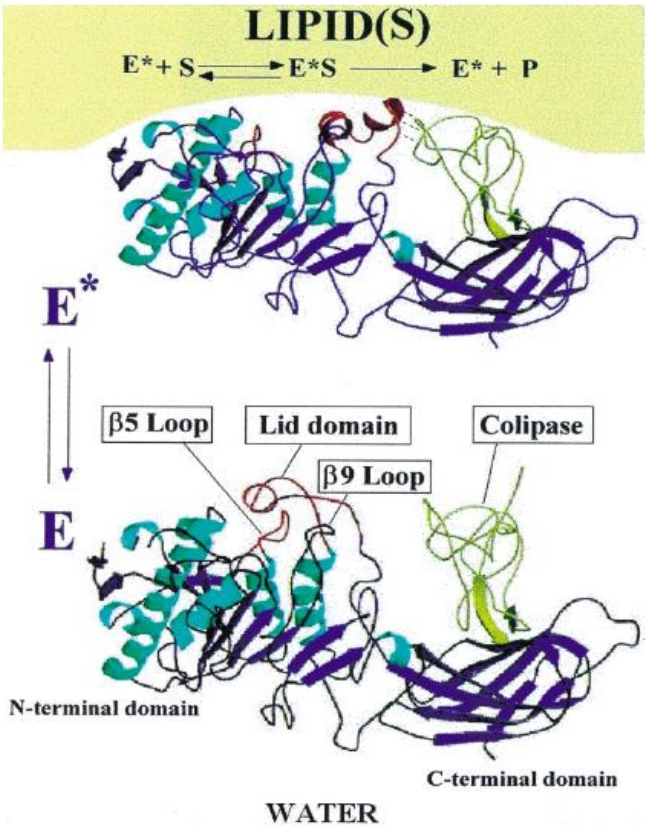

Figure 1.8 The structure of Human Pancreatic Lipase-procolipase complex. E - closed conformation; E - open conformation, S – substrate, P – product. The 3-D structure illustrates the changes during interfacial activation in the conformation of the β5-loop, colipase and the lid domain (Miled et al. 2000).*

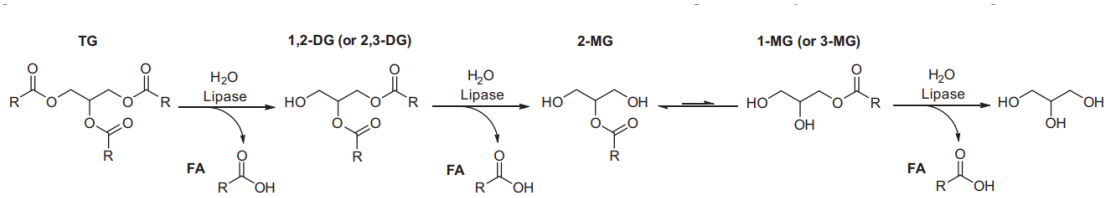

Figure 1.9. Hydrolysis of triglyceride by pancreatic lipase. The pancreatic lipase is selective towards the position sn-1 and sn-3, resulting in a 2-monoglyceride product. The intermolecular rearrangement of the monoglyceride was observed during the lipolysis(Benito-Gallo et al. 2015).

The products formed during triacylglycerol hydrolysis are displaced by BSs and solubilized in mixed micelles (Figure 1.9). Thus, the kinetics of lipolysis are altered by the removal of products from the interface, enabling lipase to continually access the substrate and increasing its overall conversion. The aqueous solubility of MAG and FFA is enhanced by a factor of 100–1000 due to micellar solubilization (Phan and Tso 2001). The rate of lipid digestion is also influenced by the droplet size of emulsified lipids. Smaller droplet sizes increase lipolysis by enlarging the total water-lipid interface, thereby facilitating enzyme access to the substrate (Armand et al. 1992). Moreover, the efficiency of lipolysis depends on the degree of TAG unsaturation. Saturated TAGs, which form lipid droplets with higher solid content, suppress lipid digestion relative to droplets composed of unsaturated TAGs. Additionally, the chain length of the released fatty acids plays a role in signaling and satiety regulation. For example, previous studies have shown that lauric acid (C12:0) suppresses energy intake and may reduce lipolysis, in contrast to oleic acid (C18:1), which is the most prevalent fatty acid in dietary TAGs (Golding and Wooster 2010).

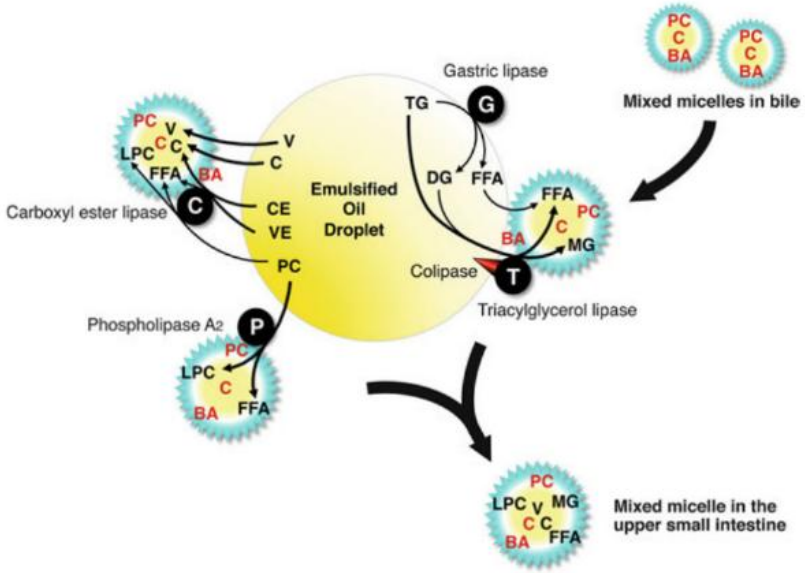

Figure 1.10. Dietary lipids hydrolysis and micellar solubilization. BA - bile acids, C- cholesterol, CE - cholesterol ester, DAG - diacylglycerol, FFA - free fatty acids, LPC - lysophosphatidylcholine, MAG - monoacylglycerol, PC - phosphatidylcholine, TAG – triacylglycerol, V – fat soluble vitamin, VE – fat-soluble vitamin ester (T. Northfield 1984).

The FFA and MAG released from TAG droplets through lipase action may either remain at the interface or become part of mixed micelles, depending on other environmental components (Wilde and Chu 2011). In the presence of BSs, FFAs are relatively easily displaced from the interface and solubilized in mixed micelles (Macierzanka et al. 2019).

In the case of PLs, their affinity for the interface is higher, and thus they rarely form mixed micelles by solubilizing interfacial FFAs and MAGs (Wilde and Chu 2011).

Fatty acids are carboxylic acids of varying lengths of the hydrocarbon chain (short, medium, long, and very long). They can be released during the hydrolysis of TAG described above or consumed in free form. They are used to generate the energy during β-oxidation in mitochondria. Fatty acids can be saturated (SFA) or unsaturated, including monounsaturated (MUFA) and polyunsaturated (PUFA). Essential FAs, like omega-3 FAs (e.g. linoleic acid) and omega-6 FAs (e.g. alpha-linolenic acid), are vital for the body and serve as precursors to PUFAs. PUFA, such as eicosapentaenoic acid (EPA) and docosahexaenoic acid (DHA), play crucial roles in the development of the nervous system and exhibit anti-inflammatory properties (Rustan and Drevon 2005).

Sterols are a group of lipids that play an important role in human metabolism. Sterols, like zoosterols in animals, phytosterols in plants, and mycosterols in fungi, all have a four-ring structure (Tietel et al. 2023). The steroid ring system contains hydroxyl group at position 3, this group can be free or esterified. The most well-known zoosterol is cholesterol, which is essential for building cell membranes, synthesizing steroid hormones (such as cortisol, estrogens, and testosterone, and producing previously mentioned bile acids. Cholesterol can be synthesized in the liver, so it is not necessary to obtain it from the diet, although cholesterol and its esters are present in animal products such as meat, eggs, and dairy. Unesterified cholesterol participates in the formation of mixed micelles and is subsequently transferred across the brush-border membrane in the intestine (Cohn et al. 2010; Sareen S. Gropper, Jack L. Smith 2022). In the body, cholesterol is transported in the blood by LDL ("bad" cholesterol) and HDL ("good" cholesterol) lipoproteins. HDL removes excess cholesterol from tissues and has anti-inflammatory and antioxidant properties. However, studies report that "good" HDL can become "bad" HDL under pathological conditions, such as coronary artery disease or chronic kidney disease. In such cases, HDL loses its protective functions and contributes to atherosclerosis and endothelial dysfunction (Xu, Liu, and Liu 2013).

Phytosterols are found in nuts, seeds, vegetable oils, and grain products. Regular consumption of phytosterols can reduce the risk of cardiovascular diseases. Moreover, research has shown that phytosterol conjugated to linoleic acid may compete with cholesterol for incorporation into micelles after digestion in the intestinal lumen, potentially competing during absorption and contributing to cholesterol reduction (Moran-Valero et al. 2012).

In the digestive system, both cholesterol and phytosterols esters are hydrolyzed by carboxyl ester lipase, also known as cholesterol esterase or BS-dependent lipase. This enzyme hydrolyses a range of substrates, primarily cleaving ester bonds between the cholesterol and the fatty acid moieties. The ester hydrolysis facilitates cholesterol absorption in the small intestine when incorporated into micelles. Cholesterol esterase forms proteolytically resistant dimers and can hydrolyze lysophospholipids (LysoPLs), fat-soluble vitamin esters, TAGs, MAGs, ceramides, as well as the sn-1 and sn-2 positions of PLs and galactolipids. This enzyme accounts for approximately 4% of the lipolytic activity in pancreatic secretions (Whitcomb and Lowe 2007; Sareen S. Gropper, Jack L. Smith 2022).

Sphingolipids contain a sphingoid base linked to fatty acid chain or PL, forming ceramides or sphingomyelin (SM), respectively. They are primarily found in animal-based foods, such as milk and meat, and support immune functions and cellular protection (Tietel et al. 2023). Sphingolipids, specifically sphingomyelin, are hydrolyzed by enzymes

primarily located in the intestinal lumen and mucosa. Sphingomyelinase converts sphingomyelin into ceramides, which are subsequently broken down by ceramidase into sphingosine and free fatty acids (Nilsson 1969). Sphingosine is readily absorbed and can be reincorporated into sphingolipids or converted into palmitic acid (Duan 2007). The presence of BSs, such as sodium taurodeoxycholate, has been shown to enhance the hydrolytic activity of both sphingomyelinase and ceramidase in the duodenal contents (Nilsson 1969).

Another class of lipid compounds commonly present in human digestion are previously described PLs. They are key components of animal and plant cell membranes The most prevalent PL is PC, followed to a lesser extent by phosphatidylethanolamine (PE) and phosphatidylinositol (PI) (Vance and Vance 2008). Phospholipids have both structural and functional roles; they participate in intercellular signaling and facilitate the transport and incorporation of nutrients (Tietel et al. 2023). In the intestinal lumen, PLs primarily originate from secreted bile (10-20g / day), and to a lesser extend from ingested food. Average daily consumption of PLs is approximately two to four times lower than the amount of PLs secreted with bile (Cohn et al. 2010). Phospholipids are digested by phospholipases. In the human digestive tract, phospholipase A2 (PLA_2) is secreted by the pancreas. Vesicles formed by PC facilitate hydrolysis by PLA_2 during digestion. This enzyme cleaves ester bonds at the sn-2 position, yielding LysoPLs and fatty acids (Smith 2019). The activity of PLA_2 depends on the BSs-to-PLs ratio (Nalbone 1980), and calcium ions are required to reduce the lag time of the enzymatic reaction (M. S. Fernández, Mejía, and Zavala 1991).

During lipid digestion, various molecules are released, including FAs, MAGs, LysoPLs, fat-soluble vitamins (A, D, E, and K), and cholesterol. These molecules then combine with BSs and PLs to create structures called mixed micelles (Figure 1.10). Mixed micelles play a crucial role in lipid absorption by increasing the solubility and mobility of digested fats within the watery environment of the intestinal lumen. They effectively ferry these lipids to the surface of the intestinal lining. This lining is composed of specialized absorptive cells called enterocytes. The close proximity provided by the micelles allows the lipids to be efficiently absorbed by the enterocytes. Enterocytes are the principal absorptive cells of the small intestine, responsible for the uptake of nutrients from digested food. These specialized cells possess a brush border of microvilli on their apical surface, significantly increasing the surface area for absorption and expressing various transporters and enzymes to facilitate this process. Following absorption by enterocytes, digestion products are re-esterified and combined with apolipoprotein B-48 in the endoplasmic reticulum to form chylomicrons. These chylomicrons are secreted into the lymphatic system, and subsequently enter the bloodstream where they distribute lipids to various tissues, such as muscle and adipose tissue (Dash et al. 2015; Kindel, Lee, and Tso 2010).

Phospholipids, besides their protective function in bile excretion, they play a role as structural and signaling lipids and have long been at the center of debate regarding their impact on the rate and extent of lipolysis. The first research on the impact of PLs on lipid hydrolysis was presented in 1967. Klein reported an inhibitory effect of lecithin on triglyceride hydrolysis by pancreatic lipase. A significant decrease in FFA release was observed at PL concentrations above 0.4 µmol/mL. The author suggested a possible mechanism of steric hindrance created by PLs, which limited substrate access to the enzyme's active center (Klein 1967).

One of the earliest studies on interfacial lipolysis, conducted by Lairon et al. (1978), investigated the influence of biliary PLs on lipase adsorption onto lipid droplets. Their findings revealed an interplay between lipase activity and PL saturation

at the interface, with the adsorption of both lipase and PLs being influenced by the PL composition (Denis Lairon et al. 1978). The authors suggested that a preformed complex of lipase, colipase, and bile lipids acts as a functional unit during the adsorption process (Lairon et al. 1978). While these observations provide valuable insights the experimental conditions described as physiological were, in fact, based on pig bile, while more recent research indicates that animal bile does not accurately reflect the physiological concentrations or profiles of human biliary lipids (Sangaraju et al. 2021).

Patton et al. (1981) reported on the inhibition of pancreatic lipase by mixed micelles of dihydroxy BSs and PC. The inhibition of TAG hydrolysis in the emulsion was attributed to the partial coating of the interface by PLs, which limited the access of lipase and colipase to the substrate. The authors explained that the components of the mixed micelles competed with lipase and colipase for adsorption at the TAG-water interface. However, they acknowledged that, although the results were consistent with previous literature (Denis Lairon et al. 1980; Borgström 1980; Bläckberg et al. 1979), they were difficult to compare due to diverse experimental conditions. Furthermore, the concentrations of enzymes and substrates did not reflect the physiological conditions of the human intestine (Patton and Carey 1981).

Erlanson-Albertsson et al. described the interactions between pancreatic lipase and colipase, which are regulated by the presence of lipids such as BSs and PLs, significantly limiting lipase's activity. Colipase overcomes this inhibition by forming a 1:1 molar complex with lipase. This complex facilitates lipase to attach to the lipid interface (Erlanson-Albertsson 1983). Larsson et al. (1986) confirmed the inhibition of lipase activity by mixed micelles of BSs and PLs. They also observed that the lag phase of triglyceride hydrolysis was longer when PC was present as a component of the substrate emulsion. However, the addition of free fatty acids (oleic acid) shortened this lag phase. The authors demonstrated that free fatty acids (lauric, oleic, and linoleic acids) could reactivate lipase, suggesting a mechanism involving the formation of a high-affinity complex between these fatty acids, lipase, and colipase, which enables effective binding of the enzyme to the interface (Larsson and Erlanson-Albertsson 1986).

Macierzanka et al. (2019) reviewed that BS-PL mixed micelles solubilize free fatty acids (lipolysis products) by removing them from the interface, thus enabling the continuation of lipolysis by shifting the reaction equilibrium (Macierzanka et al. 2019).

In (Piéroni et al. 1990), Pieroni conducted a study on lipid monolayers to understand how lipases interact with lipid surfaces, particularly in the presence of PLs and other amphiphilic compounds (including β-Lg). He demonstrated that the presence of PC at the interface leads to a reduction in lipid hydrolysis efficiency, and similarly, certain proteins, such as β-Lg, can inhibit lipase activity. In the first case, the mechanism involves a surface barrier formed by PC, which hinders enzyme adsorption to the interface. In contrast, inhibition caused by proteins like β-Lg is likely due to a long-range effect influencing lipase adsorption to, or desorption from, the lipid monolayer, rather than solely their ability to penetrate the lipid surface and their excess relative to lipase (Piéroni et al. 1990).

The combined effect of PLs and BSs was described by Lykidis in 1997 The authors described the synergistic role of PLs and BSs in lipase activation. They denied the inhibitory effect on pancreatic lipase by PLs, showing that the outcome of lipase activity depends on the ratio between these two biosurfactants (Lykidis, Avranas, and Arzoglou 1997). However, the studied concentrations of BSs and PLs were irrelevant to the actual bile composition and physiological concentrations of these biosurfactants. The assay of enzyme activity and the proposed mathematical model for evaluating lipase activity

based on BS/PL ratios did not reflect the complex digestion process occurring in the intestine in the presence of bile. Nevertheless, these studies were an important observation and provided a basis to design the experiments focused on the interplay between BSs and PLs during digestion, as presented in this dissertation.

In the review, Brockman (2000) discussed the impact of PLs on lipolysis, including the concept of "percoregulation of lipolysis" (Figure 1.11a). The review explains that at low substrate concentrations, the prevalence of PLs at the interface hinders lipase binding and activity. Efficient lipolysis occurs only when the substrate concentration surpasses a threshold, diminishing the relative dominance of PLs and promoting lipase binding at the interface. Brockman further clarifies that colipase counteracts the inhibitory effects of PLs by preferential packing with lipase substrates over PLs at the interface, and by anchoring and stabilizing the lipase at the interface. This creates a more conducive environment for lipase function (Figure 1.11b) (Brockman 2000).

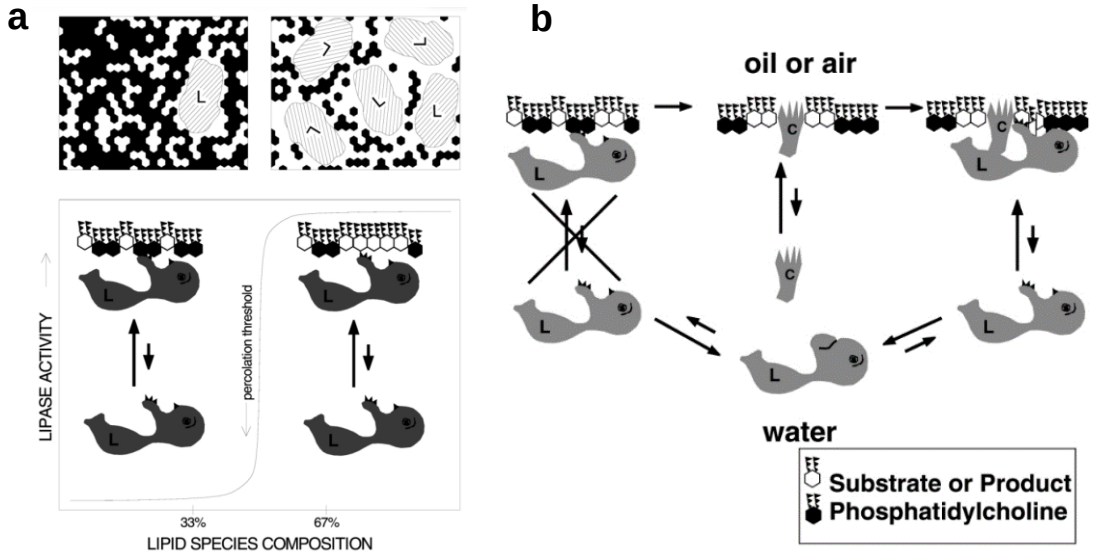

Figure 1.11. Possible inhibition of lipase activity by PLs at the interface caused by the densely packed PL film, which limits enzyme access to the substrate; a) The percolation threshold of lipolysis; b) The role of colipase in binding substrates and facilitating enzyme access to the substrate. Open hexagons represent the substrate, filled hexagons represent PC, L represents lipase, and C represents colipase (Brockman 2000).

Wickham et al. researched the effect of BSs and PLs on lipase activity. Their work explained the creation of a mixed PL/BS interface after the addition of BSs to a well-packed interface of PL-stabilized emulsion. It was discovered that the length of the lag phase of triglyceride lipolysis was inversely proportional to the level of BS incorporation. The authors hypothesized that the breakdown of the PL interface by the BSs promoted the development of substrate clusters, which made it easier for the enzyme to bind to the interface (Wickham et al. 1998). In their following experimental work (Wickham, Wilde, and Fillery-Travis 2002), the authors studied the physicochemical properties of BSs/PLs interfaces. Since there was no distinguishable difference found in the minimum interfacial tension between PC/NaTC and PC/NaTDC systems, interfacial tension was not recognized as a factor in lag time duration. The length of the lag time did not correlate with the physicochemical characteristics of the interface.

The authors of the more recent research (Tsuzuki et al. 2004) investigated the inhibitory effect of LysoPC on pancreatic lipase activity during lipid digestion. While previous studies had focused on PC and its interactions with lipids, Tsuzuki et al. (2004) went a step further by examining the role of LysoPC, a product of PC hydrolysis by PLA_2. LysoPC significantly

inhibited the hydrolysis of triolein and tricaprin, with a more pronounced effect on triolein. This inhibition was reversed by adding PC or BSs, suggesting LysoPC alters the lipid emulsion interface, hindering lipase access to the TAGs (Tsuzuki et al. 2004).

Venuti et al. (2017) observed that PL may inhibit the activity of BS simulated lipase (BSSL) in the gastrointestinal tract. BSSL is an enzyme secreted in breast milk that facilitates fat digestion in infants. Inhibition occurred as enzyme access to the substrate was obstructed by PLs. However, the addition of PLA_2 was effective in reversing this inhibition, resulting in the release of LysoPLs. This stimulated BSSL activity to some extent but LysoPLs also act as an inhibitor at higher concentrations. The study suggested that using PLA_2 in combination with BSSL could be an effective strategy for enzyme replacement therapy in patients with pancreatic exocrine insufficiency (Venuti et al. 2017).

A recent study by Mekkaoui et al. (2021) examined the effect of BSs on lipid digestion in emulsions stabilized by PLs and their impact on interfacial dilatational rheology. The study explains how BSs disrupt the lecithin layer, increasing viscoelasticity allowing lipase to access the lipid substrate. However, the research did not provide enough comprehensive data to fully explain the interplay between BSs and biliary PLs during lipolysis under physiological digestion conditions. Lecithin was introduced into the system as an exogenous food emulsifier in a medium-chain TAG/lecithin emulsion.

A recent study highlighted the importance of PLs in stabilizing infant milk emulsions and their impact on protein and lipid digestion. In the studied case, it was shown that an emulsion stabilized with sphingomyelin (SM) was more stable than one stabilized with PC. An increase in the levels of released FFAs during *in vitro* digestion of emulsions with PLs was observed. SM enhanced the surface area available for enzymes by creating emulsion droplets with smaller diameters and reduced emulsion coagulation and aggregation. However, despite more efficient lipolysis, the study noted delayed digestion of β-Lg in the SM-stabilized emulsion. Although the study did not specifically examine the effects of biliary PLs, it demonstrated the significant role of PLs in the efficiency of lipid and protein digestion (Ahn and Imm 2023).

All the findings discussed above indicate that a combination of BSs and PLs play a crucial role in the regulation of lipid digestion. However, none of these studies provides significant insights into the extent to which BSs and PLs, as components of bile at physiological concentrations, influence the progress of lipid digestion. Moreover, the interplay of biliary surfactants at the oil-water interface and its impact on the efficiency of emulsion digestion remain unclear. Therefore, further research is required to investigate the precise role of BSs and PLs under physiologically relevant conditions.

1.2 Digestion models

To understand digestive mechanisms, digestion models are developed to reflect the human gastrointestinal system (or specific compartments). These models enable the study of interactions between food and the digestive system, which is crucial for designing healthy diets and safe food products (Gouseti et al. 2019). Determining the bioavailability of nutrients aids in creating nutritionally valuable food products (Marze 2017). These models are also essential in research on digestion-related diseases and in the development of new drugs and dietary therapies. The pharmaceutical industry established the first digestion models to evaluate drug solubility and bioavailability in 1907. Since then, various types of *in vitro* digestion models have been invented and research on food digestion intensified, starting from the 1990s (Gouseti et al. 2019).

Digestion models cover various approaches, including *in vivo* (studies on living organisms), *in vitro* (laboratory simulations of digestive processes) (Figure 1.12), and *in silico* (computer modeling). *In vivo* models study digestion in living organisms. They provide the most accurate representation of physiological processes but are costly, time-consuming, and raise ethical concerns. *In silico* models use computer simulations to analyze large datasets and test hypotheses quickly. However, they may lack the accuracy of real-world experiments. *In vitro* models bridge the gap between *in vivo* and *in silico* approaches. They simulate digestion in controlled laboratory conditions. *In vitro* studies are faster and less expensive than *in vivo* studies. However, they may not fully capture all the physiological aspects of digestion, such as peristalsis, hormonal feedback, and microbial interactions. Despite these limitations, *in vitro* models are valuable tools for studying digestive mechanisms and the effects of different substances. They offer a balance between accuracy and practicality (Galanakis 2021; Tan, Zhou, and McClements 2022). As Steven Le Feunteun et al. (2021) point out, combining *in vitro* and *in silico* approaches can improve the predictive power of these models, leading to a better understanding of digestion (Feunteun et al. 2021).

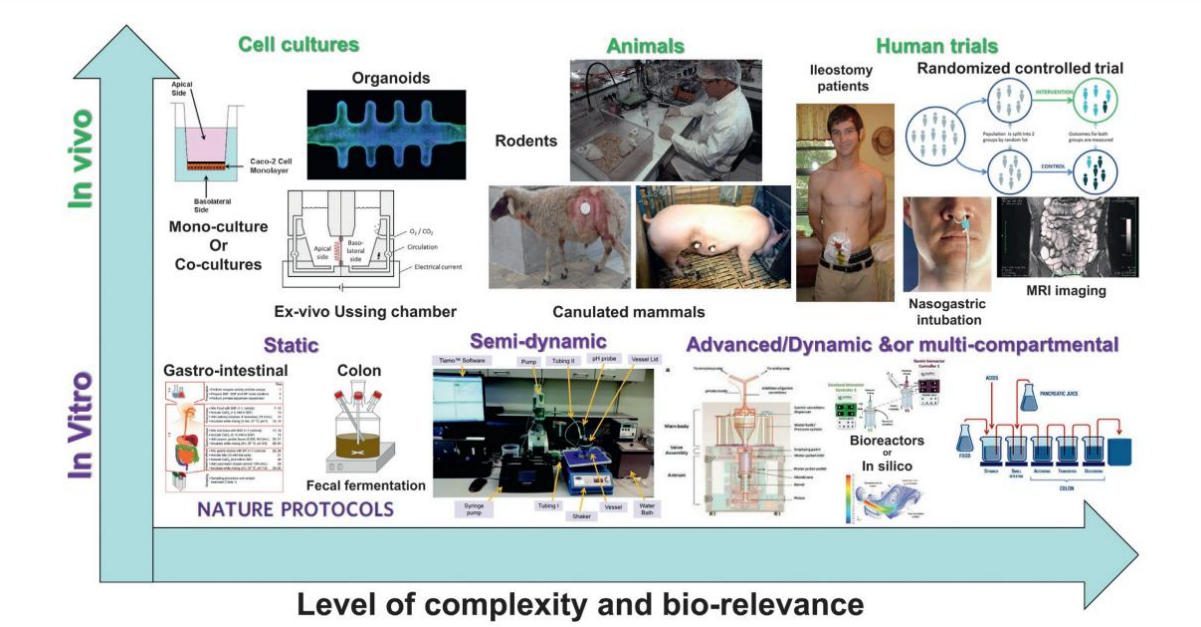

Figure 1.12 Review of in vivo and in vitro digestion models according to the level of complexity and reflection of physiological conditions (Lesmes 2023).

The primary purpose of *in vitro* digestion models is to enable the study of digestion processes outside a living organism. They are used to test various dietary components, food supplements, drugs, and other substances for digestibility and bioaccessibility. These models aim to replicate physiological conditions within the human body, such as pH, temperature, and the presence/activity of digestive enzymes (Figure 1.13). These parameters are adjusted depending on the specific segment of the digestive system being simulated (Bohn et al. 2018).

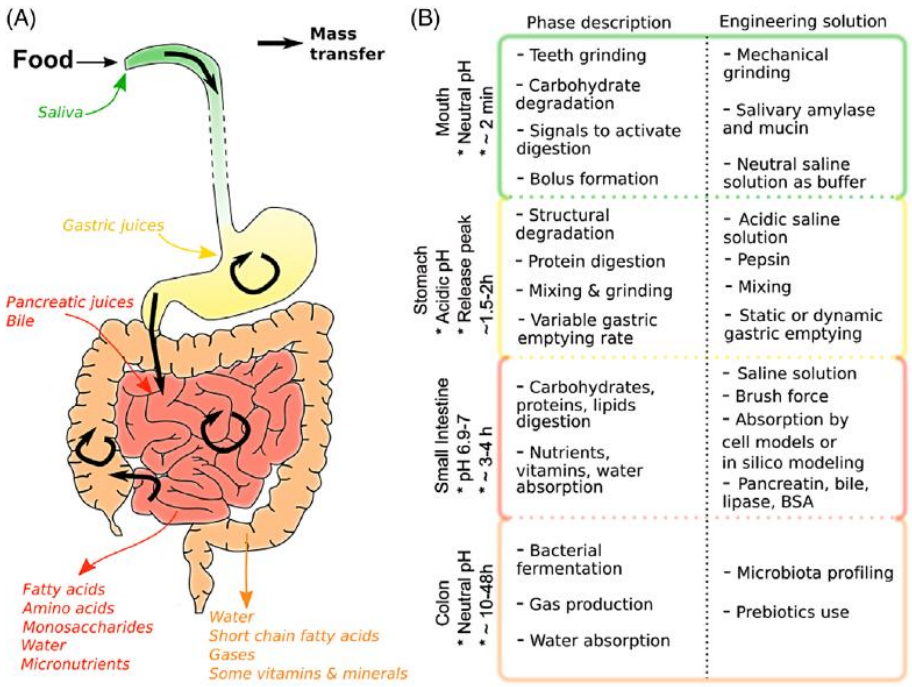

Figure 1.13 The main four compartments of alimentary system represented in different colors (A), and their main role in food digestion along with the corresponding engineering solution (B). Thin inward arrows indicate the addition of fluids by supporting organs, while outward arrows represent absorption by the small and large intestine. Thick black arrows depict mass transfer along the gastrointestinal tract and within digestive organs. BSA, Bovine serum albumin. Picture and description adopted from (K. Kristensen, David-rogeat, and Alshammari 2019).

In vitro digestion models provide an alternative to *in vivo* animal and human testing, which is important from an ethical perspective and contributes to the reduction of animal use in laboratory research (Bohn et al. 2018). There are several types of *in vitro* digestion models, generally divided into:

Static Models:

The simplest model is a static *in vitro* digestion model. They are cost-effective, quick, and easy to standardize. *In vitro* static models are used to simulate digestion processes under controlled laboratory conditions. They include oral, gastric, and intestinal digestion phases, using set parameters such as temperature, pH, and enzyme concentrations. However, they do not reflect the dynamic nature of digestive processes, such as peristalsis or fluctuating pH. The schematic process is presented in Figure 1.14. In the oral phase, α-amylase is typically used to simulate carbohydrate breakdown, while the physical process of chewing is omitted. The gastric phase involves the use of pepsin at an acidic pH and at a temperature of 37°C. Next, the intestinal phase includes the addition of pancreatic enzymes at pH 7, as well as the addition of BSs (Verhoeckx et al. 2015). These models are mainly used for quick and simple tests regarding the digestibility of nutrients or the potential bioaccessibility of bioactive substances (Xavier and Mariutti 2021).

An example of numerous static digestion models is the consensus protocol for *in vitro* gastrointestinal digestion developed by the INFOGEST scientific network. The goal of this model was to standardize *in vitro* digestive conditions and establish representative

biochemical and physicochemical conditions for food digestion in the human upper digestive tract (Brodkorb et al. 2019).

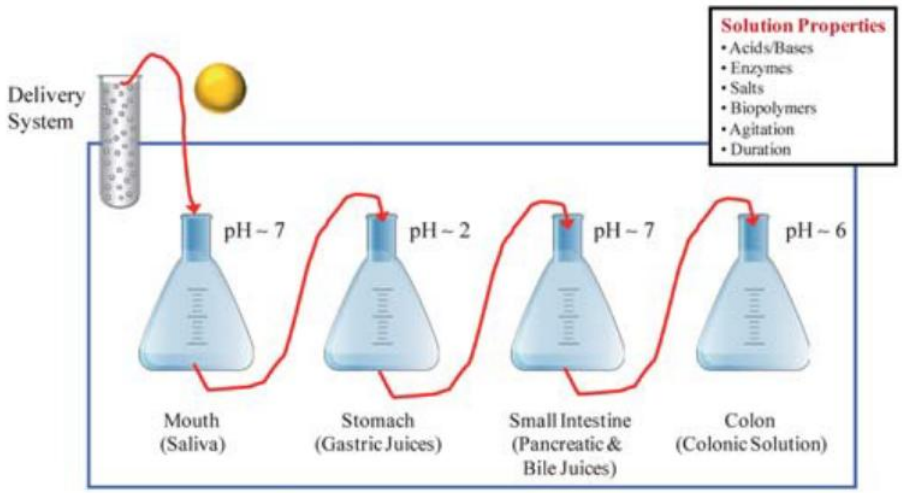

Figure 1.14 The simulation of the gastrointestinal digestion by static in-vitro digestion model (McClements and Li 2010).

Semi-dynamic Models:

Semi-dynamic *in vitro* digestion models offer a more nuanced representation of time by allowing digestive conditions, such as pH and enzyme activity, to evolve within each phase, unlike static models where conditions remain constant for the duration of each phase. These models simulate the gradual changes in the digestive environment, including the addition of enzymes, adjustment of pH, and gastric emptying, providing a better representation of the *in vivo* process. For example, during the gastric phase, semi-dynamic models can mimic the decreasing pH and the gradual emptying of gastric contents into the small intestine, as highlighted in (Xavier and Mariutti 2021). However, while semi-dynamic models are an improvement over static models, they still lack the full complexity of *in vivo* digestion, failing to fully capture processes like peristalsis, nutrient absorption, hormonal feedback (Guerra et al. 2012).

Dynamic Models:

Dynamic *in vitro* digestion models are much more complex. They allow for examination of various aspects of digestion processes, e.g., the impact of fluid dynamics on digestibility. In addition, they can recreate intricate digestive processes (Gouseti et al. 2019). Physical and chemical parameters in the various compartments are changed continuously throughout the digestion time, including pH, ionic strength, digestive enzyme concentrations, digestion product removal, peristaltic motion, and others (Dupont and Mackie 2015). The TIM model, which has been developed by TNO (the Netherlands) in the 1990s and is offered commercially, is one of the most well-known (Dupont et al. 2019).

Each in vitro model has its previously mentioned advantages and disadvantages. Despite the high level of reflection of *in vivo* studies in intestinal digestion using the INFOGEST *in vitro* static digestion protocol (Sanchón et al. 2018), many aspects remain unknown. One of the limitations of all *in vitro* models is a simulation of human bile. Some models use only selected BSs, and others use animal-derived extracts such as porcine or bovine bile extract (McClements and Li 2010). Human bile is a complex mixture. Apart from a range

of BS species, it contains other surface active ingredients such as PLs as well as a number of other components that may influence digestion (Fuchs and Dressman 2014). *In vitro* digestion models still require optimization and standardization to allow for comparison between laboratories and to more accurately reflect human physiology. This is important due to the growing need and interest in orally-administrated bioactive components and in functional foods (Lucas-González et al. 2018).

1.2.1 Methods for assessing protein digestion following *in vitro* digestion

Food analysis has been compared to looking at the sky through a telescope by Pasquale Ferranti, author of the article 'The future of analytical chemistry in foodomics'. Where once only a 'galaxy' as a whole could be seen, modern analytical techniques now allow for the examination of the 'microstructures' of food components. The article highlights how modern omics technologies have enabled the detailed study of food composition, which is crucial for the authentication and safety of food products (Ferranti 2018). Integrating data from various 'omics' fields (metabolomics, lipidomics, proteomics, peptidomics, and transcriptomics) can provide a more comprehensive understanding of the impact of diet on human health and facilitate the design of individualized nutritional strategies (Capozzi and Bordoni 2013). Foodomics employs 'omics' technologies to analyze the effects of food on health, focusing on understanding how nutrients are broken down and transformed within the body. Digestion in the gastrointestinal tract yields bioactive compounds that may have either positive or negative effects on health (Pimentel et al. 2018).

More specifically, the field that focuses on digestion is known as digestomics. In the context of food protein digestion, this term typically involves the use of proteomics and/or peptidomics (Figure 1.15) to analyze the digestive mixture - known as the digestome - and often to assess its further effects on the human body (Picariello, Mamone, et al. 2013; Picariello et al. 2020; Martini, Solieri, and Tagliazucchi 2021).

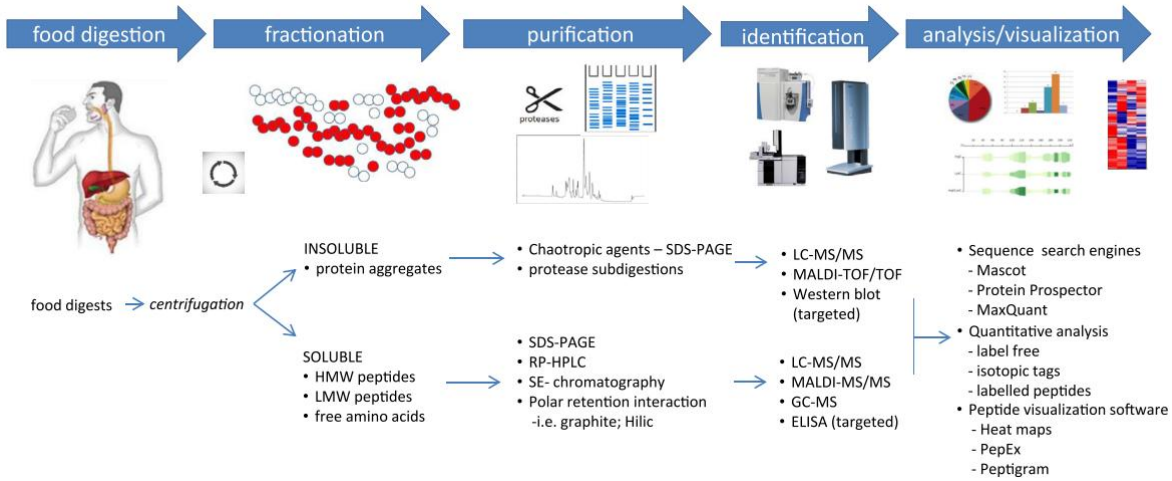

Figure 1.15 A standard workflow for the peptidomics analysis process, applicable in digestomics studies. Various choices are available at each stage, depending on the characteristics of the food matrix and the specific experimental objectives (Picariello et al. 2020).

All the fields mentioned above rely on advanced analytical techniques, particularly mass spectrometry. In the study of food digestion, 'proteomics' and 'peptidomics' are the terms most commonly used to refer to protein and peptide analysis. Two primary strategies (Figure 1.16) for protein analysis are the bottom-up and top-down approaches (Ferranti 2018).

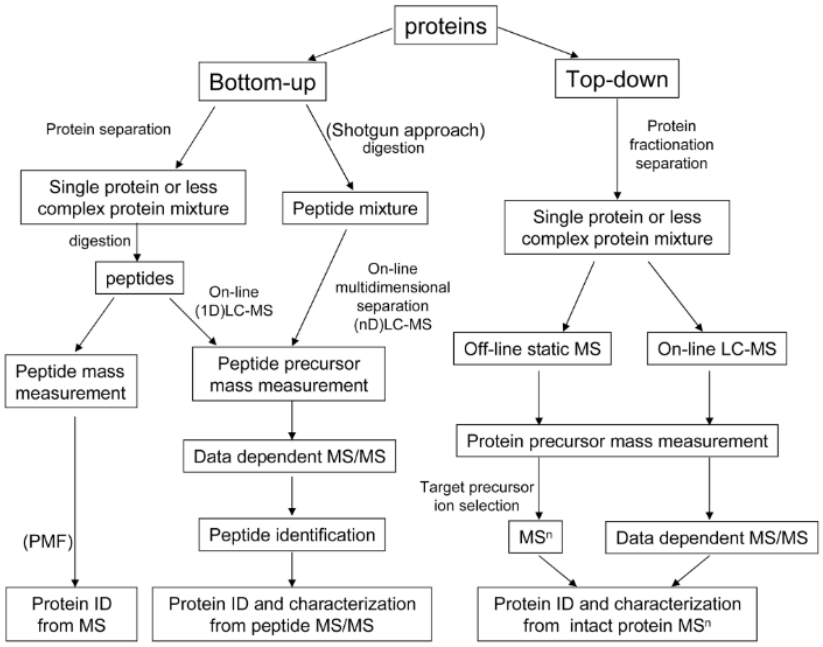

Figure 1.16 Strategies for protein identification and characterization using mass spectrometry (MS). Proteins isolated from biological samples can be analyzed through either bottom-up or top-down techniques. In the bottom-up method, proteins within complex mixtures are separated before undergoing enzymatic or chemical digestion, followed by peptide mass fingerprinting or additional peptide separation with tandem mass spectrometry (Xuemei Han, Aaron Aslanian 2008).

In the bottom-up approach (also known as shotgun proteomics), proteins are digested into peptides, which are then analyzed by MS. Alternatively, the top-down approach allows for the analysis of intact proteins without digestion, facilitating a more precise identification of post-translational modifications (PTMs) and protein isoform variants. Ionization techniques, such as MALDI and ESI, are most commonly applied in this area. MALDI, uses a laser to ionize samples embedded in a matrix, making it a rapid and efficient method, especially suitable for biological sample analysis and tissue imaging. ESI, on the other hand, creates ions by spraying the solution at atmospheric pressure, producing multiply charged ions that enable the analysis of high-mass peptides and proteins (Xuemei Han, Aaron Aslanian 2008; Yates 2004). ESI is a soft ionization technique because it provides just enough energy to convert a molecule into an ion, but not enough to break its chemical bonds. During ESI ionization, molecules are introduced into the gas phase as charged droplets. These droplets are then evaporated until only ions remain. As a result, molecules, e.g. peptides, can transition into the gas phase as ions without breaking their structure (Banerjee and Mazumdar 2012). The schematic process of ESI is illustrated in the Figure 1.17.

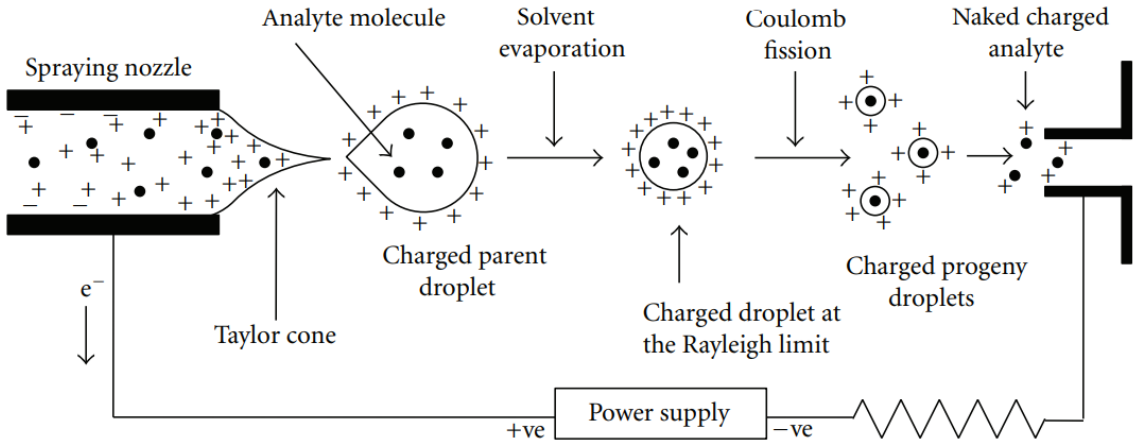

Figure 1.17 The process of the electrospray ionization (ESI) (Banerjee and Mazumdar 2012).

Next, the ions generated during ionization are sent to mass analyzers. Mass analyzers are a key component of mass spectrometry, responsible for separating ions based on their mass-to-charge ratio (m/z). The most common analyzers are Time-of-Flight (TOF), Quadrupole, and Ion Trap mass analyzers. However, different types of mass analyzers are often used in combination, which increases their versatility. One example of a hybrid tandem mass analyzer is Q-TOF, where the quadrupole selects precursor ions, and the TOF analyzes product ions. Their high resolution allows for the identification of proteins and metabolites (Clarke 2017). The example of a Q-TOF is presented in the Figure 1.18.

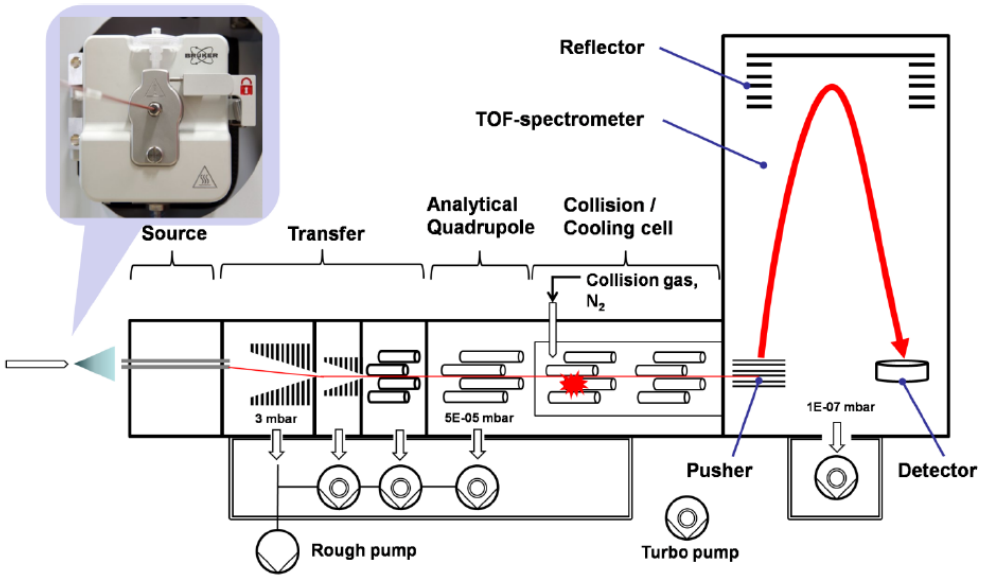

Figure 1.18 Schematic diagram of a Q-TOF mass spectrometer. The red line shows the path of ions from the source, through the quadrupole, where ion selection and collision with gas occur (red spark), to the final TOF analyzer, where fragmented ions are analyzed (Kulyyassov 2018)

In Q-TOF, a commonly used fragmentation technique is Collision-Induced Dissociation (CID). In this method, ions selected by the first analyzer (quadrupole) are introduced into a collision cell, where they undergo fragmentation. In this technique, the ions collide with an inert gas (e.g., nitrogen or argon). Fragmentation in the CID process depends on the bond energy in the molecular structure of the precursor ion, as well as the type of gas and collision energy. The fragmentation products are analyzed by the second mass analyzer, allowing for the identification of structural information about the precursor ion (Clarke 2017). During CID, fragmentation mainly occurs at the weakest bonds (Sobott et al. 2009).

There is also a complementary fragmentation method to CID called Electron-Transfer Dissociation (ETD). ETD uses the transfer of electrons from anions to positively charged peptides, leading to fragmentation without prior internal redistribution of energy. The fragmentation happens without an even energy distribution within the ion. ETD is more effective for highly charged peptides and is a softer method suitable for analyzing post-translational modifications (PTMs). On the other hand, CID is more effective for fragmenting ions with a low mass-to-charge ratio and is a more aggressive method, which can lead to the loss of PTM information (Sobott et al. 2009).

Fragmentation can occur at different sites within a peptide, resulting in the formation of various types of ions (Figure 1.19). In ETD, c- and z-type ions are formed. C-type ions contain the N-terminal end of the peptide, and the bond breaks without prior energy distribution throughout the peptide, which helps preserve side chain modifications. Z-type ions contain the C-terminal end of the peptide and are formed as a result of free radical formation. In contrast, during CID fragmentation, b- and y-type ions are formed. B- and y-type ions are peptide fragments formed by breaking the bond between nitrogen and carbon (N-C) atoms in the peptide backbone. B ions contain the N-terminal end of the peptide, meaning they start from the initial amino acid and extend to the point of fragmentation. Y ions contain the C-terminal end of the peptide, starting from the final amino acid and extending back to the fragmentation point (Sobott et al. 2009). A-type ions are frequently formed as a result of the loss of a CO group from b ions. The loss of NH_3 and H_2O groups from b or y ions is also a common phenomenon (Macias, Santos, and Brodbelt 2020).

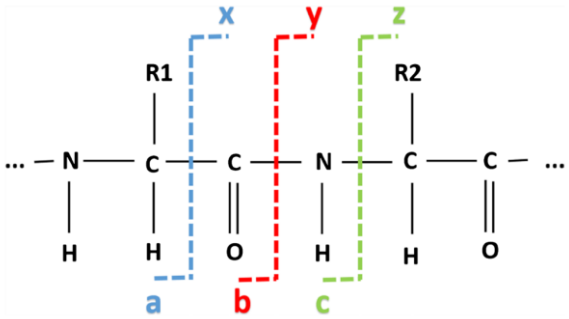

Figure 1.19 Ions created during CID and ETD fragmentation. a, b, c – N-terminal ions; x, y, z – C-terminal ions (X. Li 2023).

Two popular data acquisition modes in mass spectrometry used in digestion proteomics are Data-Independent Acquisition (DIA) and Data-Dependent Acquisition (DDA) (Picariello et al. 2020). The difference in the data acquisition process between DIA and DDA is visualized in Figure 1.20. In DIA mode, the instrument systematically scans all ions within a designated mass range and fragments them regardless of signal intensity. DIA enables a comprehensive analysis of the entire peptide content, making it useful for more thorough

digestome analysis, especially in samples with high peptide diversity and low concentrations of certain components (Picariello et al. 2020; Fernández-Costa et al. 2020). However, the drawbacks are the complex chimeric MS/MS spectra generated during DIA analysis. Chimeric MS/MS spectra contain ions originating from more than one peptide due to the simultaneous fragmentation of all precursors. This increases the complexity of the spectra and requires advanced bioinformatics algorithms that enable deconvolution (separation of ions originating from different peptides). This may lead to incorrect peptide identification if fragments are assigned to the wrong peptides (Wolf-Yadlin, Hu, and Noble 2016).

In DDA mode, the instrument selects the most intense ions at a given moment for fragmentation and identification. This approach allows for detailed analysis of the most abundant peptides but has limitations in fully identifying less intense signals. DDA is commonly used in digestion proteomics, where identifying the most frequent digestion products of food proteins is of interest (Picariello et al. 2020; Fernández-Costa et al. 2020).

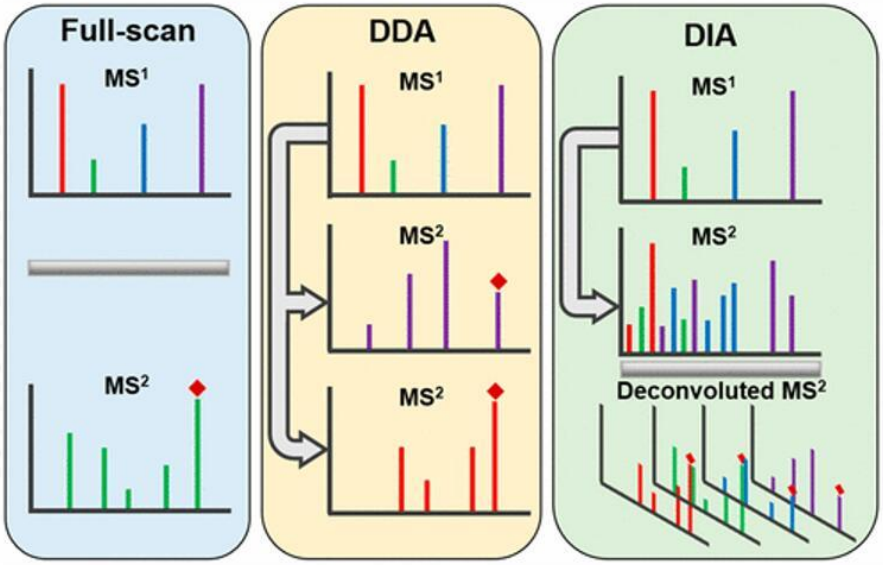

Figure 1.20 The process of data acquisition in DDA and DIA mode ("Creative Proteomics Blog" 2024).

Regardless of the chosen acquisition method, library-based spectral searching provides better reproducibility and reduces result variability. The findings suggest that developing software more suited to processing library data for DDA may increase the stability of this method and improve its reproducibility in proteomics (Fernández-Costa et al. 2020).

The acquired data require appropriate bioinformatic processing, where mass spectra are analyzed, followed by peptide identification, including de novo sequencing. Peptide identification is based on the analysis of spectra obtained from fragmentation. These spectra contain the previously mentioned b and y ions. Data on b and y ions generated from protein sequence databases are used to match theoretical peptide spectra to actual experimental spectra. This allows for the identification of proteins present in the sample based on their peptide fragments (Shuken 2023).

Once peptide sequences are identified, they must be validated through database searches and assessment of the false discovery rate (FDR) (Ferranti 2024). FDR is a measure

of the proportion of false positives among all results that have been identified as positive. Several algorithms exist for controlling FDR, including methods that calculate adjusted *p*-values, known as q-values. A q-value directly corresponds to the FDR, indicating the expected proportion of false positives if a protein with that q-value is considered significantly regulated (Marcus, Eisenacher, and Sitek 2021).

For quantitative analysis, Label-Free Quantification (LFQ) is commonly employed in proteomics to determine relative protein quantities based on mass signal intensity data, eliminating the need for isotopic or chemical labeling. There are two main LFQ strategies: spectral counting, which involves counting the number of fragment spectra for peptides, and peptide ion intensity measurement, which involves measuring the area under the chromatographic curve. Processing LFQ data requires feature detection, retention time alignment, MS intensity normalization, and noise reduction. Numerous software tools are available to facilitate bioinformatic data processing, including open-source tools such as MaxQuant and Progenesis LC-MS (Megger et al. 2013), as well as more sophisticated software like PEAKS (Bioinformatics Solution) (Ferranti 2024).

1.2.2 Analytical methods for assessing lipid hydrolysis during *in vitro* digestion

Similar to proteins, omics sciences can also be applied to studying lipids. Lipidomics provides a comprehensive approach to lipid profiling, enabling the quantification and characterization of lipids and their diversity in biological samples. It allows for the detailed analysis of lipid chemical structure, including hydrocarbon chain length, degree of saturation, bond type, and the presence of functional groups. Lipidomics covers a range of lipid classes, including PLs, triglycerides, ceramides, sterols, and fatty acids (Chen et al. 2017; Tietel et al. 2023).

MS plays a key role in lipidomics, providing a detailed view of lipid structure and enabling precise identification and quantification. Key techniques include hybrid methods such as those coupled with liquid chromatography (LC-MS) and gas chromatography (GC-MS), which separate and analyze individual lipid classes. LC-MS is used for non-volatile or thermally unstable lipids, such as PLs, TAGs, and GC-MS is used for volatile, low-molecular-weight lipids such as FFAs (Sun et al. 2020) (Z. Pan et al. 2024; Sun et al. 2020; Da et al. 2024). MS can be used for the evaluation of *in vitro* static digestion (Y. Pan et al. 2024) or dynamic *in vitro* models (Casula et al. 2024). MS analysis allowed investigation of glyceride composition in samples at different stages of digestion. This helped assess the impact of the milk fat globule membrane (MFGM) on *in vitro* static lipid digestion (Y. Pan et al. 2024). The studies on *in vitro* dynamic digestion of sheep and goat milk-based infant formulae employed UHPLC-QTOF/MS to monitor lipid hydrolysis profiles and changes in complex composition of lipids, such as TAGs, DAGs, MAGs.

In contrast, the pH-stat method offers an overall assessment of lipid digestion progress. During fat digestion, FFAs are released in the process of lipolysis, which lower the pH of the system. The pH-stat technique allows for real-time monitoring of FFA liberation by maintaining a constant pH level through the titration of the released FFAs with a neutralizing agent, such as NaOH, and thus allows to assess the digestion kinetics. This method is widely used due to its simplicity and cost-effectiveness, enabling real-time monitoring of the digestion progress and extent. It also allows for the control

of environmental pH, which is crucial for maintaining the activity of digestive enzymes, (Wang et al. 2022; Mat et al. 2016). The pH-stat method is applied in various *in vitro* digestion models, ranging from static (Figure 1.21) to dynamic systems. Models such as the TNO Gastrointestinal Model (TIM) and the Dynamic Gastric Model (DGM) frequently utilize the pH-stat method at different stages of digestion (Gouseti et al. 2019).

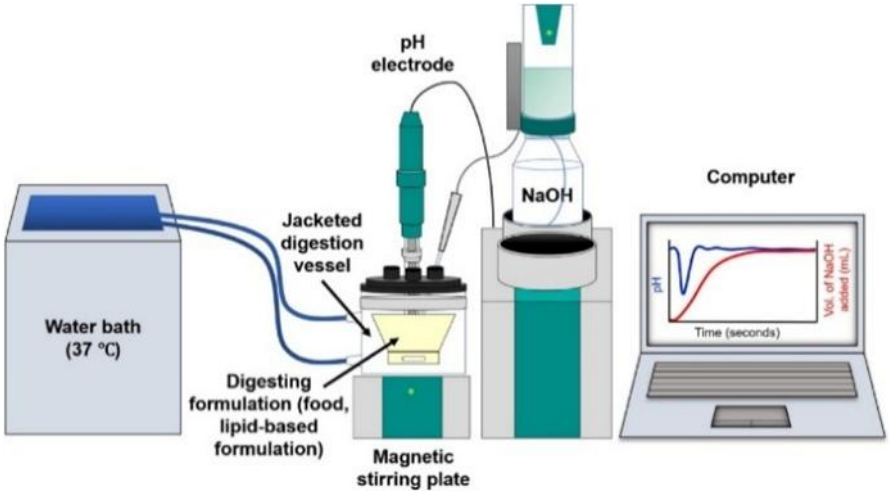

Figure 1.21 The illustration of the pH-stat apparatus used in in vitro static digestion (Pham, Clulow, and Boyd 2021).

To explain and interpret the results of quantitative changes in lipolysis, complementary techniques are used. These techniques help clarify the fundamental mechanisms occurring during digestion. For example, to evaluate the lipolysis reaction at the interfacial level, various methods can be applied, including atomic force microscopy (AFM). AFM allows for visualizing the nanoscale structure of interfaces in food systems, such as emulsion droplets, and can track changes in their surface structure during digestion by enzymes. This allows researchers to gain insights into the mechanisms of lipolysis by observing structural changes at the interface (Morris, Woodward, and Gunning 2011).

Furthermore, tensiometric techniques allow for monitoring changes in interfacial tension (IFT) between a droplet and its surrounding environment during *in vitro* digestion. This provides insights into the physical processes occurring at the surface of a single lipid droplet as it is exposed to sequential digestive phases representing different sections of the gastrointestinal tract. Two common tensiometric methods are the rising drop, where an oil droplet is immersed in an aqueous phase, and the pendant drop, where either an aqueous droplet is immersed in oil or an oil droplet is immersed in an aqueous phase. The choice between these methods depends on the specific system being studied and the research question being addressed. Pendant drop and rising drop tensiometry differ in control and interface types. Pendant drop offers versatility with both oil-in-water and water-in-oil interfaces and precise subphase exchange for simulating digestion. Rising drop is simpler, suited for oil-in-water interfaces and lipid digestion. The choice of method depends on the research question, interface type, rheology requirements, and available resources. In the context of lipid digestion, results on IFT help interpret the efficiency of surfactants at the molecular level. For example, a decrease in IFT during lipolysis may indicate high surfactant activity at the interface, explaining the progress of lipolysis in a physical-chemical context (Maldonado-Valderrama 2019).

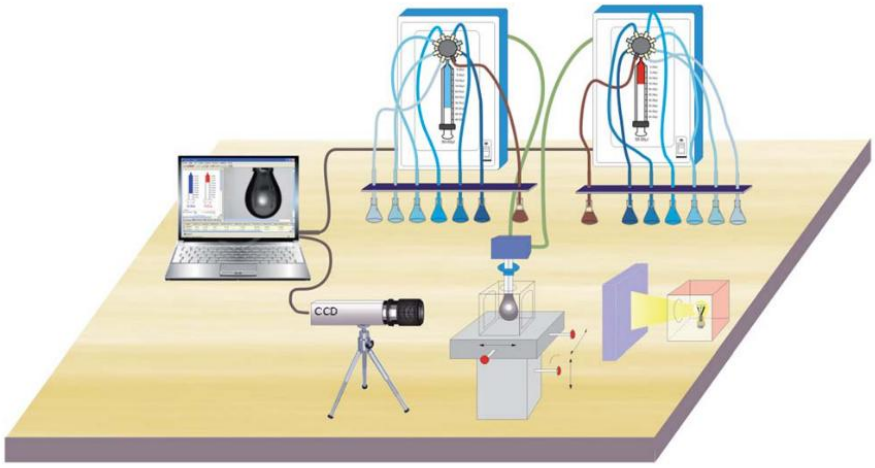

Figure 1.22 The instrument for pendant drop measurements (J. Maldonado-Valderrama et al. 2013).

The pendant drop technique was uniquely modified at the University of Granada, where the OCTOPUS device was created (Figure 1.22). It was designed to expand research capabilities by introducing a multi-exchange subphase system within a single droplet. was developed to allow for automatic subphase exchange without disturbing the droplet surface. This innovation enables real-time monitoring of IFT changes at each stage of digestion without interrupting the experiment, thus reflecting the successive phases of the digestive system: oral, gastric, and intestinal. It enables more precise studies of processes occurring at liquid-liquid interfaces (Maldonado-Valderrama et al. 2015).

2 Objectives and scope

The role of biliary phospholipids is neither well-defined nor fully understood in the context of intestinal lipolysis and proteolysis. As a result, they are often omitted from *in vitro* digestion models. However, I hypothesize that biliary phospholipids play a crucial role in both intestinal lipolysis and proteolysis, particularly through their interaction with bile salts.

This dissertation consists of two main parts: the lipolytic section, focusing on lipid digestion, and the proteolytic section, focusing on protein digestion in the presence of biliary phospholipids. The initial goal was to determine the physiological concentration of biliary phospholipids and their ratio to bile salts under the conditions of intestinal digestion in healthy individuals.

The objective of the first part of my research was to investigate the combined effect of physiologically relevant phospholipids and bile salts on small intestinal lipolysis. Specifically, the research aimed at examining the physicochemical aspects of the interplay between these biosurfactants at the oil/water interface during the simulated intestinal lipolysis process, under various ratios of the biosurfactants and in relation to their physiological concentrations. Additionally, my study aimed to investigate how phenomena observed at the interface can influence the extent of *in vitro* lipolysis in model emulsions.

The second part of my research aimed at investigating the combined effect of physiologically relevant phospholipids and bile salts, as well as their varying ratios, on the degree of β-lactoglobulin digestion, with a particular focus on differences in the peptide profiles generated during *in vitro* proteolysis. This study has also focused on evaluating the extent to which such differences could be physiologically important.

The knowledge gained from my research is expected to improve existing *in vitro* digestion models, enhancing their ability to better reflect the physiological conditions of the human small intestinal digestion.

3 Methods

3.1 Bile composition retrospective analysis.

Scientific articles regarding the composition of human hepatic bile, gallbladder bile and the concentrations of biliary surfactants in the duodenum were searched utilizing the Google Scholar and PubMed databases. The data for the concentration of biliary surfactants were transferred to an Excel database for calculations. Data were filtered by the following attributes: healthy adult individuals, fed or fasted state, and sample collection point (gallbladder, hepatic duct, or duodenal lumen). BS and PL concentrations (mM, mmol/L) were presented using weighted arithmetic means, taking into consideration the number of subjects tested in relevant, individual studies.

3.2 Lipolysis: digestion and analysis

3.2.1 Preparation of phospholipid dispersion and bile salt solution

The stock solutions of BSs and PLs were prepared using Simulated Intestinal Fluid (SIF, pH 7.0), following the INFOGEST protocol (Brodkorb et al., 2019). The BS stock solution consisted of 100 mM of equimolar quantities of sodium glycodeoxycholate (NaGDC, 97% purity; Sigma-Aldrich, G9910) and sodium taurocholate (NaTC, 95% purity; Sigma-Aldrich, T4009). The selection of the two BSs came from their frequent use in intestinal transport studies and in *in vitro* digestion models, imitating the BSs of human bile (Mandalari, Adel-Patient, et al. 2009), (Didier Dupont et al. 2009), (Chu et al. 2009), (Krupa et al. 2020), (Böttger et al. 2019), (Dulko et al. 2021).Separately, a 65 mM stock solution of PL was prepared using egg yolk-derived L-α-Phosphatidylcholine (Sigma-Aldrich, 61755), which contained approximately 58% PC, 14% PE, and 26% TAGs. Notably, the choice of PC as the primary PL source was guided by its prevalence in human bile (Gilat and Sömjen 1996), making the egg yolk-derived PLs a suitable analog for mimicking human biliary PLs. The PL preparation was carried out using an ultrasonic homogenization technique based on Silva et al. (2010) and optimized to produce a particle size below 100 nm. An ultrasound homogenizer (VCX500, Sonics & Materials Inc., CT; 20 kHz, 500 W) was employed, with the sonication conducted in two cycles (each 3 minutes long, with a 5-second pulse at 70% amplitude followed by a 10-second pause) with a 15-min break between the cycles. To prevent overheating, the PL dispersion was maintained in an ice/water/isopropanol bath (ca. 5^{o}C) during the process. The mean particle size (Z-Average, n = 4) of the prepared dispersions was determined by dynamic light scattering (DLS) using a Zetasizer Nano-ZS system, following the Malvern manual (Malvern 2013). The particle size analysis confirmed that the mean particle size of the PL stock solution was within the desired nanoscale range, ensuring a consistent starting point for subsequent experiments (Silva et al. 2010). To prepare for the subsequent experiments, aliquots of the BS and PL stock solutions were mixed in varying proportions to achieve the desired BS/PL ratios within a physiological concentration range of biliary surfactants (Table 1). These mixtures were stirred using a magnetic stirrer set at 500 rpm for 20 minutes to ensure homogeneous dispersion. The resulting BS/PL aggregates were again analyzed using DLS, with particle size data reported as the mean ± SD (n = 4) for each ratio examined.

Table 1 Experimental parameters. (I) Molar ratios and concentrations of the two biliary surfactants (BS/PL, mol/mol), in the experimental setup. (II) Intestinal enzymes activities (U/mL of reaction mixture) during in vitro lipolysis performed on interfaces and emulsions. This table have been published (Kłosowska et al. 2024).

BS/PL	BS conc. (mM)	PL conc. (mM)	Lipase[a] or pancreatin[b] (lipolytic activity)	Colipase[a]	PLA_2[a]
BS–13	1.3[a], 13[b]	0	2000 U/mL	-	-
BS–13	1.3[a], 13[b]	0	-	-	-
BS/PL–9:4	0.9[a], 9[b]	0.4[a], 4[b]	2000 U/mL	2:1 (w/w) lipase:colipase	-
BS/PL–9:4	0.9[a], 9[b]	0.4[a], 4[b]	2000 U/mL	-	170 U/mL
BS/PL–9:4	0.9[a], 9[b]	0.4[a], 4[b]	2000 U/mL	-	-
BS/PL–9:4	0.9[a], 9[b]	0.4[a], 4[b]	-	-	-
BS/PL–6.5:6.5	0.65[a], 6.5[b]	0.65[a], 6.5[b]	2000 U/mL	-	-
BS/PL–4:9	0.4[a], 4[b]	0.9[a], 9[b]	2000 U/mL	-	-
PL–13	0	1.3[a], 13[b]	2000 U/mL	-	-
PL–13	0	1.3[a], 13[b]	-	-	-
Control (no biosurfactants)	0	0	2000 U/mL	-	-

[a]used only in the interfacial lipolysis experiments (section 3.2.3), [b]used only in the emulsion lipolysis experiments (section 3.2.4).

3.2.2 Oil phase purification

Commercially available sunflower oil (Jeronimo Martins Polska S.A.) was used as a source of TAGs and purified to remove any surface-active impurities. Florisil (Sigma-Aldrich, 03286) was used for this purpose, mixed with the oil at room temperature in a 1:2 (w/w) ratio and stirred for 120 minutes at 150 rpm. The absorbent was then removed by centrifugation at 9000 rpm for 30 minutes at 20°C. The supernatant was filtered under vacuum using Millex filters (0.1 µm PDVF, Sigma Aldrich). The purified oil was stored under nitrogen at 4°C. The oil prepared in this way was used in subsequent experiments for interfacial analysis and emulsion digestion.

3.2.3 Interfacial analysis of lipolysis

The experiments described in this section were conducted during my research placement at the University of Granada, Spain (May-July 2021), in the Department of Applied Physics, within the Laboratory of Biocolloid and Fluid Physics Group, under the supervision of Professor Julia Maldonado-Valderrama, with training and support provided by Professor Teresa del Castillo-Santaella.

The simulated intestinal lipolysis experiment was conducted using the OCTOPUS device controlled by Dinaten software (Maldonado-Valderrama et al. 2015), (Maldonado-Valderrama et al. 2022), which employs a pendant drop technique to monitor

the oil-water interfacial tension (IFT) during sequential adsorption, lipolysis, and desorption phases. The experiment was carried out at a constant temperature of 37.0 ± 0.1 °C, with measurements performed in triplicate (n = 3) and the results were presented as the mean ± SD. The lipolysis conditions for various experiments are set in Table 1. The concentrations of BSs and PLs, with a combined total molarity of 13 mM and varying BS/PL ratios, were reduced by a factor of 10, as shown in Table 1. This approach has been used in previous studies, as high surfactant concentrations cause a rapid decrease in IFT (<2 mN/m), leading to droplet detachment (del Castillo-Santaella et al. 2015; Maldonado-Valderrama et al. 2015).

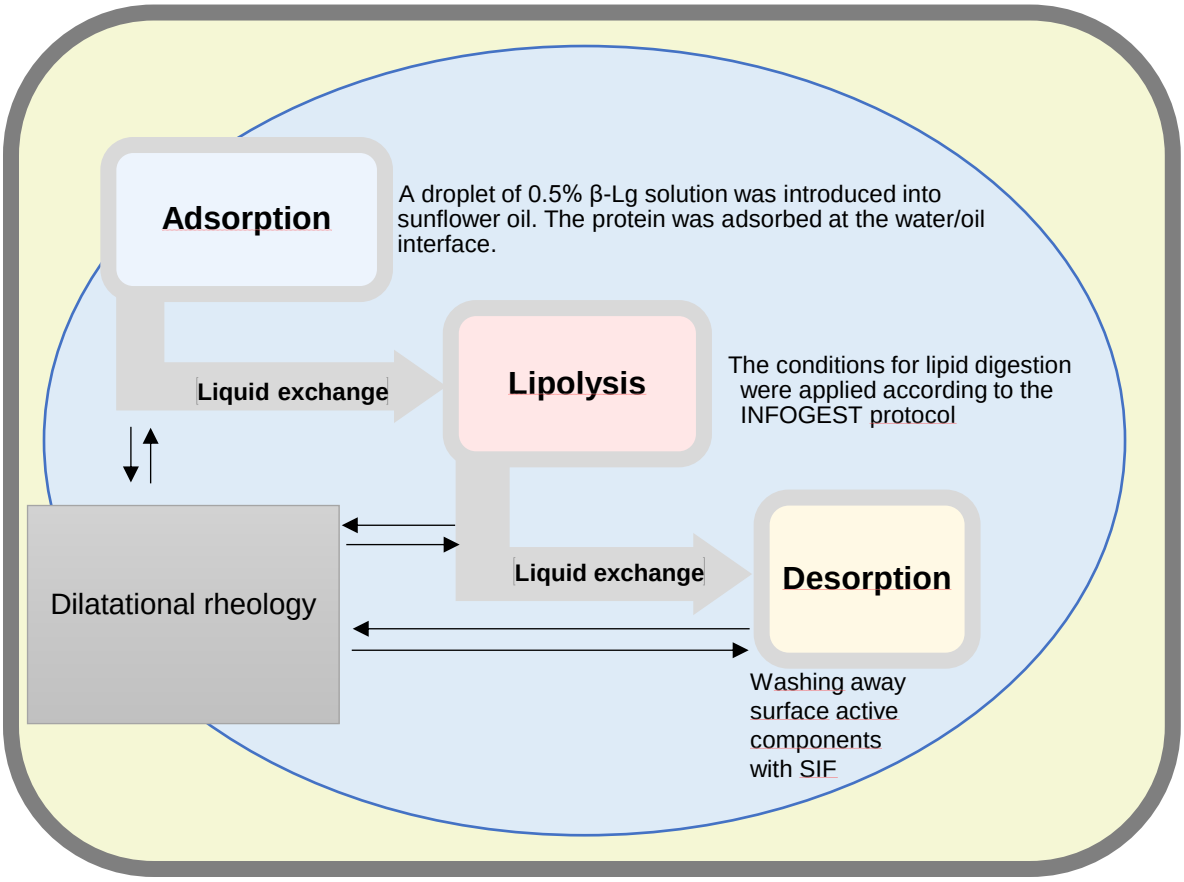

Figure 3.1 A schematic representation of the experiment at the oil-water interface during lipid digestion using the OCTOPUS pendant drop setup. The blue oval represents the droplet of the aqueous phase immersed in the oil phase (yellow rectangle). The diagram provides a cross-sectional view of the experimental cuvette setup. Narrow black arrows indicate the dilatational rheology process involving the expansion and compression of the droplet, before proceeding to the next step and liquid exchange.

Step one – Adsorption:

The first phase of the experiment involved protein adsorption. A coaxial double capillary (Patent ES 2 153 296 B1) was used to produce a 15 mm² pendant droplet of β-Lg solution (0.5 wt%), prepared by diluting the stock solution 10x in a saline buffer (150 mM NaCl, 0.02 wt% NaN_3, pH 7.0). The droplet was immersed in sunflower oil in a glass cuvette (Hellma, OG, type 6030; 10 mm optical path length) and incubated at 37°C for 60 minutes, allowing sufficient time for the protein to adsorb at the oil-water interface and reach IFT equilibrium. Dilatational rheology was then performed to assess the response of the interface to deformation. A frequency of 0.1 Hz with an amplitude below 5% was applied. This minimized disturbance of the droplet interface while allowing changes in IFT to be recorded in response to deformation of the interfacial area. The dilatational

modulus (E), obtained from these measurements, provides insights into the interfacial elasticity and viscosity. This modulus is a value expressed as $E = E' + iE'' = \varepsilon + iv\eta$, where E′ is the real component, also known as the storage modulus, which corresponds to the interfacial elasticity (ε).The imaginary component, E'', represents the loss modulus, related to the interfacial viscosity (η), with v denoting the angular frequency of the applied oscillation (Maldonado-Valderrama et al. 2021), (Del Castillo-Santaella and Maldonado-Valderrama 2023). After each deformation cycle, the interface was allowed to rest undisturbed for 5 minutes. Before the start of every experiment, specifically before initiating the protein adsorption phase, a control measurement of the interfacial tension (IFT) between sunflower oil and saline was performed. This resulted in an IFT value of 23.5 ± 1.5 mN/m at a temperature of 37.0 ± 0.1 °C.

Step two – Lipolysis:

Following the adsorption phase, the droplet content was exchanged 10 times with SIF containing porcine pancreatic lipase (Sigma-Aldrich, L3126), which was added at a concentration required to achieve an enzyme activity of 2000 U/mL, according to the INFOGEST protocol (Brodkorb et al. 2019). Additionally, the SIF contained dispersions/solutions of PLs and/or BSs, which were introduced as modifications to the original protocol, with varying BS/PL ratios as specified in the Table 1. During this phase, the droplet area remained constant at 15 mm². Control experiments (with no enzyme added) were performed for BS-13, PL-13, and BS/PL-9:4 ratios. Additional experiments tested the impact of colipase (Sigma-Aldrich, C3028) and PLA_2 (Sigma-Aldrich, P6534) on lipolysis for the BS/PL-9:4 condition, comparing three variations: lipase alone, lipase with colipase, and lipase with PLA_2 (Table 1). The lipolysis phase was maintained for 60 minutes at 37.0 ± 0.1 °C, after which dilatational rheology was performed again, following the same procedure as described previously for the adsorption process.

Step three – Desorption:

In the final step, the droplet content was exchanged with fresh SIF (10-fold exchange) to produce conditions facilitating the desorption of interfacial material. The IFT was continuously monitored for 60 minutes at 37.0 ± 0.1 °C. At the end the dilatational rheology was performed, following the same procedure as described previously for adsorption step.

3.2.4 *In vitro* lipid digestion of model food emulsion

3.2.4.1 Preparation of model food emulsion

The emulsion composition was as follows: 20 wt% sunflower oil (purified according to the procedure in section 3.2.2), 0.5 wt% Whey Protein Isolate (WPI, 93% protein; BiPRO®, Davisco Foods International Inc., Eden Prairie, MN), and 79.5 wt% saline buffer (150 mM NaCl aqueous solution with 0.02% (w/w) NaN_3).

WPI was dissolved in the saline buffer and stirred on a magnetic stirrer for 60 minutes at 720 rpm. The aqueous phase and oil phase were combined and vortexed for 3 minutes. The mixture was then sonicated using an ultrasonic device (CVX 130 Vibra Cell Ultrasonicator, 20 kHz, 130 W, 13 W/cm³) with consecutive 5-second pulses and 10-second breaks for 3 minutes; the sonication amplitude was set to 80%.

During the process, the glass vial containing the emulsion was immersed in an ice/water/isopropanol bath.

The average droplet size of the emulsion was measured using the DLS technique on a Nano-ZS Zetasizer (Malvern Instruments Ltd., Malvern, UK) operated in the size-measurement mode. Sample preparation was performed according to the Malvern manual (Malvern, 2013).

3.2.4.2 Simulation of intestinal lipolysis in emulsion

The *in vitro* lipid digestion experiments were conducted using the pH-stat technique (Figure 1.21), which maintained a constant pH throughout the digestion process by neutralizing the free fatty acids (FFAs) released during lipolysis. The experimental setup involved a pH-stat micro-titrator system (Cerko Lab Systems, Gdynia, Poland), controlled by Cerko Lab Solution software, equipped with a PID-controlled titration mechanism, which continuously adjusted the pH to 7.0 by adding 0.1 N NaOH as FFAs were liberated during TAGs enzymatic hydrolysis. The digestion vessel (20 mL conical glass), maintained at a constant temperature of 37 ± 0.1 °C with a water bath, was magnetically stirred at 700 rpm to ensure thorough mixing of the components. The pH-stat system recorded the volume of NaOH (V_{NaOH}) added every second, ensuring precise control over the reaction conditions throughout the 2-hour digestion period. The digestion followed the INFOGEST static *in vitro* digestion protocol (Brodkorb et al. 2019) for the intestinal phase, with a modification in the concentration of BSs, according to the Table 1. A freshly prepared emulsion (section 3.2.4.1) was added to the digestive conical vessel containing SIF and/or a BS solution, PL dispersion, or their mixtures (see BS/PL ratios in the Table 1; and their preparation procedure in the section 3.2.1). Then, porcine pancreatin (Sigma-Aldrich, P7545) freshly prepared in SIF was added in the quantity to achieve a final pancreatic lipase activity of 2,000 U/mL in the digestive mixture. The digestion mixture was stirred magnetically (700 rpm) at 37°C for 2h.

Moreover, blank experiments were performed, where the pancreatin was replaced with SIF, and the corresponding NaOH volumes required for background correction were recorded. These were NaOH used for adjusting the instrument to maintain a constant pH and to counteract any pH fluctuations associated with conducting the experiment in an open-air environment. The NaOH volumes obtained in the blank experiments were subtracted from the NaOH volumes measured in all active experiments, including both TAG digestion and control experiments.

Control experiments were conducted under the same conditions as the emulsion digestion experiments, but without the addition of emulsified TAGs. This allowed for the evaluation of FFAs released from PLs and/or their mixtures with BSs, due to the presence of PLA_2 and carboxyl esterase in pancreatin. All experiments were treated consistently; therefore, control experiments were also performed for BS-13 and conditions without any biosurfactants (Table 1).

The difference between the NaOH volumes recorded in the active and control experiments provided a measure of the FFAs released exclusively from TAGs hydrolysis. The digestion experiments, including controls and blanks, were performed in triplicate to ensure statistical reliability. At the end of the experiment, the data collected were used to calculate the percentage of FFAs released from the TAGs using a formula that accounted for the NaOH volumes, the molar concentration of the titrant, the molecular weight of the TAGs,

and the amount of oil used. This method allowed for the accurate assessment of lipid digestion. The control and blank experiments facilitated correction for FFA release from side reactions and any pH fluctuations. The results were presented as mean ± SD values of triplicate measurements (n = 3) for each experiment.

$$FFA\ (\%) = \frac{(V_{NaOH} - V_{blank}) \cdot C \cdot MW}{m_{oil} \cdot N \cdot 1000} \cdot 100$$

where V_{NaOH} - volume of NaOH used to neutralize FFAs released from TAGs (mL),

V_{blank} – volume of NaOH in blank sample (mL),

C - the molar concentration of the titrant (NaOH, 0.1 M),

MW is the average molecular weight of sunflower oil TAGs (885.69 g/mol; as ascertained by GC-FID analysis of fatty acid composition (Kłosowska-Chomiczewska et al., unpublished results),

m_{oil} - the amount (g) of oil incorporated into the digestion mixture via the emulsion,

N - the number of FFAs released from each TAG molecule (i.e., *N* = 2, assuming two FFAs are released from one TAG molecule by pancreatic lipase action).

Formula and its description have been published (Kłosowska et al. 2024).

3.3 Proteolysis: digestion and analysis

3.3.1 Protein *in vitro* static digestion model

The protein digestion was performed according to the INFOGEST protocol (Brodkorb et al., 2019), which provides detailed experimental procedures for *in vitro* digestion. Modifications have been implemented – especially with regard to the concentration of biliary biosurfactants used in the intestinal phase of digestion, as described below.
Stock solutions of WPI (40 mg/mL total protein) and β-Lg (40 mg/mL) were freshly prepared by dissolving whey protein isolate or β-Lg in distilled water, followed by stirring with a magnetic stirrer at 700 rpm for 60 minutes. A 20 mg/mL protein solution was then subjected to the oral phase, followed by further dilution in the gastric and intestinal phases, resulting in a theoretical protein concentration of 5 mg/mL during the intestinal phase.

Given the varying conditions in the intestinal phase (experiments conducted at different BS/PL ratios, Table 5) and to minimize errors in the peptidomic analysis, the digestion process in the oral and gastric phases was carried out in a single vessel to standardize the starting point for the subsequent intestinal phase, which was the main focus of the investigation. The post-gastric mixture was divided into equal portions, as the final stage of the gastric phase served as the uniform starting point for each condition. These portions were then subjected to further digestion in the intestinal phase, described in detail below. Stock solutions of BS/PL mixtures were prepared as previously described in section 3.2.1. All digestion steps were conducted at 37°C using an orbital shaker (170 rpm).

Oral Phase

An aliquot of the protein stock solution (10 mL) was mixed with 8 mL of simulated salivary fluid (SSF) and 50 µL of 0.3 M $CaCl_2$ solution. The volume was adjusted to 20 mL by adding distilled water (1,950 µL), and the mixture was incubated at 37°C for 2 minutes.

Gastric Phase

The post-oral mixture was diluted with pre-warmed simulated gastric fluid (SGF) (16 mL, 37°C). Then, 10 µL of 0.3 M $CaCl_2$ solution was added. The pH of the digestive mixture was adjusted to 3.0 with 1 M HCl, and the volume was brought to a final total of 40 mL by adding distilled water. At this point, 1 mL of porcine pepsin stock solution (P6887, Sigma-Aldrich, Germany) was added to initiate gastric digestion. The pepsin activity was 1,526 U/mg protein, calculated using hemoglobin as a substrate, and the enzyme was added to achieve a final concentration of 2,000 U/mL in the digestive mixture. Aliquots of 1 mL were collected during the 2-hour incubation for further analysis, with time points specified in Table 9. Each sample was treated with 13 µL of 1 M NaOH solution to reach pH 9.0, thereby inhibiting pepsin activity. The final protein concentration in the gastric phase was 10 mg/mL.

Intestinal Phase

After 2 hours of gastric digestion at pH 3.0, aliquots of 6 mL of the post-gastric digestive mixture were transferred to previously prepared and pre-incubated vessels (30 minutes at 37°C) containing solutions of simulated intestinal fluid (SIF), 10 µL of 3 M $CaCl_2$, mixtures of biosurfactants at various BS/PL ratios (Table 5), 120 µL of 1 M NaOH, and 1.068 mL of water, with volumes adjusted for each condition to reach a final

pH of 7 and a total volume of 12 mL. Details of pipetting variable volumes are provided in (Table 2). The final protein concentration in the intestinal phase was 5 mg/mL. Before use, the stock solutions of pancreatic enzymes in water were prepared separately and stored at 4 °C; these were: α-chymotrypsin from bovine pancreas (activity: 18.9 U/mg of protein calculated using BTEE as substrate; C7762, Sigma-Aldrich, Germany) and trypsin from porcine pancreas (activity: 10.309 U/mg of protein calculated using TAME as substrate; T0303, Sigma-Aldrich, Germany). 300 µL of enzyme solutions were added to achieve a total enzyme concentration of 0.1 mg/mL (1:1, w/w) in the digestive mixture (Dulko et al. 2021). For the experiment without enzymes (BS/PL-9:4 (NE)), the enzyme volume (600 µL) was replaced with water. Intestinal digestion was carried out at 37°C for 2 hours. During this phase, 1 mL samples were taken at intervals specified in Table 3. Intestinal phase samples were inhibited by adding phenylmethanesulfonyl fluoride (PMSF, Sigma-Aldrich, 93482) to reach a final PMSF concentration of 6 mM in each sample (stock solution of PMSF: 0.1 M in EtOH). Samples were divided into two 500 µL aliquots and stored at -80°C. Each experiment was conducted in triplicate for each set of conditions studied (e.g., BS/PL ratio). Digestion progress was monitored by SDS-PAGE analysis.
The experiments involving pure β-Lg digestion under two conditions (BS/PL-9:4 and Control) were conducted identically to the procedure described above.

Table 2 The pipetting volumes of variable volumes in the in vitro static intestinal phase.

Conditions	Bile		SIF
	BSs 100 mM (stock solution in SIF)	PLs 65 mM (stock solution in SIF)	
BS–13	1.560	-	2.640
BS/PL–9:4	1.080	0.738	2.382
BS/PL–6.5:6.5	0.780	1.200	2.220
BS/PL–4:9	0.480	1.662	2.058
PL–13	-	2.400	1.800
Control	-	-	4.200
BS/PL–9:4 (NE)	1.080	0.738	2.382

Table 3. Time points of sample withdrawn during the protein digestion.

Gastric phase		Intestinal phase	
Time point	Time (min)	Time point	Time (min)
G1	20	T1	0.5
G2	40	T2	1
G3	60	T3	2
G4	120	T4	5
		T5	10
		T6	20
		T7	30
		T8	60
		T9	120

3.3.2 **SDS-PAGE analysis**

Gel preparation:
The acrylamide gels were prepared according to the user guide procedure of Invitrogen SureCast™ Handcast System ("SureCast ™ Handcast System, MAN0014073, Thermo Fisher Scientific" 2021). The resolving solution of 10% polyacrylamide was prepared according to Table 4. The solution was poured into the set of gel plates, and left for complete polymerization, the surface was smoothed with water. Next, the stacking gel solution containing 4% acrylamide (Table 5) was poured, and the 12-well comb was inserted between the glass plates. The set was left for complete polymerization.

Sample preparation:
The reducing agent 0.5 M DTT (DTT (10x) Invitrogen, NP0004) was freshly prepared, and a 15 µL aliquot was added to the protein sample (50 µL of the digestion time-point sample), followed by the addition of LDS Sample Buffer (x4) (Invitrogen, NP0007) and SIF (30µL and 50 µL to intestinal and gastric phase sample, respectively). The samples were vortexed and heated for 10 min in the hot block at 70°C. The samples cooled to ambient temperature were introduced into the electrophoresis gel wells. The molecular mass of the proteins in the pre-stain marker used in the experiment was between 3 and 188 kDa (SeeBlue pre-Stained Protein Standard, Invitrogen, LC5625).

Electrophoresis conditions:
The electrophoresis was run under the following conditions: 200V, 150mA/gel, 25 min. The running buffer consisted of a solution of 5% MES SDS (Invitrogen, NP0002) in ultrapure water. The gels were stained for 30 minutes in the staining solution (Table 6), and subsequently immersed in the fixing solution (Table 7) overnight. The gels were scanned using a Gel Doc XR+ System (Bio-Rad). The densitometric analysis was done using ImageJ software and the relative amount of protein was calculated using the first time-point (T1) sample of the intestinal phase as the reference for subsequent time-point samples.

Table 4. The composition of resolving gel ("SureCast TM Handcast System, MAN0014073, Thermo Fisher Scientific" 2021).

Component	**Volume (mL)**
SureCast™ Acrylamide (40%) (HC2040)	2.0
SureCast™ Resolving Buffer (HC2212)	2.0
Distilled Water	3.5
10% SureCast APS (HC2005)	0.08
SureCast™ TEMED (HC2006)	0.008

Table 5 The composition of stacking gel ("SureCast TM Handcast System, MAN0014073, Thermo Fisher Scientific" 2021).

Component	**Volume (mL)**
SureCast™ Acrylamide (40%) (HC2040)	0.3
SureCast™ Stacking Buffer (HC2112)	0.75
Distilled Water	1.92
10% SureCast™ APS (HC2005)	0.030
SureCast™ TEMED (HC2006)	0.003

Table 6. The composition of staining solution (Dulko et al. 2021).

Component	Concentration
Methanol (STANLAB60300100X)	45% (v/v)
Acetic acid (POCH 568760114)	10% (v/v)
Coomassie brilliant blue R (Sigma Aldrich, 27816)	0,1% (w/v)
Water	45% (v/v)

Table 7. The composition of fixing solution (Dulko et al. 2021).

Component	Concentration
Methanol (STANLAB60300100X)	20% (v/v)
Acetic acid (POCH 568760114)	10% (v/v)
Water	70% (v/v)

3.3.3 **Sample preparation for mass spectrometry**

The experiments described in this and the following sections (3.3.4 and 3.3.5) were conducted during my research placement at the University of Stuttgart, Germany (June-November 2022), in the Department of Food Science, under the supervision of Professor Jens Brockmeyer, with training and support provided by Dr. Julia Bräcker.

A 100 µL aliquot of the digestive mixture was treated with 5 µL of 200 mM solution of DTT (ROTH, 6908.1) and was incubated for 1 hour at a final concentration of 10 mM. Subsequently, 250 mg of zirconium dioxide (Sigma Aldrich, 230693) was mixed with 10 mL of 1% formic acid, and the mixture was vortexed for 30 seconds. An aliquot of 0.895 mL of the a zirconium dioxide suspension (pH 2.54) was then added to the sample and incubated for 15 minutes (Houjiang Zhou et al. 2007). The pH of the sample containing the digestive mixture was lowered to 3-4 to enhance the entrapment of phosphorous groups by ZrO_2 (Hsu, Lin, and Chung 2012). The mixture was filtered using a polyethersulfone (PES) filter (Chromafil® Xtra PES-20/25, pore size 0.2 µm, membrane diameter 25 mm) (Persico et al. 2020; Marcet et al. 2022), and 500 µL of the filtrate was applied to a preconditioned solid-phase extraction (SPE) column (Strata™X, 33 µm Polymeric Reversed Phase) following an established internal protocol. SPE procedure included the following steps: conditioning the column with 1 mL methanol, equilibration with 1 mL 1% formic acid (FA), sample application, washing with 1 mL 1% FA, and elution with 1 mL of a mixture containing 90% methanol (MeOH) and 1% FA into a 1.5 mL Eppendorf tube. The samples were then evaporated in a vacuum concentrator. After evaporation, the samples were resuspended in 50 µL of the mobile phase containing 3% acetonitrile (ACN) and 0.1% FA. All samples were treated the same way, regardless of the addition of PLs in the digested sample. Before the MS measurements, the efficiency of PLs removal was visually validated in all samples using TLC plates stained with molybdate solution (Ellingson and Lands 1968).

3.3.4 **Liquid Chromatography - Mass Spectrometry analysis**

The data were collected using an Impact II quadrupol time-of-flight mass spectrometer (Bruker Daltonic, Bremen, Germany) coupled to an Elute UHPLC system (Bruker Daltonic, Bremen, Germany) controlled by software Bruker otofControl (version 6.3) and Bruker Compass HyStar (version 6.0). The ion polarity is set to positive mode, the scan mode was configured to Auto MS/MS, where the system automatically selects precursor ions for further fragmentation. The mass scan range was 50 - 2200 m/z. In the MS source settings, a VIP-HESI source was employed, with key parameters such as an end plate offset of 500 V and capillary voltage of 2500 V. The nebulizer was set to 2.5 bar, and the dry gas flow was 8 L/min at a temperature of 200°C. The dry temperature and probe gas temperature were set at 200°C and 300°C, respectively. The probe gas flow was 4 L/min. In the MS/MS acquisition section, the quadrupole ion energy was 5.0 eV, the collision energy for fragmentation was 8.0 eV. The collision cell transfer time was 50 µs, the spectra rate was 2.00 Hz.

The settings for the Liquid Chromatography (LC): The column Purospher® STAR RP-8 encapped Hibar® RT (3x150 mm, 3 µm, Merck KGaA, Darmstadt, Germany), was applied to separate analytes. The LC pump operated under a pressure range of 0 to 500 bar, accommodating the variations in backpressure during gradient elution. The flow rate was set at 0.200 mL/min, with a gradient program (Table 8) that progressively increases the proportion of acetonitrile including 0.1% formic acid up to 97% over a 65-minute run. The column oven temperature was controlled at 40°C. The injection volume for the analytes and external standard mixtures (Table 9) was 10 µL. Temperature control was enabled for the autosampler, with a setpoint of 15°C.

Table 8. Gradient conditions used in the measurements during LC.

Time (min)	Flow (mL/min)	% Water 0.1 % FA	% ACN 0.1% FA
0	0.2	97.0	3.0
2.0	0.2	85.0	15.0
52.0	0.2	70.0	30.0
58.5	0.2	2.0	98.0
61.4	0.2	2.0	98.0
61.8	0.2	97.0	3.0
65.0	0.2	97.0	3.0

Table 9. 10 mM Sodium Formate Calibrant Solution.

Component	Volume (mL)
Isopropanol	12.5
Water	10
Formic acid	0.05
Sodium hydroxide solution 0.1 M	2.5

3.3.5 **Data processing**

The data processing method for MS spectra was done using PEAKS 11 software (BioInformatics Solution, Waterloo, Canada). The raw data refinement step was performed for each sample. This step cleans raw data to improve its quality and accuracy. Mass correction and chimera association was used to ensure precise spectra for correct peptide identification. Next step, was De Novo sequencing, where amino acid sequences were determined without using the database to identify new or unknown sequences. After completing the De Novo sequencing, the data was searched against the database (335 entries, milk proteins, only one entry for all milk allergens (WHO/IUIS), created 11.06.2024), the quality filters included a PSM false discovery rare (FDR) of 1%, requiring protein identification with a -10LogP score of ≥ 50.5% and at least 1 unique peptide. Additionally, de novo identifications required an average local confidence (ALC) of ≥ 50.5 for inclusion. Subsequently, to compare relative abundance of peptides across different samples and conditions Label Free Quantification (LFQ) was performed using the same settings and filtering parameters as the de novo and database search. Detailed parameters are specified in Table 10.

The data were visualized using Microsoft Excel and Microsoft PowerBI, PyMOL (Schrodinger LLC 2010), R studio (R Core Team 2023) including packages Peptides (Osorio, Rondón-Villarreal, and Torres 2015) and R-peptidomics (Jardin 2024) supported by AI tools (OpenAI 2024).

Table 10. Parameters of data processing in PEAKS 11 software.

De novo	**DB Search:**	**LFQ parameters**:
Precursor Mass Error Tolerance: 15.00 PPM Fragment Mass Error Tolerance: 0.1 DA Enzyme: None Fixed Modifications: (none listed) Variable Modifications: Oxidation (M) (+15.99) Max Variable PTM Per Peptide: 5	Precursor Mass Error Tolerance: 15.00 PPM Fragment Mass Error Tolerance: 0.1 DA Enzyme: None Max Missed Cleavage: 40 Digest Mode: Semi-Specific Peptide Length Range: 5 - 40 Fixed Modifications: (none listed) Variable Modifications: Oxidation (M) (+15.99) Max Variable PTM Per Peptide: 5 Database: 240611_230515_Bos-taurus_Milk_allergenFocus Taxonomy: all species Searched Entries: 335 Contaminant Database: N/A Deep Learning Boost: Yes PSM FDR: 1.0% Proteins -10LgP ≥ 15.0 Proteins Unique Peptides ≥ 1 Denovo Only ALC ≥ 50.0% Denovo Only Tag Sharing: Disabled Denovo Only Fully Matched: No	Precursor Mass Error Tolerance: 15.00 PPM Fragment Mass Error Tolerance: 0.1 DA Enzyme: None Max Missed Cleavage: 40 Digest Mode: Semi-Specific Peptide Length Range: 5 - 40 Fixed Modifications: (none listed) Variable Modifications: Oxidation (M) (+15.99) Max Variable PTM Per Peptide: 5 Database: 240611_230515_Bos-taurus_Milk_allergenFocus Taxonomy: all species Searched Entries: 335 Contaminant Database: N/A Deep Learning Boost: Yes

4 Results and discussion

The results presented in sections 4.1 and 4.2 have been published in the journal *Food Research International* under the title 'The bile salt/phospholipid ratio determines the extent of in vitro intestinal lipolysis of triglycerides: interfacial and emulsion studies.' (Kłosowska et al. 2024).

4.1 Retrospective analysis of scientific literature data on biliary surfactants concentrations

The initial stage of the experimental research was preceded by a detailed literature review and data collection to determine the average concentrations of BSs and PLs in the human bile. The upper gastrointestinal system was the particular interest, as the bile is produced in the liver, stored in gallbladder and released to the proximal part of the small intestine (duodenum) (Smith 2019). For the subject of the research, it was crucial to evaluate the overall molarity of biosurfactants and the concentrations of BSs and PLs in the postprandial duodenum.

The thirty-nine research articles (from 1968 to 2021) discussed the composition of adult human bile and provided detailed information of BSs and PLs concentrations in the duodenal lumen (Table 11). The category of collected data was determined by the sampling location of human bile (Figure 4.1a). There were three main points of sourcing the human bile reported in the literature: hepatic duct, gallbladder, and the lumen of duodenum. The concentrations of biosurfactants vary significantly depending on the sample's origin as determined in the meta-analysis of the collected literature data (Figure 4.1b).

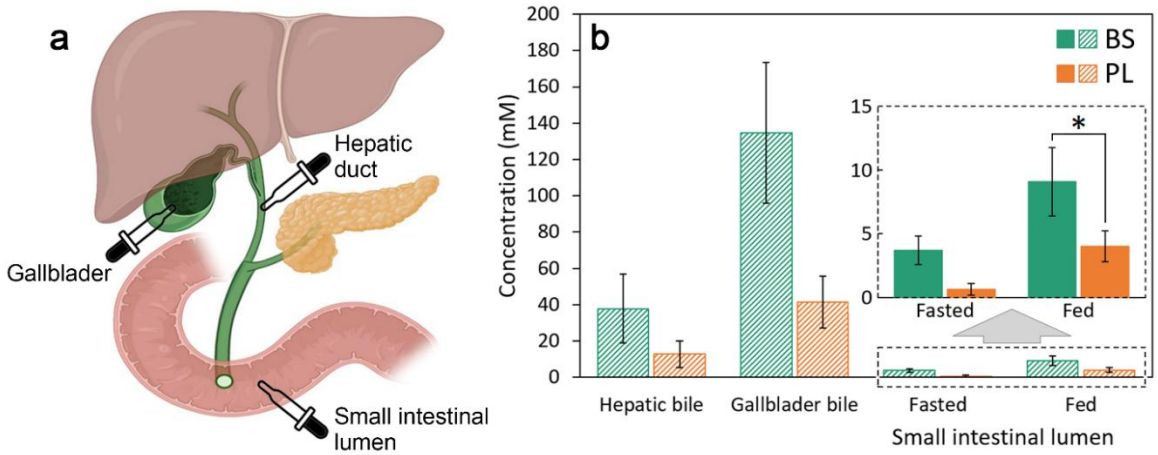

*Figure 4.1 a) The upper part of the human gastrointestinal system with the pipette symbols indicating the sampling points. b) The outcome of the data analysis presenting the comparison of the total BS and PL contents of human bile depending of the collection site. The calculations are based on a retrospective analysis of the literature. Mean concentrations (± SD) are presented for gallbladder bile, hepatic bile and the small intestinal lumen in fed and fasted state. * P<0.01, by Student's t-test. These results have been published (Kłosowska et al. 2024).*

Table 11 Research papers defining the physiological concentrations of biliary surfactants (PLs and BSs) in the duodenum (small intestine lumen in fed state and fasted state), gallbladder bile, and liver bile were used for meta-analysis of human bile in healthy adult individuals. This compilation has been published (Kłosowska et al. 2024).

Bile/Intestinal lumen	Number of scientific reports	Literature references
Hepatic bile	3	(Van Der Linden and Nakayama 1982; Lee and Nicholls 1986; Pattinson, Willis, and Frampton 1991)
Gallbladder bile	12	(Lee and Nicholls 1986; Pattinson, Willis, and Frampton 1991; Admirand and Small 1968; Heller and Bouchier 1973; Whiting, Down, and Watts 1981; Booker et al. 1992; Hay et al. 1993; Jayanthi et al. 2016; Holan et al. 1979; Cherng Z. Chuang, Ph.D., Louis F. Martin, M.D., Barbara Y. LeGardeur, M.P.H. 2001; Halpern et al. 1986; Sadaruddin, Hassan, and Zuberi 1980; Ho et al. 1980)
Small Intestinal Lumen, Fasted State	14	(Vlahcevic et al. 1972; Deferme et al. 2003; Stappaerts et al. 2014; Wuyts et al. 2015; Sarah Clarysse et al. 2009; Riethorst, Mols, et al. 2016; M. P. de la C. Moreno et al. 2010; Heikkilä et al. 2011; Armand et al. 1996; Bergstrom et al. 2020; Kalantzi, Goumas, et al. 2006; Brouwers et al. 2006; Jan Bevernage, Joachim Brouwers, Sarah Clarysse, Maria Vertzoni, Jan Tack, Pieter Annaert 2010; Lindahl et al. 1997)
Small Intestinal Lumen, Fed State	14	(Riethorst, Mols, et al. 2016; Armand et al. 1996; Kalantzi, Persson, et al. 2006; S Clarysse et al. 2009; T. C. Northfield and McColl 1973; Müllertz et al. 2012; Dahlgren et al. 2021; Kalantzi, Goumas, et al. 2006; Fausa 1974; Persson et al. 2006; Holmstock et al. 2013; Kossena et al. 2007; Riethorst, Baatsen, et al. 2016; Ladas et al. 1984)

The highest concentration of biosurfactants is observed in the gallbladder, where the bile is stored and highly concentrated (135 ± 39 mM for BSs and 42 ± 14 mM for PLs). Upon secretion into the duodenum, the bile is diluted. In the hepatic duct it reaches the values of 38 ± 19 mM for BSs and 13 ± 7 mM for PLs). In the intestinal lumen, the concentrations of BS and PL may vary depending on the ingestion state, i.e., the fasted or the fed state (FaS and FeS, respectively).

During fasting, bile secretion to the duodenum is limited; therefore, the luminal biosurfactant concentration is relatively low (Table 12). After a meal ingestion, the bile is released to the lumen of proximal small intestine, duodenum, where it is diluted with intestinal fluids and chyme (Janowitz et al. 1990). The goal here was to find the average concentration of physiological biosurfactants in intestinal lumen reported in the literature for healthy humans. The results are presented in Figure 4.1 and Table 12.

Table 12 The comparison of calculated weighted arithmetic mean (±SD) concentrations (mM) of bile biosurfactants (BS and PL) in the fasted state (FaS) and fed state (FeS) in the intestinal lumen (duodenum), including the number of individuals considered in the calculations.

FaS	Concentration (mM) ± *SD*	No. of individuals	FeS	Concentration (mM) ± *SD*	No. of individuals
BS	3.7 ± 1.1	141	**BS**	9.1 ± 2.7	127
PL	0.6 ± 0.5	108	**PL**	4.0 ± 1.2	104

The mean BS concentration was estimated to be 9 mM, and the mean concentration of PLs was 4 mM. Therefore, the physiological molar ratio of biliary biosurfactants in the postprandial proximal small intestine was established to be 9:4 (BS/PL). This indicates statistically significant (P<0.01) approximately 2.3-fold molar excess of BSs over PLs. The determined BS concentration corresponds to the 10 mM concentration recommended by the INFOGEST scientific network's *in vitro* static digestion protocol (Brodkorb et al. 2019), (Minekus et al. 2014), which is broadly applied in numerous *in vitro* digestion studies on a global scale (Hualu Zhou, Tan, and McClements 2023). However, the recognized protocol omits the concentration of PLs. As biosurfactants possess an amphiphilic structure, they may influence digestion outcomes. The impact of PLs on the extent and rate of digestion has been previously reported, though primarily in the context of protein digestion (F. J. Moreno, Mackie, and Mills 2005), (Mandalari, Mackie, et al. 2009), (Macierzanka et al. 2009), (Macierzanka et al. 2012), (Böttger et al. 2019), (Dulko et al. 2021).

The BS/PL ratio of 9:4 results in an average total molarity of 13 mM for these biosurfactants in the postprandial lumen of the human small intestine. Therefore, all experiments in this research were designed in relevance to the BS/PL ratio of 9:4. This ratio has been considered physiological in the fed state. In some experiments, the proportions of BSs or PLs were increased or decreased. However, the total molarity of both biosurfactant groups was always maintained at 13 mM. The various BS/PL ratios used in further experiments are presented in Table 13. Each following experiment in this work is based on the five combinations of the BS/PL ratio keeping the total molarity constant (13 mM). These are: the 'physiological' ratio (BS/PL -9:4) and its reversed value for assessing the excess of PLs (4:9 BS/PL); the equal molar content of each biosurfactant (BS/PL-6.5:6.5), each biosurfactant separately (BS-13 and PL-13) and the control without any surfactants.

Table 13. The various ratios of biliary biosurfactants (BS and PL) in relation to physiological concentration. Data are presented as molar concentration (mM) and approximate percentage contribution (%) of each biosurfactant in the binary mixture.

	Nomenclature of experimental conditions	BS (mM)	PL (mM)	BS (%)	PL (%)
Only BS	BS-13	13	-	100	-
'Physiological' concentration	**BS/PL-9:4**	**9**	**4**	**70**	**30**
Equal molarity	BS/PL-6.5:6.5	6.5	6.5	50	50
Excess of PL	BS/PL-4:9	4	9	30	70
Only PL	PL-13	-	13	-	100
Control (No surfactants)	Control	-	-	-	-

4.2 Lipolysis

4.2.1 The analysis of bile salts / phospholipids dispersions

Once the BSs to PLs ratios to be examined were determined, the experimental work to evaluate the size of the PL liposomes was conducted. When presented as aqueous dispersions PLs have been found to create spontaneously vesicles of 700-1000 nm in size (Naso et al. 2019).

A variety of supramolecular assemblies in colloidal fractions of the fed state human intestinal fluid aspirates has been analyzed previously. Studies revealed that the average size of PLs and BSs aggregates ranges from approximately 50 to 200 nm, with the coexistence of smaller fractions (<20 nm), being likely BS micelles (Elvang et al. 2016). The present study reproduced the physiological size attributes of the colloidal assemblies found in the human intestinal fluid, utilizing the preparation protocol described in section 3.2.1. The method of preparing PL dispersion was optimized to achieve a vesicle size lower than 100 nm. Due to possible modifications of PLs during sample preparation, the conventional method of liposome preparation using chloroform as solvent was abandoned. The organic solvents may contain impurities remaining after their production, for example, chlorine (Lin et al. 1984) that may react with double bonds of PLs' unsaturated fatty acids residues (Schwartz-Narbonne et al. 2019). In order to avoid the introduction of artificial components to the digestive mixture, the dispersion of PL was prepared by treating the PL sample with ultrasounds. The sonification allowed for disruption of large vesicles into smaller ones. According to the literature (Silva et al. 2010), the sonification amplitude, time and the type of probe let affect the size of PLs liposomes produced. The time of sonication plays a significant role, the prolongation leads to smaller vesicles; however, during the process, the heat is generated. Therefore the sonication procedure was performed under a controlled low temperature with pules-pause intervals to avoid PL oxidation and hydrolysis (Silva et al. 2010). The particle sizes in the various BS/PL preparations in simulated intestinal fluid (SIF) decreased progressively as the concentration of BS increased. The results are presented in Table 14; the Z-Average values are presented respectively for each biosurfactant ratio. The DLS examination of BS-13 solution resulted in the average diameter of 5.6 ± 0.7 nm, that indicates micelle formation.

Table 14. The mean particle size of PL and/or bile slats dispersions in Simulated Intestinal Fluid at various proportions of the surfactants used in the digestion experiments, as determined by DLS (n = 4).

BS/PL ratio	**Z-Average (nm) ± *SD***
PL–13	80.5 ± *0.58*
BS/PL–6.5:6.5	64.2 ± *1.87*
BS/PL–4:9	72.2 ± *1.60*
BS/PL–9:4	59.6 ± *2.58*
BS–13	5.6 ± *0.7*

4.2.2 **Interfacial analysis of lipolysis**

The insight into the interfacial characteristics (interfacial tension and dilatational rheology) of *in vitro* static intestinal lipolysis reaction at various concentrations of PLs and BSs has been studied using a pendant drop OCTOPUS device (Maldonado-Valderrama et al. 2013) described in the methods section 3.2.3. The elasticity and viscosity of the interface were evaluated by tracking the droplet's response to small surface expansions and compressions, which allowed for the assessment of the interface's dynamic rheology (Maldonado-Valderrama et al. 2015), (Maldonado-Valderrama et al. 2022). The experiment has been performed in three subsequent steps: STEP 1 protein adsorption, STEP 2 lipolysis, STEP 3 desorption.

Protein **adsorption** (Figure 4.2a) – at this step a single droplet interface, stabilized by adsorbed protein was employed to offer insights into the behavior of more complex protein-stabilized emulsion systems. The adsorption process started with creating a droplet by the injection of the aqueous solution of protein into the oil. The protein, β-Lg was adsorbed at the interface. In order to achieve equilibrium at the interface, the adsorption step lasted an hour. This step was identical for each measurement, and a similar decrease in the oil-water IFT was observed. The initial IFT value of the pure water-oil interface was 23.5 ± 1.5 mN/m. However, incubation with β-Lg for 60 minutes at 37°C resulted in a decrease in IFT to 12.5 ± 1.6 mN/m (n = 18).

Following interfacial tension measurements, dilatational rheology was employed. This technique, which involves controlled expansion and compression of the droplet interface, provides further insights into the viscoelastic properties of the adsorbed protein layer. After each dilatational rheology measurement, the droplet interface was allowed to stabilize before initiating the subsequent lipolysis stage via subphase exchange (Maldonado-Valderrama et al. 2015).

In the **lipolysis** step (Figure 4.2b), the droplet content was replaced with SIF containing lipase and/or biosurfactants (BS and/or PL). Initial state of this step is the rearrangement of components at the interface. There are two main aspects influencing the oil-water interface. First, the biosurfactants (BS and/or PL) might displace the adsorbed β-Lg from the interface, allowing lipase access to the TAG substrate. That effect was described previously (Maldonado-Valderrama et al. 2008), (Macierzanka et al. 2009), (Macierzanka et al. 2012). The effect depends on the surfactant type and its concentration, as well as the type of adsorbed protein (Bellesi, Pizones Ruiz-Henestrosa, and Pilosof 2014). Second, the composition of the oil-water interface might be influenced by the lipase activity. This occurs because lipase at the interface converts TAGs into surface-active compounds, such as FFAs and MAGs (Janowitz et al. 1990).

The lipolysis step was designed to mimic the digestion of single droplet of emulsion and was based on principles of intestinal digestion from *in vitro* static digestion protocol released by INFOGEST network (Brodkorb et al. 2019) The BS/PL ratios used in the interfacial tension measurements spanned the physiological range observed in healthy, fed-state individuals, including a ratio of 9:4 for BSs to PLs. However, other ratios were also investigated to assess the impact of varying BS/PL proportions on interfacial tension. This range of ratios allowed for the evaluation of how variations in the relative concentrations of PLs and BSs, within physiologically relevant levels, influence the dynamics of oil-water interfacial tension during intestinal lipolysis.

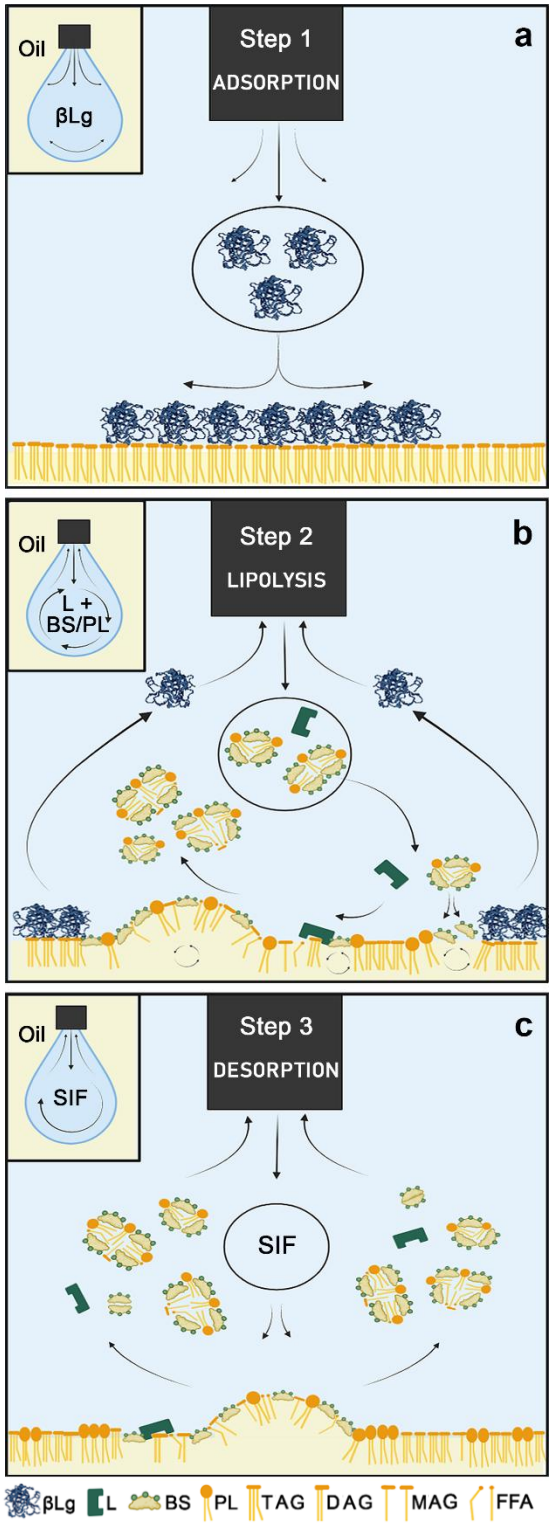

Figure 4.2 The graphical representation of the interfacial phenomena for three-stage experiment performed using OCTOPUS device, a) protein adsorption, b) lipolysis, and c) desorption. Abbreviations: β-Lg, β-lactoglobulin; L, lipase; BS, bile salt; PL; phospholipid; TAG, triglyceride DAG; diglyceride; MAG; monoglyceride; FFA, free fatty acid; SIF, simulated intestinal fluid. These results have been published (Kłosowska et al. 2024).

Given that pancreatic juice contains a mixture of enzymes, including not only lipase but also colipase and phospholipases (Smith 2019), initial experiments were performed using combinations of lipase and colipase, as well as lipase and PLA_2, to better simulate physiological conditions and establish experimental parameters. In the early stages of lipolysis experiments (Figure 4.3a), a sharp drop in interfacial tension was observed, regardless of the presence of colipase or PLA_2 (Figure 4.3b). This suggests that the combined action of lipase and biosurfactants, rather than biosurfactants alone, was responsible for the initial rapid decrease in IFT. While biosurfactants likely contributed to β-Lg displacement from the interface, the observed IFT reduction might not be solely attributed to them. Given the negligible impact of colipase and PLA_2 on the initial IFT drop, subsequent experiments were conducted using lipase only, to focus on the interplay between lipase and biosurfactants.

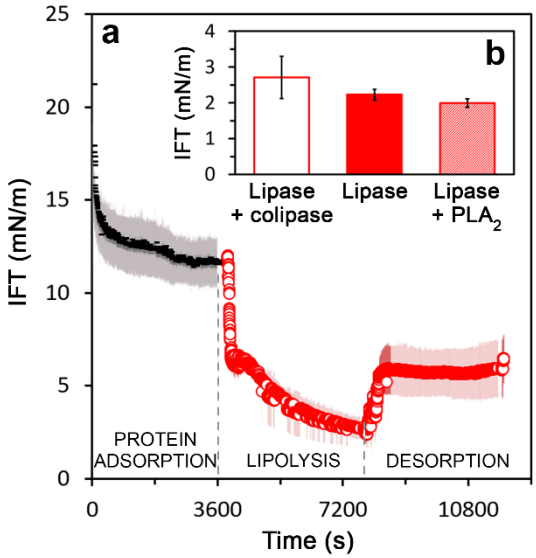

Figure 4.3 Interfacial experiments of lipolytic enzymes conducted using the OCTOPUS setup. a) This panel depicts the changes in oil-water interfacial tension over time. The three-step experiment comprises: (i) protein adsorption (n = 18), (ii) lipolysis with pancreatic lipase and colipase under BS/PL-9:4 conditions (n = 3), and (iii) desorption (n = 3). Data are presented as mean ± SD. b) Impact of enzymatic conditions on interfacial tension. This panel presents the final IFT values after the lipolysis step under various enzymatic conditions for BS/PL-9:4: (i) pancreatic lipase and colipase ('lipase + colipase'), (ii) lipase alone ('lipase'), or (iii) lipase and phospholipase A2 ('lipase + PLA_2'). Data are presented as mean ± SD (n = 3). These results have been published (Kłosowska et al. 2024).

In order to evaluate the impact of biosurfactants (BS and/or PL) on the decline in IFT, the control studies without enzyme were performed. Figure 4.4 presents the results for experiments with only BSs (BS-13), PLs (PL-13) and a physiological biosurfactant ratio (BS/PL 9:4), comparing the individual effect of biosurfactants with the combined effect of biosurfactants and lipase. In general, the control experiments resulted in limited IFT reduction. However, the largest decrease was noted for the biosurfactant combination BS/PL-9:4. Substantial differences in IFT decline were observed for each active experiment involving lipase and respective control. These results suggest that surface-active products were possibly released from TAGs at the interface during incubation with enzyme. However, to gain a more comprehensive understanding of the process, the third step of the experiment was conducted and the results are discussed in the following section of this chapter.

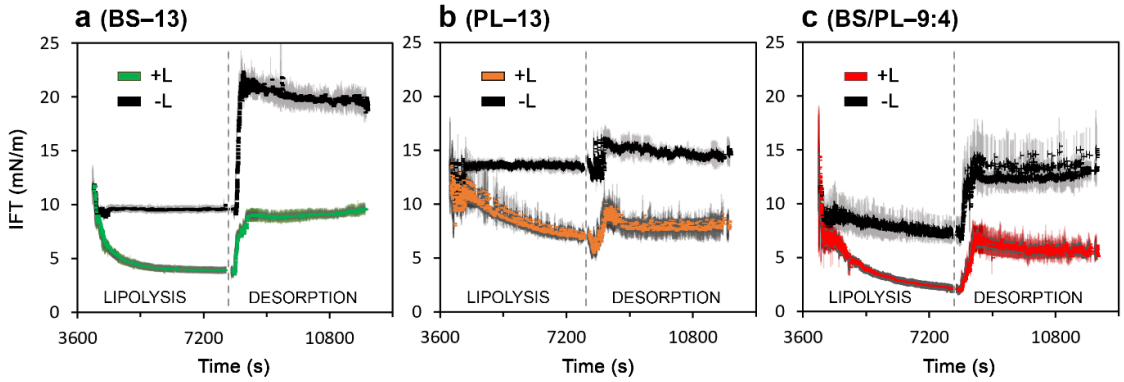

Figure 4.4 The oil-water interfacial tension (IFT) evolution under control conditions (without lipase, -L) and in active experiments (with lipase, +L) of simulated intestinal lipolysis (mean ± SD, n = 3) for a) BS-13, b) PL-13 and c) BS/PL-9:4). All experiments were conducted at 37 ± 0.1 °C and consisted of β-Lg adsorption step (not shown in here, please see Figure 4.5), followed by the lipolysis and desorption steps. These results have been published (Kłosowska et al. 2024).

The lipolysis studies were continued by performing experiments with other molar proportions of biliary surfactants, according to Table 13, in order to better explore the combined action of BSs and PLs (Figure 4.5). The lowest value at the end of the lipolysis step was observed for physiologically relevant conditions BS/PL-9:4 (2.2 ± 0.1 mN/m). The equal molar ratio of BSs and PLs (BS/PL-6.5:6.5) resulted in higher value 3.1 ± 0.3 mN/m, and the excess of PLs lead to similar results giving the value 3.2 ± 0.3 mN/m. Although the values for equimolar biosurfactant ratio and the excess of PLs were higher than those observed under the physiologically relevant conditions, they were still lower than the outcomes from experiments with only BSs (i.e., 4.0 ± 0.3 mN/m for BS–13) or only PLs (PL-13) (Figure 4.5). This demonstrates that the combination of these biosurfactants reduces IFT more effectively than BSs or PLs used separately. In the control experiment, where only the enzyme was utilized, the IFT decreased to just 12.0 ± 0.4 mN/m (Figure 4.5), indicating minimal hydrolysis of TAGs into surface-active products. It is important to highlight that these *in vitro* lipolysis experiments only demonstrate how IFT evolved during the incubation time. However, these measurements were unable to definitively determine whether, and to what extent, the BS/PL mixtures contributed to the enzymatic hydrolysis of TAGs and the production of surface-active compounds such as MAGs, DAGs, and FFAs, though all lipolysis experiments involving BSs, BS/PL mixtures, or PLs resulted in a larger reduction in IFT compared to the control lipolysis without the addition of biosurfactants.

Desorption, was the final experimental phase of the interfacial studies (Figure 4.2c). The liquid within the droplet was exchanged with SIF to wash away any excessive surface-active compounds, and produce conditions for potential desorption of adsorbed compounds, providing information about the affinity of specific components to the interface. The ease of desorption of compounds indicates their lower affinity to the interface. Effective desorption is reflected by an increase in IFT (Maldonado-Valderrama et al. 2015), (Maldonado-Valderrama et al. 2022); the higher the value, the more successful the desorption process, as surface-active compounds remove the interface approaching the initial value of a bare oil-water interface, 23.5 ± 1.5 mN/m. In the absence of enzyme (Control), BS-13 exhibited the most effective desorption, with interfacial tension increasing from 9.7 ± 0.6 mN/m after the initial adsorption phase to 21.7 ± 1.2 mN/m during the subsequent desorption phase (Figure 4.4a). This substantial desorption of BS from interfaces aligns with previous reports, notably the work of Maldonado-Valderrama et al. demonstrating significant desorption of NaTC and NaGDC from both oil-water and air-water interfaces (Maldonado Valderrama et al. 2014), (del Castillo-Santaella and Maldonado-Valderrama

2023). In contrast, the experiment with PL-13 (Figure 4.4b) after the lipolysis step, increased to 15.8 ± 1.0 mN/m during the desorption step. This indicates a strong PL affinity for the interface, resulting in a persistent adsorbed layer even after the desorption phase. While BSs also exhibit interfacial affinity, they appear to desorb more readily than PLs under these conditions.

The combined use of BSs and PLs (BS/PL 9:4) resulted in a substantially lower IFT during the lipolysis step compared to using either BSs or PLs alone (Figure 4.5) suggesting a synergistic effect. This synergy is evident even in the absence of enzymes (control experiments, Figure 4.4), indicating an inherent interaction between BSs and PLs at the interface. However, it is crucial to consider the subsequent desorption step when evaluating the overall impact on interfacial properties. While the initial reduction in IFT during lipolysis is enhanced by the combined use of BSs and PLs, their individual desorption behaviors influence the final IFT value. Therefore, a complete analysis should consider both the synergistic reduction during lipolysis and the individual contributions to desorption.

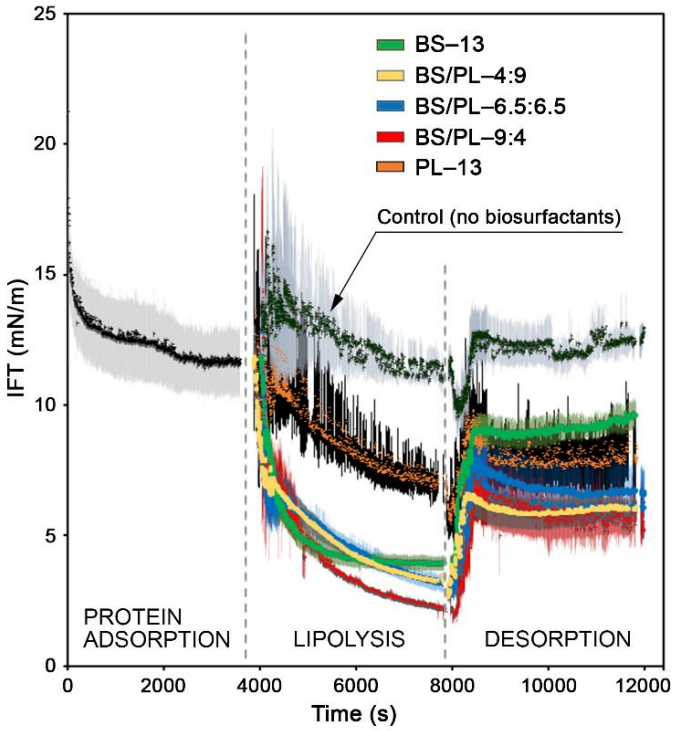

Figure 4.5 Changes in oil-water interfacial tension measured during three sequential steps: β-Lg protein adsorption (n = 18); lipolysis (n = 3 for each condition); and desorption (n = 3 for each condition). The lipolysis step was performed without the biosurfactants (Control), or in the presence of biosurfactants at different molar ratios, including sole BSs, sole PLs, or their mixtures (i.e., BS-13, PL–13 or BS/PL-9:4, BS/PL-6.5:6.5, and BS/PL-4:9). Each experimental step lasted 60 minutes and were conducted at 37.0 ± 0.1 °C. Values are presented as mean ± SD. These results have been published (Kłosowska et al. 2024).

The final desorption result for BS/PL–9:4 showed slightly lower values than for PL-13 (Figure 4.6). However, the IFT for BS/PL–9:4 before desorption was significantly lower than for PL-13 ($p < 0.01$), indicating partial removal of surface-active components, likely predominantly. These results highlight the complex interfacial behavior of the biliary surfactant mixtures used in this experiment.

In the active experiments (BS-13, PL-13, BS/PL-9:4) involving lipase (Figure 4.4) the IFT values observed during the desorption process were lower than for their respective control experiments. This is likely due to lipase activity, which produces surface-active

compounds that remains partially adsorbed at the interface during subphase exchange. In experiments containing PLs (PL-13 and BS/PL-9:4), the difference in IFT between the second step (lipolysis) and the third step (desorption) was consistent for both the active and control experiments with the increase of approximately 2-5 mN/m. However, notable differences were observed for BSs: in the control experiment, the IFT increase was about 11 mN/m, whereas in the active experiment, the desorption process was less efficient, leading to an increase of only about 5 mN/m. That suggests the products of TAG hydrolysis and not only BSs may remain partially at the interface during the desorption process. The highest values of IFT after the desorption process were noted for BS-13 and PL-13, 9.9 ± 0.9 mN/m and 8.1 ± 1.2 mN/m, respectively. However, the lowest value observed for BS/PL–9:4 (5.7 ± 0.7 mN/m) highlights the synergistic effect of BSs and PLs in reducing interfacial tension.

The full spectrum of results from the third step of the active experiments with lipase is presented in Figure 4.5, demonstrating the complex impact of various ratios of biosurfactants and lipolytic products on the desorption process. For a more in-depth analysis of desorption process, Figure 4.6 presents the calculated relative differences between the values obtained at the end of the second and third step (lipolysis and desorption), expressed as ΔIFT.

The higher the PL content and the lower the BS content applied in the experiment, the lower the relative ΔIFT value. Figure 4.6 shows an approximately six-fold reduction observed between BS-13 and PL-13. A high ΔIFT value indicates ease of desorption, suggesting a facilitated solubilization of lipolytic products. The high ΔIFT value for BS-13 suggests effective solubilization of interfacial compounds, whereas the low ΔIFT value for PL-13 implies limitations in solubilizing lipolytic products from the interface. Experiments involving both biosurfactants, BSs and PLs, resulted in intermediate ΔIFT values. Several factors could explain these results; however, the effect may be influenced by the concentration of BSs and the BS/PL ratio. First, PLs may hinder the desorption process. Second, the presence of PLs may make it more difficult for BSs to desorb or solubilize lipolytic products, while PLs themselves may facilitate the formation of interfacial complexes with lipolytic products. Third, PLs may not be completely displaced by BSs, or only to a limited degree. Ultimately, the difficulties in desorption of interfacial products may influence the intestinal lipolysis of TAG emulsion.

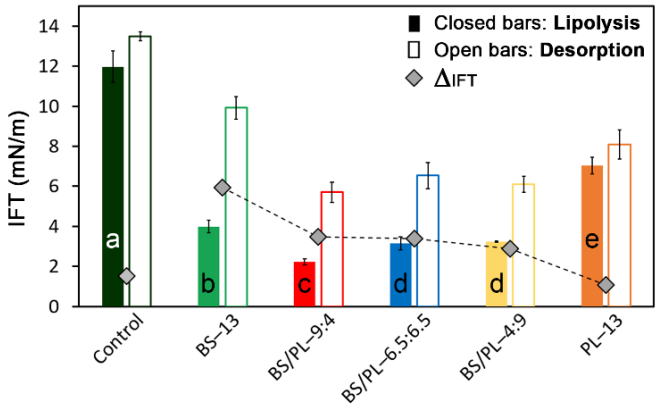

Figure 4.6 Interfacial tension changes during in vitro lipolysis and desorption. This figure presents the interfacial tension values at the end of the lipolysis step (closed bars) and after the completion of the desorption step (open bars) under various biosurfactant ratios, as detailed in Table 5. Data represent mean ± SD (n = 3 for each condition). The relative difference in IFT between the end of lipolysis and the end of desorption is represented by diamonds (dashed line serves as a visual reference). Different letters indicate statistically significant differences (P < 0.05). The 'Control' condition represents the IFT measurements in the absence of any biosurfactants. These results have been published (Kłosowska et al. 2024).

At the end of each experimental step (protein adsorption, lipolysis, and desorption), dilatational rheological measurements were performed as described in methods section 3.2.3. The experimental conditions, particularly the oscillation frequency, were adjusted to reflect the previously reported peristaltic frequency observed during digestion in the small intestine. In the duodenum, this frequency is approximately 11.7 per minute (Kellow et al. 1986), which is considered to nearly align with the 0.1 Hz frequency used in the experiment. The rheological measurements provide insights into the viscoelastic properties of the interfacial layers, specifically the storage and loss moduli. The dilatational modulus (E) is a complex quantity comprising two components: the real part, known as the storage modulus (E′), which reflects the elastic behavior of the interface, and the imaginary part, known as the loss modulus (E″), which represents the viscous behavior (Maldonado-Valderrama et al. 2021).

In this research, the focus has been placed on the real component of the dilatational modulus, E′ (Figure 4.7). The E′ consistently exceeded the E″ by approximately a factor of ten across all analyzed cases. A complete set of E′ and E″ values for all conditions is presented in Figure 4.7 and Figure 4.8.

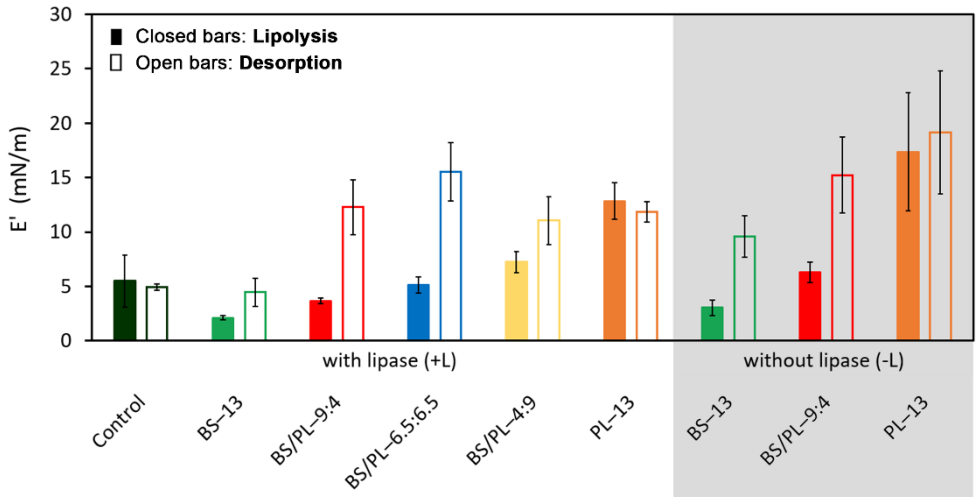

Figure 4.7 The dilatational elasticity (storage modulus, E') at various biosurfactant ratios, as shown in Table 1 (mean ± SD, n = 3 for each condition). E' was measured at the final stage of the lipolysis step (closed bars) and the desorption step (open bars) at an oscillation frequency of 0.1 Hz and a deformation area of <5%. These results have been published (Kłosowska et al. 2024).

Upon completion of the protein adsorption step (identical for each experiment), the E′ of the desorbed β-Lg interfacial layer was measured to be 21.9 ± 2.9 mN/m. This value is consistent with previously published data (del Castillo-Santaella et al. 2014), (Maldonado-Valderrama et al. 2013).

Results for the control condition (Figure 4.7), without biosurfactants, confirm that lipolysis progressed and released surface-active products. The E′ decreased to 5.5 ± 2.4 mN/m after the lipolysis step, indicating a less elastic interfacial layer compared to the result after the protein adsorption process. This reduction in elasticity was most likely attributed to the accumulation of lipolytic products at the interface, which altered the interfacial rheological properties.

In the control experiment (without biosurfactants), the desorption step did not significantly affect the rheological properties. The E′ measured 4.9 ± 0.3 mN/m after desorption, which is consistent with the small change in interfacial tension (ΔIFT) observed between

the lipolysis and desorption steps in Figure 4.6. Although the ΔIFT was minor after the adsorption and lipolysis steps in the control condition, the rheological measurements provided valuable insights into interfacial elasticity and supported the conclusions regarding the progress of lipolysis.

For the BS-13 condition (Figure 4.7), the E′ after the lipolysis step was 3.0 ± 0.7 mN/m under control conditions (without lipase) and 2.1 ± 0.2 mN/m under active lipolysis conditions (with lipase). The low E′ values observed indicate a rapid interchange of BS molecules between the bulk solution and the interface during the oscillation process (Maldonado-Valderrama et al. 2011). This rapid exchange is facilitated by the planar configuration of BSs, which promotes their rapid adsorption at the interface and a consequent immediate decline in interfacial tension, as documented in the literature (Maldonado-Valderrama et al. 2011), (Macierzanka et al. 2019), (del Castillo-Santaella and Maldonado-Valderrama 2023). Furthermore, the even lower E′ value observed in the presence of the enzyme (+L) suggests that surface-active compounds released during lipolysis contributed to a further reduction in the elasticity of the interfacial layer. Characteristically low dilatational moduli have been previously observed for BSs adsorbed at the interface, likely due to weak lateral interactions between BS molecules within the adsorbed layers (Maldonado-Valderrama et al. 2008), (Matubayasi et al. 1996) The findings presented in (Figure 4.7) confirm this behavior of BSs.

Conducting lipolysis under increasing proportion of PLs in BS/PL mixtures resulted in progressively higher E′ values: 3.7 ± 0.3 mN/m for BS/PL–9:4, 5.1 ± 0.8 mN/m for BS/PL-6.5:6.5, and 7.2 ± 0.9 mN/m for BS/PL–4:9. These increasing values indicate the formation of more elastic interfacial layers, while also suggest the coexistence of both biosurfactants at the interface. The increased elasticity observed during the desorption steps, with E′ increasing to approximately 11–16 mN/m (Figure 4.7), likely resulted from the partial removal of adsorbed substances from the interface. The relatively low IFT combined with the increased E′ after desorption (Figure 4.7) suggests the presence of strong intramolecular interactions driven by PLs. These interactions likely contribute to the formation of a dense interfacial film, limiting the mobility of BSs. This is further supported by the contrasting result for BS-13, which exhibited a much lower E′ of 4.5 ± 1.3 mN/m after the desorption step (Figure 4.7). This difference highlights the key role of PLs in enhancing the elasticity of the interfacial layer. Subphase exchange with SIF likely promoted the formation of an interfacial layer predominantly composed of PLs, which appeared partially resistant to desorption, while BSs were preferentially removed. Lower values of the dilatational modulus for interfaces with BSs compared to their mixtures with PC were also reported in previous studies (Mekkaoui et al. 2021).

The E’ value for PL-13 after lipolysis and desorption remained almost unchanged (11.9 ± 0.9 mN/m after lipolysis and 12.8 ± 1.7 mN/m after desorption). These results confirm the endurance of interfacial layers created by PLs to the desorption process. The high value of E’ for PL-13 after desorption process, is consistent with previous studies suggesting restricted lipolysis under conditions where a PL-stabilized olive oil-water interface is exposed to lipase (Torcello-Gómez et al. 2011). In the current study, surface-active products and remaining PLs likely persisted at the interface after SIF exchange. This observation is consistent with the static experiments (Figure 4.6), where interfacial tension values remained largely unchanged after the desorption step.
The molecular structure of PLs facilitates their anchoring at the interface due to the presence of two long fatty acid chains. This leads to the formation of elastic and densely packed interfacial layers of irreversibly adsorbed molecules with strong intermolecular interactions (De Vleeschauwer and Van der Meeren 1999), (Torcello-Gómez et al. 2011), (Wilde and Chu 2011). The anchoring properties of PLs may restrict the mobility of BSs at the interface. Mixed BS-PL films have been shown to exhibit

reduced dilatational elasticity compared to more ordered structures. This reduced elasticity can associated with their disordered and less compact structure (Chu et al. 2010), (Torcello-Gómez et al. 2012), (Pabois et al. 2019).

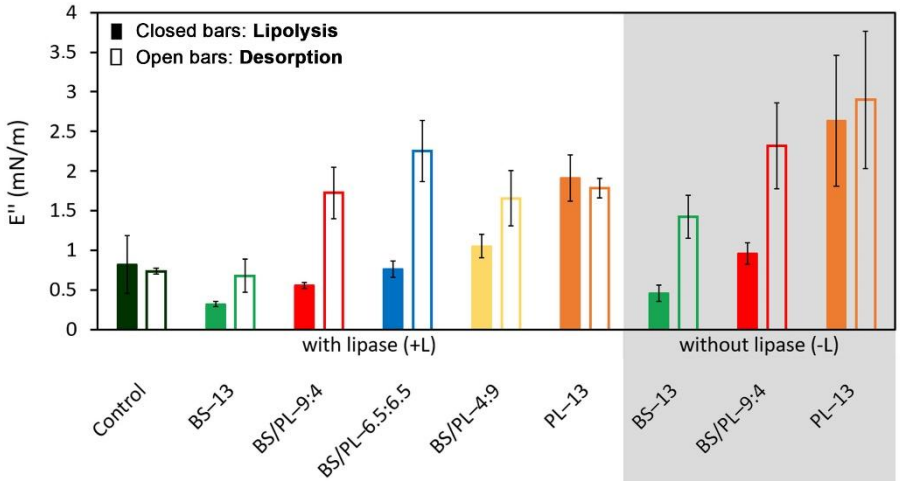

Figure 4.8 The dilatational viscosity (loss modulus, E") at various biosurfactant ratios, as shown in Table 1 (mean ± SD, n = 3 for each condition). E" was measured at the final stage of the lipolysis step (closed bars) and the desorption (open bars) at an oscillation frequency of 0.1 Hz and a deformation area of <5%. These results have been published (Kłosowska et al. 2024).

4.2.3 *In vitro* static digestion of model food emulsion.

The experiments were conducted on WPI-stabilized emulsions (mean droplet size of 2280 ± 140 nm (n = 27)), used as a source of TAGs. For the purpose of emulsion digestion, static *in vitro* digestion method was applied. The consensus protocol published by Brodkorb et al. was followed, with modifications to the biliary surfactants. Porcine pancreatin was employed as a source of pancreatic lipase to study the digestion of TAG emulsions, where the FFAs released during enzymatic hydrolysis were monitored using a titration approach. This method is commonly used as a classical approach in *in vitro* digestion studies (Grundy et al. 2021), (Brodkorb et al. 2019), (Minekus et al. 2014), (Menard et al. 2023). Nevertheless, the pancreatin used in the experiment contains a variety of digestive enzymes, including PLA_2, which may act on the PLs in the digestive mixture, potentially leading to the production of additional FFAs. To consider the extra FFAs possibly released through this side reaction, control studies (Table 1) were conducted alongside the digestion experiments. In these control experiments, the TAG emulsion was replaced with SIF. The actual experimental data for the TAG emulsion were calculated by subtracting the results of the control experiments (the volume of titrant (NaOH) used for the digestion of PLs) from the volume of titrant required to neutralize the FFAs liberated during the TAG emulsion digestion. This approach yielded titrant volumes, which were then used to determine the percentage of FFAs released exclusively from the emulsified TAGs. These results are presented in Figure 4.10. Control measurements were carried out for all experiments, including conditions with only BSs (BS–13), as well as in the absence of any biosurfactants, to guarantee uniformity across all pH-stat lipolysis experiments (Figure 4.9).

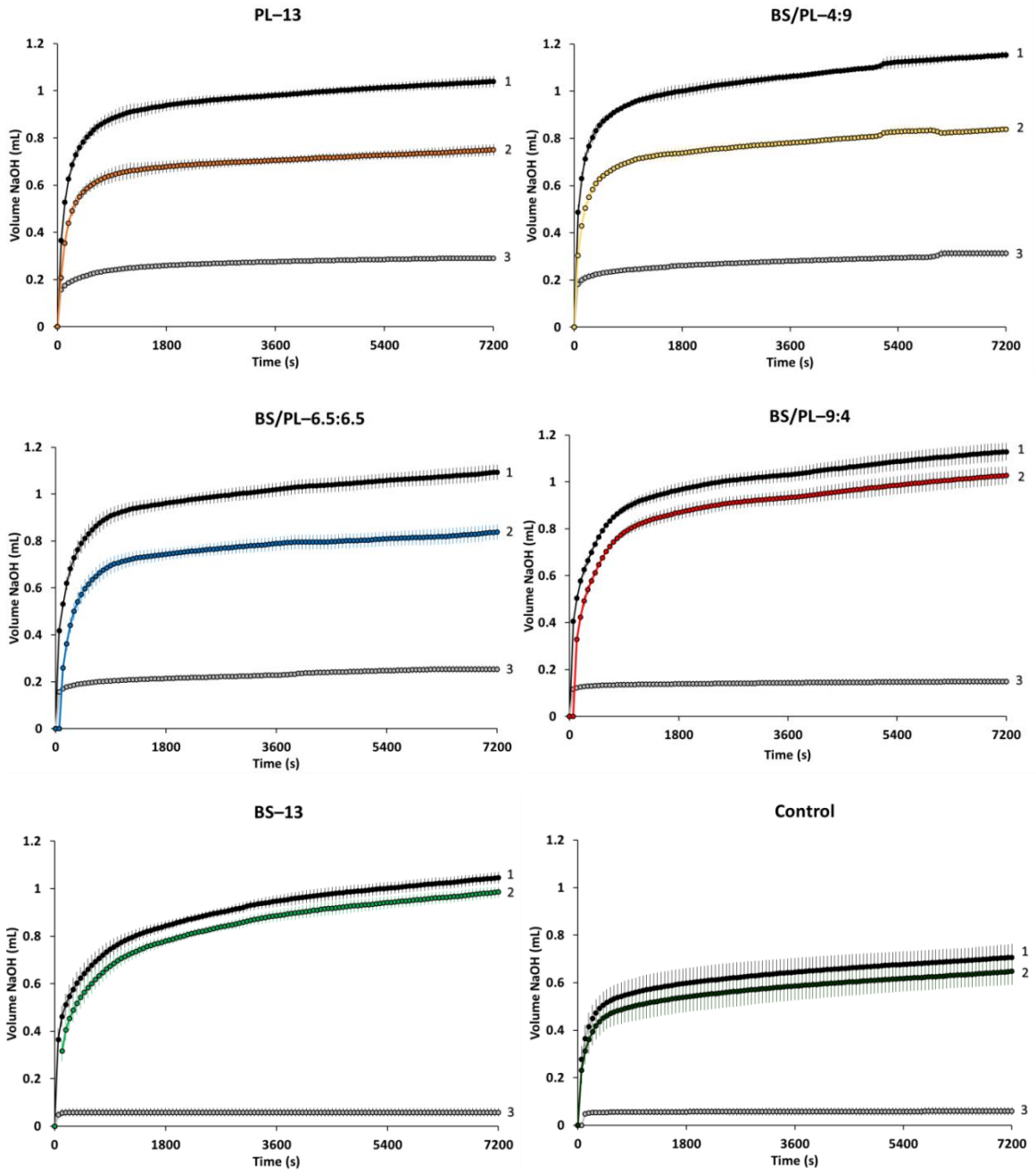

Figure 4.9 The charts presents the raw data, background measurements and corrected values for pH-stat measurements of emulsion digestion under various BS/PL ratios, as well as for conditions with PL or BS alone (PL-13, BS-13) or without any biosurfactants (BS/PL-0:0). Curve 1 - raw measurements: This represents the total volume of NaOH added during the digestion of the TAG emulsion in the presence of either PL alone, BS alone, Control or various BS/PL ratios; curve 2 - calculated result: This is the actual amount of NaOH used to neutralize the FFAs released specifically from the TAG emulsion during intestinal lipolysis, obtained by subtracting the background measurement (curve 3) from the raw measurement (curve 1). These corrected data were used for calculating the results shown in Figure 4.5; curve 3 - background correction: This represents the volume of NaOH consumed in control experiments with only PL alone, BS alone, or a BS/PL dispersion, without the TAG emulsion. This accounts for the NaOH consumed to neutralize any free fatty acids present in the system or released from PLs themselves. The data is presented as the mean ± SD (n = 3) for each set of conditions studied. These results have been published (Kłosowska et al. 2024).

While a physiologically relevant proportion of BSs and PLs (BS/PL–9:4) resulted in a significantly lower interfacial tension during lipolysis compared to other BS/PL ratios and BS–13 ($p < 0.05$, Figure 4.6), the BS and PL proportions also impacted on the TAG to FFA conversion in emulsion experiments. Specifically, the highest conversion was observed with BS/PL–9:4 (Figure 4.10a). Following 900 s of digestion, the BS/PL–9:4 ratio was the only proportion in which the quantity of liberated FFAs was significantly higher (P<0.01) in comparison to PL–13 (Figure 4.10b). When the *in vitro* digestion experiments continued to 1800 s, this difference turned out to be even more noticeable (p<0.001) (Figure 4.10c). At this time, the amounts of FFAs produced from TAGs in the experiment with BS/PL–9:4 was likewise considerably higher (p<0.05) than the amounts seen with the other two BS/PL ratios (BS/PL–6.5:6.5 and BS/PL–4:9, Figure 4.10c). Furthermore, it was found that employing BS/PL–9:4 was more efficient than employing BSs alone (i.e., BS–13) to enhance lipolysis, especially within the first 3600s (Figure 4.10a). However, beyond this time there was no significant difference between the studies for BS/PL-9:4 and BS–13 (Figure 4.10b,c,d). After 3600 s, the patterns of FFA liberation in these two systems were highly similar for the rest of the digestion experiments (Figure 4.10a,e). In the end, following 7200 s of digestion, 57.8 ± 2.2% FFAs were released from emulsified TAGs when BSs and PLs were present in physiologically relevant concentrations (BS/PL–9:4) (Figure 4.10e). This resulted in a value about 9% higher compared to all other investigated BS/PL ratios (p<0.001), and approximately 20% increase in comparison to control lipolysis in the absence of biosurfactants (p<0.001).

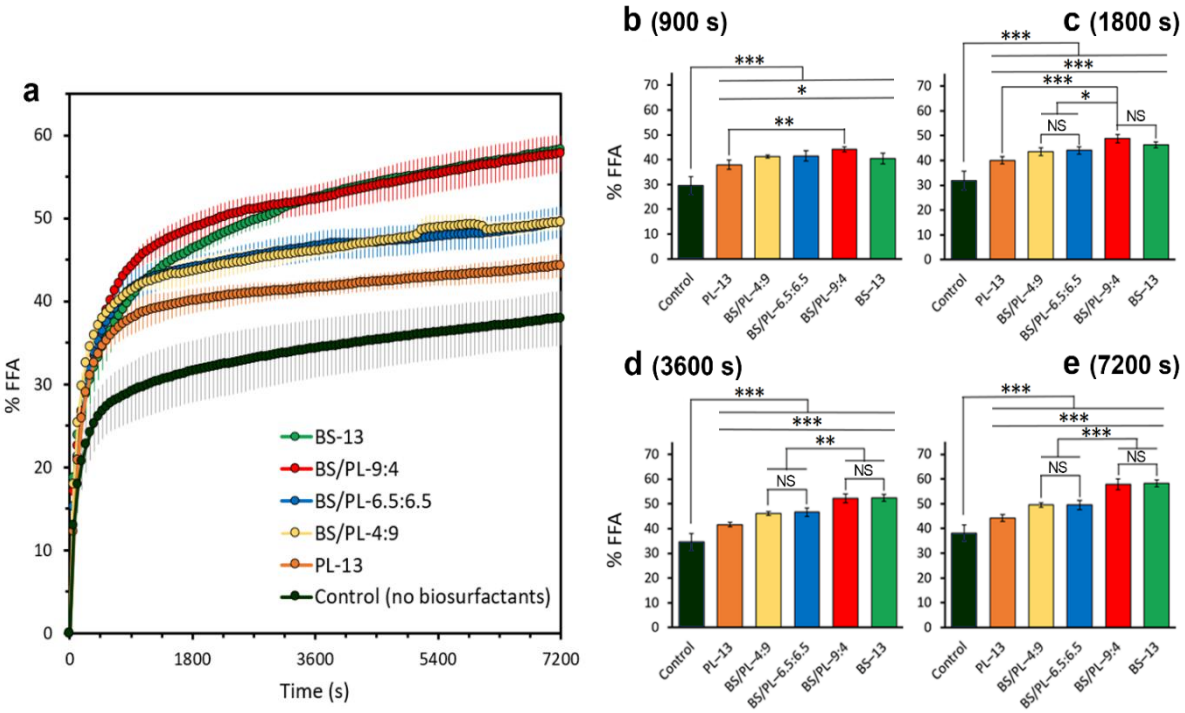

*Figure 4.10 a) The digestion progress of emulsion, expressed in percentage of FFA released from TAGs during simulated intestinal lipolysis at various biosurfactant ratios, as shown in Table 13 (mean ± SD, n = 3 for each condition). b-e) Statistical analysis of digestion progress at time points 900, 1800, 3600 and 7200 s (t-test and ANOVA) * P<0.05, ** P<0.01, *** P<0.001, NS (not significant, P>0.05). These results have been published (Kłosowska et al. 2024).*

The combined results of the interfacial and emulsion studies suggest that the desorption of biliary surfactants from the oil-water interface is a key factor in the overall lipolysis process controlled by the ratio of BSs and PLs. The biosurfactants solubilize lipolysis products, facilitating their desorption from the interface and enabling further

TAG interfacial hydrolysis (Macierzanka et al. 2019), (Acevedo-Fani and Singh 2022). This study examined the impact of different BS/PL ratios on this process. The BS-13 lipolysis/desorption experiment (Figure 4.6) showed the largest ΔIFT value (5.9 mN/m) *in vitro* indicating the most effective desorption of post-lipolysis interfacial material. The ΔIFT decreased with the increasing incorporation of PLs in the BS/PL mixture, which correlated with the efficacy observed in the emulsion lipolysis experiments. In the emulsion lipolysis experiments, lower ΔIFT values obtained from interfacial studies correlated with a reduced conversion of TAG to FFA (Figure 4.10).

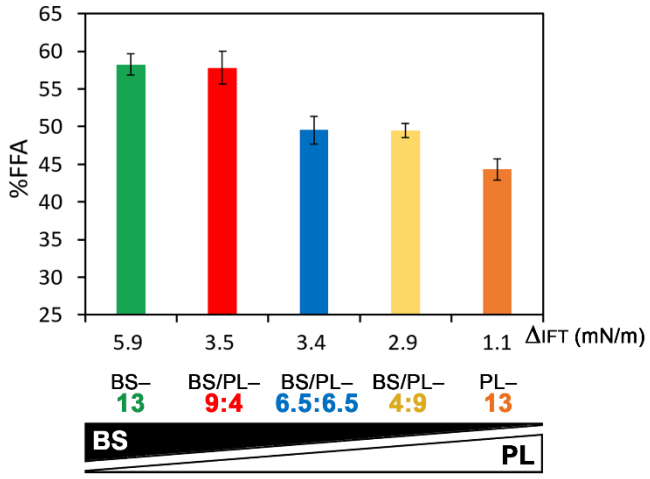

Figure 4.11 The correlation between the percentage of free fatty acids (%FFA) released from sunflower oil emulsions at 7200 s of in vitro lipolysis (Figure 4.10) and the values of ΔIFT obtained from interfacial lipolysis/desorption experiments performed under various BS/PL conditions (Table 13). Means ± SD, n = 3 for each condition. These results have been published (Kłosowska et al. 2024).

In interfacial experiments, purified pancreatic lipase was used, while emulsion digestion studies employed pancreatin (which may contain PLA_2, accounted for in the analysis). Despite this difference, it was demonstrated that even PLs alone significantly enhanced TAG conversion compared to the control without biosurfactants (Figure 4.10). This PL-dependent enhancement remained consistent across both experimental setups (Figure 4.10 and Figure 4.5).

The synergistic effect of BSs and PLs in BS/PL–9:4, observed in the interfacial experiments (Figure 4.5), appeared to enhance the conversion of TAGs to FFAs during the initial 3600 s of emulsion digestion (Figure 4.10a). This BS-PL combination proved particularly effective in reducing the IFT during lipolysis, as demonstrated in Figure 4.5 and Figure 4.6. The BS/PL–9:4 experiments indicated that the addition of small quantities of PLs to BSs did not reduce overall FFA generation. Experiments with BS–13 and BS/PL–9:4 showed comparable rates of the FFA release after 3600 s (Figure 4.10a,e), despite BS/PL–9:4 having a lower ΔIFT value than BS–13; 3.5 mN/m and 5.9 mN/m, respectively (Figure 4.11). According to this, efficient digestion of TAGs is facilitated by the combined effects of BSs and PLs under physiologically relevant conditions (BS/PL–9:4 ratio), that reduce the oil-water IFT as well as facilitate relatively good desorption from the interface. Taken together, these results demonstrate the increased effectiveness of the physiologically relevant combination of biliary surfactants (BS/PL-9:4) in promoting TAG intestinal digestion compared to other, non-physiological BS/PL ratios.

There have been relatively few studies that specifically look at how both types of biosurfactants affect intestinal lipolysis, despite the fact that both PLs and BSs are present in the small intestinal content during digestion. According to Lykidis et al. (1997), PLs and BSs can work together to activate pancreatic lipase. Although, the positive impact of PL addition was only evident at BS concentrations above 5 mM and with a PL/BS ratio below 0.6 (Lykidis, Avranas, and Arzoglou 1997). The BS/PL–9:4 ratio in the present emulsion lipolysis study met these criteria. Under these conditions, it resulted in the most significant increase in the release of FFAs from digested TAGs, when compared to control experiments without biosurfactants (Figure 4.10). However, the authors of the referenced article did not investigate the digestion of TAGs under intestinal simulation. They did not examine the individual impact of PLs on enzyme activity either. According to a recent study (Ahn and Imm 2023), medium-chain triglyceride (MCT) emulsions stabilized with milk proteins and PLs showed a slight increase in the extent of *in vitro* intestinal lipolysis compared to those produced without PLs. Nevertheless, in that investigation, PLs were primarily used as a co-stabilizer for the emulsions in small quantities. Mekkaoui et al. (2021) studied the digestion of soybean lecithin-stabilized MCT emulsion under simulated intestinal conditions. It was determined that the addition of 5 mg/mL sodium cholate (BS) to the digestion medium notably enhanced the release of FFAs from TAGs digested with pancreatic lipase, in comparison to control trials conducted without sodium cholate. A tight film of PL molecules at the surface of the emulsion droplets, which limited the enzyme's access to the TAG substrate, has been proposed as the reason for the reduced lipolysis observed under control conditions. The authors suggested that BS may counteract the limiting action of PLs by creating a mixed BS/PL interfacial coating that promoted lipolysis. Similar conclusions were drawn in previous studies. Brockman (2000) have suggested that a higher concentration of PLs might restrict enzyme access to the substrate. This effect was attributed to the formation of a densely packed PL layer at the interface (Brockman 2000). Nevertheless, the research by Mekkaoui et al. (2021) did not provide data on the digestion results when both biosurfactants (PLs and BSs) were absent. Consequently, unambiguous conclusions regarding the specific role of PLs serving whether as catalysts or inhibitors - on the hydrolysis of emulsified TAGs could not be made from that research. My findings, presented in this section, shed more light on this important aspect of intestinal lipolysis.

4.3 Proteolysis

4.3.1 Protein digestion

After analyzing emulsion digestion and the interfacial behavior of PLs and BSs during TAG lipolysis, I also investigated the effect of the BS/PL ratio on the proteolysis of a model food-grade protein material – whey protein isolate (WPI). The dry basis composition of WPI consists of approximately 93% protein, with the remainder comprising fats, carbohydrates, vitamins, and minerals. The main proteins present are β-Lg (45%), α-La, (15%), glycomacropeptide (16%), immunoglobulins (4%), and bovine serum albumin (1%), while the rest are minor components (Zajac et al. 2019).

Proteolysis starts in the gastric phase, where proteins are subjected to pepsin digestion. Many proteins undergo significant digestion in the gastric phase, with pepsin fragmenting them into smaller peptides before they reach the small intestine (Picariello et al. 2020). To monitor the intestinal phase, β-Lg was selected as the model protein due to its resistance to pepsinolysis. It is well established that β-Lg, the major whey protein, is largely resistant to gastric digestion by pepsin (Sousa et al. 2020). The partially digested and undigested β-Lg is then transferred to the small intestine (Dulko et al. 2021), where proteolytic activity is significantly increased (Sousa et al. 2020). The aim of this part of the research was to investigate how protein digestion in the intestinal phase is affected by various BS/PL concentrations (Table 13). A control experiment without any biosurfactants was conducted, along with an experiment under physiological BS/PL conditions (BS/PL-9:4(NE)) but in the absence of intestinal enzymes (trypsin and chymotrypsin).

The INFOGEST protocol for proteolysis was applied with modifications to various biliary conditions (Table 13). Since β-Lg digestion in the presence of pancreatin occurred rapidly (Sousa et al. 2020), the conditions were adjusted to slow down the reaction, and the enzyme amount was reduced according to Dulko et al. (2021).

Since the study focused on the intestinal phase, the gastric phase was conducted in a single vessel to standardize the starting point for each condition in the intestinal phase. This approach aimed to minimize uncertainty and variability at the peptide level that might have been caused by uneven gastric digestion between biological replicates, providing a consistent basis for comparing experiments involving different compositions of biliary surfactants. Gass et al. (2007) examined the intestinal proteolysis of β-Lg that had been pre-treated with pepsin under simulated gastric conditions. They found that gastric treatment did not significantly affect the subsequent degradation of β-Lg during the intestinal phase; however, their conclusions were drawn at the level of whole protein, without analysis of the peptide profile. In contrast, Sousa et al. (2020) demonstrated that although β-Lg exhibits resistance to pepsinolysis, specific peptide fragments can still be detected during the gastric phase.

Three replicates of *in vitro* proteolysis of WPI and β-Lg were performed under the conditions described in the method section 3.3.1. A total of 27 digestion experiments were conducted, with 263 time-point samples collected during these experiments for subsequent analysis of proteolysis progress and peptide profiles.

The digestion progress of WPI for each experiment at various BS/PL ratio was monitored by SDS-PAGE, and the results are presented in Figure 4.12.The results shown in Figure 4.12e indicate strong reduction of β-Lg hydrolysis during *in vitro* intestinal proteolysis in the presence of PLs alone, consistent with previously published data (Mandalari, Mackie, et al. 2009). Intestinal digestion performed in the sole presence of BSs (13 mM) proceeded more rapidly, with only trace amounts of β-Lg fragments detected within the first ten minutes of digestion (Figure 4.12a). Comparable results were reported by Sousa et al. (2020), where β-Lg was fully digested at the protein level almost instantaneously under the conditions specified by the INFOGEST protocol (10 mM BSs and pancreatin) (Sousa et al. 2020).

In contrast under physiologically relevant concentrations of biosurfactants (BS/PL-9:4) (Figure 4.12b), the protein was fully digested after 60 minutes. Increased levels of PLs in the digestion mixture resulted in a delay in protein hydrolysis (Figure 4.12c-d). The intestinal digestion experiment conducted without biosurfactants (Control) (Figure 4.12f) demonstrated a slow progression of digestion, with the last visible band at 30 minutes, similar to the BS/PL 9:4 condition. However, the β-Lg band disappeared entirely during the second hour of the experiment, indicating a higher rate of proteolysis compared to the experiment conducted in the presence of PLs only (PL13) (Figure 4.12e). This observation suggests that PLs may protect β-Lg from intestinal proteolysis, as the undigested protein band remained visible after 2 hours of digestion (Figure 4.12g). The interactions of PLs with milk allergens, resulting in the retardation of in vitro digestion, were studied by Moreno et al. (2005). The study found that pepsinolysis of α-lactalbumin (α-La), a protein typically easily digested in the gastric phase, was inhibited in the presence of PLs. The authors suggested that the reduced digestion was due to the penetration of α-La into PL vesicles. However, the protein was subsequently fully digested during the intestinal phase, likely due to the action of BSs, which disrupted potential electrostatic interactions between the protein and the charged PL head groups, and diminished the steric barrier of the PL layer (F. J. Moreno, Mackie, and Mills 2005). Mandalari et al. (2009) reported on the protection of β-Lg from simulated gastrointestinal proteolysis in the presence of PC. The vesicular PC was found to slow down β-lg digestion, and an excess of PC changed the digesta peptide pattern. The authors proposed three possible mechanisms. Two were possible ligand bindings to the peptides, stabilizing the polypeptide mobility and thus protecting from digestion. Suggested binding sites were a peptide calyx and the strand of α-helix. The third suggested mechanism was that the PLs enclosed the proteins in the vesicles (Mandalari, Mackie, et al. 2009).

The results of the densitometric analysis of the electrophoresis gels presented in Figure 4.12a-g are summarized in Figure 4.13. The analysis indicated approximately 81% and 66% of the protein remaining after 30 minutes of digestion for the BS/PL 9:4 and Control conditions, respectively (Figure 4.13). The relative densitometric analysis was performed with reference to the initial point of the intestinal phase, providing an approximate measure of the progression of intestinal digestion.

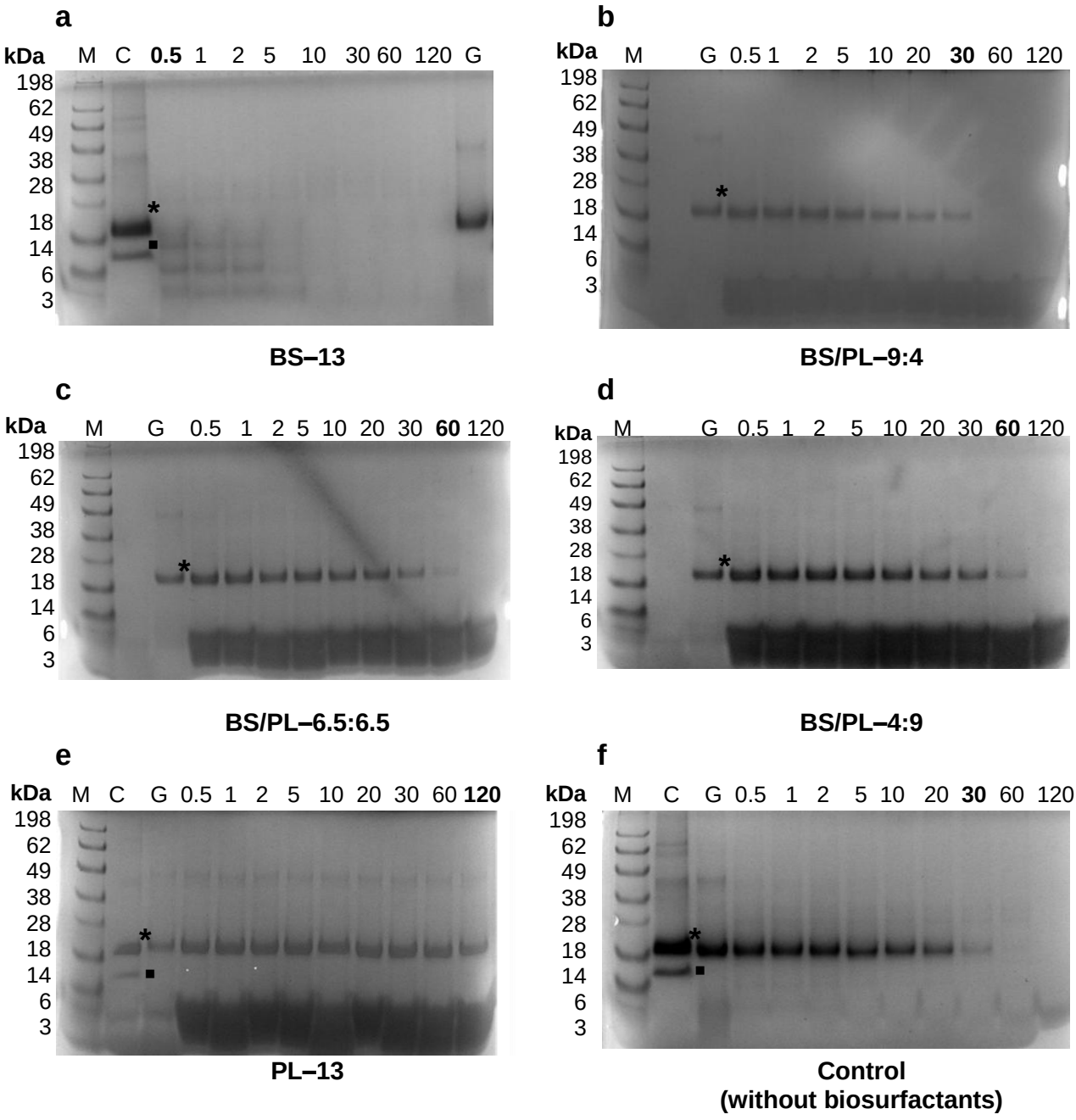

*Figure 4.12 SDS-PAGE gels of whey protein isolate (WPI) digestion (40 mg/mL) at various BS/PL ratios (a-g). M represents the molecular weight marker, C indicates the control (undigested WPI), and G denotes the final time point of the gastric phase (at 120 min). The numbers 0.5, 1, 2, 5, 10, 20, 30, 60, and 120 correspond to time points (in minutes) of the intestinal phase, where bold numbers indicate the last time point with a visible band. * β-lactoglobulin (molecular weight 18.281 Da); ■ α-lactalbumin; NE stands for the experiment without trypsin and chymotrypsin.*

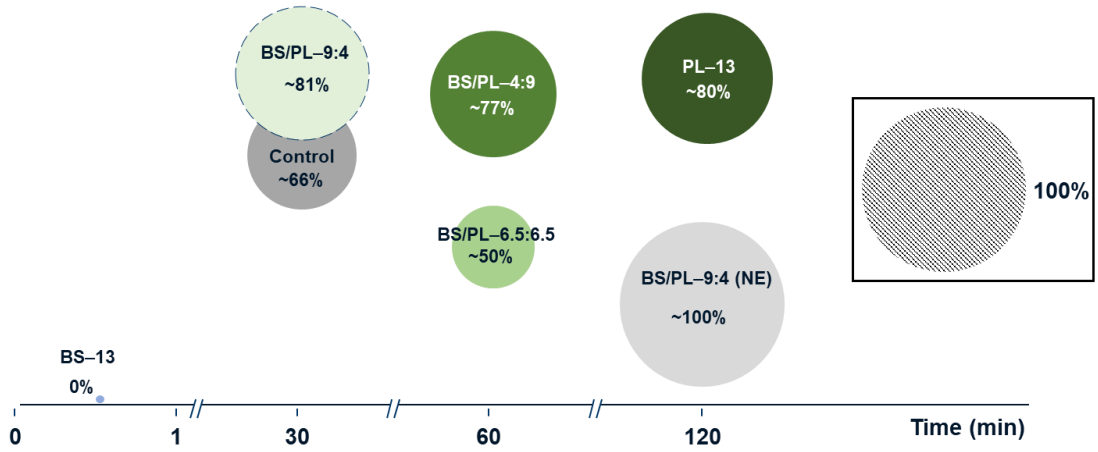

Figure 4.13. Densitometric analysis of WPI digestion, shown in Figure 4.12, in the presence of various biosurfactant concentrations (Table 13). The graph represents the relative percentage of undigested β-Lg remaining in the final visible bands at different time points during the intestinal phase.

Densitometric analysis indicated only an approximately 20% progress in β-Lg intestinal digestion under the PL-13 condition over a period of 2 hours. In contrast, protein digestion under conditions involving both PLs and BSs, specifically BS/PL 6.5:6.5 and BS/PL 4:9, reached approximately 50% and 23%, respectively, within the first hour of digestion. The BS/PL 9:4 condition resulted in approximately 19% digestion within a shorter time frame (30 minutes) and complete degradation within 1 hour. These results indicate the influence BSs, which is consistent with the literature describing their enhanced effect on some protein digestion (Gass et al. 2007; Dulko et al. 2021). Gass et al. (2007) conducted proteolysis experiments in the presence of a mixture of six physiologically relevant BSs and in the presence of mixed micelles comprising BSs, oleic acid, and monoolein. Their results demonstrated an increased effect on β-Lg proteolysis in the presence of BSs, with a moderate increase observed when mixed micelles were present. They showed that even a low concentration of BSs (2 mM) enhanced β-Lg digestion, with the most effective enhancement occurring at concentrations above the critical micelle concentration of the BS mixture (3.5 mM). Although the authors claimed to use physiologically relevant conditions for intestinal digestion, the 10 mM concentration of the BS mixture might not accurately reflect the natural composition of human bile, and the micelles used in their experiments did not include PLs, which are an integral component of human bile. This was confirmed in more recent research by Dulko et al. (2021), who conducted experiments using real human bile samples and individual BSs. The authors demonstrated that the total bile concentration has a more significant impact than the composition of individual BSs. They also showed that results obtained with human bile closely matched those with a mixture of BSs and PLs, indicating that this mixture can effectively simulate human bile. Furthermore, their study highlighted the influence of BS concentration on the increased rate of β-Lg proteolysis.

Following the analysis of WPI digestion, the digestion of pure β-Lg was conducted to facilitate in-depth mass spectrometry analysis, aiming to evaluate the influence of biliary surfactants at physiological concentration on β-Lg digestion and to determine whether significant differences exist in the peptide profile. Two experimental conditions were selected for this purpose: physiologically relevant condition BS/PL 9:4 and a Control condition (without biliary surfactants), as both conditions exhibited comparable protein degradation times during WPI digestion. SDS-PAGE analysis of pure β-Lg digestion (Figure 4.14a) indicated complete disappearance of the protein within the first hour under physiologically relevant conditions, while the Control condition (Figure 4.14b) remained undigested at the 120-minute time point. A detailed comparison at the peptide level is presented in the subsequent section 4.3.3, which focuses on mass spectrometry analysis.

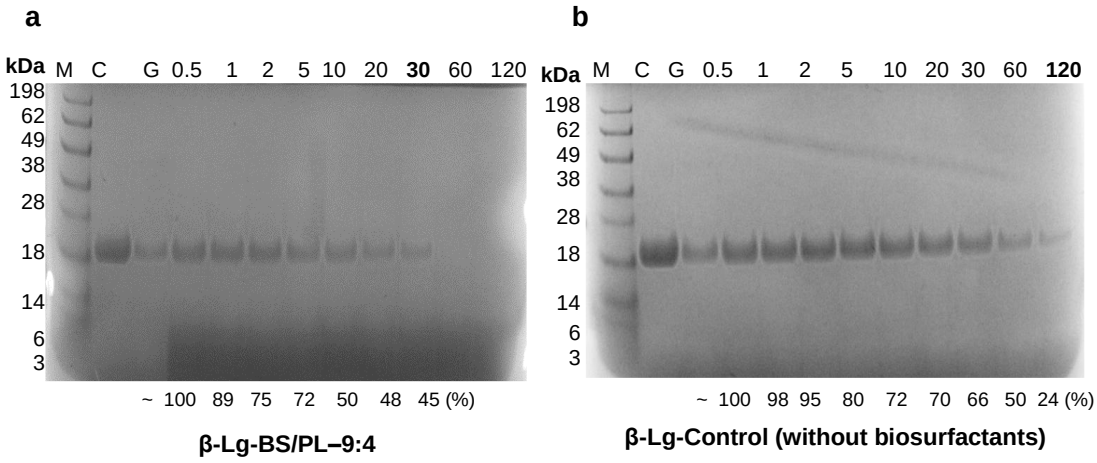

Figure 4.14. SDS-PAGE of the progress of pure β-Lg (MW 18.281 Da) digestion in the intestinal phase at various conditions, b) physiological concentration of biliary surfactants (BS/PL–9:4), b) Control - the intestinal β-Lg digestion without any biosurfactants indicates the control (undigested WPI), and G denotes the final time point during the gastric phase (at 120 min). The numbers 0.5, 1, 2, 5, 10, 20, 30, 60, and 120 correspond to time points (in minutes) of the intestinal phase, where the bold numbers indicate the last time point with a visible band. Values below the bands correspond to the approximate percentage of the undigested protein remaining at each particular time point.

There is very limited scientific literature available regarding the effect of biliary biosurfactants on protein digestion. The aforementioned articles can lead to the conclusion that PLs retard and BSs enhance digestion of β-lg. However, this study demonstrates that the rate of digestion depends on the BS/PL ratio. For WPI digesta, the extent of β-Lg digestion without any biosurfactants is comparable to the digestion observed with the lowest amount of PL addition (BS/PL-9:4). In contrast, the outcome differed for pure β-Lg digestion, where biosurfactants under physiological concentrations (β-Lg-BS/PL-9:4) showed an enhanced effect. The differences between WPI and pure β-Lg digestion might be attributed to the distinct digestive matrix of WPI digesta, which could limit β-Lg molecules aggregation. Consequently, under conditions with biosurfactants the digestion of the protein was more efficient.

4.3.2 **Analysis of Whey Protein Isolate digesta**

For a deeper analysis at the peptide level, mass spectrometry coupled with liquid chromatography was conducted. The analytical method used was DDA, in which precursor ions with the highest signal intensity were selected for further analysis by CID. The acquired data were processed using PEAKS software, where LFQ was applied to normalize data and quantify detected peptides. The software provides comprehensive analysis with an advanced peptide quality scoring method, which defines the quality of each peptide feature (including differences in retention time (rt), mass-to-charge ratio (m/z), similarity in chromatogram shape (XIC), and feature intensity). A higher quality score indicates a more reliable and reproducible peptide quantification outcome.

Since WPI proteins like BSA and α-La are easily digested during pepsinolysis, while β-Lg remains undigested after 120 min (X. Wang et al. 2018; Sutantawong et al. 2025), the focus of this study was on β-Lg. The results for the sum peak area and sequence coverage for BSA and α-La are presented in the Appendix Figure 7.1 and Table 17.

As previously mentioned, protein digestion experiments (WPI and β-Lg) were performed in a single vessel during the gastric phase to ensure the highest quality analysis during the intestinal phase, allowing for comparison across different conditions (Table 13) with high sample correlation at the peptide level. The average sample correlation outcomes for each condition were as follows: PL-13, 0.76 ± 0.17; BS/PL-6.5:6.5, 0.67 ± 0.21; BS/PL-4:9, 0.69 ± 0.18; BS/PL-9:4, 0.52 ± 0.29; BS-13, 0.97 ± 0.29; Control, 0.73 ± 0.18; and BS/PL-9:4(NE), 0.96 ± 0.04. As digestion progressed dynamically at the peptide level under the conditions PL-13, BS/PL-6.5:6.5, BS/PL-4:9, BS/PL-9:4, and Control, the sample correlation of biological replicates decreased. The very high correlation in BS-13 (0.97 ± 0.29) suggests stable digestion pattern at peptide level, similar to BS/PL-9:4(NE) (0.96 ± 0.04), where the experiment was conducted without intestinal enzymes. The high correlation in these experiments reflects good laboratory practices and repeatability. It rules out errors related to sample preparation, biosurfactant removal, and associated losses. Since all samples were handled in the same manner, it can be concluded that as digestion progresses, a variety of peptides are produced, which causes a reduction in the sample correlation of biological replicates. The sequence coverage for β-Lg in WPI digestion experiments was as follows: 100% for experiments BS/PL-9:4 and BS/PL-4:9, 97.2% for Control, 96.6% for BS-13, and 91.6% for BS/PL-6.5-6.5 and PL-13.

Since the aim of the study was to observe protein digestion in the presence of PLs, a similar approach as in lipolysis was used, replacing pancreatin with pure enzymes. Two main digestive enzymes, trypsin and chymotrypsin, were used instead of pancreatin. Pancreatin contains PLA_2 and carboxyl esterase, which would digest PLs and change their ratio compared to BSs. As reported previously, lysolecithin may promote the destabilization of β-Lg's native conformation, comparable to thermal or alkaline denaturation (Korver and Meder 1974). It would introduce too many variables, making the experiment too complex for drawing specific conclusions about the effect of PLs on protein digestion.

The results for the sum peak area are presented in Figure 4.15, providing overall information about the relative total quantity of peptides released from β-Lg over two hours of WPI digestion. This measure reflects the progress of protein digestion at the peptide level. The results for physiologically relevant condition (BS/PL-9:4) show that the initial phase of β-Lg digestion is highly intense, as illustrated in the graph (Figure 4.15a). The intensity of the sum peak area for physiologically relevant conditions decreases over the first hour and stabilizes in the second hour, and becomes similar to the pattern observed in experiments with BS-13.

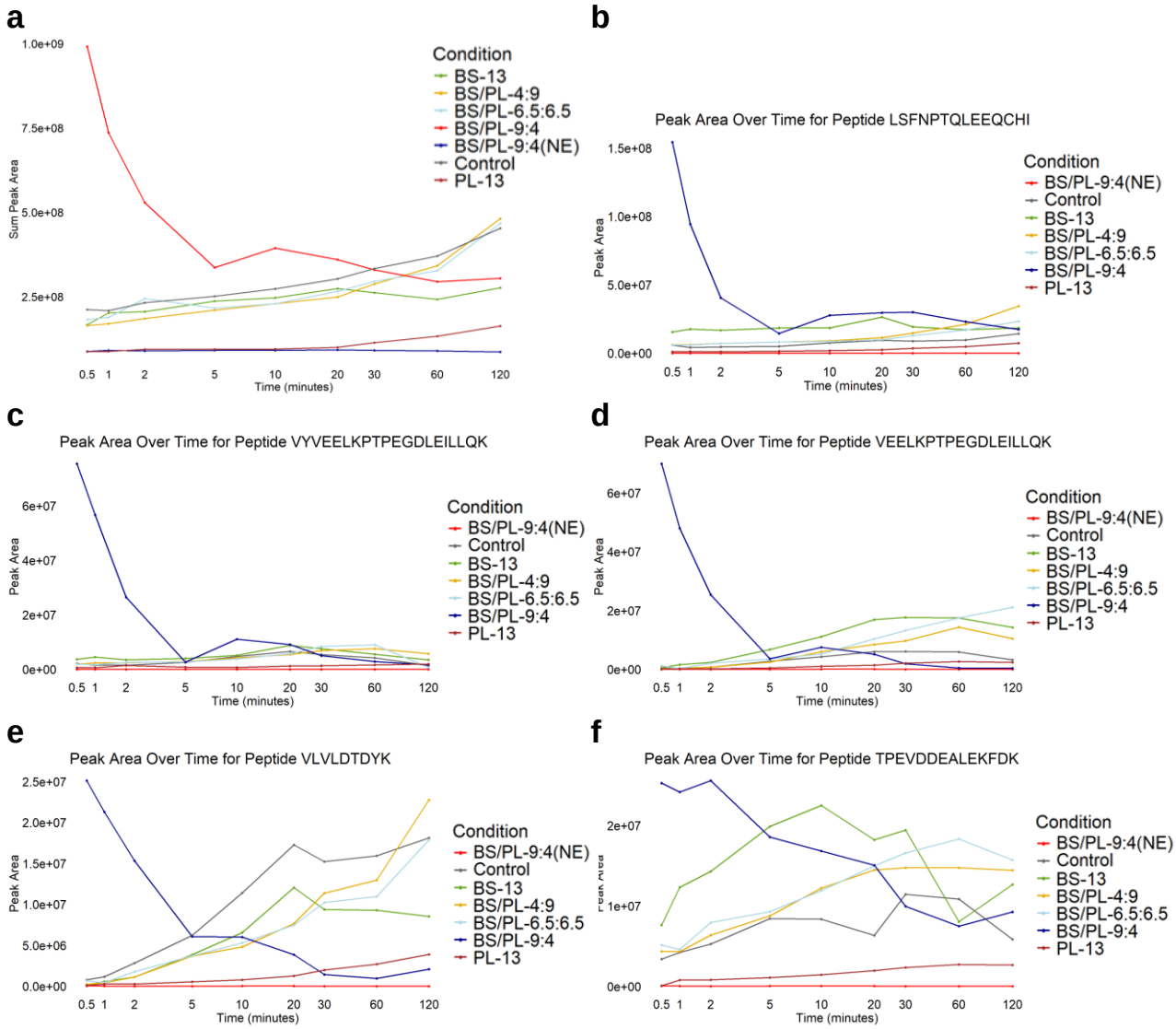

Figure 4.15 a) Sum of peak area for β-Lg peptides released over 2 hours of WPI digestion at various ratios of biosurfactants (Table 13). BS/PL-9:4(NE) represents an experiment without intestinal digestive enzymes; b-f) Peak area of peptides with exceptionally high signal intensity under BS/PL-9:4 conditions. Figures showing the kinetics of each corresponding peptide with standard deviation (SD) are provided in the Appendix, Figure 7.3a-e.

In contrast, the intensity of sum peak area in the experiment with only PLs (PL-13) was very low, remaining comparable to the control experiment (BS/PL-9:4(NE)), conducted without any intestinal digestive enzymes) for up to 20 minutes. Over the next 90 minutes, the intensity gradually increased but never reached levels comparable to other experiments with biosurfactants or even to the Control experiment without any biosurfactants. The Control, BS/PL-4:9, and BS/PL-6.5:6.5 experiments exhibited a similar trend in changes in the sum area over time, with a steady increase.

The initial high intensity of BS/PL-9:4 was mainly caused by five peptides. These peptides had a peak area above 10^7: VYVEELKPTPEGDLEILLQK (41-60), VEELKPTPEGDLEILLQK (43-60), TPEVDDEALEKFDK (125-138), and VLVLDTDYK (92-100) (Figure 4.15c-f). One peptide stood out: LSFNPTQLEEQCHI (149-162) (Figure 4.15b). Its peak area was one order of magnitude higher than other peptides, exceeding 10^8, and will be discussed later. Peptides VYVEELKPTPEGDLEILLQK, VLVLDTDYK, and LSFNPTQLEEQCHI have been described in the literature as stable, β-Lg-specific peptides. They are resistant to matrix complexity interference and were selected as milk biomarkers for studying the authenticity of animal feed (Lecrenier et al. 2018) and

identification of milk allergens (Planque et al. 2016). These peptides are discussed in more detail in section 4.3.5.

The heatmap at Figure 4.16 represents the evolution over 2 hours of WPI digestion at various conditions aligned to β-Lg protein sequence for each intestinal condition according to Table 13. Dark blue color indicates low count of amino acids belonged to the particular peptide sequence (starting from one count), fading color converting into yellow and orange indicate the increase of counts. The heat map reveals visible differences between experiments under various intestinal conditions. Experiments with only PLs (PL-13) and only BSs (BS-13) as well as Control resulted in a lower occurrence of peptides in the 29-39 region, while at the physiological concentration (BS/PL-9:4), a noticeably higher number of released peptides was observed in this region. Additionally, the regions around 83-99 and 129-149 showed a higher abundance of released peptides under these conditions compared to other experiments. Moreover, the sequence segments around 20-42 (especially 24-28) and 105-117 exhibited an intense orange color, indicating a greater presence of peptides in these regions. In the other experiments with PLs, the color intensity in these sequence regions decreases as the BS content decreases. However, it can be observed that the color intensity for BSs alone is not as strong as in physiologically relevant conditions or even in PL-only conditions. In general, the experiments with only BSs (BS-13) resulted in regions with deep blue colors, indicating a low presence of released peptides in these areas. This may suggest complete digestion of peptides originating from certain parts of the protein (e.g., 1-20, 70-77, 99-104, 138-141), as observed in the SDS-PAGE gels (Figure 4.12a).

Considering the peptide pattern in the context of the interplay between BS and PL, it can be observed that the addition of BSs changes the digestion pattern depending on their concentration. Excluding the physiological concentration BS/PL-9:4, which stands out among the other combinations, the similarities are observed in the BS-13 and BS/PL-6.5:6.5 experiments (regions 1-20, 69-83, terminal part 120-149). However, in these experiments, disparities are observed in some regions, making the digestive pattern of BS/PL-6.5:6.5 conditions similar to those experiments containing PLs. These regions include 1–8, 86–100, and 120–148. The differences in these segments become evident as the PLs ratio increases, as in BS/PL-4:9 (particularly the proximal part 1-20 and the segment 120–148), which approaches the physiological ratio BS/PL-9:4. In the initial region of the protein sequence (1–20), the intensity of the yellow color increases with a higher PL content and decreases with a higher BS content. Under Control conditions, this segment (1–20) is similar to the experiment with BSs alone, and it appears dark blue, indicating a low number of peptides found in this range. The regions that differentiate Control conditions from BS-13 are 83–100 and 125–149, which have a color shade similar to conditions containing PLs. In the condition without intestinal enzymes (BS/PL-9:4(NE)), representing the final point of gastric digestion, peptides from the sequence ranges 1–54, 103–117, and 140–146 are visible. The regions with the lowest number of peptides are the central part of the protein sequence, approximately 54–104, as well as the fragment and 117–136 and terminal part 146–162.

The physiologically relevant condition (BS/PL-9:4) differs substantially from the experiments conducted under other conditions. The results obtained for BS/PL-9:4 are consistent with those of in vivo digestion of β-Lg performed by Sanchón et al (2018). The main digestion regions identified in their *in vivo* studies were sequences approximately 40–80 and 90–140 (Sanchón et al. 2018). Specifically, under physiologically relevant conditions (BS/PL-9:4), the sequence 121–138 showed substantial differences compared to other conditions.

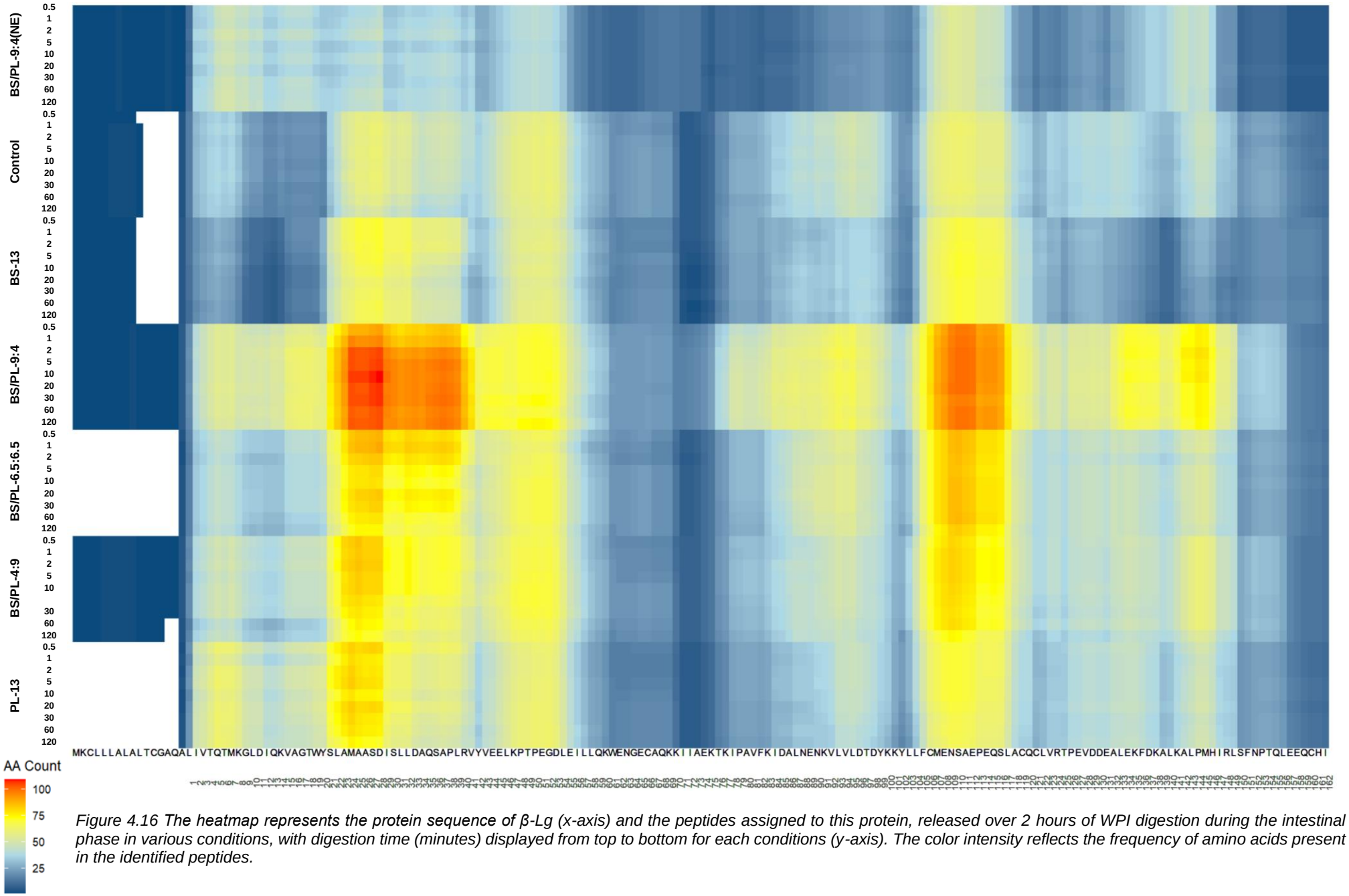

Figure 4.16 The heatmap represents the protein sequence of β-Lg (x-axis) and the peptides assigned to this protein, released over 2 hours of WPI digestion during the intestinal phase in various conditions, with digestion time (minutes) displayed from top to bottom for each conditions (y-axis). The color intensity reflects the frequency of amino acids present in the identified peptides.

In the study by Sanchón et al. (2018), the *in vivo* results closely reflected the *in vitro* digestion of β-Lg conducted following the INFOGEST protocol. Importantly, the protocol recommends using bovine or porcine bile extracts at BSs concentration of 10 mM but does not address the standardization or specific concentrations of PLs (Brodkorb et al. 2019). In Sanchón's study (2018), pig bile extract was used. As is known, bile extracts are not fully purified mixtures and may contain PLs as impurities. However, the effect of PLs combined with BSs on β-Lg digestion and the resulting peptide profile has not yet been investigated. To accurately reflect human bile and improve *in vitro* digestion models, it is essential to account for appropriate PLs concentrations. The present results, illustrated on the heatmap, provide crucial insights into differences in the digestion of specific protein sequences. These differences, in turn, influence the release of peptides that may have biological significance, as discussed in the following sections of this dissertation (section 4.3.3). Despite the high consistency between *in vivo* and *in vitro* studies reported in Sanchón's article (2018), certain regions from *in vivo* digestion were not fully covered in the *in vitro* experiments. These included sequences 20–40 and 70–100. In my study, under physiologically relevant conditions, these protein regions (sequences 20–40 and 70–100) also showed alignment with the cited *in vivo* results. This may serve as evidence that the physiological conditions are well reflected in the applied model system.

Moreover, Figure 7.2 (Appendix), shows the heatmap for the gastric phase. These results are consistent with those obtained by Sousa et al. (2020), particularly in the relatively intensive digestion of the initial segment (1–20) and the terminal region (above position 100), with lower effectiveness observed in the middle part of the sequence (55–80).

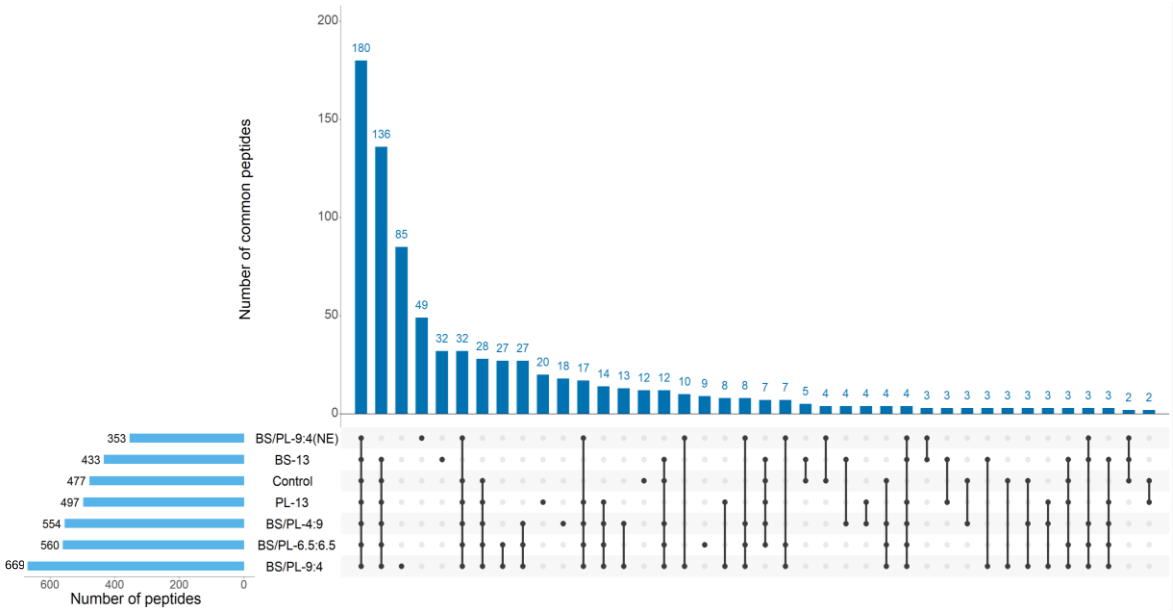

Figure 4.17 The figure shows the number of peptides identified for β-Lg during 2 hours of WPI digestion. It includes the intestinal phase under different BS/PL ratios. The Control was performed without any biosurfactant, while BS/PL-9:4(NE) represents an experiment without intestinal enzymes. The total number of peptides is shown by horizontal bars. Vertical bars represent number of peptides common to the conditions, indicated by black dots connected by lines. A single black dot represents unique peptides for a given condition that were not shared with other conditions.

The highest total number of peptides was observed during the gastric phase, with 721 different peptides identified over 2 hours of digestion. The total number of peptides found during intestinal digestion under various conditions is presented in the Figure 4.17. For the physiologically relevant conditions (BS/PL-9:4), the total number of peptides was the highest among all intestinal experiments, reaching 669 peptides. The physiologically relevant condition is especially distinguished by the number of unique peptides, with 85 peptides being unique to this condition (BS/PL-9:4). The lowest peptide count was observed in the experimental condition without intestinal enzymes (BS/PL-9:4(NE)), with

353 total peptides and 49 unique peptides. BS/PL-9:4(NE) represents the final point of the gastric phase, where pepsin was the only active enzyme. However, comparing conditions with trypsin and chymotrypsin, the condition with BSs alone (BS-13) yielded the lowest peptide count (433 total, 32 unique) and Control 477 of total number with only 12 unique peptides.

The mean (± SD) molecular weight for peptides found in physiologically relevant conditions BS/PL-9:4 was the highest 1382.98 ± 654.19 (median 1262.62), PL-13 1321.88 ± 713.27, BS/PL-4:9 1313. 56 ± 651.13, BS/PL-6.5:6.5 resulted in 1299 ± 619.69 Da, next comparable for Control 1235.00 ± 650.68 Da and BS-13 1225.95 ± 632.81 Da. The size distribution over time across the different conditions is presented in Figure 7.5 (Appendix).

The number of peptides found for each specific condition did not significantly change over time, as presented in Table 15. This is most likely due to the equilibrium formed by peptides generated during digestion, caused by the lack of other proteolytic enzymes, such as carboxypeptidases A and B. These enzymes would further break down the peptides formed by trypsin and chymotrypsin. This process would lead to greater diversification of the peptide profile over time and eventually result in the complete breakdown of some peptides.

Table 15 The evolution of peptide number found over 2 hours of digestion for intestinal phase at various experimental conditions. The outcome represents number of peptides after LFQ analysis.

Time:	0.5 min	1 min	2 min	5 min	10 min	20 min	30 min	60 min	120 min
BS-13	405	414	411	411	404	401	402	404	395
BS/PL-4:9	538	538	544	541	546	539	534	529	509
BS/PL-6.5:6.5	544	543	529	544	544	551	545	536	525
BS/PL-9:4	636	645	655	654	655	652	650	650	650
BS/PL-9:4(NE)	348	347	351	344	349	348	348	347	349
Control	459	467	462	464	459	467	460	456	445
PL-13	484	475	478	482	476	479	475	473	468

The low number of peptides in BS-13 may indicate less diverse protein breakdown, resulting in a relatively uniform peptide profile, achieved through tryptic and chymotryptic digestion. This is evidenced by the high correlation of samples between biological replicates (0.97). This can also be seen in Figure 7.7 (Appendix), which distinguishes BS-13 from other conditions of intestinal digestion. The diagram shows the percentage contribution of cleavage sites across the peptide sequence. In BS-13, cleavages typical for trypsin dominate over those from the gastric phase, which are typical for pepsin, such as Leu, Trp or Phe (Keil 1992). This is due to the complete digestion of the protein and achieving the maximum percentage contribution of cleavage sites typical for intestinal proteolytic enzymes. Specific cleavage sites dominate at particular positions of the protein sequence, such as Lys70, Lys60, Lys83, Lys91, Lys100, Lys101, Lys138, Arg40 and Arg124. This cleavage pattern leads to a more uniform peptide profile, and consequently, fewer detected peptides compared to other conditions where cleavage sites from gastric and intestinal phase are more evenly distributed across the protein sequence. This is also confirmed by the relatively stable trend of the sum intensity curve for BS-13, with only a slight increase in intensity over time, which may indicate a lower number of detected peptides, although the protein was fully digested Figure 4.15a.

Furthermore, the SDS-PAGE gels show degradation to relatively large protein fragments within the first 5 minutes, which disappear after about 10 minutes of digestion Figure 4.12a. This also shows evidence of a different protein cleavage pattern compared to all other conditions, where the protein stayed intact for a longer digestion period, and no bands of cleaved protein were visible below the band of undigested β-Lg molecules Figure 4.12b-g.

Although under PL-13 conditions the number of peptides is higher than in BS-13 (497), it is still relatively low compared to the physiologically relevant condition (Figure 4.17). The heatmap shows the presence of peptides across the entire protein sequence, indicating complete digestion of the β-Lg molecule. Hence, the number of peptides may reflect an equilibrium between the undigested protein and released peptides, as slowed digestion was observed at the protein level on the SDS-PAGE gels. The relatively low number of peptides may suggest slower protein cleavage due to protection and steric hindrance by PLs, which could have obstructed enzyme access to the substrate (Mandalari, Mackie, et al. 2009). This is further confirmed by the sum intensity, which starts to increase only after 20 minutes, indicating delayed peptide release from the protein (Figure 4.15).

Moreover, the conditions with the mixture of PLs and BSs (BS/PL-9:4, BS/PL-6.5:6.5, BS/PL-4:9) as well Control, exhibit more disordered protein cleavage sites compared to BS-13, leading to a high number of peptides and diverse peptide profile. The Figure 7.7 (Appendix) shows diverse contribution of cleavage sites across the protein sequence coming from both gastric and intestinal enzymes. Indicating that peptides with cleavage sites from the gastric phase have a relatively high contribution in the total percentage of cleavage sites. A peptide profile with a high number of peptides may indicate a state where peptides from the gastric phase accumulate along with newly formed peptides in the intestinal phase, leading to a diverse peptide profile. The persistence of peptides from the gastric phase could be due to interactions or aggregation with PLs or mixed micelles (Banerjee and Onyuksel 2012; Groleau et al. 2003), which prevent them from digestion. The kinetic of very long peptide originating from the gastric phase, VRTPEVDDEALEKFDKALKALPMHIRLSFNPTQLEEQCHI (123-162) and IVTQTMKGLDIQKVAGTWYSLAMAASDISLLDAQSAPLRV (2-41) may support these assumptions. It persisted throughout the entire intestinal digestion period under PL-13 conditions but was not found in other intestinal conditions.

Additionally, the results presented in Figure 7.7 (Appendix) show clear differences in the percentage contribution of various cleavage sites depending on the conditions. Specifically, the example is Leu149 (Appendix Figure 7.7). It has a negligible contribution under BS-13 conditions (only 3 peptides ending with this amino acid were found), while in other conditions, it has a higher percentage contribution: 2.3% for Control (11 peptides), 2.9% for BS/PL-6.5:6.5 (16 peptides), 2.8% for PL-13 (14 peptides), 2.4% for BS/PL-9:4 (16 peptides) and 2.5% for BS/PL-4:9 (14 peptides). Under gastric conditions of the final time point represented by BS/PL-9:4(NE) the percentage contribution of the cleavage site at position Leu149 was 1.4% (9 peptides). These results indicate the extensive digestion of peptides ending with Leu149 in the case of BS-13, whereas in other conditions, peptides from the gastric phase remained in digestive mixture, undergoing partial breakdown. This leads to a more diverse peptide profile. An example is the long peptide VRTPEVDDEALEKFDKALKALPMHIRL (123-149), which originated from the gastric phase. In all intestinal conditions including Control and PLs addition, it showed similar kinetics (Appendix Figure 7.4) and underwent slow degradation over time. However, this peptide was not identified in the experiment with BSs alone, indicating its immediate breakdown during the initial stage of intestinal digestion. Where the cleavage site was centered on Lys138 (Appendix Figure 7.7), as discussed earlier. The low number of peptides in this region for BS-13 is illustrated by the dark blue area on the heatmap (Figure 4.16). Furthermore, another possibility is that the diverse peptide profile results from miss-cleavages during trypsin and chymotrypsin digestion due to varied digestion conditions, as well as the rate of digestion could be influenced by the interactions of intestinal enzymes with biosurfactants. It has been reported that the cleavage sites and miss-cleavages of tryptic digestion of β-Lg depend on factors such as the type of buffer and its concentration, leading to different peptide patterns (Cheison et al. 2011). Additionally, studies conducted by Verma et al. (Verma et al. 2015) demonstrated the effect of surfactants in increasing trypsin activity by better stabilizing catalytic sites through micellar complexes. The strongest enhancement of activity was observed in the presence of

cationic surfactants due to strong electrostatic interactions, while zwitterionic surfactants showed a smaller, but still higher, effect compared to the control experiment (Verma et al. 2015). Moreover, Najar studied the interactions between BSs and trypsin, showing that significant unfolding of trypsin occurs during these interactions, with the effect depending on the type of BSs. The strongest interactions were observed in the presence of the hydrophobic NaTDC, while the weakest were noted for NaTC and NaC (Najar et al. 2021). Unfortunately, the influence of these interactions on enzyme activity was not investigated. Additionally, the activity of α-chymotrypsin was investigated in the presence of sodium glycocholate (NaGC) micelles and linoleic acid, which accelerated insulin degradation. The catalysis could result either from the direct attack of linoleic acid on insulin or from the allosteric regulation of α-chymotrypsin activity (Y. Li, Shao, and Mitra 1993). It cannot be ruled out that the combination of biliary surfactants, particularly at physiologically relevant concentrations, may influence the activity and cleavage specificity of enzymes resulted in high number of unique peptides (85) and outstanding intensities of certain peptides. This is discussed in further detail later in this dissertation (section 4.3.5). However, the mechanism behind specificity and missed cleavages during tryptic and chymotryptic digestion, caused by changing conditions during digestion, as well as enzyme activity and its selectiveness under various BS/PL conditions, has not been confirmed and remains unexplored.

Under Control conditions (without any surfactants), digestion is also delayed but to a much lesser extent than under PL-13 conditions. The high intensity of the sum area indicates that digestion is more efficient than in PL-13. However, the number of detected peptides in Control is comparable to number of peptides found under PL-13 conditions differing by only 20 peptides. The low number of peptides and the slowed digestion under Control conditions likely result from reduced intestinal enzyme activity due to less accessible substrate structure. This might be caused by the absence of BSs in the digestive mixture, which unfold the spatial structure of the protein and accelerate cleavage, as previously described by Robic et al. (2011). This article shows that BAs play a key role in protein digestion by supporting trypsin and chymotrypsin through the destabilization of large protein substrates, facilitating their cleavage. However, for small substrates, the lack of impact on enzymatic activity suggests that cholic acid or glycocholic acid do not directly affect the enzymes (Robic et al. 2011). This may explain the very rapid breakdown of the β-Lg protein into smaller fragments during the initial stage of digestion, but not necessarily the fast degradation of all generated peptides. It may explain the similarity of the kinetics of many peptides observed under BS-13 conditions to the kinetics of the same peptides released in other conditions, as shown below. This indicates that despite differences in the digestion rate, certain peptides follow comparable release and degradation patterns (Id et al. 2020). However, while there were many similarities in the kinetics of certain peptides, numerous disparities occurred depending on the conditions, as shown in the heatmap below (Figure 4.18). The heatmap presents a comparison of the kinetics of 50 peptides released from β-Lg during 2 hours of intestinal digestion under different conditions. Figure 4.18, shows that peptide VYVEELKPTPEGDLEILLQK dominated in signal intensity under BS/PL-9:4 conditions (among the compared list of peptides), while the peptide TPEVDDEALEKFDK was the dominant peptide under BS-13 conditions. In the other conditions, which contained higher PL concentrations (PL-13, BS/PL-4:9, BS/PL-6.5:6.5), as well as the Control, peptides VYVEELKPTPEGDLEILLQK and TPEVDDEALEKFDK showed lower signal intensity. In contrast, the peptide IPAVF had the highest intensity in these conditions (PL-13, BS/PL-4:9, BS/PL-6.5:6.5), while its intensity was lower in BS-13 and BS/PL-9:4 conditions. Under conditions without intestinal enzymes (BS/PL-9:4(NE)), the intensity of peptide DAQSAPLRV was predominant. This peptide was gradually degraded under all intestinal conditions; however, the saturation in yellow color under PL-13 conditions indicates a high concentration of this peptide, which suggests a slowed digestion process (Figure 4.18).

BS/PL-9:4(NE) *

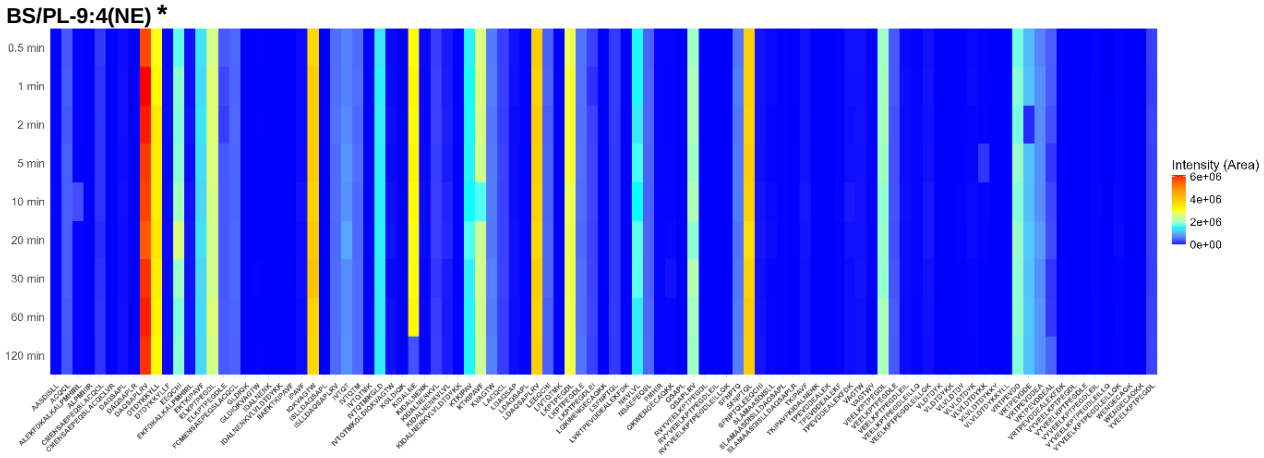

Control

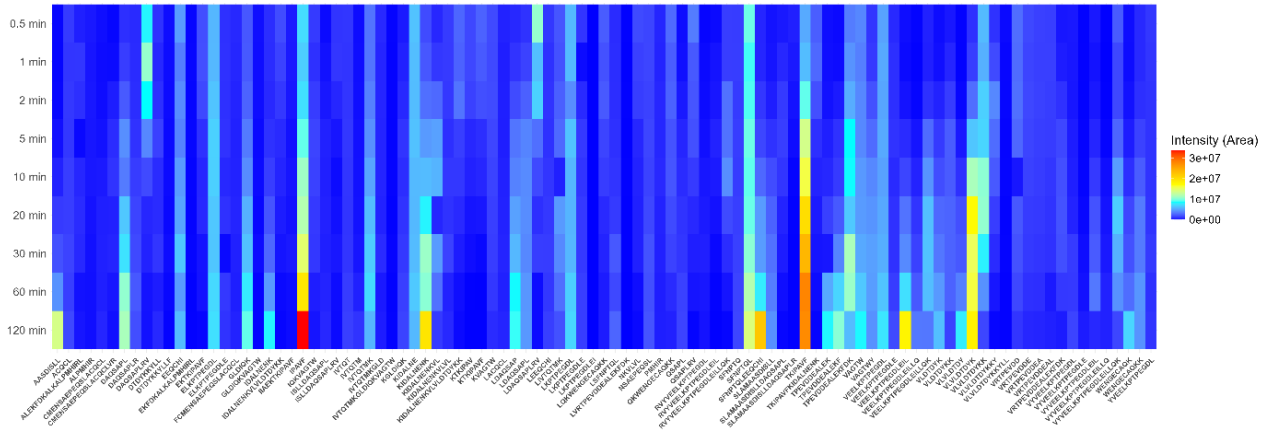

BS-13

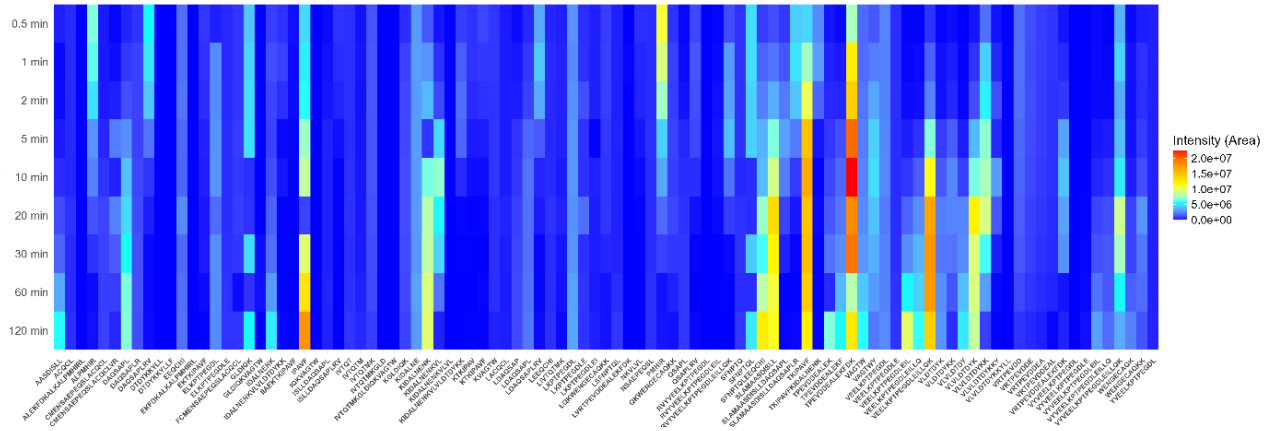

BS/PL-9:4

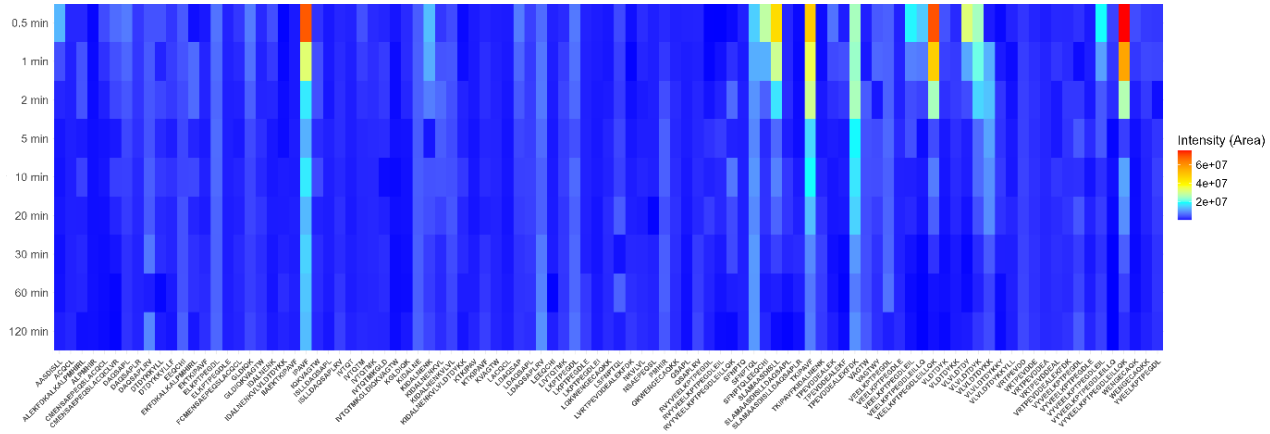

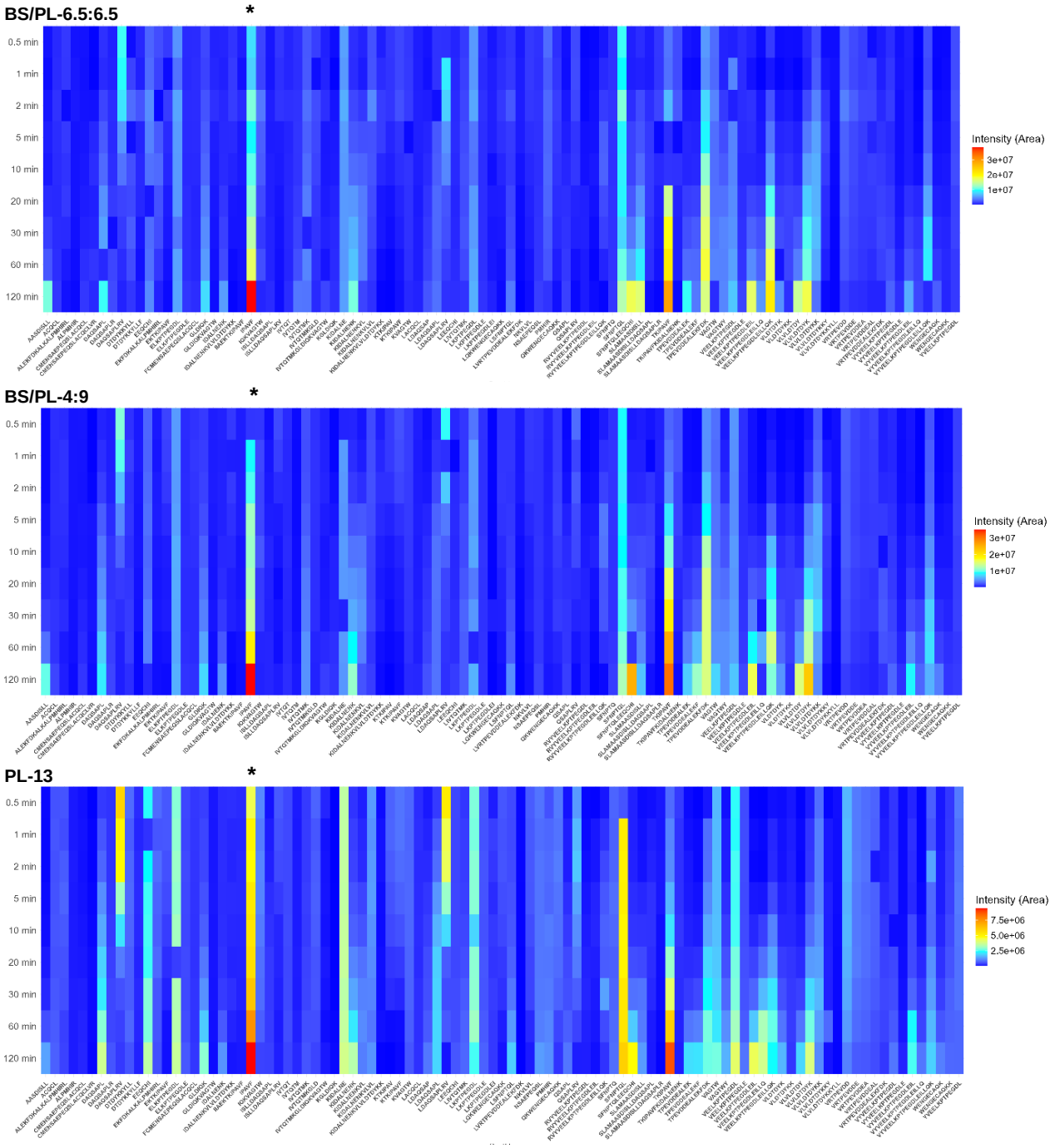

Figure 4.18 The heatmap presents the relative comparison of kinetic evolution (formation and degradation) of peptides found over 2 hours of WPI intestinal digestion at various biliary surfactant ratios. Top 50 peptides from physiologically relevant conditions (BS/PL-9:4) were chosen as a reference list for x-axis. Peptide LSFNPTQLEEQCHI was excluded from the list, due to high intensity and is discussed in details in section 4.3.5. Asterisk indicates the peptide with the highest intensity among the compared list of peptides within a given condition.

The peptides TPEVDDEALEKFDK (125-136) (Figure 4.15f and Appendix Figure 7.3e) and VRTPEVDDEALEKFDK (123-136) (Figure 4.19) under BS-13 were metastable, meaning they were released from larger fragments or the parent protein and were further degraded. The signal intensity of TPEVDDEALEKFDK (Appendix Figure 7.3e) peptide increased and reached its peak at 10 minutes of digestion, after which it gradually decreased in signal intensity by 120 minutes. In other conditions (BS/PL-4:9, BS/PL-6.5:6.5), this peptide showed very low intensity during the first 1-5 minutes, and increased over time, reaching its maximum signal intensity at the end of digestion. Under physiological conditions (BS/PL9:4), peptide TPEVDDEALEKFDK (Appendix Figure 7.3e) appeared in substantial quantities within the first 30 seconds, then largely diminished after 2 hours of digestion.
The peptide VRTPEVDDEALEKFDK (Figure 4.19) was metastable under conditions such as Control, BS/PL-6.5:6.5, and BS/PL-4:9, similar to BS-13. However, under BS/PL-9:4 conditions, the signal intensity fluctuated at a relatively high intensity level.

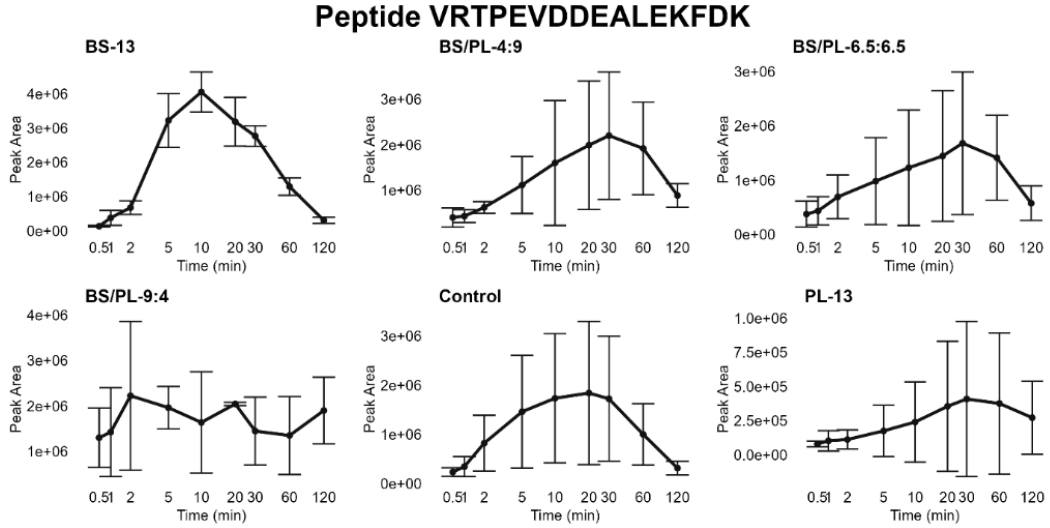

Figure 4.19 The kinetics of peptide VRTPEVDDEALEKFDK (123-136) assigned for β-Lg found during 2-hour WPI intestinal digestion under various biliary surfactant concentrations (only BSs: BS-13; BS/PL mixtures: BS/PL-9:4, BS/PL-6.5:6.5, BS/PL-4:9; only PLs: PL-13; and Control, without biosurfactants).

The formation of the peptide VEELKPTPEGDLEILLQK (43-60) was reversed under physiologically relevant conditions (BS/PL-9:4) compared to other conditions (BS-13, PL-13, BS/PL-6.5;6.5, BS/PL-4:9). It reached its highest intensity in the first 30 seconds of digestion and then decreased over time. However, in other conditions, its intensity increased over time, reaching the highest intensity within the first hour of digestion (BS-13, BS/PL-4-9, PL-13, Control) and within 2 hours for BS/PL-6.5:6.5. A similar pattern was observed for peptides from the same protein region, such as VYVEELKPTPEGDLEILLQK (41-60) and VYVEELKPTPEGDLEIL (41-57). Their kinetics are provided in (Figure 4.15c-d).

The signal intensity of the peptide IPAVF (78-82) (Figure 4.20) gradually increased under BS-13 conditions reaching its peak at the second hour of digestion. This trend is opposite to physiologically relevant conditions, where the intensity started very high initially, dropped sharply, and remained at a much lower but stable level from the second minute until the end of digestion. The same situation was observed for peptides KIDALNENK and AASDISLL (Figure 4.18).

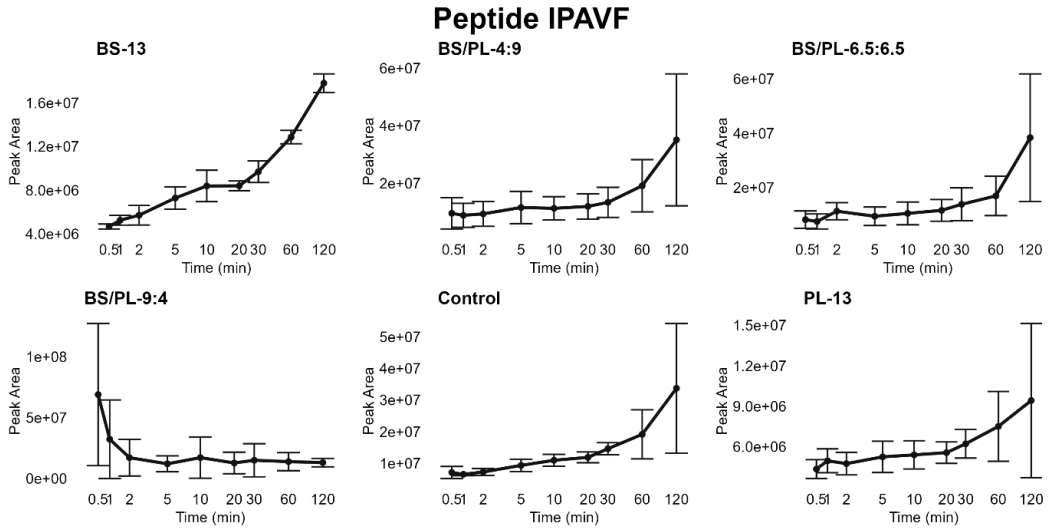

Figure 4.20 The kinetics of peptide IPAVF assigned for β-Lg found during 2-hour WPI intestinal digestion under various biliary surfactant concentrations (only BSs: BS-13; BS/PL mixtures: BS/PL-9:4, BS/PL-6.5:6.5, BS/PL-4:9; only PLs: PL-13; and Control, without biosurfactants).

The kinetics of the peptide VAGTW (15-19) (Figure 4.21) was similar across all conditions, with intensity increasing over time, except physiologically relevant conditions. For conditions BS-13, BS/PL-4:9, Control, and PL-13, the increased was gradual. In the case of BS/PL-9:4, there was a sharp decrease in the second minute of digestion. Similar trend was observed for peptide DAQSAPL (Figure 4.22).

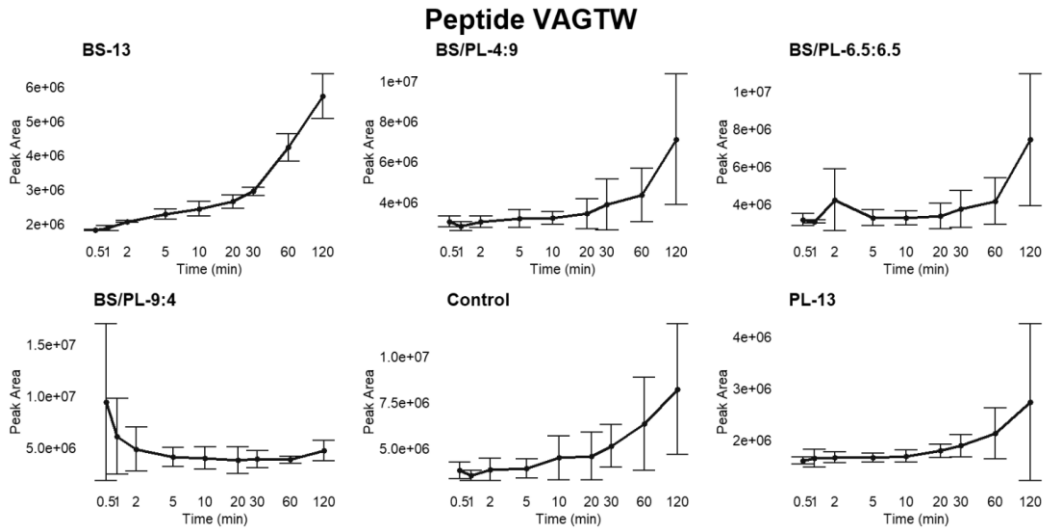

Figure 4.21 The kinetics of peptide VAGTW (15-19) assigned for β-Lg found during 2-hour WPI intestinal digestion under various biliary surfactant concentrations (only BSs: BS-13; BS/PL mixtures: BS/PL-9:4, BS/PL-6.5:6.5, BS/PL-4:9; only PLs: PL-13; and Control, without biosurfactants).

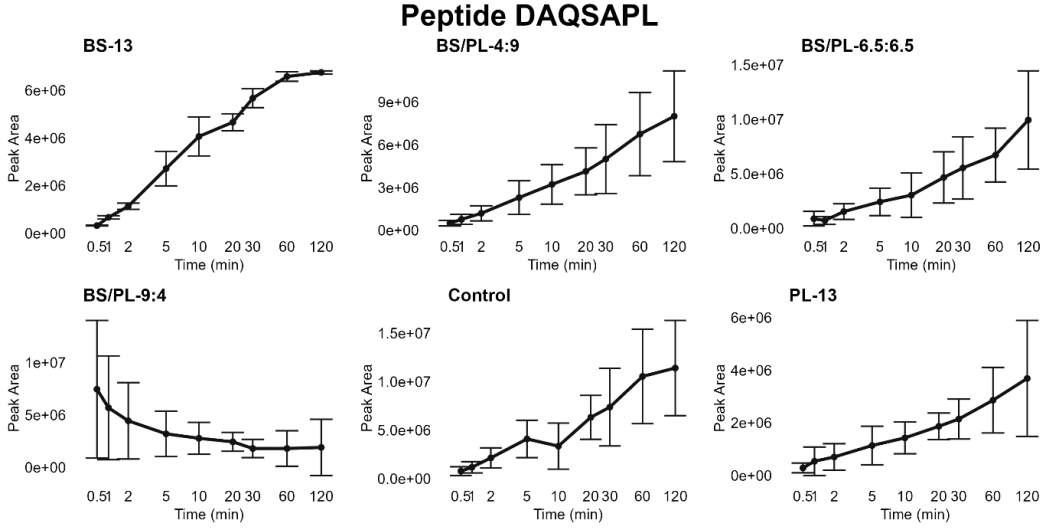

Figure 4.22 The kinetics of peptide DAQSAPL assigned for β-Lg found during 2-hour WPI intestinal digestion under various biliary surfactant concentrations (only BSs: BS-13; BS/PL mixtures: BS/PL-9:4, BS/PL-6.5:6.5, BS/PL-4:9; only PLs: PL-13; and Control, without biosurfactants).

The peptides originating from the gastric phase, IVTQTMKGLDIQKVAGTW (Appendix Figure 7.8a) and the peptide IVTQTMKGLD (Appendix Figure 7.8b), were not present under BS-13 conditions. Its intensity fluctuated over time under physiologically relevant conditions (BS/PL-9:4), Control condition and in the presence of PLs (PL-13, BS/PL-4:9, BS/PL-6.5:6.5). This indicates that some peptides originating from the gastric phase remained undigested over time under Control conditions and in the presence of PLs, while in BS-13 conditions, intestinal enzymes action was immediate. This is confirmed by the kinetics of the peptides IVTQTMK, IVTQTM and IVTQT (Appendix Figure 7.8c-e), which were detected in all intestinal conditions. Peptide IVTQTM showed increasing intensity over time with a relatively low standard deviation under BS-13 conditions. This might suggest that IVTQTM was more stable and was the predominant product released from this protein region (2-19). In contrast, the signal intensity of peptides IVTQTMK and IVTQT fluctuated over time.

In summary, the kinetics of peptides in BS-13 are clearer, with more logical and evident transitions between peptide formation and degradation over time. In many cases, the peptide kinetics under Control conditions, PL-only conditions, BS/PL mixtures of equimolar concentrations and the excess of PLs showed similar behavior to BS-13. However, there were exceptions. For example, FKIDALNENK (Appendix Figure 7.9a) was found only in BS-13 and Control, and its kinetics differed substantially. In BS-13, its intensity dropped sharply during the first 5 minutes of digestion, while in Control, it increased, reaching a maximum at the end of digestion.

Physiologically relevant conditions (BS/PL-9:4) differed from the other conditions. However, some peptides not found in BS-13 showed similar kinetics across all other conditions including physiologically relevant conditions, such as EALEKFDKALKALPMHIRL and FKIDALNENKVLVL (Appendix Figure 7.9b-c). Additionally, there were peptides, which exhibited very similar kinetic trend under all conditions e.g. LSFNPTQL, VYVEEL (Appendix Figure 7.9d-e), which showed growing intensity over digestion time. There are also peptides that were not present in PL-13 conditions and their kinetics were similar across all other conditions e.g. metastable peptide KIDALNENKVLVLDTDYKKY (Appendix Figure 7.9f), and finally, there were peptides, which exhibited kinetics in physiologically relevant conditions (BS/PL-9:4) similar to BS-13 e.g. LKPTPEGD (Appendix Figure 7.9g).

The complex kinetics observed under physiologically relevant conditions (BS/PL-9:4) might result from multiple simultaneous pathways of peptide formation and degradation. These include pathways specific to BSs conditions and delayed digestion caused by the presence of PLs, as well as their interplay. The impact of these two biosurfactants is a complicated issue that requires further research to fully understand the digestive pattern and explain the mechanism under the combined effect of BS/PL. Nonetheless, the current findings confirm the distinct kinetics of peptides depending on the conditions involving various proportions of BSs and/or PLs. The diversity of created peptides and their varying kinetics across conditions highlights the necessity of including PLs alongside BSs in *in vitro* digestion models to reflect reliable conditions of the physiological digestion.

As the heat map revealed Figure 4.16 differences in the peptide pattern, an analysis of hydropathy was performed. The hydropathic character of the released peptides was calculated using the Kyte method. The most hydrophilic peptides were found under BS/PL-9:4(NE) (-0.17 ± 0.85) and BS-13 (-0.15 ± 0.98) conditions. Average of the hydropathic character was the highest for physiologically relevant conditions (BS/PL-9:4) resulting in -0.07 ± 0.84. Than -0.09 ± 0.89 for BS/PL-4:9, -0.1 ± 0.89 for only PLs (PL-13), and Control -0.13 ± 0.96.

Additionally, average hydropathy character by protein sequence is shown at the Figure 4.23. It presents the differences in hydropathic character of peptide profile in digestive mixture at various conditions. The black curve represents the hydropathic profile of undigested B-lg protein, calculated using a sliding window method with a mean of five amino acids (two to the right and two to the left of each position), based on the hydropathy scale published by Kyte and Doolittle (Kyte and Doolittle 1982). This line provides the information of hydrophobic and hydrophilic regions over the protein sequence and serves, as a reference point for analyzing the hydropathic character of peptides released during a two-hour digestion. For the experimental data the hydropathic character for each position in protein sequence was calculated based on hydropathic character of peptides released during digestion. Each amino acid in the sequence represents the average of hydropathic character of peptides released from this region during the digestion. This visualization allows for a deeper analysis of the peptide profile in terms of hydropathy.

The results reveal that, in the experiment with BSs, low hydropathic values dominate (-0.15 ± 0.98), which is visible as intensely blue bars pointing toward negative values indicating hydrophilic character of released peptides from these regions. Even thought, there are also regions where a hydrophobic character prevails. It differs from physiologically relevant conditions (BS/PL-9:4), where in the sequence above position 100, no or minor positive values are noticeable for physiologically relevant conditions. Negative values of hydrophobic character were observed around positions 11–16 under BS-13 conditions, as well as slightly in the Control. This differs from all conditions containing PLs and the BS/PL-9:4(NE) condition, where values in this fragment (11-16) are clearly positive (indicated by the black arrow A in Figure 4.23). In contrast, in the segment 138–150, hydropathy values are positive under BS-13 conditions but are close to zero under physiologically relevant conditions (BS/PL-9:4) (arrow B). In the fragment 70–79 (indicated by arrow C), more positive values are observed under Control, physiologically relevant conditions and all other conditions containing BSs, compared to the conditions with only PLs, making it more similar to the gastric condition BS/PL-9:4(NE). In the segment 118–124 (arrow D), noticeable differences are observed between the physiologically relevant condition (BS/PL-9:4) and other conditions, particularly Control and BS-13. The segment 118–124 contains two cysteine residues (Cys119 and Cys124), with the former forming a disulfide bond with Cys106. This aspect is discussed in detail in

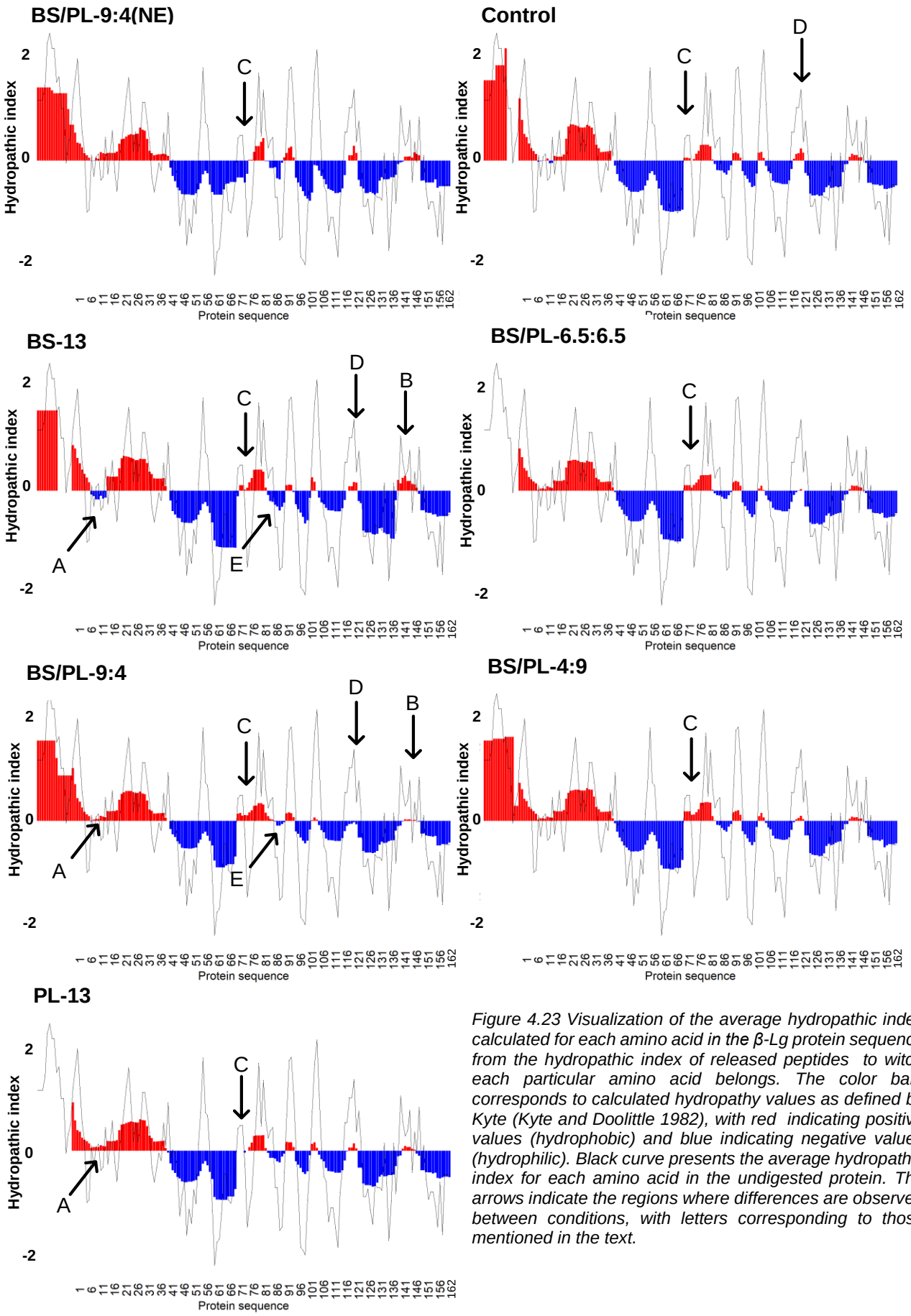

Figure 4.23 Visualization of the average hydropathic index calculated for each amino acid in the β-Lg protein sequence from the hydropathic index of released peptides to witch each particular amino acid belongs. The color bars corresponds to calculated hydropathy values as defined by Kyte (Kyte and Doolittle 1982), with red indicating positive values (hydrophobic) and blue indicating negative values (hydrophilic). Black curve presents the average hydropathic index for each amino acid in the undigested protein. The arrows indicate the regions where differences are observed between conditions, with letters corresponding to those mentioned in the text.

subsequent sections. On the other hand, the region indicated by arrow E, around position 86, shows more negative values under all conditions compared to the physiologically relevant condition BS/PL-9:4, where the contribution of hydrophilic character is the smallest.

The observed differences result from variations in the peptide profile and may be due to preferred cleavage sites depending on the condition and/or the accumulation of peptides of different lengths caused by delayed digestion. It allows to conclude that β-Lg protein digestion under different conditions, with varying proportions of biosurfactants, results in distinct peptide profiles, and consequently their various hydropathic character. Moreover, it may be influenced by peptide interactions with biosurfactants (Bellesi and Pilosof 2021), due to the interfacial properties of some peptides, as β-Lg is reported as a good source of surface-active peptides (Turgeon et al. 1992).

Bioactive peptides and epitopes

The list of peptides obtained from the 2-hour intestinal digestion was searched against the Milk Bioactive Peptide Database (MBPDB) (Nielsen et al. 2017), and a total of 39 bioactive peptides were found in the WPI digests (Figure 4.24a) assigned to β-Lg. Thirty-two peptides were assigned to BS-13 conditions, 33 to PL-13, 39 to BS/PL-4:9, 37 to BS/PL-9:4, and 36 to BS/PL-6.5:6.5. Only two unique peptides were found in BS/PL-4:9. The number of common peptides was 30, while two peptides were shared exclusively among the BS-13, physiologically relevant concentration (BS/PL-9:4), and equimolar biosurfactant ratios (BS/PL-6.5:6.5). The remaining five peptides were shared across experiments involving PLs, with three peptides common to each PL experiment (PL-13, BS/PL-4:9, BS/PL-6.5:6.5, BS/PL-9:4). The number of bioactive peptides found in WPI digestion under Control conditions (not shown in the graph) was 34. There were no unique bioactive peptides, as all of them were also found under BS/PL-9:4 conditions.

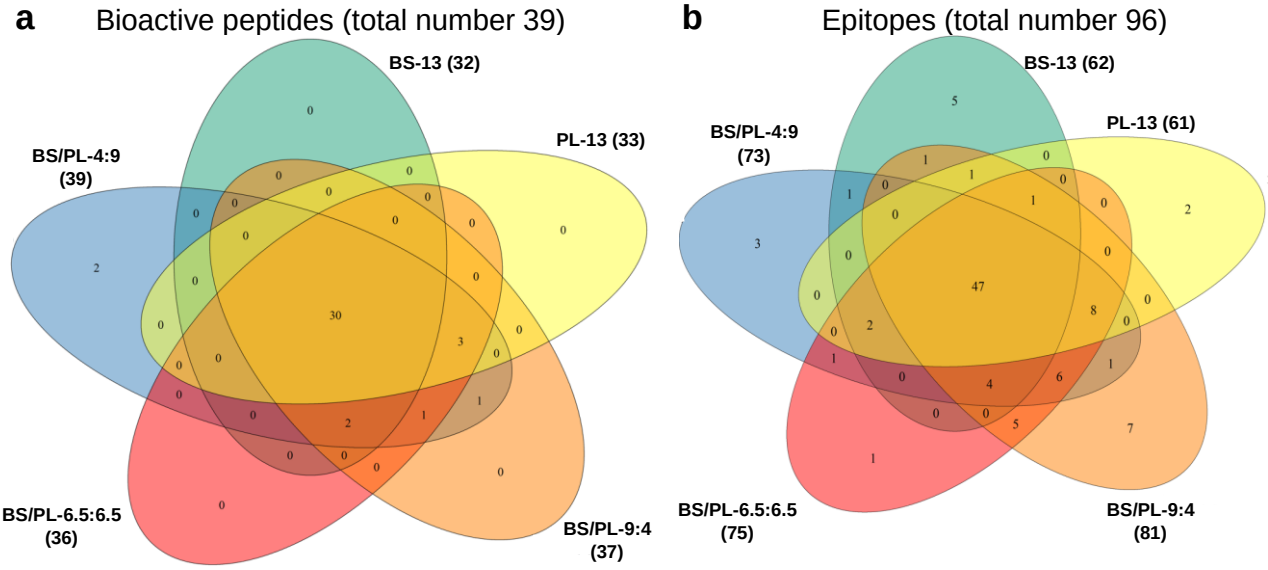

Figure 4.24 The Venn diagrams represent the comparison of the number of bioactive peptides (a) and epitopes (b) assigned to β-Lg, found under various BS/PL ratio conditions during the intestinal digestion of WPI. The total number of bioactive peptides/epitopes found in each condition is shown in brackets.

Peptides VAGTWY (15-20), AASDISLLDAQSAPLR (25-40), IPAVFK (78-83), and VLVLDTDYK (92-100) exhibit antibacterial activity, mainly against Gram-positive bacteria. The authors of the article (Pellegrini et al. 2001) suggest that β-Lg may play an antibacterial role after proteolytic degradation. This indicates potential benefits in functional nutrition or infant formulas. AASDISLLDAQSAPLR (25-40) is an antimicrobial peptide that acts against Gram-positive bacteria, including *Bacillus subtilis* and *Staphylococcus lentus*. This peptide is relatively polar, which may affect its selectivity towards different types of bacteria (Pellegrini et al. 2001). It shows decreasing signal intensity under all conditions except BS/PL-9:4 (Appendix Figure 7.6a).

The peptide IPAVFK (78-83), shown in Figure 7.6b (Appendix), stayed stable at relatively high signal intensity level over time (BS-13, BS/PL-9:4, BS/PL-4:9, BS/PL-6.5:6.5, PL-13, Control). Further digestion of this peptide leads to the formation of IPAVF (78–82). Peptide IPAVF has potential therapeutic properties, particularly in the context of DPP-IV enzyme inhibition, which may help regulate blood glucose levels. IPAVF (78–82) exhibited strong inhibitory activity, suggesting its potential use as a component of functional foods in the treatment of type 2 diabetes (Silveira et al. 2013). The kinetics of this peptide have been described above and are presented in Figure 4.20. Additionally, Figure 4.18, marked with an asterisk under PL-13, BS/PL-4:9, BS/PL-6.5:6.5, and Control, shows that it exhibited the highest intensity among the peptides released under these particular conditions.

Peptide VLVLDTDYK (92-100) is amphipathic, containing both hydrophobic (VLVL) and hydrophilic regions (DTDYK). This allows it to interact with bacterial cell membranes. It has shown activity against Gram-positive bacteria, such as *Bacillus subtilis* and *Staphylococcus lentus* (Pihlanto-Leppälä et al. 2000). Additionally, it has been found that this peptide shows moderate DPP-IV inhibitory activity (Silveira et al. 2013). In the BS/PL-9:4 experiment (Appendix Figure 7.6c), it appears at high intensity at the very beginning, then decreases over time. For all other conditions, it shows an increasing trend over time.

DAQSAPLRVY (33-42) (Figure 4.25a) exhibits inhibitory properties against angiotensin I-converting enzyme (ACE) (Tavares et al. 2011). Under physiologically relevant conditions, the intensity of this peptide remains at a similar level over the whole digestion period, whereas in all other conditions, the trend is decreasing. Peptide VAGTWY (Appendix Figure 7.6d), in addition to its antimicrobial and antioxidant properties, also has ACE-inhibitory properties (Pihlanto-Leppälä et al. 2000). The kinetics of this peptide is distinct under BS-13 conditions. This peptide clearly shows metastability, with a peak intensity at 10 minutes of digestion with only BSs. In other conditions (PL-13, BS/PL-6.5:6.5, BS/PL-4:9, Control), the peptide shows a slow increasing trend, but under physiologically relevant conditions (BS/PL-9:4), its intensity decreases over time.

Peptides ALKALPMHIR (139-148) and EILLQK (55-60) have a positive impact on the immune system, particularly by stimulating the proliferation of immune cells, such as splenocytes, and modulating cytokine secretion, which is crucial for immune response (Jacquot et al. 2010). Peptide ALKALPMHIR (Figure 4.25b) in physiologically relevant conditions (BS/PL-9:4) shows a clear upward trend, while in other conditions, it decreases. In the case of BS-13, a substantial drop is observed within 5 minutes. This peptide is broken down into shorter fragments, ALPHMIR and ALPMH. In the presence of only BSs (BS-13), the intensity of ALPHMIR decreases over time (Figure 4.25c), while ALPMH increases (Figure 4.25d), indicating the conversion of one peptide into the other. Under physiologically relevant conditions, these changes are less pronounced, as the

longer peptides (ALKALPMHIR and ALPHMIR) show a clear increasing trend. For their shorter fragment, the initial intensity is the highest, suggesting it may be released from other peptides coming from this region of the protein not discussed here. Importantly, each of the three discussed peptides maintains relatively high intensity throughout the entire digestion time under physiologically relevant conditions (BS/PL-9:4). The kinetics of the shorter fragments of ALKALPMHIR are also important, as each of them has been shown to have bioactive properties. ALPMHIR (142-148) acts as an ACE inhibitor and influences the release of endothelin-1 (ET-1) by endothelial cells. This action may play a role in lowering blood pressure by modulating the release of ET-1, a potent vasoconstrictive peptide (Maes et al. 2004). Peptide ALPMH (142-146) had an impact on reducing cholesterol absorption (Nagaoka et al. 2001). It is worth noting that the peptide ALKALPMHIR was not observed under conditions with only PLs (PL-13), but its shorter fragments were detected and showed an increasing trend over digestion time. This provides evidence of protein digestion in this region, occurring with a different pattern.

The general trend for most bioactive peptides under BS-13 conditions is a decrease over time. However, there are interesting exceptions, including GLDIQK (9–14) (Figure 4.25e), ALPMH (142–146), and VYVEELKPTPEGDLEILLQK (41-60). These peptides have been shown to reduce cholesterol absorption (Nagaoka et al., 2001). It is natural to assume that short peptides form over time, with their intensity increasing as larger protein fragments are digested. However, the persistence of the long peptide (41-60) at high signal intensity may indicate interactions with BSs. These interactions are discussed in more detail in later section of this dissertation (section 4.3.4). Interestingly, the peptide EILLQK (55-60) (Figure 4.25f) is a part of peptide (41-60) and it was not identified under BS-13 conditions. Kinetics of peptide EILLQK were linear in BS/PL-6.5:6.5, BS/PL-4:9, and Control, with a slight increase after 30 minutes of digestion. In conditions with only PLs (PL-13) the intensity of this peptide slightly fluctuated at the very low level. In physiologically relevant conditions (BS/PL-9:4), the signal intensity of this peptide increased noticeably until the 5th minute, next it rapidly decreased and fluctuated until the end of digestion, without reaching the intensity observed during the initial 5 minutes.

Although the biological implications of peptide release kinetics during digestion under different conditions remain a complex puzzle, some conclusions can be drawn. The kinetics of many bioactive peptides differ considerably between conditions. In particular, noticeable differences are observed between BS-13 conditions and physiologically relevant conditions (BS/PL-9:4). In general, it can be concluded that under BS/PL-9:4 conditions discussed bioactive peptides maintain relatively high intensity levels throughout the digestion time, even if they originate from the same protein sequence region. This is different from the kinetics under BS-13 conditions, where changes mainly involve the conversion of one peptide into another, its shorter fragment. This confirms earlier observations of a more ordered and uniform digestion pattern under BS-13 conditions. Where the decrease in intensity of the longer peptide coincides with the increase in intensity of its shorter fragments. This phenomenon is not as clearly observed under physiologically relevant conditions (BS/PL-9:4). In physiologically relevant conditions, the protein is broken down more slowly, but digestion probably occurs through multiple possible pathways simultaneously over the digestion time.

a

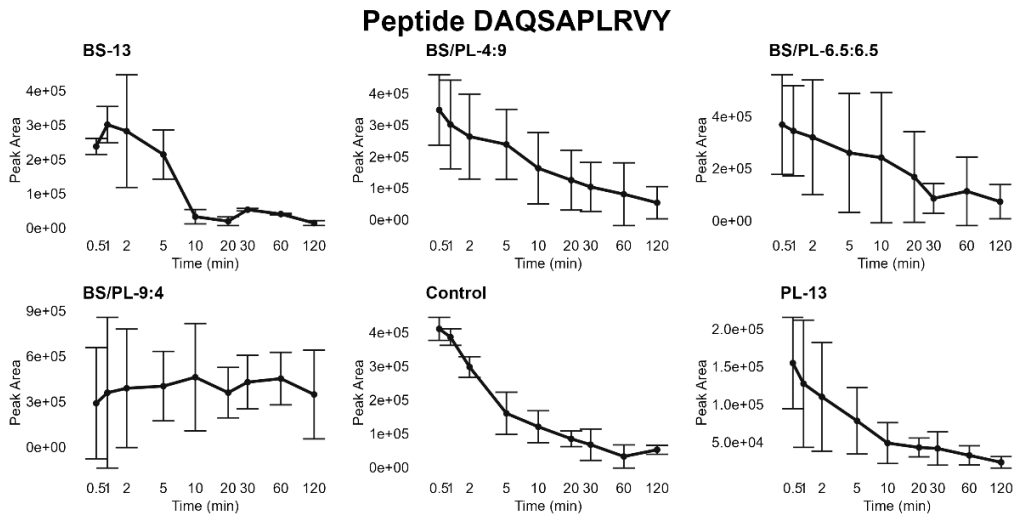
Peptide DAQSAPLRVY
BS-13
BS/PL-4:9
BS/PL-6.5:6.5
BS/PL-9:4
Control
PL-13
Peak Area
Time (min)
0.5 1 2 5 10 20 30 60 120

b

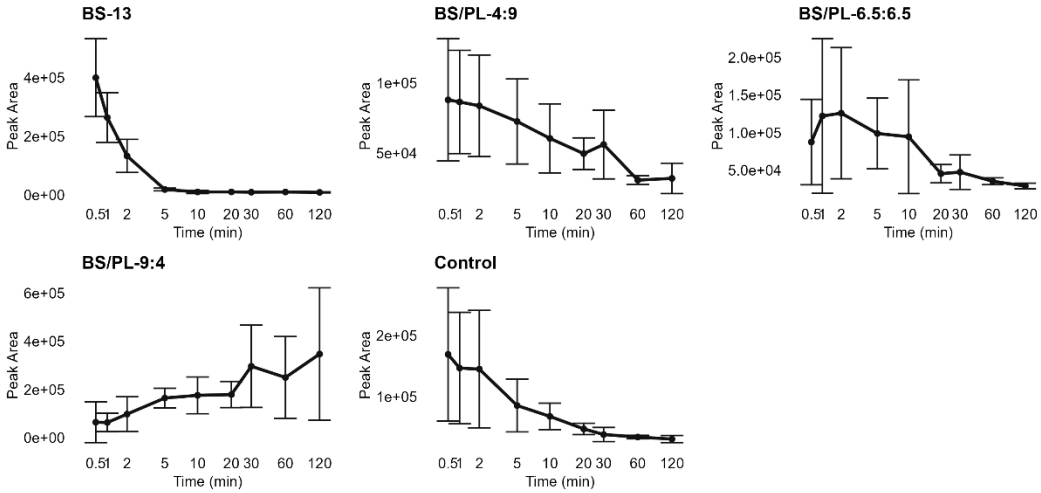
Peptide ALKALPMHIR
BS-13
BS/PL-4:9
BS/PL-6.5:6.5
BS/PL-9:4
Control
Peak Area
Time (min)
0.5 1 2 5 10 20 30 60 120

c

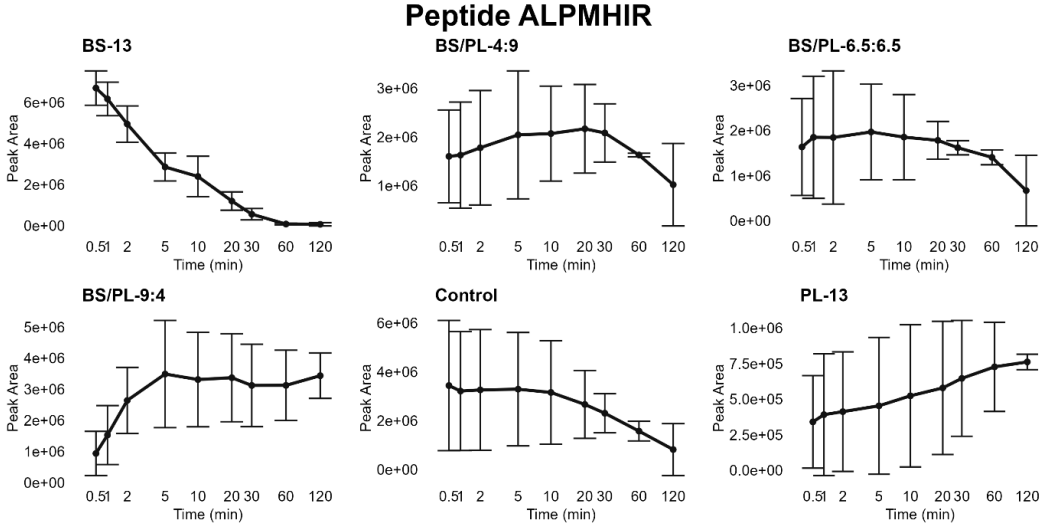
Peptide ALPMHIR
BS-13
BS/PL-4:9
BS/PL-6.5:6.5
BS/PL-9:4
Control
PL-13
Peak Area
Time (min)
0.5 1 2 5 10 20 30 60 120

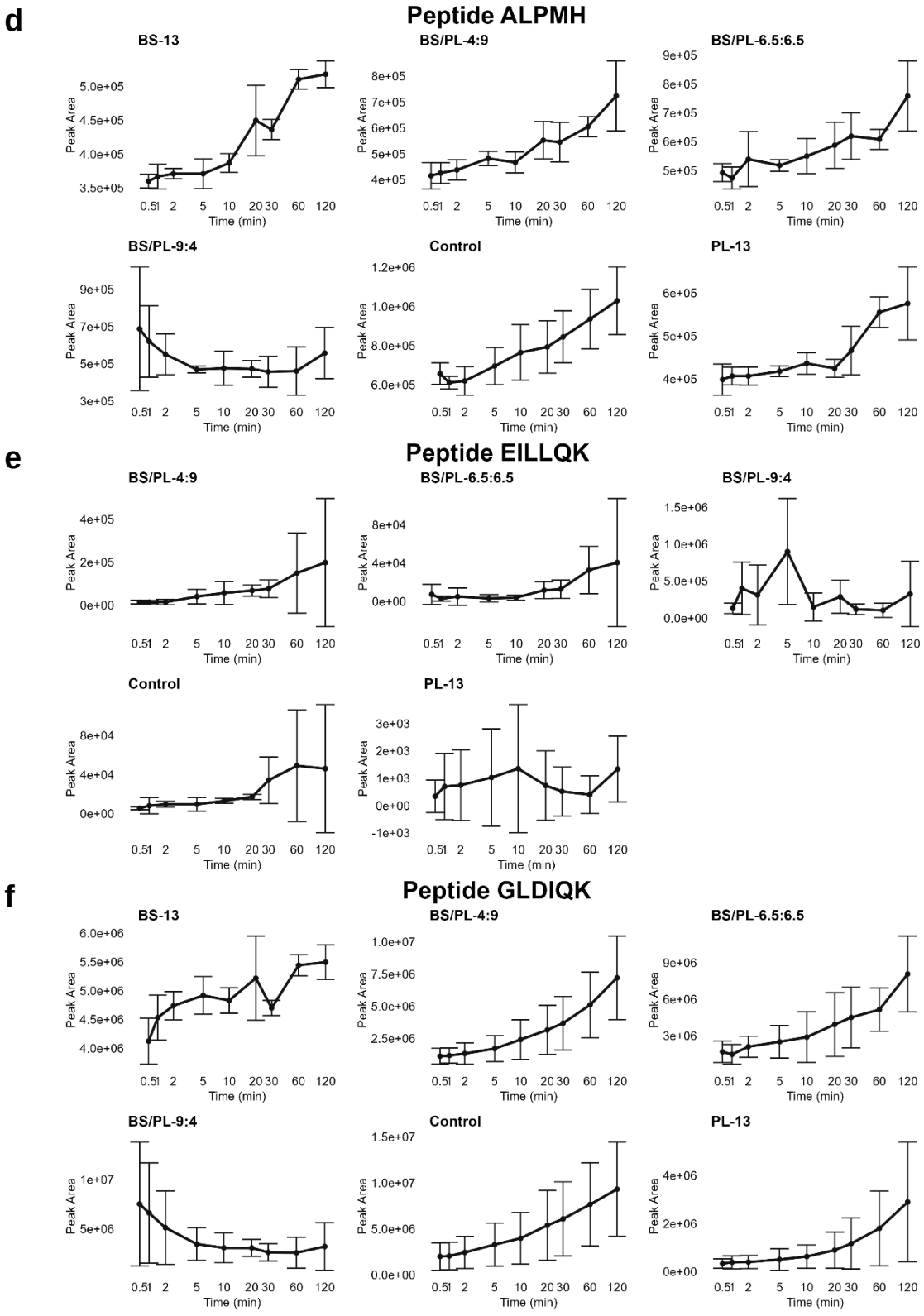

Figure 4.25 The kinetics of bioactive peptides (a-f) assigned for β-Lg found during 2-hour WPI intestinal digestion under various biliary surfactant concentrations (only BSs: BS-13; BS/PL mixtures: BS/PL-9:4, BS/PL-6.5:6.5, BS/PL-4:9; only PLs: PL-13; and Control, without biosurfactants). The absence of a graph for a specific condition indicates the non-detection of that peptide under these conditions.

In addition to bioactive peptides, the focus shifted to identifying potential epitopes generated during the 2-hour digestion period. To achieve this, the list of peptides obtained from all experiments was searched against the Immune Epitope Database (IEDB) for β-Lg (P02754) from 24.02.2023 (Vita et al. 2018). This search identified a total of 96 epitopes, the results are presented in the Figure 4.24b. The highest number of peptides was found under physiologically relevant conditions BS/PL-9:4 (81 peptides), followed by 75 peptides in BS/PL-6.5:6.5, 73 in BS/PL-4:9, and the lowest numbers under conditions with only PL-13 and BS-13, yielding 61 and 62 peptides, respectively. The number of common peptides was 47, while the number of unique peptides for each condition was as follows: 7 in the physiological biosurfactant concentration, 5 in conditions with only BSs, 3 in excess PL conditions, and 2 in experiments with PLs only. The highest number of shared peptides was found across experiments with various PL ratios. The number of epitopes found under Control conditions was 66 (not shown in the graph).

The allergenic reactivity of β-Lg was studied by Bossios et al. (2011), who conducted digestion using *in vitro* models with and without BSs and PLs. The authors highlighted the role of physiological surfactants, such as PC, in assessing the potential allergenicity of food proteins. Their results suggest that PC protects β-Lg from degradation, potentially increasing its allergenic potential, while BSs contribute to the breakdown of PC protecting the protein, thereby allowing β-Lg digestion. Gastro-duodenal digestion without PC significantly reduced the IgE-binding capacity of β-Lg. An *in vivo* skin prick test (SPT) showed a general trend of reduced wheal diameter after exposure to digested β-Lg; however, digestion in the presence of PC resulted in an increase in wheal size. These analyses were conducted at the protein level rather than the peptide level (Bossios et al. 2011). However, the entire digestive mixtures were analyzed by ELISA and SPT, and the response was influenced by the whole digestive mixture, without identifying specific potential epitopes that may cause this effect.

The results obtained in the current study provide a general peptide profile that was not examined in the experiments by Bossios et al (2011). Nevertheless, the findings are consistent with those of Bossios et al. (2011), showing bioinformatic alignment regarding the potential allergenicity of β-Lg digestive mixtures, as indicated by the high number of epitopes detected in PLs-containing digestive mixtures Figure 4.24b. However, there is a difference in experimental approaches, as in some experiments by Bossios et al. (2011), PC was added at the gastric phase, which may have influenced pepsinolysis outcomes. The issue of allergenicity is complex, and a thorough analysis of this topic is beyond the scope of this study.

Considering the kinetics of epitopes under different conditions, it can be observed that in BS/PL-9:4, the peptides LIVTQTMK (1-8) and VRTPEVDDEA (123-132) (Figure 4.26a,b) appear within the first minute and maintain relatively high intensity over 2 hours of digestion. According to the literature (Jacquot et al. 2010) the peptide LIVTQTMK exhibited cytotoxic activity at high concentrations, which may lead to damage to immune system cells. The cytotoxicity may have resulted from its high hydrophobicity and poor solubility, leading to aggregation and a negative impact on cells (Jacquot et al. 2010). The signal intensity of peptide LIVTQTMK (Figure 4.26a) under all conditions slightly fluctuated over time at the maintained relatively high intensity range, suggesting its stability over digestion time, unlike under BS-13, where its intensity decreases substantially during digestion. Peptide VRTPEVDDEA (Figure 4.26b) showed decreasing trend under all conditions, except BS/PL-9:4.

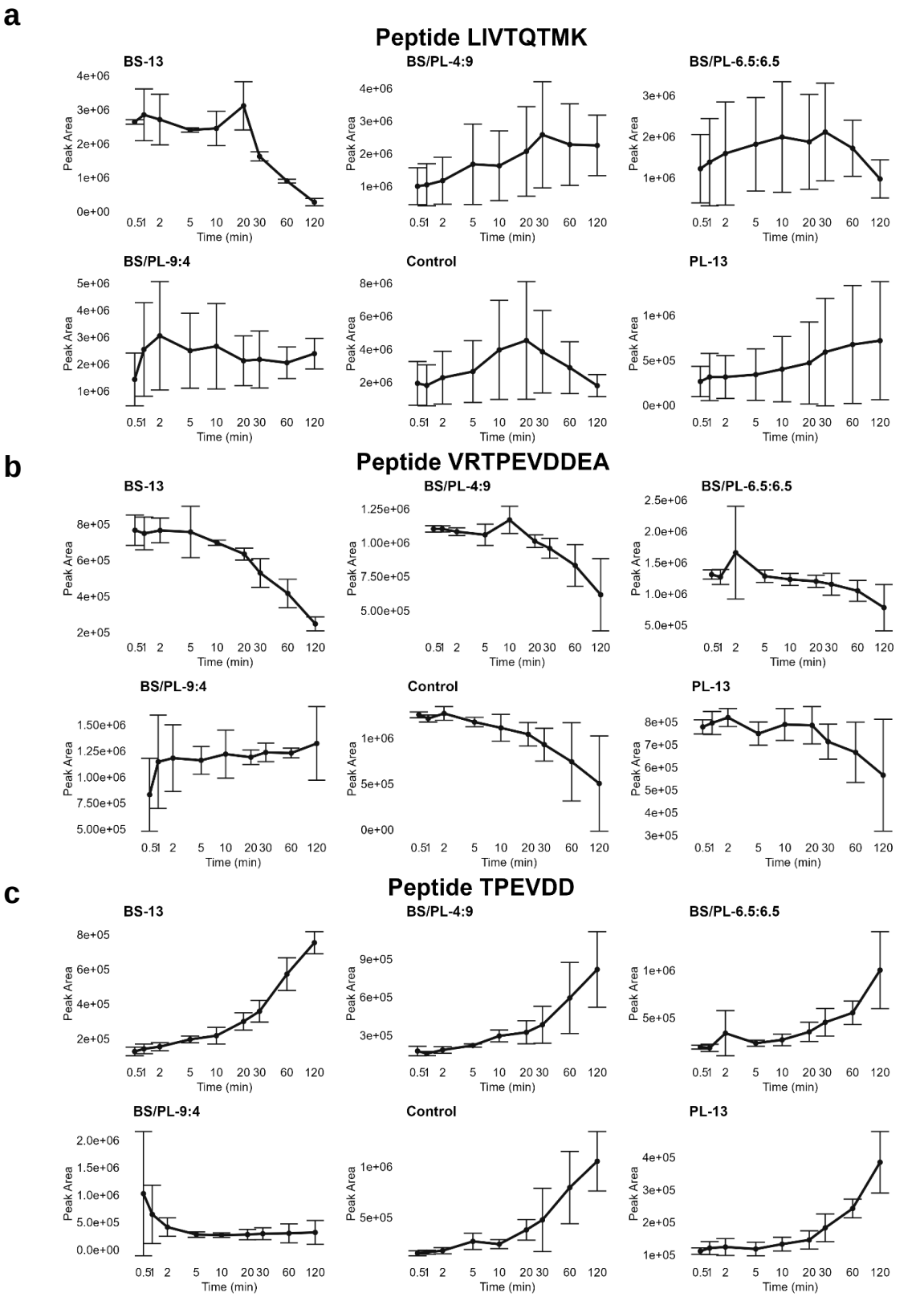
a
Peptide LIVTQTMK
BS-13
BS/PL-4:9
BS/PL-6.5:6.5
BS/PL-9:4
Control
PL-13
b
Peptide VRTPEVDDEA
BS-13
BS/PL-4:9
BS/PL-6.5:6.5
BS/PL-9:4
Control
PL-13
c
Peptide TPEVDD
BS-13
BS/PL-4:9
BS/PL-6.5:6.5
BS/PL-9:4
Control
PL-13
Peak Area
Time (min)
0.5 1 2 5 10 20 30 60 120

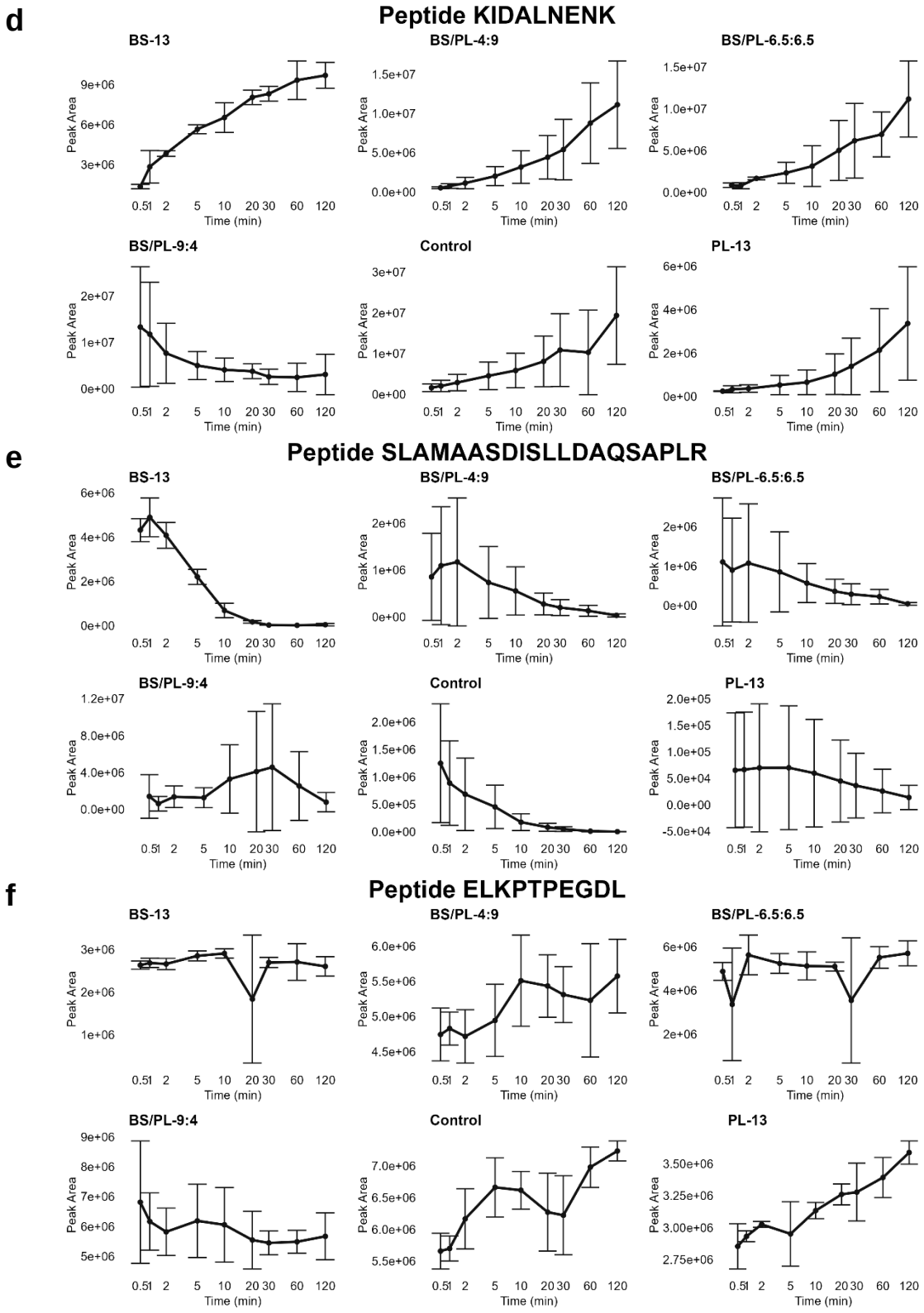

Figure 4.26 The kinetics of epitopes (a-f) assigned for β-Lg found during 2-hour WPI intestinal digestion under various biliary surfactant concentrations (only BSs: BS-13; BS/PL mixtures: BS/PL-9:4, BS/PL-6.5:6.5, BS/PL-4:9; only PLs: PL-13; and Control, without biosurfactants).

For the peptides TPEVDD (125-130) (Figure 4.26c) and KIDALNENK (83-91) (Figure 4.26d), their signal intensity decreases under physiologically relevant conditions (BS/PL-9;4) but increases in all other conditions. Similarly, the signal intensity of SLAMAASDISLLDAQSAPLR (Figure 4.26e) decreases across all conditions. However, under physiologically relevant conditions, it is metastable, reaching its maximum intensity after 30 minutes. The peptide ELKPTPEGDL (Figure 4.26f) shows a clearly increasing trend in the Control condition and in conditions with high PL content (PL-13 and BS/PL-4:9). In conditions with high concentrations of BSs (BS-13 and BS-6.5:6.5), its tendency is decreasing. The peptides mentioned at the beginning of this section (Figure 4.15), LSFNPTQLEEQCHI, VEELKPTPEGDLEILLQK, TPEVDDEALEKFDK, and VYVEELKPTPEGDLEILLQK, are reported as epitopes. Among them, the peptide VYVEELKPTPEGDLEILLQK is also reported as bioactive, as it was discussed above.

In summary, it was analyzed that during digestion in the presence of PLs, more bioactive peptides are released under BS/PL-4:9 conditions, while more epitopes are released under BS/PL-9:4 conditions, compared to digestion with BSs alone (BS-13). While it is not yet possible at this stage of research to fully explain the biological implications of these differences, the observations highlighted in this chapter provide valuable insights into the peptide patterns generated under various BS/PL ratios. The findings presented in this chapter offer important observations for the proper design of studies focused on bioactive peptides and epitopes. This is particularly relevant for the development of functional foods and nutraceuticals enriched with bioactive peptides. Moreover, the presence of epitopes and their release kinetics play a crucial role in the design of hypoallergenic foods for special dietary needs.

4.3.3 Analysis of digesta obtained from pure β-lactoglobulin

Due to high biological variance observed between some experiments of WPI digestion, experiments with pure β-Lg were performed to allow for a more detailed analysis. Digestion experiments with pure β-Lg were conducted at the physiologically relevant BS/PL ratio of 9:4, as well as under a control condition without any biosurfactants. The sample correlation of biological replicates outcome for experiments with only β-Lg was highly satisfactory: β-Lg-BS/PL-9:4, 0.97 ± 0.02; β-Lg-Control, 0.96 ± 0.03. It is important to underscore that these experiments differ from previous experiments with WPI, where the digestive matrix was a much more complex mixture of peptides derived from other proteins in the sample, which could potentially influence the overall kinetics and enzyme behavior during digestion, as well the mass spectrometry analysis with DDA method. However, the high quality of single-protein digestion data enhances the reliability of the data obtained through the DDA method, allowing for more in-depth statistical analysis and comparison of two conditions.

The graph (Figure 4.27) shows the digestive progress at the peptide level of β-Lg under two examined conditions (physiologically relevant concentration of biosurfactants, β-Lg-BS/PL-9:4 and their absence, β-Lg-Control), expressed by changes in the overall sum area over time. The sum area increases over time in both cases, reaching a maximum at 60 minutes for the physiologically relevant concentration of biosurfactants (β-Lg-BS/PL-9:4) and then showing a decrease during the second hour. This differs from the kinetics under control conditions, where the sum area for the β-Lg-Control continuously increases, indicating slowed digestion.

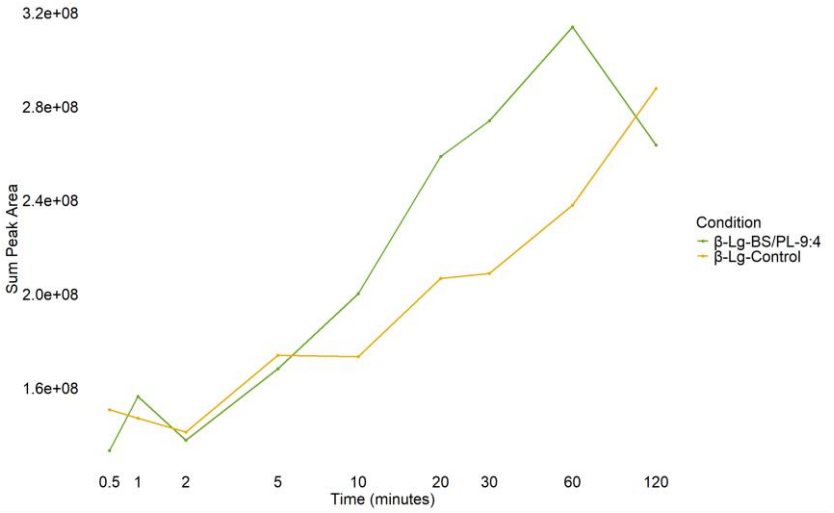

Figure 4.27 Sum peak area evolution of β-Lg 2-hour digestion in intestinal phase in the presence of biosurfactants at physiologically relevant concentration (BS/PL-9:4) and Control without any biosurfactants.

The total number of peptides identified in both conditions was comparable: 478 for the control and 494 for the physiologically relevant condition. However, the number of common peptides was only 392, with 188 peptides differing between conditions (Figure 4.28).

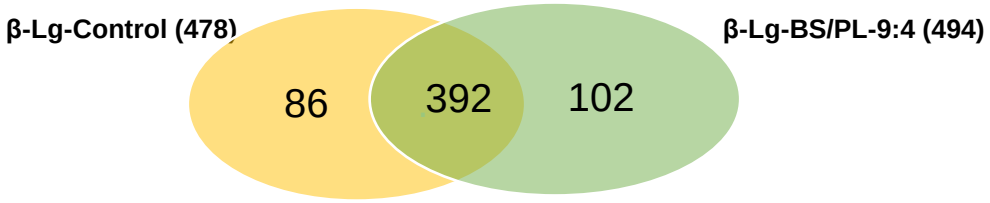

Figure 4.28 Venn diagram represents the number of peptides found during β-Lg intestinal proteolysis at physiologically relevant conditions (β-Lg-BS/PL-9:4) and control (β-Lg-Control). The values in brackets indicate the total number of peptides found in each condition.

The average molecular mass of peptides found under β-Lg-BS/PL-9:4 was 1220.13 ± 631.39 Da (median 999.08 Da), closely comparable to the control conditions (β-Lg-Control) at 1211.47 ± 652.49 Da (median 981.11 Da). The size distribution over time is shown in (Figure 4.29), where no substantial differences appeared between the two conditions. However, the first 10 minutes (T1-T5) of digestion under physiologically relevant conditions showed a higher frequency of high molecular weight peptides than under control conditions.

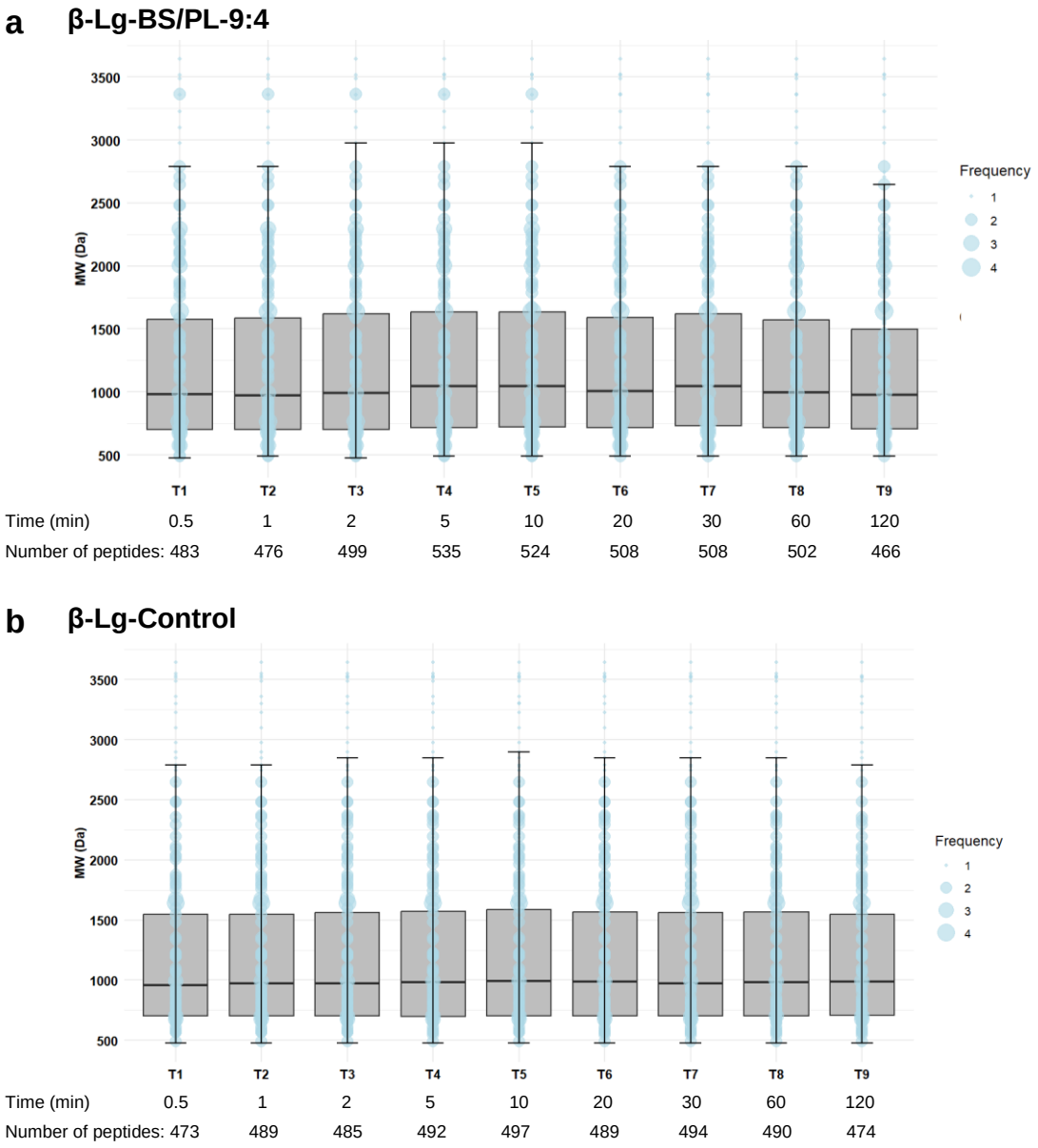

Figure 4.29 Size distribution and number of peptides evolving over time during β-Lg intestinal digestion under physiologically relevant conditions (β-Lg-BS/PL-9:4) (a) and control, without biosurfactants (β-Lg-Control) (b). On the x-axis: time points T1-T9 and the corresponding minutes, as well as the number of peptides found at each time point.; y-axes – molecular weight, MW (Da).

The visualized peptide pattern of β-Lg digestion reveals differences in protein digestion across certain regions that evolve over time. The heat map (
Figure 4.30) illustrates the intestinal phase for both conditions, β-Lg-BS/PL-9-4 and β-Lg-Control. Notably, a difference is visible within the first 2 minutes (T1-T3). Peptides covering the sequence from 39-60 are less abundant under physiologically relevant conditions (β-Lg-BS/PL-9:4), than in the β-Lg-Control. In the control this region shows a higher abundance (indicated by the yellow color), especially in sequence 45-55, which suggests a higher presence of peptides. Another noteworthy region is 70-75, which appears dark blue in the control condition (indicating a low number of peptides covering this sequence) but is lighter in the presence of biosurfactants (indicating higher coverage). In the initial region (8–20), fewer peptides were released compared to physiologically relevant conditions, which was similar to WPI digestion under control conditions (Figure 4.16). However, in the region 133–141, more peptides were released under physiologically relevant conditions (β-Lg-BS/PL9:4) than in control conditions (β-Lg-Control).

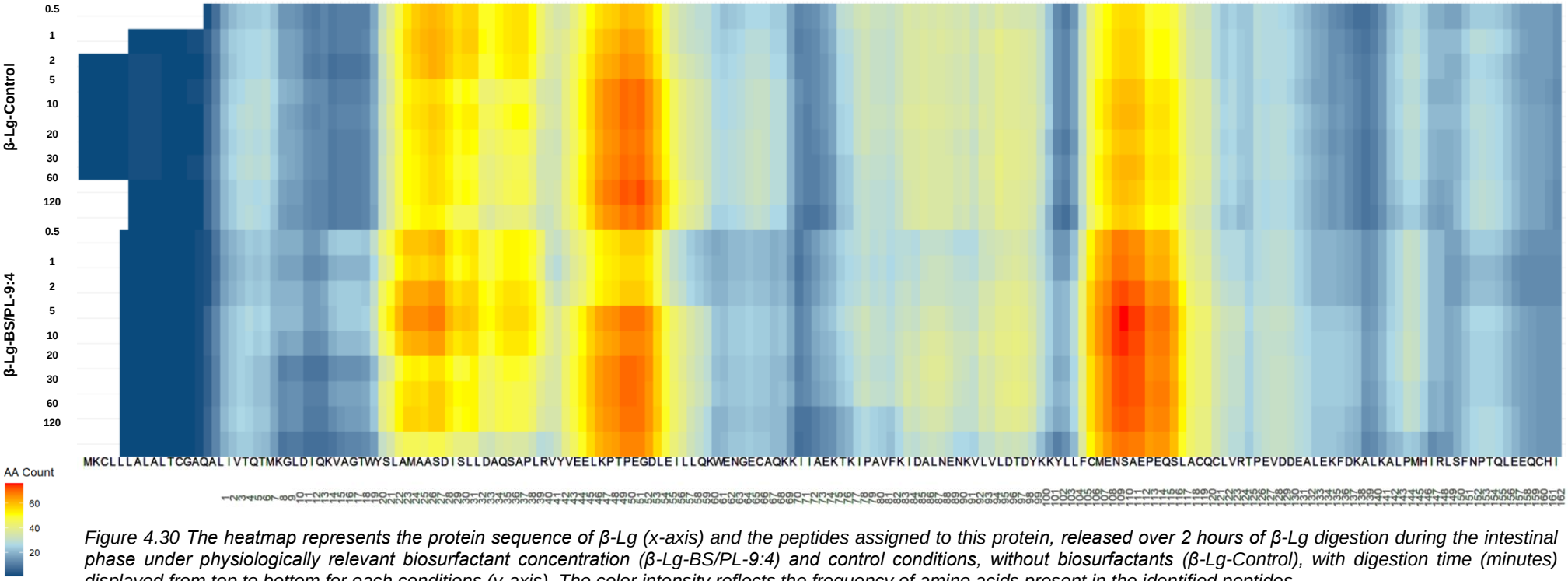

Figure 4.30 The heatmap represents the protein sequence of β-Lg (x-axis) and the peptides assigned to this protein, released over 2 hours of β-Lg digestion during the intestinal phase under physiologically relevant biosurfactant concentration (β-Lg-BS/PL-9:4) and control conditions, without biosurfactants (β-Lg-Control), with digestion time (minutes) displayed from top to bottom for each conditions (y-axis). The color intensity reflects the frequency of amino acids present in the identified peptides.

The Figure 4.31 presents differences between physiologically relevant conditions and control in the favored cleavage sites, most notably Lys138. At the physiologically relevant surfactant concentration, the percentage of cleavage at Lys138 is 2.4%, whereas in the Control condition, it is only 1% (indicated by a red arrow in the Figure 4.31). According to research by Fernández and Riera (2013), this position (Lys138) is located on the outer surface of the protein but is near acidic amino acid residue, Asp137, which reduced the rate of hydrolysis, leading to a slower release of peptides despite the physical accessibility of this site (A. Fernández and Riera 2013). The results for the β-Lg-Control condition align with the literature. Similar to the article, digestion was conducted without biliary surfactants, resulting in a slower release of peptides from this region (A. Fernández and Riera 2013). Under physiologically relevant conditions (β-Lg-BS/PL-9:4), the presence of biosurfactants mitigated the effect of missed cleavage caused by the acidic residue in the second position from the scissile bond. This resulted in more efficient cleavage at Lys138. These findings are consistent with those obtained during WPI digestion (Appendix Figure 7.7), where the Lys138 residue showed low percentage contribution among all intestinal conditions, except BS-13 and BS/PL-9:4. In BS-13 and BS/PL-9:4, the percentages were the highest, at 2.3% and 2.1%, respectively. In contrast, the Control condition was only 1.5%, while PL-13 and BS/PL-6.5:6.5 showed 1.6%, and BS/PL-4:9 showed 1.8%.

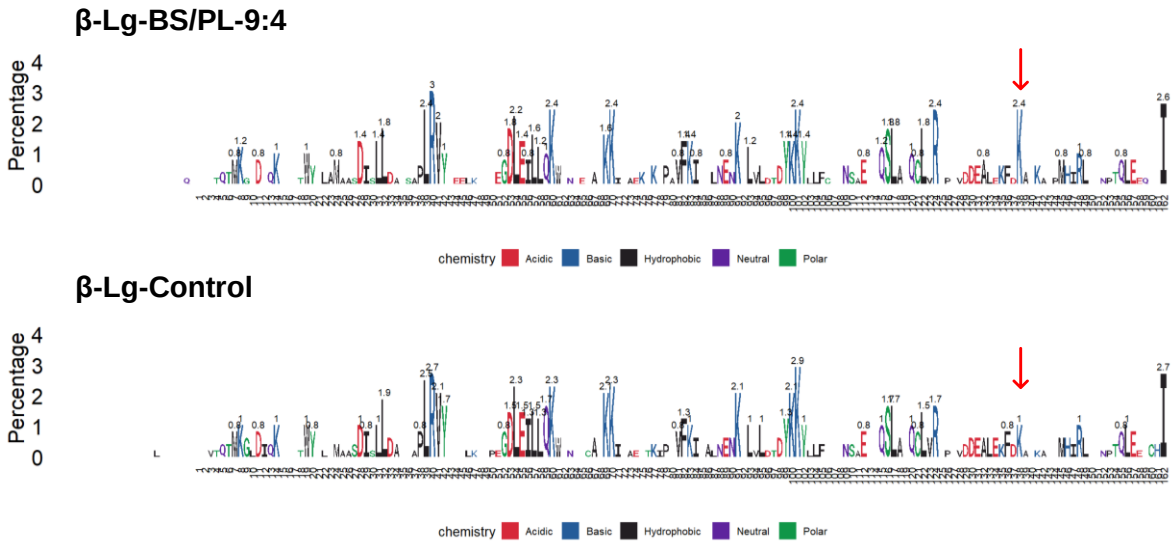

Figure 4.31 The enzyme cleavage sites are displayed as the percentage occurrence of specific amino acids at the ends of peptides generated during a 2-hour digestion. Amino acid symbols are aligned with positions in the protein sequence, and the labels indicate the percentage frequency of peptides with a particular terminal amino acid under the experimental conditions, β-Lg-BS/PL-9:4 and β-Lg-Control.

The overall hydropathy values calculated for peptides released under physiologically relevant conditions and control were closely aligned, with an average of -0.21 ± 0.97 for β-Lg-Control and 0.23 ± 0.97 for β-Lg-BS/PL-9:4. However, differences in the average hydropathic character are observed in the protein sequence regions 75–84 and 117–122, indicated by arrows A' and B', respectively, in Figure 4.32. These results are consistent with data obtained for WPI digestion (Figure 4.23), where the region around 75-84 is more hydrophobic under physiologically relevant conditions (BS/PL-9:4) and less so in the Control, while the region around 117-122 is more hydrophilic in the Control than under BS/PL-9:4 conditions (indicated by arrow D in Figure 4.23). These differences provide evidence of distinct peptide patterns generated under various conditions.

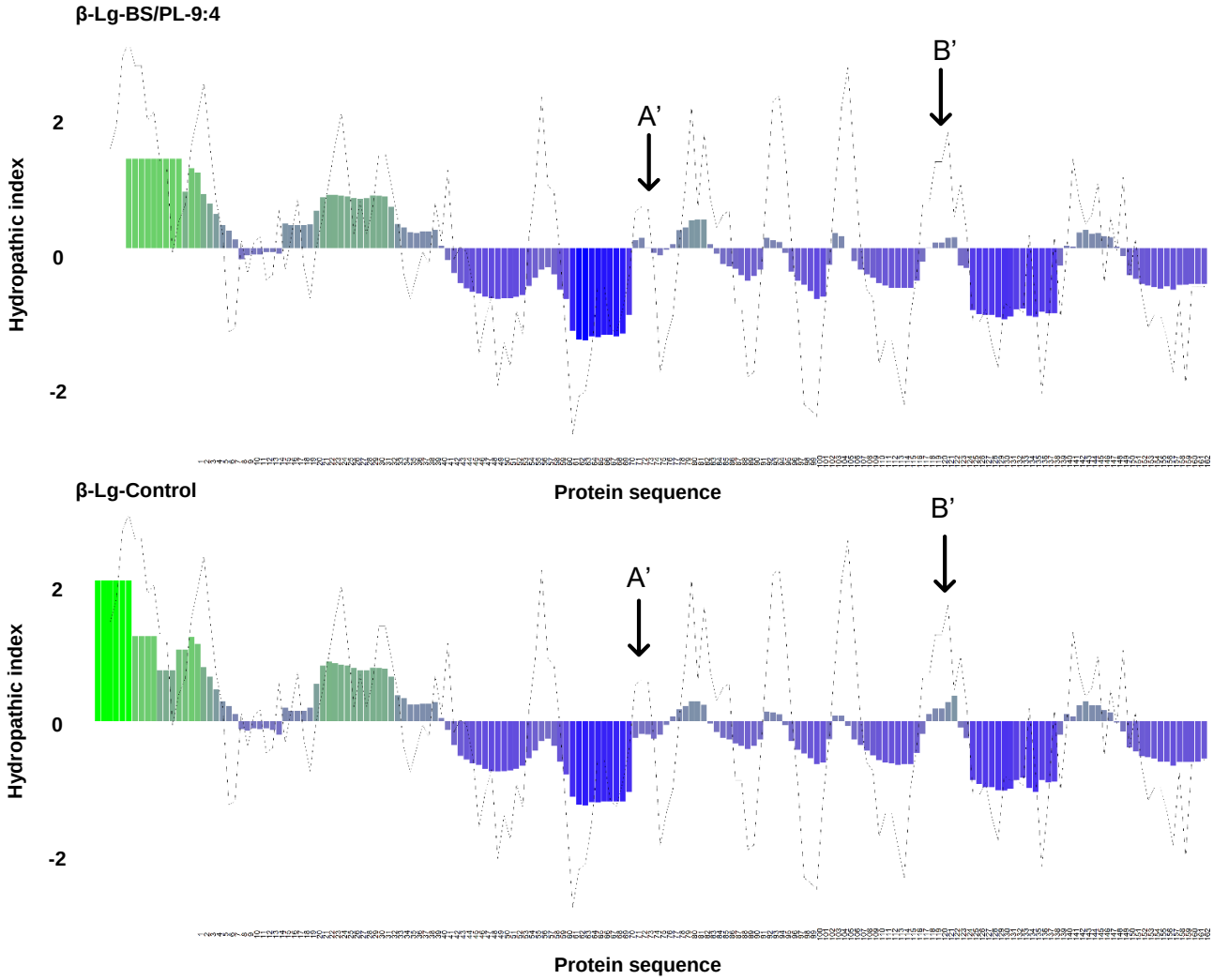

Figure 4.32 Visualization of the average hydropathic index calculated for each amino acid in the β-Lg protein sequence from the hydropathic index of released peptides to witch each particular amino acid belongs. The color gradient bars corresponds to calculated hydropathy values as defined by Kyte (Kyte and Doolittle 1982), with green indicating positive values (hydrophobic) and blue indicating negative values (hydrophilic). Black curve presents the average hydropathic index for each amino acid in the undigested protein. The arrows indicate the regions where differences are observed between conditions, with letters corresponding to those mentioned in the text.

The subsequent step was to analyze differences at each time point and assess whether these differences might reflect significant changes. This is particularly relevant for the digestion process, which occurs over time, as the outcomes at specific intervals might have implications for the body's response, such as the rate of formation, persistence, and degradation of epitopes or bioactive peptides (Picariello et al. 2010; Sutantawong et al. 2025; Id et al. 2020). For this purpose, an ANOVA test was performed according to the PEAKS Studio 11 Manual (Yang 2023), with a False Discovery Rate of 0.05 applied. Volcano plots were generated to compare groups (time points) under the physiologically relevant condition to the control. Peptides with a Log2 Fold Change (FC) greater than 1 or less than -1 and an adjusted *p*-value below 0.05 were considered significantly changed (Marcus, Eisenacher, and Sitek 2021). On the left side of the volcano plot, values corresponding to peptides with higher peak area values in the control over the physiologically relevant condition are displayed. On the right side of the plot, peptides with peak area values in the physiologically relevant condition over the control are displayed.

Due to an uneven number of peptides (a high number of unique peptides) between the conditions, two approaches were applied to handle missing values (Marcus, Eisenacher, and Sitek 2021). The first approach omitted missing values, generating a volcano plot for common peptides found in both groups (Appendix Figure 7.10). The second approach imputed missing values as the minimum detected value of peak area, which was found to be 639.5797. This approach allows unique peptides to be included in calculations, to check if those peptides could show a significant change. This is especially important when a peptide appears in one group with high peak area value but is not detected in the other group. This absence could be due to technical issues or biological differences between the groups, and relaying only on the first approach may cause the substantial information loss. Therefore, two approaches are presented: the first approach indicates significant change in a strict statistical manner, while the second approach, though less conservative, highlights biologically important differences.

The results of the second approach are presented in (Figure 4.34). The statistical analysis showed several significantly changed peptides between the two groups of each time point. This provides an in-depth analysis and indicates the differences over time in β-Lg digestion. The highest number of peptides considered significant changes were observed at the initial state (30 seconds, T1) resulting in 106 peptides and after 1 hour (T8) of intestinal digestion resulting in 114 peptides. Interestingly, the outcome for the last time point (120 min, T9) shows a significant change only in the peptides on the left-side plots, indicating differences between the control and physiologically relevant conditions after two hours of β-Lg digestion. This may be related to the delayed digestion of β-Lg in Control condition observed in the SDS-PAGE images (Figure 4.14). Even after adopting more restrictive assumptions in statistical calculations, differences between the conditions reach about 10% at T1, T6, and T7, and up to 14.6% at T8 (Appendix Figure 7.10). These differences confirm the importance of using biosurfactants in *in vitro* digestion models. Properly reflected conditions can improve the reliability of *in vitro* simulations in mimicking physiological digestion. This is particularly important to provide results with the highest possible consistency between simulated and biological conditions.

The overall result of significant change between the physiologically relevant condition and control was 9.1% in the first approach, which considered only common peptides, and 15.9% in the second approach, which included unique peptides. The total number of peptides with significant change, obtained for the second approach, was 304, of which 51 were unique to the physiologically relevant condition (β-Lg-BS/PL-9:4) and 54 were unique to the β-Lg-Control. The other 199 peptides were common to both conditions (Figure 4.33).

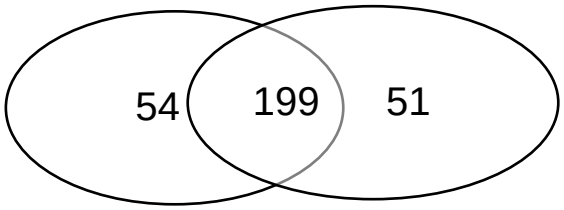

Figure 4.33 Venn diagram presenting the number of significant peptides in physiologically relevant conditions β-Lg-BS/PL-9:4 and β-Lg-Control, without any biosurfactants. The values in brackets indicate the total number of significant peptides assigned to each condition.

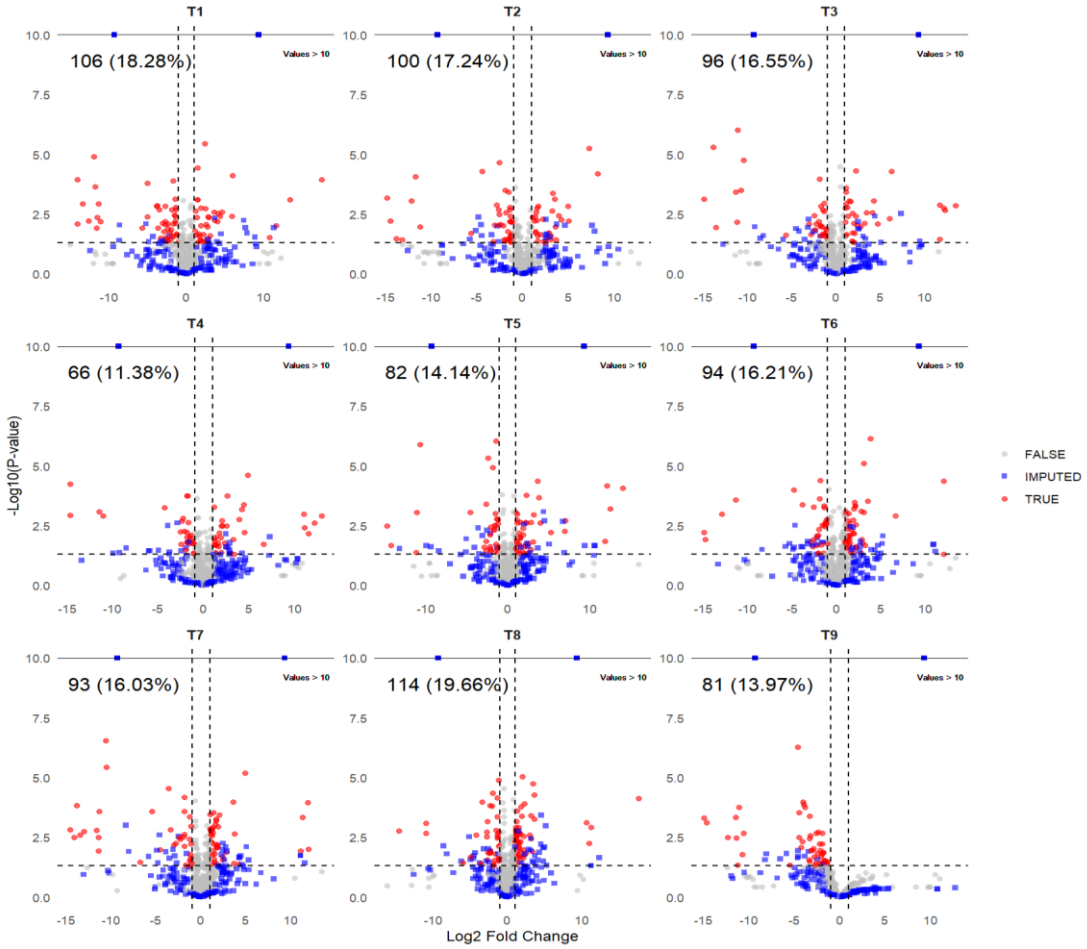

Figure 4.34 Volcano plots for each intestinal digestion time point present the differences in peak area of peptides between the physiologically relevant condition (β-Lg-BS/PL-9:4) and control (β-Lg-Control). The x-axis shows the Log2 Fold Change with a cut-off Fold Change of <0.5 and >2, and the y-axis shows -log10(p-value) with a cut-off p-value of <0.05 after FDR correction (dashed lines). Horizontal line indicates values threshold of -log10(p-value) >10. Gray dots indicate peptides that do not reach the cutoffs, red dots indicate peptides with statistical relevance, blue squares indicate imputed minimum detected values missing in one experiment. Values in the top left corners indicate numbers of statistically relevant peptides and their percentage contribution of total number of peptides taken to the analysis, n = 580.

Furthermore, 158 peptides showed a positive log2FC, meaning their intensity in physiologically relevant conditions was at least twice that of the control, while 163 peptides had a negative log2FC, indicating that their concentration was at least half as much under physiologically relevant conditions compared to the control. This may be significant for bioactive peptides and epitopes. Therefore, the list of peptides extracted from the volcano plots (Figure 4.34) was searched against the Milk Bioactive Peptides Database (MBPDB) (Nielsen et al. 2017) and the Immune Epitope Database (IEDB) for β-Lg (P02754) from 24.02.2023 (Vita et al. 2018).

Before conducting volcano analysis, 33 and 32 bioactive peptides as well as 73 and 64 epitopes were identified in physiologically relevant and control conditions, respectively. After the analysis, 16 bioactive peptides were identified during intestinal digestion in both conditions and were considered as statistically significant peptides. Of these, 13 peptides were found under physiologically relevant conditions and 11 in the control (Figure 4.35). For epitopes, the total number identified was 47, with 44 assigned to physiologically relevant conditions and 37 to the control (Figure 4.36).

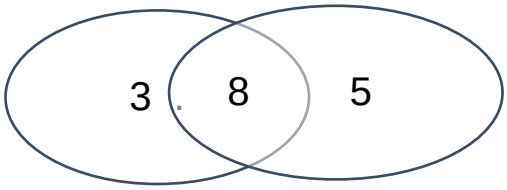

Figure 4.35 The Venn diagram presenting the number of bioactive peptides that showed significant difference in the signal intensity between two conditions, β-Lg-BS/PL-9:4 and β-Lg-Control, during 2 hours of intestinal digestion of β-Lg.

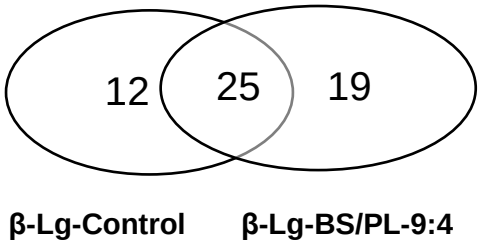

Figure 4.36 The Venn diagram presenting the number of epitopes that showed significant difference in the signal intensity between two conditions, β-Lg-BS/PL-9:4 and β-Lg-Control, during 2 hours of intestinal digestion of β-Lg.

Analyzing the results from the volcano plot obtained for each time point, the formation of epitopes and bioactive peptides during digestion were tracked, and their statistical significance in terms of changes between physiologically relevant conditions (β-Lg-BS/PL-9:4) and the control (β-Lg-Control) was determined. The number of bioactive peptides and epitopes showing statistical differences at each time point is presented in (Table 16). In the epitope analysis, the highest number of peptides was found at time points T4-T8, exceeding the signal intensity of the control. However, after one hour of digestion, only two significant epitopes remained under physiologically relevant conditions, compared to ten in the control. At the last time point, T9, despite the high number of significant peptides (81 peptides, Figure 4.34) under β-Lg-Control conditions, only three were bioactive, similar to what was found at T8. Under physiologically relevant conditions (β-Lg-BS/PL-9:4), the number of bioactive peptides was twice as high, reaching six, and remained constant from T5 to T8.

Table 16 The number of significant bioactive peptides and epitopes (p<0.05, FC <0.5 and >2) with assigned positive or negative log2FC at each time point of intestinal digestion. A negative log2FC indicates higher expression in the control (β-Lg-Control), while a positive log2FC indicates higher expression under physiologically relevant conditions (β-Lg-BS/PL-9:4).

Time point	Number of bioactive peptides		Number of epitopes	
	-log2FC	+log2FC	-log2FC	+log2FC
T1	2	0	13	8
T2	1	2	8	9
T3	0	2	9	8
T4	0	2	5	12
T5	1	6	4	18
T6	3	6	3	17
T7	2	6	5	15
T8	3	6	7	18
T9	3	0	10	2

The above analysis provides important insights into the impact of control and physiologically relevant conditions on the formation of bioactive peptides and epitopes. The results presented in Table 16 show that although the total number of bioactive peptides and epitopes detected before the volcano analysis was high and comparable between conditions, about 34% of bioactive peptides and 60% of epitopes showed statistically significant differences during digestion. Nevertheless, many peptides with significantly varying kinetics were identified under both conditions, which may have important biological implications, such as influencing regulatory mechanisms or immune response.

As previously mentioned, Nagaoka et al. (2001) studied hypocholesterolemic peptides derived from milk proteins. The β-Lg hydrolysate showed significant taurocholate-binding capacity and influenced the micellar solubility of cholesterol. Among the identified peptides, IIAEK (71–75) and VYVEELKPTPEGDLEILLQK (41-60) were highlighted for their ability to inhibit cholesterol absorption in Caco-2 cells *in vitro*. The peptide IIAEK (71–75) reduces cholesterol absorption by lowering its solubility in micelles, hindering uptake in the digestive tract (Nagaoka et al. 2001). This peptide was absent under Control conditions but was uniquely present under physiologically relevant conditions studied in my research (β-Lg-BS/PL-9:4). Its intensity peaked after one hour of digestion and then slowly declined (Appendix Figure 7.11a). The IIAEK peptide originates from a region that distinguishes physiologically relevant conditions (β-Lg-BS/PL-9:4) from the β-Lg-Control based on the average hydropathic properties of the protein sequence (arrow A' in Figure 4.32). Specifically, this peptide exhibits a hydrophobic character (+1.02), whereas, in the corresponding region, a hydrophilic character predominated in the β-Lg-Control experiment. The occurrence of this peptide serves as evidence of the differences between the two conditions. Moreover, the peptide IIAEK originates from the region with previously mentioned disparities in the heatmap (Figure 4.30). This highlights the distinctions between the conditions in the region 70–75. Similarly, as mentioned earlier, differences were observed on the heatmap in the region around 40–60, from which another bioactive peptide originates. The peptide VYVEELKPTPEGDLEILLQK (41-60) showed positive log2FC and increasing intensity over 120 minutes under physiologically relevant conditions (Figure 4.37a). In contrast, under Control conditions, its intensity peaked at 20 minutes and then dropped substantially. Its shorter fragments, peptide VEELKPTPEGDLEIL (43–57) (Figure 4.37d) and peptide LKPTPEGDLEILLQ (46-60) have been reported as an epitope (Q. Zhao et al. 2023). The kinetics of peptide 43–57 increased over time and remained very high under control conditions (β-Lg-Control). In contrast, under physiologically relevant conditions (β-Lg-BS/PL-9;4), its intensity is substantially lower, peaking at 60 minutes and decreasing after two hours of digestion (Figure 4.37f). The peptide 46–60, on the contrary, showed increasing kinetics under physiologically relevant conditions while in the control (β-Lg-Control) it was metastable at low signal intensity level (Figure 4.37e). Additionally, significant peptides from the same protein fragment include the metastable peptide RVYVEELKPTPEGDLEILLQ (40–59), which was also reported as an epitope (Järvinen et al. 2001). It shows a negative log2FC and is predominantly found at higher intensities under control conditions (Figure 4.37f). Another is the peptide LKPTPEGDLEIL (46–57), reported as a bioactive peptide, identified only under physiologically relevant conditions (Figure 4.37b). Similarly, the peptide EILLQK, also a bioactive peptide, had a positive log2FC, and surpassed control conditions in of peak area intensity under physiologically relevant conditions (Figure 4.37c).

In summary, six significant peptides were identified from the 41–60 sequence region. Of these, three were bioactive peptides and one epitope with higher release under physiologically relevant conditions, while the remaining two were epitopes with increased release under control conditions.

Interestingly, in WPI digestion, peptides 41-60 demonstrated a notable peak area under physiologically relevant conditions. Under BS-13, despite its relatively long sequence (19 amino acids), it exhibited an increasing trend up to 20 minutes of digestion (Appendix Figure 7.3b), unlike most long peptides in BS-13 conditions. Although Nagaoka et al. (2001) examined NaTC binding with the β-Lg hydrolysate as a fraction of a peptide mixture, including the distinguished peptide 41-60, recent studies confirmed interactions between BSs and β-Lg in this specific region (Takkella et al., 2024). A detailed discussion on this subject can be found in section 4.3.4.

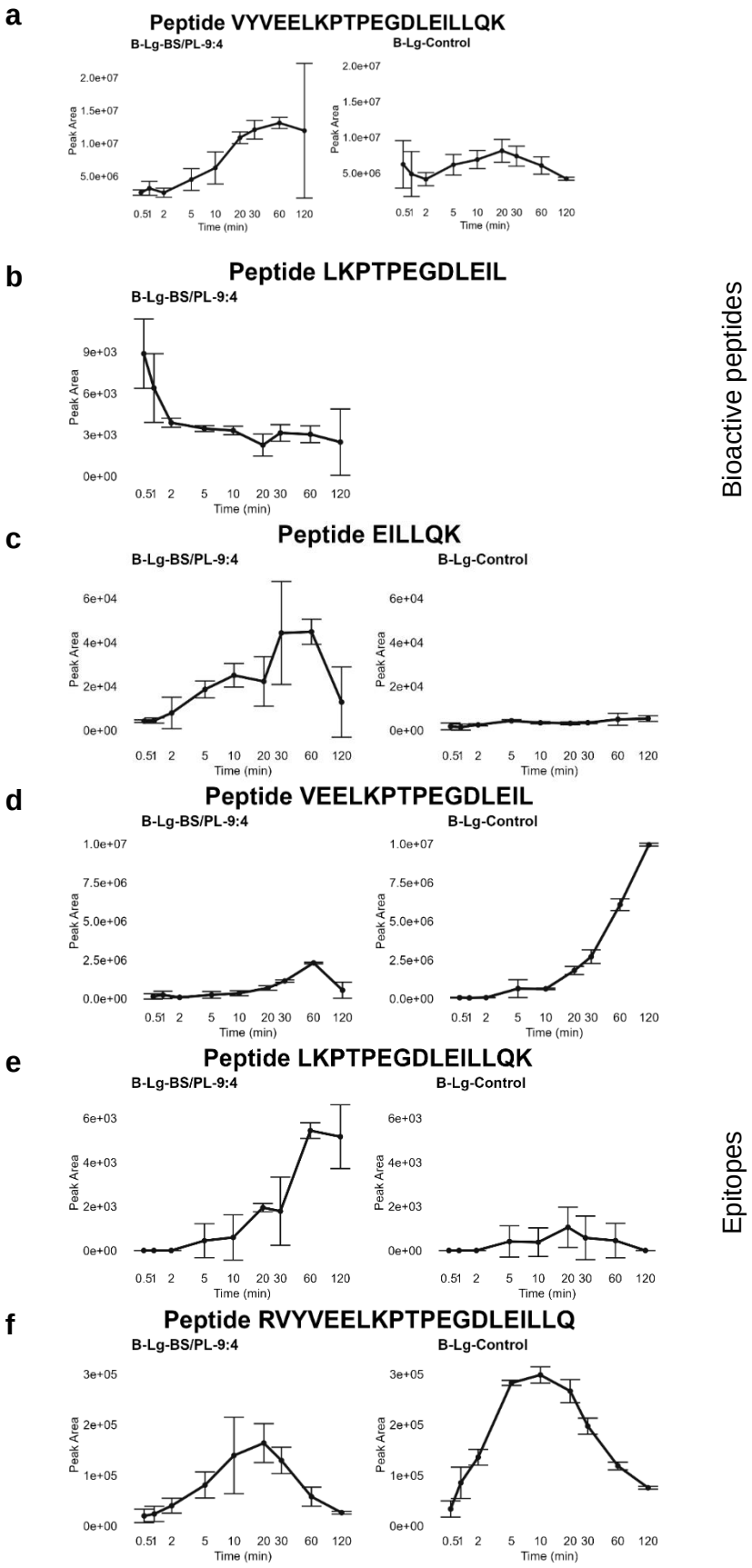

Figure 4.37 The kinetics of biologically significant peptides originating from the 40–60 β-Lg region, which were released during 2 hours of intestinal digestion of β-Lg under physiologically relevant concentrations of biosurfactants (β-Lg-BS/PL-9:4) and control conditions (β-Lg-Control).a-c bioactive peptides, d-f epitopes.

4.3.4 β-Lactoglobulin interactions with biliary surfactants and possible unique features of its digestion

Interactions between β-Lg and BS micelles have been studied by many authors; however, these studies did not identify specific binding sites, attributing the interaction to the overall hydrophobicity of the protein (Saitoh et al. 1996; Naso et al. 2019). In contrast, the latest study by Takkela et al. (2024) investigated the interaction between β-Lg and BSs, specifically NaTC, in greater detail. The authors examined β-Lg–NaTC interactions under pH 3.0 (gastric phase) and pH 6.2 (intestinal phase). It was observed that NaTC forms stable micelles at both pH 3.0 and pH 6.2. At pH 6.2, NaTC does not cause significant conformational changes in β-Lg. The interactions between NaTC and β-Lg are limited to the protein surface and are mainly hydrophobic interactions. These interactions preserve the dimeric structure of β-Lg under intestinal conditions in presence of NaTC. In contrast, during the gastric phase (pH 3), the key interaction site of the protein monomer was Trp61, where NaTC strongly binds through hydrogen bonds and van der Waals forces (Figure 4.38a). However, it should be noted that the study by Takkela et al. (2024) provided insights into the behavior of β-Lg in the presence of BSs at pH 3.0 and pH 6.2 and it did not simulate the sequential transition of the protein from the gastric to the intestinal phase, which could provide a more realistic picture of β-Lg digestion in the presence of NaTC. Nonetheless, these findings offer valuable insights into the stability of this protein in the small intestine and may explain the formation of a uniform and less diverse peptide profile during β-Lg digestion in the presence of BSs alone (BS-13).

Interestingly, the peptide YVEELKPTPEGDLEILLQKWENGECAQKKI (42-71) was found only under the BS-13 digestion conditions. This peptide was degraded after 5 minutes, among others, to peptides PTPEGDLEILLQ and WENGECAQKKI, which were also unique to BS-13 (Figure 4.39). Considering this peculiarity, the peptide 42-71 contains the key Trp61 residue involved in binding to BSs, along with other residues forming hydrogen bonds (Gln68, Lys70, Glu62), van der Waals interactions with Ile71 and Leu58, and alkyl interactions with Lys60 and Lys69 (Takkella et al., 2024). Since the fragment fully overlaps with the region of β-Lg involved in strong hydrophobic interactions with NaTC, as described by the Takkela et al. and shown in Figure 4.38, this may explain the distinct digestion pattern observed in the presence of BS-13 compared to other conditions (Figure 4.16). It is important to note that the fragment 42-71 was not detected in the gastric phase at all. This demonstrates the unique digestive pattern observed in the presence of BSs, likely resulting from their interactions with this specific region of β-Lg.

Additionally, the peptide originating from this region, LKPTPEGDLEILLQK (46–60), was found in all conditions (Control, PL-13, BS/PL-9:4, BS/PL-6.5:6.5 and BS/PL-4:9) except BS-13. This proves that discussed protein fragment (42-71) was digested in other conditions, but with a different pattern. Another example is shorter fragment, peptide LKPTPEGDLEIL (46–57), which was detected in all experiments with BSs (BS-13, BS/PL-9:4, BS/PL-6.5:6.5 and BS/PL-4:9) but was absent in the conditions with only PLs (PL-13) and in Control. These results are consistent with studies of pure β-Lg digestion, where fragment 46–60 was present in control (β-Lg-Control) and physiologically relevant conditions (β-Lg-BS/PL-9:4). However, fragment 46–57 was found only in conditions containing BSs (β-Lg-BS/PL-9:4) (Figure 4.37b).

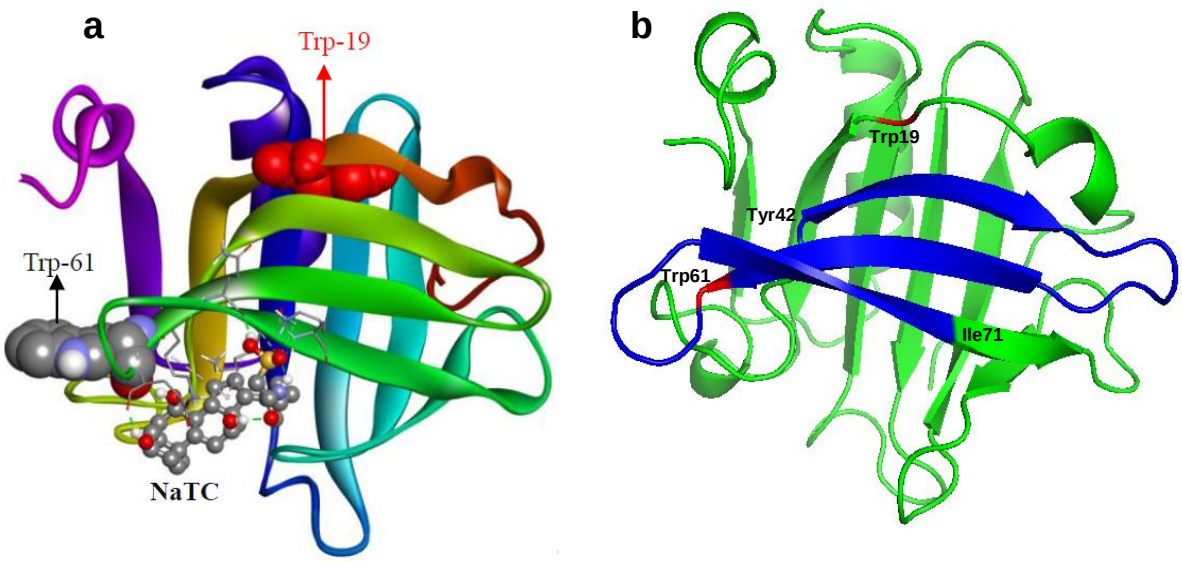

Figure 4.38 The structure of β-Lg and molecular docking of NaTC, by Takkela et al. (2024) (a); The structure of β-Lg with the fragment 42–71 highlighted in blue found only in the BS-13 conditions and the Trp61 and Trp19 residues marked in red (b). PyMol (PDB ID: 1B0O).

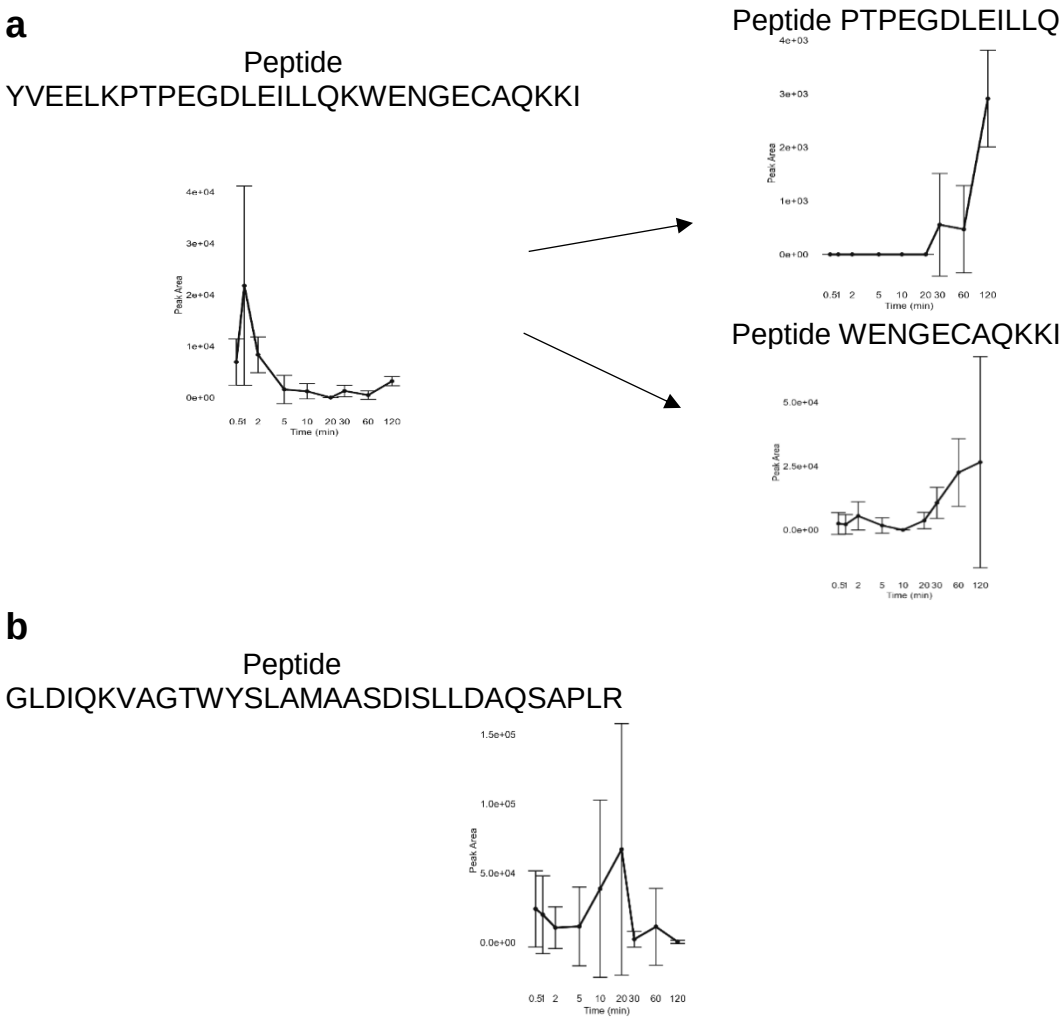

Figure 4.39 The kinetics of unique peptides found in BS-13 conditions during intestinal phase of WPI digestion. a) Peptide 42-71 and its possible break down peptides present only in the conditions of BS-13; b) Peptide 9-40.

The kinetic model of β-Lg digestion proposed by Fernández and Riera (2013) aligns in many cases with the results of this study. However, the model is simplified and limited to a small number of peptides. For example, the kinetics of the digestion of the 41–70 fragment, which is broken down into 41–60 and 61–70 (A. Fernández and Riera 2013), represents a significant oversimplification. Although the current results are consistent with the proposed pathway, it is not the only pathway occurring during intestinal digestion, which is preceded by gastric digestion. In this study, numerous peptides were released from the fragment 41–70 (89 peptides under β-Lg-BS/PL-9:4 and 94 peptides under β-Lg-Control conditions). This is particularly important in a biological context, as six different biologically important peptides are released from this fragment (Figure 4.37a-f), showing statistically significant differences between the conditions. Peptides from aforementioned region 41–60 were characterized as having good interfacial properties due to their hydrophobic/hydrophilic residue distribution (Turgeon et al. 1992). This specific fragment with amphipathic character leads to aggregation with other peptides and also makes it effective emulsifier (Groleau et al. 2003). However, weaker interfacial properties were assigned to peptides 61–70 and 149–162. The authors suggest that the weak interfacial properties could be caused by the rigidity of these peptides due to the presence of disulfide bonds and the even distribution of hydrophobic/hydrophilic residues (Turgeon et al. 1992).

Furthermore, a comparable pattern is observed in the region surrounding Trp19. The peptide GLDIQKVAGTWYSLAMAASDISLLDAQSAPLR (9-40) is found only in BS-13 conditions and reaches its maximum peak area after 20 minutes of digestion. Similarly, to previous example, this peptide has not been found in gastric phase (Figure 4.39b). Its shorter fragment (15-40) appears in all conditions containing BSs but is absent in Control and PL-13. This is consistent with the digestion experiment of pure β-Lg, where the peptide 9-40 and its shorter forms (9-23, 9-24, 9-22, 9-31, 9-28) are unique to physiologically relevant conditions (β-Lg-BS/PL-9:4). Similarly, the peptide 15-40 and its shorter forms, such as 15-31, 15-28, and 15-24, are also found only in physiologically relevant conditions and are absent in control (β-Lg-Control). For experiments of WPI digestion, the peptide 15-28 is present in BS-13, PL-13, and BS/PL mixtures but is absent in Control. In addition, the peptide 15-27 appears only in PL-13, while 15-24 is detected in experiments with BS/PL mixtures but none of them was found in Control conditions. Although Takkella et al. does not specifically investigate the interactions involving Trp19, due to its location in the central hydrophobic part of the protein, within its calyx (Takkella et al., 2024), these studies were conducted on the native structure of the protein and do not account for the structural changes occurring during digestion. The unique presence of the 9–40 fragment may suggest interactions similar to those observed for the 42–71 fragment. However, binding might have occurred only after partial protein digestion, as indicated by the kinetics of the metastable peptide 9–40 (Figure 4.39b).

In addition to BSs, also PLs have been studied for their interactions with the β-Lg protein. The studies by Brown et al. (1983) have shown the dynamics associated with structural changes in β-Lg in the presence of PLs. The study demonstrated dynamic transitions in the protein's structure driven by electrostatic and hydrophobic interactions between β-Lg and PLs. These changes involve partial unfolding of the protein structure and an increase in the proportion of α-helical structures from approximately 10% to 25-30%. The conformational changes are strongly dependent on pH and environmental conditions (e.g., the presence of lipids and ionic strength). The article suggests that these structural changes are partially reversible, depending on the environment. For instance, the protein partially renatures when transferred from an organic solvent to an aqueous environment (Brown et al. 1983). Other studies, such as (Kristensen et al. 1997) and (Lefèvre 2000), showed that zwitterionic PLs (e.g., PC and PE) have lower affinity for interaction with β-Lg compared to negatively charged PLs, such as distearoylphosphatidic acid or phosphatidylserine, respectively. However, these studies were conducted with the native

form of β-Lg, which does not reflect the partial denaturation of the protein caused by gastric conditions. Therefore, the use of organic solvents in the initial stage of Brown et al.'s experiments, which induced protein pre-denaturation, may better explain the interaction of PLs with β-Lg under intestinal digestion conditions. The protein's dynamic ability to temporarily adopt different structures as a result of interaction with PLs may explain the diversity of the peptide profile during digestion in the presence of PL resulting in increased number of peptides. This may result from the lack of protein stabilization or a more complex mechanism as a result of interplay of BSs and PLs. Interactions of β-Lg in the presence of BS and PL micelles were studied by Dulko et al. (2021), who demonstrated that PLs, even at low concentrations such as 0.18 mM, have a reducing effect on the denaturing properties of BSs and mitigate structural changes within the secondary structure. This suggested a protective effect of PLs against the action of BSs (Maldonado-Valderrama et al. 2011; Dulko 2021). Although this study provides important observations, it does not provide clear information that can be directly applied to the current research, as these studies were also conducted on the native form of β-Lg, without considering the digestion process over time, and potential protein structural changes. This issue requires further analysis and research, which is beyond the scope of this study. As mentioned earlier, very long fragments (2–41 and 123–162) were observed only in the presence of PLs alone (Appendix Figure 7.4b,c), which persisted throughout the entire 2-hour digestion period. This suggests potential interactions between these fragments and PLs. The mechanism behind these interactions remains unknown; however, this observation underscores the importance of PLs and their equally important role during β-Lg digestion.

In summary, the peculiarity of β-Lg digestion in the regions of Trp19 and Trp61 proximity may depend on the interplay of BSs and PLs and their possible interactions with the protein sequence at these regions. However, further research is required to explain the interactions between the β-Lg molecule, its fragments, and biliary surfactants in these specific regions.

4.3.5 Distinctiveness of β-lactoglobulin digestion under the physiologically relevant ratio of biliary surfactants

The kinetics of peptide LSFNPTQLEEQCHI warrants additional discussion. It is the C-terminal fragment (149-162) of β-Lg (Nika et al. 2013), and it is marked in red at the 3D structure of β-lg (Figure 4.40). This peptide contains cysteine at position 160, which forms a disulfide bond with the Cys66 (Figure 4.40). This disulfide bond is one of the main bonds stabilizing the tertiary structure of β-Lg (Barbiroli, Iametti, and Bonomi 2022). The fragment 149-162 has been reported as one of the main β-Lg epitopes (Sélo et al. 1999). It is well-documented in the literature as a signature peptide for β-Lg from cow milk (Chen et al. 2016). Moreover, it is one of the most valuable markers in the analysis of milk proteins. It stands out not only for its specificity to β-Lg but also for its stability in complex matrices such as ripened cheese (von Oesen et al. 2023). Furthermore, it has been reported as a potential marker (Nika et al. 2013) for tracking the β-Lg oxidation process during food storage or food processing (Du et al. 2021).

Cavalcante et al. (2023) found the differences in the peptide profile of the tryptic digestion depended on the pasteurization process. The absence of peptide (149-162) in the β-Lg hydrolysate was reported when the digestion was performed on the protein pre-treated with UV-C. The UV-C irradiation causes photochemical reductive cleavage of disulfide bonds present in β-Lg, leading to changes in the conformational structure of the protein,

and consequently differences in the obtained peptide profile during digestion (Cavalcante et al. 2023).
In current research, the peptide (149-162) exhibits contrasting trend in the kinetics under physiologically relevant conditions (BS/PL-9:4) compared to other conditions during intestinal digestion. This trend is consistent in both WPI and pure β-Lg digestion (Figure 4.41). The peptide shows very high signal intensity during the initial phase of digestion (first minute), followed by a decrease in signal intensity in the presence of biosurfactants at physiologically relevant concentration (BS/PL-9:4). Conversely, under other digestion conditions, its intensity increases, reaching a maximum during the final stage of digestion (BS/PL-6.5:6.5, BS/PL-4:9, PL-13, Control). The exception is the experiment with only BSs (BS-13), where this peptide reaches its maximum peak area at 20 minutes of digestion.

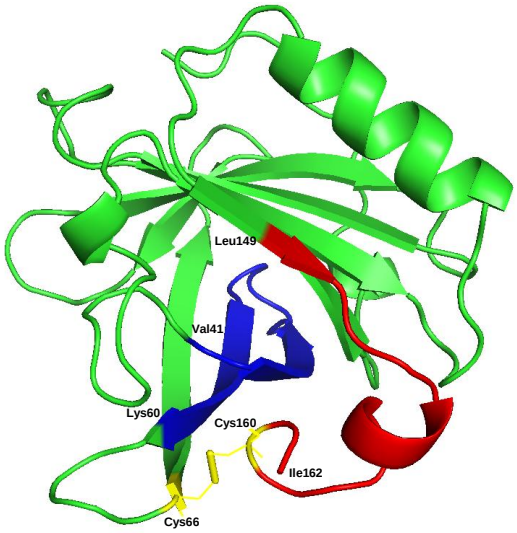

Figure 4.40 3D structure of β-Lg showing fragments released with the highest signal intensity under physiologically relevant conditions during intestinal digestion. The yellow color indicates the disulfide bond between Cys66 and Cys160. The red fragment represents peptide LSFNPTQLEEQCHI (residues 149-162), while the blue fragment represents peptide VYVEELKPTPEGDLEILLQK (residues 41-60). PyMol (PDB ID: 1B0O).

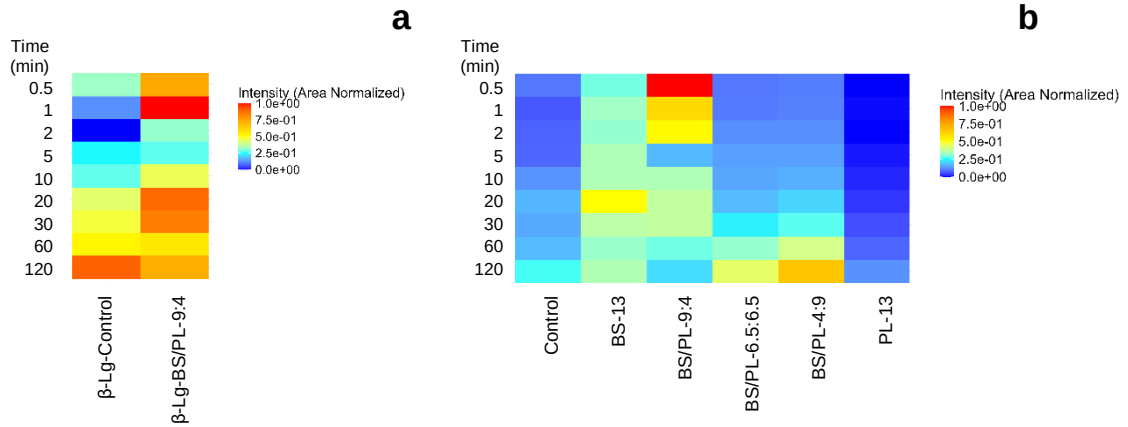

Figure 4.41 The heatmap for LSFNPTQLEEQCHI illustrates the relative comparison of kinetic evolution (a) in the pure β-Lg intestinal digestion for control and physiologically relevant concentration. Min-max normalization was applied to enhance the visual representation of the kinetic pattern; (b) in the WPI intestinal digestion across various conditions. To reduce the impact of the exceptionally high signal intensity under physiologically relevant conditions (BS/PL-9:4) in WPI digestion, the values of this particular experiment were divided by 2. Min-max normalization was applied to enhance the visual representation of the kinetic pattern.

Two additional peptides that also showed outstanding peak area values in the early stage of WPI digestion under BS/PL-9:4 conditions were VYVEELKPTPEGDLEILLQK (41–60) and VEELKPTPEGDLEILLQK (43–60) (Figure 4.15c-d). These peptides originate from a region previously discussed in detail in the context of β-Lg – BSs interactions (section 4.3.4) as well as their roles as bioactive peptides and epitopes. During the digestion of pure β-Lg, these peptides also exhibited significantly higher signal intensity under physiologically relevant conditions compared to the control. Their kinetics showed a gradual increase over time, reaching maximum intensity at the final stage of digestion. The region (41-60) is highlighted in Figure 4.40, where its spatial arrangement in the protein is shown, along with its proximity to peptide 149–162 and the disulfide bond Cys66-Cys160.

Similarly, peptides mentioned earlier, which had the highest sum peak area under physiologically relevant conditions of WPI digestion (Figure 4.15e-f), originate from the region surrounding the second disulfide bond in β-Lg, Cys106-Cys119 (Barbiroli, Iametti, and Bonomi 2022). The peptide VLVLDTDYK precedes the Cys106 residue, while the peptide TPEVDDEALEKFDK follows Cys119 (Figure 4.42).

In the case of β-Lg digestion alone, the peptide VLVLDTDYK (92-100) showed no significant difference between conditions and had similar kinetics, with increasing intensity over time in both physiologically relevant biosurfactant concentrations (β-Lg-BS/PL-9:4) and control conditions (β-Lg-Control) (Appendix Figure 7.11a). However, the peptide TPEVDDEALEKFDK (125-138) under β-Lg-BS/PL-9:4 conditions had significantly higher peak area intensity compared to β-Lg-Control (Appendix Figure 7.11b).

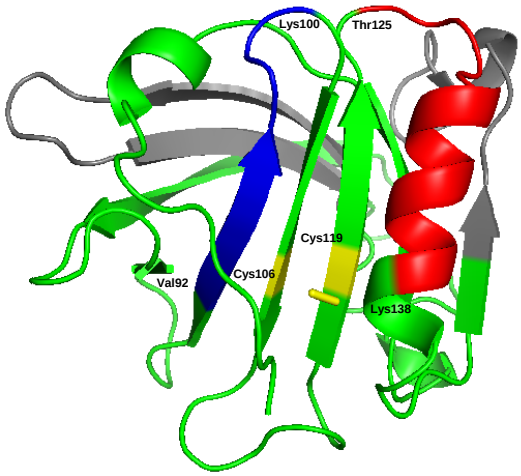

Figure 4.42 3D structure of β-Lg showing fragments released with the highest signal intensity under physiologically relevant conditions during intestinal digestion of WPI. The yellow color indicates the disulfide bond between Cys106 and Cys119. The red fragment represents peptide TPEVDDEALEKFDK (125-138), while the blue fragment represents peptide VLVLDTDYK (94-100), grey fragments represent peptides discussed above (LSFNPTQLEEQCHI and VYVEELKPTPEGDLEILLQK) and shown in the Figure 4.40. PyMol (PDB ID: 1B0O).

In the Figure 4.42, the peptides with the outstanding peak area are visualized, along with the cleavage sites: Lys100-Lys101, Lys91-Val92, Arg124-Thr125, Lys138-Arg139. By cleaving at these sites, the fragment 101–124, containing the disulfide bond Cys106-Cys119 is detached from the protein. There have been 80 peptides detected in physiologically relevant conditions from the β-Lg region 101–124 (ranging in length from 23 to 5 amino acids). However, the highest intensity was observed for the peptides CMENSAEPEQSLACQCLVR (106–124) and CMENSAEPEQSLACQCL (106–122). The

kinetics of these peptides (Appendix Figure 7.3f-g) is similar to all peptides with outstanding intensity, discussed in this subsection. The coexisting peptide KYLLF (101-105) also shows decrease in its intensity in the course of digestion but has a slightly lower peak area intensity (Appendix Figure 7.3h).

Taking all the above under consideration, it can be concluded that under physiologically relevant biosurfactant concentrations (BS/PL-9:4) the release of outermost fragments which are in proximity of the disulfide bonds is likely favored. This phenomenon could facilitate the unfolding of the protein structure and its exposure to further digestion. As shown earlier, the breaking of disulfide bonds causes changes in the tertiary structure of the protein and exposes hydrophobic sites (Du et al. 2021). Additionally, the selectivity of trypsin was previously observed in its interaction with the capsid protein VP1 of type 3 poliovirus, where intestinal trypsin cleaved the BC-loop located between two β-sheets, what could influence biological response (Cusi, Rossolini, Valensin 1988). These observations could explain the exceptionally high and distinct area values characteristic of the mentioned peptides under digestion conditions involving the physiologically relevant BS/PL ratio (BS/PL-9:4) (Figure 4.15b-f).

5 Conclusions

Accurately mimicking bile composition is essential for reflecting physiological digestion under *in vitro* conditions. The primary and most extensively studied components of bile are BSs. However, the results of my research show that biliary PLs, second most abundant biliary biosurfactants, play a significant role, especially when combined with BSs. The physiological ratio of biliary biosurfactants was determined in my study to be 9 mM BSs to 4 mM PLs in healthy individuals.

One of the main findings of this study is the synergistic effect of BSs and PLs, combined at physiologically relevant 9:4 ratio, in efficiency of TAG lipolysis, compared to other proportions of biliary surfactants. The physiological ratio shows the largest conversion of TAGs to FFAs in the emulsion lipolysis experiments, as well as the most effective reduction in IFT during lipolysis. This research provides a pioneering study on the significance of the ratio of BSs and PLs in simulating the physiological role of biliary biosurfactants in intestinal lipolysis.

For the first time, a correlation was established between the extent of *in vitro* digestion of TAG emulsions and the evolution in the TAG/water IFT during interfacial lipolysis and desorption, depending on the concentration of PLs. This finding provides insights into the desorption capacities of PLs, BSs, and the lipolytic products generated at the interface. Our results underscore the importance of the desorption step, when lipolysis products are removed from the interface and solubilized, enabling further TAG hydrolysis at the interface. Systems containing PLs alongside BSs were found to form a complex interfacial layer that presents resistant to desorption. This resistance may influence the efficiency of TAG lipolysis in the intestine, particularly at higher PL ratios.

This study also demonstrates the effect of PLs on the digestion rate of the model food protein β-Lg, where, for the first time, the relationship between digestion slowdown and the molar ratios of biosurfactants has been shown. Furthermore, the peptide profile analysis revealed that the slowed digestion of β-Lg in the presence of biliary PLs may possess a physiological significance in the kinetics of bioactive peptide and epitope release. The peptide profile resulting from β-Lg digestion under the physiologically relevant concentrations of biosurfactants (BSs 9mM and PLs 4mM) differs significantly from digestion without the biosurfactants, with a higher number of biologically significant peptides observed under physiologically relevant conditions compared to the control.

Additionally, for the first time, differences have been identified in the peptide profiles of β-Lg between the digesta produced in the presence of BSs alone, PLs alone, and the physiological ratio BS/PL-9:4. These differences may result from specific interactions between the biosurfactants and protein fragments, leading to diversification of the peptide profile. My observations suggest further research directions required for understanding the impact of biliary surfactants on β-Lg digestion and their mutual interactions during the digestion process.

To sum up, the study of the lipolytic section provides thorough knowledge of the interfacial dynamics in the simulated digestive system, especially as they apply to food colloids. The results emphasize the synergistic effects of biliary biosurfactants in intestinal lipolysis and the crucial role that the BS/PL ratio plays in effective digestion of TAGs.

The results of the proteolytic section show a diverse peptide profile, with a substantially higher number of bioactive peptides and epitopes, observed during β-Lg digestion in the presence of BS/PL mixtures compared to BSs alone.

Together, the differences identified from the digestion experiments emphasize the critical role of biliary PLs in the physiologically relevant digestion β-Lg and TAGs. Moreover, demonstrating differences in the outcomes of both lipolysis and proteolysis at various molar ratios of biliary surfactants can provide valuable insights for pathological conditions of the gut, where the concentrations of BSs and PLs may vary, such as in bile secretion disorders or in BSs and/or PLs deficiencies (Razafindrazoto et al. 2023).

The main goal of *in vitro* digestion models used in scientific research is often to reflect the conditions of the human digestive system. Therefore, the *in vitro* models should be designed as close as possible to physiological conditions. This is also important for any further physiologically relevant assessment of nutrient or bioactive peptide absorption, as well as the evaluation of allergenicity, which may depend on the release of epitopes. Delayed lipolysis may impact e.g. the transport and absorption of fat-soluble vitamins and other lipophilic substances in the intestine. Likewise, delayed proteolysis may impact the release, persistence and absorption of biologically important peptides in the intestine. Therefore, the importance of PLs should not be omitted in *in vitro* digestive models. The results obtained through my research may contribute substantially to the improvement of *in vitro* digestion models by highlighting the importance of PLs alongside BSs. The findings presented in this dissertation can also provide a foundation for future studies, e.g. on the design of hypoallergenic foods, nutraceuticals, and functional foods enriched with bioactive peptides or lipid-soluble vitamins, etc.

6 Literature

Abd El-Salam, M. H., Safinaz El-Shibiny, and Aida Salem. 2009. “Factors Affecting the Functional Properties of Whey Protein Products: A Review.” *Food Reviews International* 25 (3): 251–70. https://doi.org/10.1080/87559120902956224.

Acevedo-Fani, Alejandra, and Harjinder Singh. 2022. “Biophysical Insights into Modulating Lipid Digestion in Food Emulsions.” *Progress in Lipid Research* 85: 101129. https://doi.org/10.1016/j.plipres.2021.101129.

Adhikari, Shiksha, Marijke Schop, Imke J.M. de Boer, and Thom Huppertz. 2022. “Protein Quality in Perspective: A Review of Protein Quality Metrics and Their Applications.” *Nutrients* 14 (5): 1–31. https://doi.org/10.3390/nu14050947.

Admirand, W. H., and D. M. Small. 1968. “The Physicochemical Basis of Cholesterol Gallstone Formation in Man.” *The Journal of Clinical Investigation* 47 (5): 1043–52. https://doi.org/10.1172/JCI105794.

Ahn, Nahyun, and Jee-Young Imm. 2023. “Effect of Phospholipid Matrix on Emulsion Stability, Microstructure, Proteolysis, and in Vitro Digestibility in Model Infant Formula Emulsion.” *Food Research International* 163 (July): 112218. https://doi.org/10.1016/j.foodres.2022.112218.

Akkerdaas, Jaap, Muriel Totis, Brian Barnett, Erin Bell, Tom Davis, Thomas Edrington, Kevin Glenn, et al. 2018. “Protease Resistance of Food Proteins: A Mixed Picture for Predicting Allergenicity but a Useful Tool for Assessing Exposure.” *Clinical and Translational Allergy* 8 (1): 1–12. https://doi.org/10.1186/s13601-018-0216-9.

Alvarez, F J, and V J Stella. 1989. “The Role of Calcium Ions and Bile Salts on the Pancreatic Lipase-Catalyzed Hydrolysis of Triglyceride Emulsions Stabilized with Lecithin.” *Pharmaceutical Research* 6 (6): 449–57. https://doi.org/10.1023/a:1015956104500.

Armand, Martine. 2007. “Lipases and Lipolysis in the Human Digestive Tract: Where Do We Stand?” *Current Opinion in Clinical Nutrition and Metabolic Care* 10 (2): 156–64. https://doi.org/10.1097/MCO.0b013e3280177687.

Armand, Martine, Patrick Borel, Berengere Pasquier, Christophe Dubois, Michele Senft, Marc Andre, Jacques Peyrot, Jacques Salducci, and Denis Lairon. 1996. “Physicochemical Characteristics of Emulsions during Fat Digestion in Human Stomach and Duodenum.” *American Journal of Physiology - Gastrointestinal and Liver Physiology* 271 (1 34-1). https://doi.org/10.1152/ajpgi.1996.271.1.g172.

Armand, Martine, Patrick Borel, Pascale Ythier, Guy Dutot, Christian Melin, Michèle Senft, Huguette Lafont, and Denis Lairon. 1992. “Effects of Droplet Size, Triacylglycerol Composition, and Calcium on the Hydrolysis of Complex Emulsions by Pancreatic Lipase: An in Vitro Study.” *The Journal of Nutritional Biochemistry* 3 (7): 333–41. https://doi.org/10.1016/0955-2863(92)90024-D.

Bai, Jane P.F. 1994. “Effects of Bile Salts on Brush-Border and Cytosolic Proteolytic Activities of Intestinal Enterocytes.” *International Journal of Pharmaceutics* 111 (2): 147–52. https://doi.org/10.1016/0378-5173(94)00117-0.

Balakireva, Anastasia V., and Andrey A. Zamyatnin. 2016. “Properties of Gluten Intolerance: Gluten Structure, Evolution, Pathogenicity and Detoxification Capabilities.” *Nutrients* 8 (10). https://doi.org/10.3390/nu8100644.

Banerjee, Amrita, and Hayat Onyuksel. 2012. “Human Pancreatic Polypeptide in a Phospholipid-Based Micellar Formulation.” *Pharmaceutical Research* 29 (6): 1698–1711. https://doi.org/10.1007/s11095-012-0718-4.

Banerjee, Shibdas, and Shyamalava Mazumdar. 2012. “Electrospray Ionization Mass Spectrometry: A Technique to Access the Information beyond the Molecular Weight of the Analyte.” *International Journal of Analytical Chemistry* 2012: 1–40. https://doi.org/10.1155/2012/282574.

Barak, Sheweta, Deepak Mudgil, and B. S. Khatkar. 2015. “Biochemical and Functional Properties of Wheat Gliadins: A Review.” *Critical Reviews in Food Science and Nutrition* 55 (3): 357–68. https://doi.org/10.1080/10408398.2012.654863.

Barbiroli, Alberto, Stefania Iametti, and Francesco Bonomi. 2022. “Beta-Lactoglobulin as a Model Food Protein: How to Promote, Prevent, and Exploit Its Unfolding Processes.”

Bellesi, Fernando A., and Ana M.R. Pilosof. 2021. “Potential Implications of Food Proteins-Bile Salts Interactions.” *Food Hydrocolloids* 118 (March): 106766. https://doi.org/10.1016/j.foodhyd.2021.106766.

Bellesi, Fernando A., Víctor M. Pizones Ruiz-Henestrosa, and Ana M.R. Pilosof. 2014. “Behavior of Protein Interfacial Films upon Bile Salts Addition.” *Food Hydrocolloids* 36 (May): 115–22. https://doi.org/10.1016/j.foodhyd.2013.09.010.

Benito-Gallo, Paloma, Alessandro Franceschetto, Jonathan C.M. Wong, Maria Marlow, Vanessa Zann, Peter Scholes, and Pavel Gershkovich. 2015. “Chain Length Affects Pancreatic Lipase Activity and the Extent and PH-Time Profile of Triglyceride Lipolysis.” *European Journal of Pharmaceutics and Biopharmaceutics* 93 (June): 353–62. https://doi.org/10.1016/j.ejpb.2015.04.027.

Berge Henegouwen, G. P. van, S. D.J. van der Werf, and A. T. Ruben. 1987. “Fatty Acid Composition of Phospholipids in Bile in Man: Promoting Effect of Deoxycholate on Arachidonate.” *Clinica Chimica Acta* 165 (1): 27–37. https://doi.org/10.1016/0009-8981(87)90215-4.

Bergstrom, Christel A.S., Albin Parrow, Per Larsson, and Patrick Augustijns. 2020. “Molecular Dynamics Simulations on Interindividual Variability of Intestinal Fluids: Impact on Drug Solubilization.” *Molecular Pharmaceutics* 17 (10): 3837–44. https://doi.org/10.1021/acs.molpharmaceut.0c00588.

Bhagavan, N.V., and Chung-Eun Ha. 2015. “Gastrointestinal Digestion and Absorption.” *Essentials of Medical Biochemistry*, 137–64. https://doi.org/10.1016/b978-0-12-416687-5.00011-7.

Bläckberg, L., O. Hernell, G. Bengtsson, and T. Olivecrona. 1979. “Colipase Enhances Hydrolysis of Dietary Triglycerides in the Absence of Bile Salts.” *The Journal of Clinical Investigation* 64 (5): 1303–8. https://doi.org/10.1172/JCI109586.

Bohn, T, F Carriere, L Day, A Deglaire, L Egger, D Freitas, M Golding, et al. 2018. “Correlation between in Vitro and in Vivo Data on Food Digestion. What Can We Predict with Static in Vitro Digestion Models?,” 1–48. https://doi.org/10.1080/10408398.2017.1315362.

Boland Mike; Golding Matt. 2014. *Food Structures, Digestion and Health*. https://doi.org/https://doi.org/10.1016/B978-0-12-404610-8.01001-X.

Booker, M. L., W. W. LaMorte, S. A. Ahrendt, K. D. Lillemoe, and H. A. Pitt. 1992. “Distribution of Phosphatidylcholine Molecular Species between Mixed Micelles and

Phospholipid-Cholesterol Vesicles in Human Gallbladder Bile: Dependence on Acyl Chain Length and Unsaturation." *Journal of Lipid Research* 33 (10): 1485–92.

Borgström, Bengt. 1980. "Importance of Phospholipids, Pancreatic Phospholipase A2, and Fatty Acid for the Digestion of Dietary Fat. In Vitro Experiments with the Porcine Enzymes." *Gastroenterology* 78 (5 PART 1): 954–62. https://doi.org/10.1016/0016-5085(80)90777-5.

Bossios, Apostolos, Maria Theodoropoulou, Lucie Mondoulet, Neil M. Rigby, Nikolaos G. Papadopoulos, Hervé Bernard, Karine Adel-Patient, Jean Michel Wal, Clare EN Mills, and Photini Papageorgiou. 2011. "Effect of Simulated Gastro-Duodenal Digestion on the Allergenic Reactivity of Beta-Lactoglobulin." *Clinical and Translational Allergy* 1 (1): 1–11. https://doi.org/10.1186/2045-7022-1-6.

Böttger, Franziska, Didier Dupont, Dorota Marcinkowska, Balazs Bajka, Alan Mackie, and Adam Macierzanka. 2019. "Which Casein in Sodium Caseinate Is Most Resistant to in Vitro Digestion? Effect of Emulsification and Enzymatic Structuring." *Food Hydrocolloids* 88 (March): 114–18. https://doi.org/10.1016/j.foodhyd.2018.09.042.

Bradley, Sterling Gaylen, and Don W. Bradley. 2022. *Digestive Proteases: Roles in the Human Alimentary Tract*. *Encyclopedia of Cell Biology: Volume 1-6, Second Edition*. Vol. 1. Elsevier Ltd. https://doi.org/10.1016/B978-0-12-821618-7.00207-8.

Brix, Klaudia, and Walter St. 2013. *Proteases: Structure and Function*. Edited by Klaudia Brix and Walter Stöcker. Vienna: Springer Vienna. https://doi.org/10.1007/978-3-7091-0885-7.

Brockman, H. L. 2000. "Kinetic Behavior of the Pancreatic Lipase-Colipase-Lipid System." *Biochimie* 82 (11): 987–95. https://doi.org/10.1016/S0300-9084(00)01185-8.

Brodkorb, André, Lotti Egger, Marie Alminger, Paula Alvito, Ricardo Assunção, Simon Ballance, Torsten Bohn, et al. 2019. "INFOGEST Static in Vitro Simulation of Gastrointestinal Food Digestion." *Nature Protocols* 14 (4): 991–1014. https://doi.org/10.1038/s41596-018-0119-1.

Brouwers, Joachim, Jan Tack, Frank Lammert, and Patrick Augustijns. 2006. "Intraluminal Drug and Formulation Behavior and Integration in in Vitro Permeability Estimation: A Case Study with Amprenavir." *Journal of Pharmaceutical Sciences* 95 (2): 372–83. https://doi.org/10.1002/jps.20553.

Brown, Eleanor M., Robert J. Carroll, Philip E. Pfeffer, and Joseph Sampugna. 1983. "Complex Formation in Sonicated Mixtures of β-Lactoglobulin and Phosphatidylcholine." *Lipids* 18 (2): 111–18. https://doi.org/10.1007/BF02536104.

Capozzi, Francesco, and Alessandra Bordoni. 2013. "Foodomics: A New Comprehensive Approach to Food and Nutrition." *Genes and Nutrition* 8 (1): 1–4. https://doi.org/10.1007/s12263-012-0310-x.

Capuano, Edoardo, and Anja E.M. Janssen. 2021. "Food Matrix and Macronutrient Digestion." *Annual Review of Food Science and Technology* 12: 193–212. https://doi.org/10.1146/annurev-food-032519-051646.

Carbonaro, Marina, George Grant, Marsilio Cappelloni, and Arpad Pusztai. 2000. "Perspectives into Factors Limiting in Vivo Digestion of Legume Proteins: Antinutritional Compounds or Storage Proteins?" *Journal of Agricultural and Food Chemistry* 48 (3): 742–49. https://doi.org/10.1021/jf991005m.

Carey, Martin C. 1972. “Micelle Formation by Bile Salts.” *Archives of Internal Medicine* 130 (4): 506. https://doi.org/10.1001/archinte.1972.03650040040005.

Carver, J. D. 1999. “Dietary Nucleotides: Effects on the Immune and Gastrointestinal Systems.” *Acta Paediatrica, International Journal of Paediatrics, Supplement* 88 (430): 83–88. https://doi.org/10.1111/j.1651-2227.1999.tb01306.x.

Castillo-Santaella, Teresa del, and Julia Maldonado-Valderrama. 2023. “Adsorption and Desorption of Bile Salts at Air–Water and Oil–Water Interfaces.” *Colloids and Interfaces* 7 (2): 31. https://doi.org/10.3390/colloids7020031.

Castillo-Santaella, Teresa Del, Julia Maldonado-Valderrama, Miguel Ángel Cabrerizo-Vílchez, Ceferino Rivadeneira-Ruiz, Deyanira Rondón-Rodriguez, and María José Gálvez-Ruiz. 2015. “Natural Inhibitors of Lipase: Examining Lipolysis in a Single Droplet.” *Journal of Agricultural and Food Chemistry* 63 (47): 10333–40. https://doi.org/10.1021/acs.jafc.5b04550.

Castillo-Santaella, Teresa del, Esther Sanmartín, Miguel Angel Cabrerizo-Vílchez, Juan Carlos Arboleya, and Julia Maldonado-Valderrama. 2014. “Improved Digestibility of β-Lactoglobulin by Pulsed Light Processing: A Dilatational and Shear Study.” *Soft Matter* 10 (48): 9702–14. https://doi.org/10.1039/C4SM01667J.

Casula, Mattia, Cristina Manis, Olivia Menard, Giulia Tolle, Marie Francoise Cochet, Didier Dupont, Paola Scano, Viviana Garau, and Pierluigi Caboni. 2024. “Lipidomics of Sheep and Goat Milk-Based Infant Formulae during in Vitro Dynamic Digestion.” *Food Chemistry* 461 (August): 140850. https://doi.org/10.1016/j.foodchem.2024.140850.

Cavalcante, Keila N., Jessica F. Feitor, Sinara T.B. Morais, Renata T. Nassu, Lilia M. Ahrné, and Daniel R. Cardoso. 2023. “Impact of UV-C Pretreatment on β-Lactoglobulin Hydrolysis by Trypsin: Production and Bioavailability of Bioactive Peptides.” *International Dairy Journal* 142. https://doi.org/10.1016/j.idairyj.2023.105650.

Cevc Gregor. 2018. *Phospholipids Handbook*. Edited by Gregor Cevc. *Marel Deker Inc.* CRC Press. https://doi.org/10.1201/9780203743577.

Cheison, Seronei Chelulei, Elena Leeb, Thomas Letzel, and Ulrich Kulozik. 2011. “Influence of Buffer Type and Concentration on the Peptide Composition of Trypsin Hydrolysates of β-Lactoglobulin.” *Food Chemistry* 125 (1): 121–27. https://doi.org/10.1016/j.foodchem.2010.08.047.

Chen, Hong, Fang Wei, Xu yan Dong, Ji qian Xiang, Siew young Quek, and Xuemin Wang. 2017. “Lipidomics in Food Science.” *Current Opinion in Food Science* 16: 80–87. https://doi.org/10.1016/j.cofs.2017.08.003.

Chen, Q., X. Ke, J. S. Zhang, S. Y. Lai, F. Fang, W. M. Mo, and Y. P. Ren. 2016. “Proteomics Method to Quantify the Percentage of Cow, Goat, and Sheep Milks in Raw Materials for Dairy Products.” *Journal of Dairy Science* 99 (12): 9483–92. https://doi.org/10.3168/jds.2015-10739.

Cherng Z. Chuang, Ph.D., Louis F. Martin, M.D., Barbara Y. LeGardeur, M.P.H., and Alfredo Lopez-S. 2001. “Physical Activity, Biliary Lipids, and Gallstones in Obese Subjects.” *American Journal of Gastroenterology* 96 (6): 1860–65. https://doi.org/10.1016/S0002-9270(01)02447-9.

Chu, Boon Seang, A. Patrick Gunning, Gillian T. Rich, Mike J. Ridout, Richard M. Faulks, Martin S.J. Wickham, Victor J. Morris, and Peter J. Wilde. 2010. “Adsorption of Bile Salts and Pancreatic Colipase and Lipase onto Digalactosyldiacylglycerol and

Dipalmitoylphosphatidylcholine Monolayers." *Langmuir* 26 (12): 9782–93. https://doi.org/10.1021/la1000446.

Chu, Boon Seang, Gillian T. Rich, Mike J. Ridout, Richard M. Faulks, Martin S.J. Wickham, and Peter J. Wilde. 2009. "Modulating Pancreatic Lipase Activity with Galactolipids: Effects of Emulsion Interfacial Composition." *Langmuir* 25 (16): 9352–60. https://doi.org/10.1021/la9008174.

Clarke, W. 2017. *Mass Spectrometry in the Clinical Laboratory: Determining the Need and Avoiding Pitfalls*. *Mass Spectrometry for the Clinical Laboratory*. Elsevier Inc. https://doi.org/10.1016/B978-0-12-800871-3.00001-8.

Clarysse, S, J Tack, F Lammert, G Duchateau, C Reppas, and P Augustijns. 2009. "Postprandial Evolution in Composition and Characteristics of Human Duodenal Fluids in Different Nutritional States." *Journal of Pharmaceutical Sciences* 98 (3): 1177–92. https://doi.org/https://doi.org/10.1002/jps.21502.

Clarysse, Sarah, Dimitrios Psachoulias, Joachim Brouwers, Jan Tack, Pieter Annaert, Guus Duchateau, Christos Reppas, and Patrick Augustijns. 2009. "Postprandial Changes in Solubilizing Capacity of Human Intestinal Fluids for BCS Class II Drugs." *Pharmaceutical Research* 26 (6): 1456–66. https://doi.org/10.1007/s11095-009-9857-7.

Claudel, Thierry, and Michael Trauner. 2010. *Bile Acids and Their Receptors*. *Signaling Pathways in Liver Diseases*. https://doi.org/10.1007/978-3-642-00150-5_21.

Cohen, David E. 1996. "Hepatocellular Transport and Secretion of Biliary Phospholipids." *Seminars in Liver Disease* 16 (2): 191–200. https://doi.org/10.1055/s-2007-1007231.

Cohn, Jeffrey S., Alvin Kamili, Elaine Wat, Rosanna W.S. Chung, and Sally Tandy. 2010. "Dietary Phospholipids and Intestinal Cholesterol Absorption." *Nutrients* 2 (2): 116–27. https://doi.org/10.3390/nu2020116.

"Creative Proteomics Blog." 2024. 2024. https://www.creative-proteomics.com/blog/index.php/principles-applications-and-comparative-workflow-of-dia-and-dda/.

Cserhåti, T., and M. Szögyi. 1993. "Interaction of Phospholipids with Proteins and Peptides. New Advances III." *International Journal of Biochemistry* 25 (2): 123–46. https://doi.org/10.1016/0020-711X(93)90001-U.

Cusi, M. G., G. M. Rossolini, C. Cellesi, and P. E. Valensin. 1988. "Antibody Response to Wild Rubella Virus Structural Proteins Following Immunization with RA 27/3 Live Attenuated Vaccine." *Archives of Virology* 101 (1–2): 25–33. https://doi.org/10.1007/BF01314649.

Da, Xuanbo, Yukai Xiang, Hai Hu, Xiangyu Kong, Chen Qiu, Zhaoyan Jiang, Gang Zhao, and Jingli Cai. 2024. "Identification of Changes in Bile Composition in Pancreaticobiliary Reflux Based on Liquid Chromatography / Mass Spectrometry Metabolomics," 1–8.

Dahlgren, D., M. Venczel, J. P. Ridoux, C. Skjöld, A. Müllertz, R. Holm, P. Augustijns, P. M. Hellström, and H. Lennernäs. 2021. "Fasted and Fed State Human Duodenal Fluids: Characterization, Drug Solubility, and Comparison to Simulated Fluids and with Human Bioavailability." *European Journal of Pharmaceutics and Biopharmaceutics* 163 (February): 240–51. https://doi.org/10.1016/j.ejpb.2021.04.005.

Dallas, David C., Florine Citerne, Tian Tian, Vitor L.M. Silva, Karen M. Kalanetra, Steven A. Frese, Randall C. Robinson, David A. Mills, and Daniela Barile. 2016. “Peptidomic Analysis Reveals Proteolytic Activity of Kefir Microorganisms on Bovine Milk Proteins.” *Food Chemistry* 197: 273–84. https://doi.org/10.1016/j.foodchem.2015.10.116.

Dash, Satya, Changting Xiao, Cecilia Morgantini, and Gary F. Lewis. 2015. “New Insights into the Regulation of Chylomicron Production.” *Annual Review of Nutrition* 35 (1): 265–94. https://doi.org/10.1146/annurev-nutr-071714-034338.

Deferme, Sven, Jan Tack, Frank Lammert, and Patrick Augustijns. 2003. “P-Glycoprotein Attenuating Effect of Human Intestinal Fluid.” *Pharmaceutical Research* 20 (6): 900–903. https://doi.org/10.1023/A:1023891320858.

Du, Peng cheng, Zong cai Tu, Hui Wang, Yue ming Hu, Jing jing Zhang, and Bi zhen Zhong. 2021. “Investigation of the Effect of Oxidation on the Structure of β-Lactoglobulin by High Resolution Mass Spectrometry.” *Food Chemistry* 339 (March 2020): 127939. https://doi.org/10.1016/j.foodchem.2020.127939.

Duan, Rui Dong. 2007. “Sphingomyelinase and Ceramidase in the Intestinal Tract.” *European Journal of Lipid Science and Technology* 109 (10): 987–93. https://doi.org/10.1002/ejlt.200700074.

Dulko, Dorota, Robert Staroń, Lukasz Krupa, Neil M. Rigby, Alan R. Mackie, Krzysztof Gutkowski, Andrzej Wasik, and Adam Macierzanka. 2021. “The Bile Salt Content of Human Bile Impacts on Simulated Intestinal Proteolysis of β-Lactoglobulin.” *Food Research International* 145. https://doi.org/10.1016/j.foodres.2021.110413.

Dupont, D., M. Alric, S. Blanquet-Diot, G. Bornhorst, C. Cueva, A. Deglaire, S. Denis, et al. 2019. “Can Dynamic in Vitro Digestion Systems Mimic the Physiological Reality?” *Critical Reviews in Food Science and Nutrition* 59 (10): 1546–62. https://doi.org/10.1080/10408398.2017.1421900.

Dupont, Didier, and Alan R. Mackie. 2015. “Static and Dynamic in Vitro Digestion Models to Study Protein Stability in the Gastrointestinal Tract.” *Drug Discovery Today: Disease Models* 17–18: 23–27. https://doi.org/10.1016/j.ddmod.2016.06.002.

Dupont, Didier, Giuseppina Mandalari, Daniel Molle, Julien Jardin, Joëlle Léonil, Richard M. Faulks, Martin S.J. Wickham, E. N.Clare Mills, and Alan R. Mackie. 2010. “Comparative Resistance of Food Proteins to Adult and Infant in Vitro Digestion Models.” *Molecular Nutrition and Food Research* 54 (6): 767–80. https://doi.org/10.1002/mnfr.200900142.

Dupont, Didier, Giuseppina Mandalari, Daniel Molle, Julien Jardin, Joëlle Léonil, Richard M Faulks, Martin S J Wickham, E. N. Clare Mills, and Alan R Mackie. 2009. “Comparative Resistance of Food Proteins to Adult and Infant in Vitro Digestion Models.” *Molecular Nutrition & Food Research* 54 (6): 767–80. https://doi.org/10.1002/mnfr.200900142.

Duranti, Marcello, and Cristina Gius. 1997. “Legume Seeds: Protein Content and Nutritional Value.” *Field Crops Research* 53 (1–3): 31–45. https://doi.org/10.1016/S0378-4290(97)00021-X.

Edwards Patrick. 2014. *Structure and Stabiolity of Whey Proteins*. *Milk Proteins*. Second Edi. Elsevier Inc. https://doi.org/10.1016/B978-0-12-40561471-3.00007-6.

Ellingson, John S., and William E.M. Lands. 1968. “Phospholipid Reactivation of Plasmalogen Metabolism.” *Lipids* 3 (2): 111–20. https://doi.org/10.1007/BF02531727.

Elmadfa, Ibrahim, and Alexa L. Meyer. 2017. “Animal Proteins as Important Contributors to a Healthy Human Diet.” *Annual Review of Animal Biosciences* 5: 111–31. https://doi.org/10.1146/annurev-animal-022516-022943.

Elvang, Philipp A., Askell H. Hinna, Joachim Brouwers, Bart Hens, Patrick Augustijns, and Martin Brandl. 2016. “Bile Salt Micelles and Phospholipid Vesicles Present in Simulated and Human Intestinal Fluids: Structural Analysis by Flow Field–Flow Fractionation/Multiangle Laser Light Scattering.” *Journal of Pharmaceutical Sciences* 105 (9): 2832–39. https://doi.org/10.1016/j.xphs.2016.03.005.

Erlanson-Albertsson, Charlotte. 1983. “The Interaction between Pancreatic Lipase and Colipase: A Protein-Protein Interaction Regulated by a Lipid.” *FEBS Letters* 162 (2): 225–29. https://doi.org/10.1016/0014-5793(83)80760-1.

Fausa, O. 1974. “Duodenal Bile Acids after a Test Meal.” *Scandinavian Journal of Gastroenterology* 9 (6): 567–70. https://doi.org/10.1080/00365521.1974.12096876.

Fernández-Costa, Carolina, Salvador Martínez-Bartolomé, Daniel B. McClatchy, Anthony J. Saviola, Nam Kyung Yu, and John R. Yates. 2020. “Impact of the Identification Strategy on the Reproducibility of the DDA and DIA Results.” *Journal of Proteome Research* 19 (8): 3153–61. https://doi.org/10.1021/acs.jproteome.0c00153.

Fernández, Ayoa, and Francisco Riera. 2013. “β-Lactoglobulin Tryptic Digestion: A Model Approach for Peptide Release.” *Biochemical Engineering Journal* 70: 88–96. https://doi.org/10.1016/j.bej.2012.10.001.

Fernández, M. S., R. Mejía, and E. Zavala. 1991. “The Interfacial Calcium Ion Concentration as Modulator of the Latency Phase in the Hydrolysis of Dimyristoylphosphatidylcholine Liposomes by Phospholipase A2.” *Biochemistry and Cell Biology = Biochimie et Biologie Cellulaire* 69 (10–11): 722–27. https://doi.org/10.1139/o91-108.

Ferranti, Pasquale; 2024. *Proteomics Applied to Foods*. Edited by Pasquale; Ferranti. Methods and Protocols in Food Science. New York, NY: Springer US. https://doi.org/10.1007/978-1-0716-4075-3.

Ferranti, Pasquale. 2018. “The Future of Analytical Chemistry in Foodomics.” *Current Opinion in Food Science* 22: 102–8. https://doi.org/10.1016/j.cofs.2018.02.005.

Ferreira, I. M.P.L.V.O., O. Pinho, D. Monteiro, S. Faria, S. Cruz, A. Perreira, A. C. Roque, and P. Tavares. 2010. “Short Communication: Effect of Kefir Grains on Proteolysis of Major Milk Proteins.” *Journal of Dairy Science* 93 (1): 27–31. https://doi.org/10.3168/jds.2009-2501.

Feunteun, Steven Le, Sarah Verkempinck, Juliane Floury, Anja Janssen, Sebastien Marze, Pierre-sylvain Mirade, Anton Pluschke, et al. 2021. *Mathematical Modelling of Food Hydrolysis during in Vitro Digestion : From Single Nutrient to Complex Foods in Static and Dynamic Conditions To Cite This Version : HAL Id : Hal-03348081*.

Flint, Harry J., Karen P. Scott, Petra Louis, and Sylvia H. Duncan. 2012. “The Role of the Gut Microbiota in Nutrition and Health.” *Nature Reviews Gastroenterology and Hepatology* 9 (10): 577–89. https://doi.org/10.1038/nrgastro.2012.156.

Fuchs, Alexander, and Jennifer B. Dressman. 2014. “Composition and Physicochemical Properties of Fasted-State Human Duodenal and Jejunal Fluid: A Critical Evaluation of the Available Data.” *Journal of Pharmaceutical Sciences* 103 (11): 3398–3411. https://doi.org/10.1002/jps.24183.

Galanakis, Charis M. 2021. *Sustainable Food and Engineering Challenges*. https://doi.org/10.1016/B978-0-12-822714-5.00011-5.

Gass, Jonathan, Harmit Vora, Alan F. Hofmann, Gary M. Gray, and Chaitan Khosla. 2007. “Enhancement of Dietary Protein Digestion by Conjugated Bile Acids.” *Gastroenterology* 133 (1): 16–23. https://doi.org/10.1053/j.gastro.2007.04.008.

Gilat, Tuvia, and Giora J. Sömjen. 1996. “Phospholipid Vesicles and Other Cholesterol Carriers in Bile.” *Biochimica et Biophysica Acta - Reviews on Biomembranes* 1286 (2): 95–115. https://doi.org/10.1016/0304-4157(96)00005-6.

Golding, Matt, and Tim J. Wooster. 2010. “The Influence of Emulsion Structure and Stability on Lipid Digestion.” *Current Opinion in Colloid and Interface Science* 15 (1–2): 90–101. https://doi.org/10.1016/j.cocis.2009.11.006.

Goodman, Barbara E. 2010. “Insights into Digestion and Absorption of Major Nutrients in Humans.” *American Journal of Physiology - Advances in Physiology Education* 34 (2): 44–53. https://doi.org/10.1152/advan.00094.2009.

Gouseti, Ourania, Gail M. Bornhorst, Serafim Bakalis, and Alan Mackie. 2019. *Interdisciplinary Approaches to Food Digestion*. *Interdisciplinary Approaches to Food Digestion*. https://doi.org/10.1007/978-3-030-03901-1.

Groleau, Paule Emilie, Pierre Morin, Sylvie F. Gauthier, and Yves Pouliot. 2003. “Effect of Physicochemical Conditions on Peptide-Peptide Interactions in a Tryptic Hydrolysate of β-Lactoglobulin and Identification of Aggregating Peptides.” *Journal of Agricultural and Food Chemistry* 51 (15): 4370–75. https://doi.org/10.1021/jf0259720.

Grundy, Myriam M.L., Evan Abrahamse, Annette Almgren, Marie Alminger, Ana Andres, Renata M.C. Ariëns, Shanna Bastiaan-Net, et al. 2021. “INFOGEST Inter-Laboratory Recommendations for Assaying Gastric and Pancreatic Lipases Activities Prior to in Vitro Digestion Studies.” *Journal of Functional Foods* 82 (July): 104497. https://doi.org/10.1016/j.jff.2021.104497.

Guerra, Aurélie, Lucie Etienne-Mesmin, Valérie Livrelli, Sylvain Denis, Stéphanie Blanquet-Diot, and Monique Alric. 2012. “Relevance and Challenges in Modeling Human Gastric and Small Intestinal Digestion.” *Trends in Biotechnology* 30 (11): 591–600. https://doi.org/10.1016/j.tibtech.2012.08.001.

Halpern, Z., M. A. Dudley, A. Kibe, M. P. Lynn, A. C. Breuer, and R. T. Holzbach. 1986. “Rapid Vesicle Formation and Aggregation in Abnormal Human Biles. A Time-Lapse Video-Enhanced Contrast Microscopy Study.” *Gastroenterology* 90 (4): 875–85. https://doi.org/10.1016/0016-5085(86)90863-2.

Hay, D. W., M. J. Cahalane, N. Timofeyeva, and M. C. Carey. 1993. “Molecular Species of Lecithins in Human Gallbladder Bile.” *Journal of Lipid Research* 34 (5): 759–68.

Heikkilä, Tiina, Milja Karjalainen, Krista Ojala, Kirsi Partola, Frank Lammert, Patrick Augustijns, Arto Urtti, Marjo Yliperttula, Leena Peltonen, and Jouni Hirvonen. 2011. “Equilibrium Drug Solubility Measurements in 96-Well Plates Reveal Similar Drug Solubilities in Phosphate Buffer PH 6.8 and Human Intestinal Fluid.” *International Journal of Pharmaceutics* 405 (1–2): 132–36. https://doi.org/10.1016/j.ijpharm.2010.12.007.

Heller, F., and I. A. Bouchier. 1973. “Cholesterol and Bile Salt Studies on the Bile of Patients with Cholesterol Gallstones.” *Gut* 14 (2): 83–88. https://doi.org/10.1136/gut.14.2.83.

Herrera, Anashareth W., Julieta N. Naso, Fernando A. Bellesi, and Ana M.R. Pilosof. 2024. “Unraveling the Potential Health Impact of the Interactions between Pea Hydrolysates/Peptides Originating under Gastric Digestion and Bile Salts.” *Food Hydrocolloids* 146 (PA): 109225. https://doi.org/10.1016/j.foodhyd.2023.109225.

Ho, K. J., L. C. Ho, S. C. Hsu, and J. S. Chen. 1980. “Bile Acid Pool Size in Relation to Functional Status of Gallbladder and Biliary Lipid Composition in Chinese.” *American Journal of Clinical Nutrition* 33 (5): 1026–32. https://doi.org/10.1093/ajcn/33.5.1026.

Holan, Keith R., R. Thomas Holzbach, Robert E. Hermann, Avram M. Cooperman, and William J. Claffey. 1979. “Nucleation Time: A Key Factor in the Pathogenesis of Cholesterol Gallstone Disease.” *Gastroenterology* 77 (4): 611–17. https://doi.org/10.1016/0016-5085(79)90209-9.

Holmstock, Nico, Tom De Bruyn, Jan Bevernage, Pieter Annaert, Raf Mols, Jan Tack, and Patrick Augustijns. 2013. “Exploring Food Effects on Indinavir Absorption with Human Intestinal Fluids in the Mouse Intestine.” *European Journal of Pharmaceutical Sciences* 49 (1): 27–32. https://doi.org/10.1016/j.ejps.2013.01.012.

Hsu, Shih Hong, Yi Feng Lin, and Tsair Wang Chung. 2012. “Potential of Metal Oxides on the Removal of Phospholipids in Crude Jatropha Curcas Oil.” *Journal of the Taiwan Institute of Chemical Engineers* 43 (5): 659–62. https://doi.org/10.1016/j.jtice.2012.02.012.

Id, Rong Wang, Yanfei Wang, Thomas C Edrington, Zhenjiu Liu, Thomas C Lee, Andre Silvanovich Id, Hong S Moon, Zi L Liu, and Bin Li. 2020. “Presence of Small Resistant Peptides from New in Vitro Digestion Assays Detected by Liquid Chromatography Tandem Mass Spectrometry : An Implication of Allergenicity Prediction of Novel Proteins ?,” 1–19. https://doi.org/10.1371/journal.pone.0233745.

Jackson, Anthony D., and John Mclaughlin. 2006. “Digestion and Absorption.” *Surgery* 24 (7): 250–54. https://doi.org/10.1383/surg.2006.24.7.250.

Jacquot, Arnaud, Sylvie F. Gauthier, Rejean Drouin, and Yvan Boutin. 2010. “Proliferative Effects of Synthetic Peptides from β-Lactoglobulin and α-Lactalbumin on Murine Splenocytes.” *International Dairy Journal* 20 (8): 514–21. https://doi.org/10.1016/j.idairyj.2010.02.013.

Jan Bevernage, Joachim Brouwers, Sarah Clarysse, Maria Vertzoni, Jan Tack, Pieter Annaert, Patrick Augustijns. 2010. “Drug Supersaturation in Simulated and Human Intestinal Fluids Representing Different Nutritional States.” *Journal of Pharmaceutical Sciences* 99 (11): 4525–34. https://doi.org/https://doi.org/10.1002/jps.22154.

Janowitz, P., W. Swobodnik, J. G. Wechsler, A. Zoller, K. Kuhn, and H. Ditschuneit. 1990. “Comparison of Gall Bladder Bile and Endoscopically Obtained Duodenal Bile.” *Gut* 31 (12): 1407–10. https://doi.org/10.1136/gut.31.12.1407.

Järvinen, Kirsi-Marjut, Pantipa Chatchatee, Ludmilla Bardina, Kirsten Beyer, and Hugh A Sampson. 2001. “IgE and IgG Binding Epitopes on α-Lactalbumin and β-Lactoglobulin in Cow’s Milk Allergy.” *International Archives of Allergy and Immunology* 126 (2): 111–18. https://doi.org/10.1159/000049501.

Jayanthi, V., S. Sarika, Joy Varghese, V. Vaithiswaran, Malay Sharma, Mettu Srinivas Reddy, Vijaya Srinivasan, G. M.M. Reddy, Mohamed Rela, and S. Kalkura. 2016. “Composition of Gallbladder Bile in Healthy Individuals and Patients with Gallstone Disease from North and South India.” *Indian Journal of Gastroenterology* 35 (5): 347–53. https://doi.org/10.1007/s12664-016-0685-5.

Jenkins, Gereth; Hardie, Laura. 2008. *Bile Acids: Toxicology and Bioactivity*.

Julien Jardin. 2024. “R-Peptidomics.” 2024. https://forgemia.inra.fr/julien.jardin/r-peptidomics.

Kalantzi, Lida, Konstantinos Goumas, Vasilios Kalioras, Bertil Abrahamsson, Jennifer B. Dressman, and Christos Reppas. 2006. “Characterization of the Human Upper Gastrointestinal Contents under Conditions Simulating Bioavailability/Bioequivalence Studies.” *Pharmaceutical Research* 23 (1): 165–76. https://doi.org/10.1007/s11095-005-8476-1.

Kalantzi, Lida, Eva Persson, Britta Polentarutti, Bertil Abrahamsson, Konstantinos Goumas, Jennifer B. Dressman, and Christos Reppas. 2006. “Canine Intestinal Contents vs. Simulated Media for the Assessment of Solubility of Two Weak Bases in the Human Small Intestinal Contents.” *Pharmaceutical Research* 23 (6): 1373–81. https://doi.org/10.1007/s11095-006-0207-8.

Keil, Borivoj. 1992. *Specificity of Proteolysis*. *Specificity of Proteolysis*. https://doi.org/10.1007/978-3-642-48380-6.

Kellow, J.E., T.J. Borody, S.F. Phillips, R.L. Tucker, and A.C. Haddad. 1986. “Human Interdigestive Motility: Variations in Patterns from Esophagus to Colon.” *Gastroenterology* 91 (2): 386–95. https://doi.org/10.1016/0016-5085(86)90573-1.

Kindel, Tammy, Dana M. Lee, and Patrick Tso. 2010. “The Mechanism of the Formation and Secretion of Chylomicrons.” *Atherosclerosis Supplements* 11 (1): 11–16. https://doi.org/10.1016/j.atherosclerosissup.2010.03.003.

Klein, E. 1967. “The Effect of Lecithin on the Activity of Pancreatic Lipase.” *Life Sciences* 6 (5): 1305–7.

Kłosowska-Chomiczewska, Ilona E., Dorota Dulko, Mateusz Semborski, Mariia Yakoviv, Noel Si, Robert Staroń, Łukasz Krupa, and Adam Macierzanka. n.d. “In Vitro Intestinal Lipolysis of Protein-Stabilised Emulsion: Simulating the Impact of Human Bile Using Individual Bile Salts and Phospholipids.” *Submitted*.

Kłosowska, K, Teresa Castillo-santaella, Julia Maldonado-valderrama, and Adam Macierzanka. 2024. “The Bile Salt / Phospholipid Ratio Determines the Extent of in Vitro Intestinal Lipolysis of Triglycerides : Interfacial and Emulsion Studies” 187 (January). https://doi.org/10.1016/j.foodres.2024.114421.

Koirala, Pankaj, Merina Dahal, Sampurna Rai, Milan Dhakal, Nilesh Prakash, and Nirmal Sajid. 2023. “Dairy Milk Protein – Derived Bioactive Peptides : Avengers Against Metabolic Syndrome.” *Current Nutrition Reports*, 299–317. https://doi.org/10.1007/s13668-023-00472-1.

Korver, O., and H. Meder. 1974. “The Influence of Lysolecithin on the Complex Formation between β-Lactoglobulin and κ-Casein.” *Journal of Dairy Research* 41 (1): 9–17. https://doi.org/10.1017/S0022029900014850.

Kossena, Greg A., William N. Charman, Clive G. Wilson, Bridget O’Mahony, Blythe Lindsay, John M. Hempenstall, Christopher L. Davison, Patrick J. Crowley, and Christopher J.H. Porter. 2007. “Low Dose Lipid Formulations: Effects on Gastric Emptying and Biliary Secretion.” *Pharmaceutical Research* 24 (11): 2084–96. https://doi.org/10.1007/s11095-007-9363-8.

Kristensen, Annika, Tommy Nylander, Marie Paulsson, and Anders Carlsson. 1997. “Calorimetric Studies of Interactions between β-Lactoglobulin and Phospholipids in Solutions.” *International Dairy Journal* 7 (1): 87–92. https://doi.org/10.1016/S0958-

6946(96)00038-6.

Kristensen, Kaja, Noémie David-rogeat, and Norah Alshammari. 2019. *Chapter 10 - Food Digestion Engineering*. *Sustainable Food Processing and Engineering Challenges*. Elsevier Inc. https://doi.org/10.1016/B978-0-12-822714-5/00010-3.

Krupa, Lukasz, Balazs Bajka, Robert Staroń, Didier Dupont, Harjinder Singh, Krzysztof Gutkowski, and Adam Macierzanka. 2020. “Comparing the Permeability of Human and Porcine Small Intestinal Mucus for Particle Transport Studies.” *Scientific Reports* 10 (1): 20290. https://doi.org/10.1038/s41598-020-77129-4.

Kulyyassov, A T, and Ramankulov Ye M. 2018. “APPLICATIONS OF THE IMPACT II HIGH RESOLUTION QUADRUPOLE TIME-OF-FLIGHT (QTOF) INSTRUMENT FOR SHOTGUN PROTEOMICS Mass Spectrometry Is a Central Analytical Method for Protein Research and Other Biomolecules Which Also Demonstrated Capability to Detect Pe.” *Euroasian Journal of Applied Biotechnology*, no. Cid.

Kyte, Jack, and Russell F. Doolittle. 1982. “A Simple Method for Displaying the Hydropathic Character of a Protein.” *Journal of Molecular Biology* 157 (1): 105–32. https://doi.org/10.1016/0022-2836(82)90515-0.

Ladas, S. D., P. E.T. Isaacs, G. M. Murphy, and G. E. Sladen. 1984. “Comparison of the Effects of Medium and Long Chain Triglyceride Containing Liquid Meals on Gall Bladder and Small Intestine Function in Normal Man.” *Gut* 25 (4): 405–11. https://doi.org/10.1136/gut.25.4.405.

Lairon, D. 2009. *Digestion and Absorption of Lipids*. *Designing Functional Foods: Measuring and Controlling Food Structure Breakdown and Nutrient Absorption*. Woodhead Publishing Limited. https://doi.org/10.1533/9781845696603.1.66.

Lairon, Denis, Gilles Nalbone, Huguette Lafont, Jeannie Leonardi, Nicole Domingo, Jacques Christian Hauton, and Robert Verger. 1978. “Possible Roles of Bile Lipids and Colipase in Lipase Adsorption.” *Biochemistry* 17 (24): 5263–69. https://doi.org/10.1021/bi00617a028.

Lairon, Denis, Gilles Nalbone, Huguette Lafont, Jeannie Leonardi, Jean Louis Vigne, Christiane Chabert, Jacques C. Hauton, and Robert Verger. 1980. “Effects of Bile Lipids on the Adsorption and Activity of Pancreatic Lipase on Triacylglycerol Emulsions.” *Biochimica et Biophysica Acta (BBA)/Lipids and Lipid Metabolism* 618 (1): 119–28. https://doi.org/10.1016/0005-2760(80)90059-4.

Larsson, Anita, and Charlotte Erlanson-Albertsson. 1986. “Effect of Phosphatidylcholine and Free Fatty Acids on the Activity of Pancreatic Lipase-Colipase.” *Biochimica et Biophysica Acta (BBA)/Lipids and Lipid Metabolism* 876 (3): 543–50. https://doi.org/10.1016/0005-2760(86)90042-1.

Lecrenier, M. C., M. Planque, M. Dieu, P. Veys, C. Saegerman, N. Gillard, and V. Baeten. 2018. “A Mass Spectrometry Method for Sensitive, Specific and Simultaneous Detection of Bovine Blood Meal, Blood Products and Milk Products in Compound Feed.” *Food Chemistry* 245 (September 2017): 981–88. https://doi.org/10.1016/j.foodchem.2017.11.074.

Lee, S. P., and J. F. Nicholls. 1986. “Nature and Composition of Biliary Sludge.” *Gastroenterology* 90 (3): 677–86. https://doi.org/10.1016/0016-5085(86)91123-6.

Lefevre, T.; M. Subirade. 2000. “Interaction of B-Lactoglobulin with Phospholipid Bilayers: A Molecular Level Elucidation as Revealed by Infrared Spectroscopy.” *International Journal of Biological Macromolecules* 122: 873–81. https://doi.org/10.1016/j.ijbiomac.2018.10.211.

Lesmes, Uri. 2023. *In Vitro Digestion Models for the Design of Safe and Nutritious Foods*. *Advances in Food and Nutrition Research*. 1st ed. Vol. 104. Elsevier Inc. https://doi.org/10.1016/bs.afnr.2022.10.006.

Li, Xinming. 2023. “Classification of B and Y Ions in Peptide MS/MS Spectra Based on Machine Learning.” *Journal of Computer and Communications* 11 (03): 99–109. https://doi.org/10.4236/jcc.2023.113008.

Li, Yuping, Zezhi Shao, and Ashim K Mitra. 1993. “Chemical and α-Chymotrypsin-Mediated Proteolytic Degradation of Insulin in Bile Salt-Unsaturated Fatty Acid Mixed Micellar Systems.” *Pharmaceutical Research* 10 (11): 1638–41. https://doi.org/10.1023/A:1018933022150.

Lin, Secholng, Robert J. Llukkonen, Rebecca E. Thom, John G. Bastian, Marta T. Lukasewycz, and Robert M. Carlson. 1984. “Increased Chloroform Production from Model Components of Aquatic Humus and Mixtures of Chlorine Dioxide/Chlorine.” *Environmental Science and Technology* 18 (12): 932–35. https://doi.org/10.1021/es00130a007.

Lindahl, Anders, Anna Lena Ungell, Lars Knutson, and Hans Lennernäs. 1997. “Characterization of Fluids from the Stomach and Proximal Jejunum in Men and Women.” *Pharmaceutical Research*. https://doi.org/10.1023/A:1012107801889.

Linden, W. Van Der, and F. Nakayama. 1982. “Hepatic versus Duodenal Bile.” *Scandinavian Journal of Gastroenterology* 17 (4): 497–502. https://doi.org/10.3109/00365528209182238.

Lucas-González, Raquel, Manuel Viuda-Martos, José Angel Pérez-Alvarez, and Juana Fernández-López. 2018. “In Vitro Digestion Models Suitable for Foods: Opportunities for New Fields of Application and Challenges.” *Food Research International* 107 (2017): 423–36. https://doi.org/10.1016/j.foodres.2018.02.055.

Lykidis, Athanasios, Antonis Avranas, and Pantelis Arzoglou. 1997. “Combined Effect of a Lecithin and a Bile Salt on Pancreatic Lipase Activity.” *Comparative Biochemistry and Physiology - B Biochemistry and Molecular Biology* 116 (1): 51–55. https://doi.org/10.1016/S0305-0491(96)00153-8.

Macias, Luis A., Inês C. Santos, and Jennifer S. Brodbelt. 2020. “Ion Activation Methods for Peptides and Proteins.” *Analytical Chemistry* 92 (1): 227–51. https://doi.org/10.1021/acs.analchem.9b04859.

Macierzanka, Adam, Franziska Böttger, Neil M. Rigby, Martina Lille, Kaisa Poutanen, E. N.Clare Mills, and Alan R. Mackie. 2012. “Enzymatically Structured Emulsions in Simulated Gastrointestinal Environment: Impact on Interfacial Proteolysis and Diffusion in Intestinal Mucus.” *Langmuir* 28 (50): 17349–62. https://doi.org/10.1021/la302194q.

Macierzanka, Adam, Ana I. Sancho, E. N. Clare Mills, Neil M. Rigby, and Alan R. Mackie. 2009. “Emulsification Alters Simulated Gastrointestinal Proteolysis of β-Casein and β-Lactoglobulin.” *Soft Matter* 5 (3): 538–50. https://doi.org/10.1039/B811233A.

Macierzanka, Adam, Amelia Torcello-Gómez, Christian Jungnickel, and Julia Maldonado-Valderrama. 2019. “Bile Salts in Digestion and Transport of Lipids.” *Advances in Colloid and Interface Science* 274. https://doi.org/10.1016/j.cis.2019.102045.

Madenci, D., and S. U. Egelhaaf. 2010. “Self-Assembly in Aqueous Bile Salt Solutions.” *Current Opinion in Colloid and Interface Science* 15 (1–2): 109–15.

https://doi.org/10.1016/j.cocis.2009.11.010.

Maes, Wim, John Van Camp, Vanessa Vermeirssen, Mattias Hemeryck, Jean Marie Ketelslegers, Jürgen Schrezenmeir, Patrick Van Oostveldt, and André Huyghebaert. 2004. “Influence of the Lactokinin Ala-Leu-Pro-Met-His-Ile-Arg (ALPMHIR) on the Release of Endothelin-1 by Endothelial Cells.” *Regulatory Peptides* 118 (1–2): 105–9. https://doi.org/10.1016/j.regpep.2003.11.005.

Mahony, J A O, and P F Fox. 2014. *Milk: An Overview*. *Milk Proteins*. Second Edi. Elsevier Inc. https://doi.org/10.1016/B978-0-12-405171-3/00002-7.

Maldonado-Valderrama, J., J. L. Muros-Cobos, J. A. Holgado-Terriza, and M. A. Cabrerizo-Vílchez. 2014. “Bile Salts at the Air-Water Interface: Adsorption and Desorption.” *Colloids and Surfaces B: Biointerfaces* 120: 176–83. https://doi.org/10.1016/j.colsurfb.2014.05.014.

Maldonado-Valderrama, J., J. A.Holgado Terriza, A. Torcello-Gómez, and M. A. Cabrerizo-Vílchez. 2013. “In Vitro Digestion of Interfacial Protein Structures.” *Soft Matter* 9 (4): 1043–53. https://doi.org/10.1039/c2sm26843d.

Maldonado-Valderrama, Julia. 2019. “Probing in Vitro Digestion at Oil–Water Interfaces.” *Current Opinion in Colloid and Interface Science* 39: 51–60. https://doi.org/10.1016/j.cocis.2019.01.004.

Maldonado-Valderrama, Julia, Teresa del Castillo-Santaella, María José Gálvez-Ruiz, Juan Antonio Holgado-Terriza, and Miguel Ángel Cabrerizo-Vílchez. 2021. “Structure and Functionality of Interfacial Layers in Food Emulsions.” In *Food Structure and Functionality*, 1–22. Elsevier. https://doi.org/10.1016/B978-0-12-821453-4.00010-7.

Maldonado-Valderrama, Julia, Teresa del Castillo Santaella, Juan Antonio Holgado-Terriza, and Miguel Ángel Cabrerizo-Vílchez. 2022. “In Vitro Digestion of Emulsions in a Single Droplet via Multi Subphase Exchange of Simulated Gastrointestinal Fluids.” *Journal of Visualized Experiments* 2022 (189). https://doi.org/10.3791/64158.

Maldonado-Valderrama, Julia, Amelia Torcello-Gómez, Teresa Del Castillo-Santaella, Juan A. Holgado-Terriza, and Miguel A. Cabrerizo-Vílchez. 2015. “Subphase Exchange Experiments with the Pendant Drop Technique.” *Advances in Colloid and Interface Science* 222: 488–501. https://doi.org/10.1016/j.cis.2014.08.002.

Maldonado-Valderrama, Julia, Pete Wilde, Adam MacIerzanka, and Alan MacKie. 2011. “The Role of Bile Salts in Digestion.” *Advances in Colloid and Interface Science* 165 (1): 36–46. https://doi.org/10.1016/j.cis.2010.12.002.

Maldonado-Valderrama, Julia, Nicola C. Woodward, A. Patrick Gunning, Mike J. Ridout, Fiona A. Husband, Alan R. Mackie, Victor J. Morris, and Peter J. Wilde. 2008. “Interfacial Characterization of β-Lactoglobulin Networks: Displacement by Bile Salts.” *Langmuir* 24 (13): 6759–67. https://doi.org/10.1021/la800551u.

Malvern. 2013. “Malvern Zetasizer ZS DLS User Manual.” *MAN0485 Issue 1.1 April 2013* 67 (1.1): 13-1-13–3.

Mandalari, G., K. Adel-Patient, V. Barkholt, C. Baro, L. Bennett, M. Bublin, S. Gaier, et al. 2009. “In Vitro Digestibility of β-Casein and β-Lactoglobulin under Simulated Human Gastric and Duodenal Conditions: A Multi-Laboratory Evaluation.” *Regulatory Toxicology and Pharmacology* 55 (3): 372–81. https://doi.org/10.1016/j.yrtph.2009.08.010.

Mandalari, Giuseppina, Alan M. Mackie, Neil M. Rigby, Martin S.J. Wickham, and E. N.Clare Mills. 2009. “Physiological Phosphatidylcholine Protects Bovine β-Lactoglobulin from Simulated Gastrointestinal Proteolysis.” *Molecular Nutrition and Food Research* 53 (SUPPL. 1): 131–39. https://doi.org/10.1002/mnfr.200800321.

Marcet, Ismael, Jaime Delgado, Natalia Díaz, Manuel Rendueles, and Mario Díaz. 2022. “Peptides Recovery from Egg Yolk Lipovitellins by Ultrafiltration and Their in Silico Bioactivity Analysis.” *Food Chemistry* 379 (July 2021): 132145. https://doi.org/10.1016/j.foodchem.2022.132145.

Marcus, Katrin, Martin Eisenacher, and Barbara Sitek. 2021. *Quantitative Methods in Proteomics Second Edition Methods in Molecular Biology 2228*. http://www.springer.com/series/7651.

Martini, Serena, Lisa Solieri, and Davide Tagliazucchi. 2021. “Peptidomics: New Trends in Food Science.” *Current Opinion in Food Science* 39: 51–59. https://doi.org/10.1016/j.cofs.2020.12.016.

Marze, Sébastien. 2017. “Bioavailability of Nutrients and Micronutrients: Advances in Modeling and in Vitro Approaches.” *Annual Review of Food Science and Technology* 8: 35–55. https://doi.org/10.1146/annurev-food-030216-030055.

Mat, Damien J.L., Steven Le Feunteun, Camille Michon, and Isabelle Souchon. 2016. “In Vitro Digestion of Foods Using PH-Stat and the INFOGEST Protocol: Impact of Matrix Structure on Digestion Kinetics of Macronutrients, Proteins and Lipids.” *Food Research International* 88: 226–33. https://doi.org/10.1016/j.foodres.2015.12.002.

Mathai, John K., Yanhong Liu, and Hans H. Stein. 2017. “Values for Digestible Indispensable Amino Acid Scores (DIAAS) for Some Dairy and Plant Proteins May Better Describe Protein Quality than Values Calculated Using the Concept for Protein Digestibility-Corrected Amino Acid Scores (PDCAAS).” *British Journal of Nutrition* 117 (4): 490–99. https://doi.org/10.1017/S0007114517000125.

Matubayasi, Norihiro, Makoto Kanzaki, Satoko Sugiyama, and Asako Matuzawa. 1996. “Thermodynamic Study of Gaseous Adsorbed Films of Sodium Taurocholate at the Air/Water Interface.” *Langmuir* 12 (7): 1860–62. https://doi.org/10.1021/la950832o.

McClements, David Julian, and Yan Li. 2010. “Review of in Vitro Digestion Models for Rapid Screening of Emulsion-Based Systems.” *Food and Function* 1 (1): 32–59. https://doi.org/10.1039/c0fo00111b.

Megger, Dominik A., Thilo Bracht, Helmut E. Meyer, and Barbara Sitek. 2013. “Label-Free Quantification in Clinical Proteomics.” *Biochimica et Biophysica Acta - Proteins and Proteomics* 1834 (8): 1581–90. https://doi.org/10.1016/j.bbapap.2013.04.001.

Mekkaoui, Aicha, Yang Liu, Pingping Zhang, Sana Ullah, Ce Wang, and Baocai Xu. 2021. “Effect of Bile Salts on the Interfacial Dilational Rheology of Lecithin in the Lipid Digestion Process.” *Journal of Oleo Science* 70 (8): 1069–80. https://doi.org/10.5650/jos.ess21081.

Menard, O, U Lesmes, C S Shani-Levi, A Araiza Calahorra, A Lavoisier, M Morzel, A Rieder, et al. 2023. “Static in Vitro Digestion Model Adapted to the General Older Adult Population: An INFOGEST International Consensus.” *Food & Function* 14 (10): 4569–82. https://doi.org/10.1039/D3FO00535F.

Miled, Nabil, Stephane Canaan, Liliane Dupuis, Alain Roussel, Mireille Rivière, Frederic Carrière, Alain De Caro, Christian Cambillau, and Robert Verger. 2000. “Digestive Lipases: From Three-Dimensional Structure of Physiology.” *Biochimie* 82 (11): 973–86. https://doi.org/10.1016/S0300-9084(00)01179-2.

Minekus, M., M. Alminger, P. Alvito, S. Ballance, T. Bohn, C. Bourlieu, F. Carrière, et al. 2014. “A Standardised Static in Vitro Digestion Method Suitable for Food-an International Consensus.” *Food and Function* 5 (6): 1113–24. https://doi.org/10.1039/c3fo60702j.

Monaci, Linda, Virginie Tregoat, Arjon J. Van Hengel, and Elke Anklam. 2006. *Milk Allergens, Their Characteristics and Their Detection in Food: A Review*. *European Food Research and Technology*. Vol. 223. https://doi.org/10.1007/s00217-005-0178-8.

Moran-Valero, Maria I., Diana Martin, Guzman Torrelo, Guillermo Reglero, and Carlos F. Torres. 2012. “Phytosterols Esterified with Conjugated Linoleic Acid. in Vitro Intestinal Digestion and Interaction on Cholesterol Bioaccessibility.” *Journal of Agricultural and Food Chemistry* 60 (45): 11323–30. https://doi.org/10.1021/jf303148d.

Moreno, F. Javier, Alan R. Mackie, and E. N.Clare Mills. 2005. “Phospholipid Interactions Protect the Milk Allergen α-Lactalbumin from Proteolysis during in Vitro Digestion.” *Journal of Agricultural and Food Chemistry* 53 (25): 9810–16. https://doi.org/10.1021/jf0515227.

Moreno, Mariangeles Perez de la Cruz, Marianne Oth, Sven Deferme, Frank Lammert, Jan Tack, Jennifer Dressman, and Patrick Augustijns. 2010. “Characterization of Fasted-State Human Intestinal Fluids Collected from Duodenum and Jejunum.” *Journal of Pharmacy and Pharmacology* 58 (8): 1079–89. https://doi.org/10.1211/jpp.58.8.0009.

Morita, Shin Ya, and Tomohiro Terada. 2014. “Molecular Mechanisms for Biliary Phospholipid and Drug Efflux Mediated by ABCB4 and Bile Salts.” *BioMed Research International* 2014. https://doi.org/10.1155/2014/954781.

Morris, Victor J., Nicola C. Woodward, and Allan P. Gunning. 2011. “Atomic Force Microscopy as a Nanoscience Tool in Rational Food Design.” *Journal of the Science of Food and Agriculture* 91 (12): 2117–25. https://doi.org/10.1002/jsfa.4501.

Müller, Karl. 1984. “Structural Aspects of Bile Salt-Lecithin Mixed Micelles.” *Hepatology* 4 (2 S): 134S-137S. https://doi.org/10.1002/hep.1840040823.

Müllertz, Anette, Dimitrios G. Fatouros, James R. Smith, Maria Vertzoni, and Christos Reppas. 2012. “Insights into Intermediate Phases of Human Intestinal Fluids Visualized by Atomic Force Microscopy and Cryo-Transmission Electron Microscopy Ex Vivo.” *Molecular Pharmaceutics* 9 (2): 237–47. https://doi.org/10.1021/mp200286x.

Nagaoka, Satoshi, Yu Futamura, Keiji Miwa, Takako Awano, Kouhei Yamauchi, Yoshihiro Kanamaru, Kojima Tadashi, and Tamotsu Kuwata. 2001. “Identification of Novel Hypocholesterolemic Peptides Derived from Bovine Milk □ -Lactoglobulin” 17: 11–17. https://doi.org/10.1006/bbrc.2001.4298.

Najar, Muzaffar Hussain, Oyais Ahmad Chat, Parvaiz Ahmad Bhat, Mohammad Amin Mir, Ghulam Mohamamd Rather, and Aijaz Ahmad Dar. 2021. “Structural Changes in Trypsin Induced by the Bile Salts: An Effect of Amphiphile Hydrophobicity.” *International Journal of Biological Macromolecules* 180: 121–28. https://doi.org/10.1016/j.ijbiomac.2021.03.041.

Nalbone, G.; Lairon D.; Charbonnier-Augeire M.; Vigne J-L.; Leonardi J.; Chabert C.; Hauton C.; Verger R. 1980. “Pancreatic Phospholipase A2, Hydrolysis of Phosphatydylcholines in Various Physicochemical States” 620 (May): 612–25.

Naso, Julieta N., Fernando A. Bellesi, Víctor M. Pizones Ruiz-Henestrosa, and Ana M.R. Pilosof. 2019. “Studies on the Interactions between Bile Salts and Food Emulsifiers under in Vitro Duodenal Digestion Conditions to Evaluate Their Bile Salt Binding Potential.” *Colloids and Surfaces B: Biointerfaces* 174: 493–500. https://doi.org/10.1016/j.colsurfb.2018.11.024.

Nervi, Flavio. 2000. “Significance of Biliary Phospholipids for Maintenance of the Gastrointestinal Mucosal Barrier and Hepatocellular Integrity.” *Gastroenterology* 118 (6): 1265–67. https://doi.org/10.1016/S0016-5085(00)70380-5.

Nielsen, Søren Drud, Robert L. Beverly, Yunyao Qu, and David C. Dallas. 2017. “Milk Bioactive Peptide Database: A Comprehensive Database of Milk Protein-Derived Bioactive Peptides and Novel Visualization.” *Food Chemistry* 232: 673–82. https://doi.org/10.1016/j.foodchem.2017.04.056.

Nielsen, Søren Drud Heydary, Ningjian Liang, Harith Rathish, Bum Jin Kim, Jiraporn Lueangsakulthai, Jeewon Koh, Yunyao Qu, Hans Jörg Schulz, and David C. Dallas. 2023. “Bioactive Milk Peptides: An Updated Comprehensive Overview and Database.” *Critical Reviews in Food Science and Nutrition* 0 (0): 1–20. https://doi.org/10.1080/10408398.2023.2240396.

Nika, H., E. Nieves, David H. Hawke, and Ruth Hogue Angeletti. 2013. “C-Terminal Protein Characterization by Mass Spectrometry Using Combined Micro Scale Liquid and Solid-Phase Derivatization.” *Journal of Biomolecular Techniques* 24 (1): 17–31. https://doi.org/10.7171/jbt.13-2401-003.

Nilsson, Åke. 1969. “The Presence of Sphingomyelin- and Ceramide-Cleaving Enzymes in the Small Intestinal Tract.” *Biochimica et Biophysica Acta (BBA)/Lipids and Lipid Metabolism* 176 (2): 339–47. https://doi.org/10.1016/0005-2760(69)90192-1.

Northfield, T. C., and I. McColl. 1973. “Postprandial Concentrations of Free and Conjugated Bile Acids down the Length of the Normal Human Small Intestine.” *Gut* 14 (7): 513–18. https://doi.org/10.1136/gut.14.7.513.

Northfield, T. 1984. *Bile Acids in Gastroenterology*. *Gut*. Vol. 25. https://doi.org/10.1136/gut.25.11.1305.

Oesen, Tobias von, Mascha Treblin, Ingrid Clawin-Rädecker, Dierk Martin, Ronald Maul, Wolfgang Hoffmann, Katrin Schrader, et al. 2023. “Identification of Marker Peptides for the Whey Protein Quantification in Edam-Type Cheese.” *Foods* 12 (10). https://doi.org/10.3390/foods12102002.

OpenAI. 2024. “ChatGPT.” 2024. https://openai.com.

Osorio, Daniel, Paola Rondón-Villarreal, and Rodrigo Torres. 2015. “Peptides: A Package for Data Mining of Antimicrobial Peptides.” *The R Journal* 7 (1): 4. https://doi.org/10.32614/RJ-2015-001.

Ozorio, Luísa, Caroline Mellinger-Silva, Lourdes M.C. Cabral, Julien Jardin, Gaelle Boudry, and Didier Dupont. 2020. “The Influence of Peptidases in Intestinal Brush Border Membranes on the Absorption of Oligopeptides from Whey Protein Hydrolysate: An Ex Vivo Study Using an Ussing Chamber.” *Foods* 9 (10). https://doi.org/10.3390/foods9101415.

Pabois, Olivia, Christian D. Lorenz, Richard D. Harvey, Isabelle Grillo, Myriam M.L. Grundy, Peter J. Wilde, Yuri Gerelli, and Cécile A. Dreiss. 2019. “Molecular Insights into the Behaviour of Bile Salts at Interfaces: A Key to Their Role in Lipid Digestion.” *Journal of Colloid and Interface Science* 556: 266–77. https://doi.org/10.1016/j.jcis.2019.08.010.

Pan, Yue, Yibo Liu, Jiayi Zhao, Liqin Cui, Xiaodong Li, Lu Liu, Kouadio Jean Eric Parfait Kouame, et al. 2024. “Simulated in Vitro Infant Digestion and Lipidomic Analysis to Explore How the Milk Fat Globule Membrane Modulates Fat Digestion.” *Food Chemistry* 447 (600): 139008. https://doi.org/10.1016/j.foodchem.2024.139008.

Pan, Zheng, Aiqian Ye, Karl Fraser, Siqi Li, Anant Dave, and Harjinder Singh. 2024. “Comparative Lipidomics Analysis of in Vitro Lipid Digestion of Sheep Milk: Influence of Homogenization and Heat Treatment.” *Journal of Dairy Science* 107 (2): 711–25. https://doi.org/10.3168/jds.2023-23446.

Pattinson, N. R., K. E. Willis, and C. M. Frampton. 1991. “Comparative Analysis of Cholesterol Transport in Bile from Patients with and without Cholesterol Gallstones.” *Journal of Lipid Research* 32 (2): 205–14.

Patton, J. S., and M. C. Carey. 1981. “Inhibition of Human Pancreatic Lipase-Colipase Activity by Mixed Bile Salt-Phospholipid Micelles.” *American Journal of Physiology - Gastrointestinal and Liver Physiology* 4 (4): 328–36. https://doi.org/10.1152/ajpgi.1981.241.4.g328.

Pekar, Judith, Davide Ret, and Eva Untersmayr. 2018. “Stability of Allergens.” *Molecular Immunology* 100 (March): 14–20. https://doi.org/10.1016/j.molimm.2018.03.017.

Pellegrini, Antonio, Carmen Dettling, Ursula Thomas, and Peter Hunziker. 2001. “Isolation and Characterization of Four Bactericidal Domains in the Bovine β-Lactoglobulin.” *Biochimica et Biophysica Acta - General Subjects* 1526 (2): 131–40. https://doi.org/10.1016/S0304-4165(01)00116-7.

Perrocheau, Ludivine, Benedicte Bakan, Patrick Boivin, and Didier Marion. 2006. “Stability of Barley and Malt Lipid Transfer Protein 1 (LTP1) toward Heating and Reducing Agents: Relationships with the Brewing Process.” *Journal of Agricultural and Food Chemistry* 54 (8): 3108–13. https://doi.org/10.1021/jf052910b.

Persico, Mathieu, Gaétan Daigle, Sabita Kadel, Véronique Perreault, Geneviève Pellerin, Jacinthe Thibodeau, and Laurent Bazinet. 2020. “Predictive Models for Determination of Peptide Fouling Based on the Physicochemical Characteristics of Filtration Membranes.” *Separation and Purification Technology* 240 (January): 116602. https://doi.org/10.1016/j.seppur.2020.116602.

Persson, Eva M., Ralf G. Nilsson, Göran I. Hansson, Lars J. Löfgren, Fredrik Libäck, Lars Knutson, Bertil Abrahamsson, and Hans Lennernäs. 2006. “A Clinical Single-Pass Perfusion Investigation of the Dynamic in Vivo Secretory Response to a Dietary Meal in Human Proximal Small Intestine.” *Pharmaceutical Research* 23 (4): 742–51. https://doi.org/10.1007/s11095-006-9607-z.

Phan, C. T., and P. Tso. 2001. “Intestinal Lipid Absorption and Transport.” *Frontiers in Bioscience : A Journal and Virtual Library* 6 (5): 299–319. https://doi.org/10.2741/a612.

Picariello, Gianluca, Pasquale Ferranti, Olga Fierro, Gianfranco Mamone, Simonetta Caira, Aldo Di Luccia, Stefano Monica, and Francesco Addeo. 2010. “Peptides Surviving the Simulated Gastrointestinal Digestion of Milk Proteins: Biological and Toxicological Implications.” *Journal of Chromatography B: Analytical Technologies in the Biomedical and Life Sciences* 878 (3–4): 295–308. https://doi.org/10.1016/j.jchromb.2009.11.033.

Picariello, Gianluca, Giuseppe Iacomino, Gianfranco Mamone, Pasquale Ferranti, Olga Fierro, Carmen Gianfrani, Aldo Di Luccia, and Francesco Addeo. 2013. “Transport across Caco-2 Monolayers of Peptides Arising from in Vitro Digestion of Bovine Milk Proteins.” *Food Chemistry* 139 (1–4): 203–12.

https://doi.org/10.1016/j.foodchem.2013.01.063.

Picariello, Gianluca, Gianfranco Mamone, Chiara Nitride, Francesco Addeo, and Pasquale Ferranti. 2013. “Protein Digestomics: Integrated Platforms to Study Food-Protein Digestion and Derived Functional and Active Peptides.” *TrAC - Trends in Analytical Chemistry* 52: 120–34. https://doi.org/10.1016/j.trac.2013.08.001.

Picariello, Gianluca, Luigia Di Stasio, Chiara Nitride, Gianfranco Mamone, and Pasquale Ferranti. 2020. *Food Protein Digestomics*. *Comprehensive Foodomics*. Elsevier. https://doi.org/10.1016/B978-0-08-100596-5.23032-1.

Pichot, Roman, Richard L. Watson, and Ian T. Norton. 2013. “Phospholipids at the Interface: Current Trends and Challenges.” *International Journal of Molecular Sciences* 14 (6): 11767–94. https://doi.org/10.3390/ijms140611767.

Piéroni, G., Y. Gargouri, L. Sarda, and R. Verger. 1990. “Interactions of Lipases with Lipid Monolayers. Facts and Questions.” *Advances in Colloid and Interface Science* 32 (4): 341–78. https://doi.org/10.1016/0001-8686(90)80023-S.

Pihlanto-Leppälä, Anne, Päivi Koskinen, Kati Phlola, Tuomo Tupasela, and Hannu Korhonen. 2000. “Angiotensin I-Converting Enzyme Inhibitory Properties of Whey Protein Digests: Concentration and Characterization of Active Peptides.” *Journal of Dairy Research* 67 (1): 53–64. https://doi.org/10.1017/S0022029999003982.

Pimentel, Grégory, Kathryn J. Burton, Guy Vergères, and Didier Dupont. 2018. “The Role of Foodomics to Understand the Digestion/Bioactivity Relationship of Food.” *Current Opinion in Food Science* 22: 67–73. https://doi.org/10.1016/j.cofs.2018.02.002.

Planque, M., T. Arnould, M. Dieu, P. Delahaut, P. Renard, and N. Gillard. 2016. “Advances in Ultra-High Performance Liquid Chromatography Coupled to Tandem Mass Spectrometry for Sensitive Detection of Several Food Allergens in Complex and Processed Foodstuffs.” *Journal of Chromatography A* 1464: 115–23. https://doi.org/10.1016/j.chroma.2016.08.033.

Pohl, Antje, Philippe F. Devaux, and Andreas Herrmann. 2005. “Function of Prokaryotic and Eukaryotic ABC Proteins in Lipid Transport.” *Biochimica et Biophysica Acta - Molecular and Cell Biology of Lipids* 1733 (1): 29–52. https://doi.org/10.1016/j.bbalip.2004.12.007.

Polgár, L. 2005. “The Catalytic Triad of Serine Peptidases.” *Cellular and Molecular Life Sciences* 62 (19–20): 2161–72. https://doi.org/10.1007/s00018-005-5160-x.

R Core Team. 2023. “R: A Language and Environment for Statistical Computing.” R Foundation for Statistical Computing, Vienna, Austria. https://www.r-project.org/.

Ragona, L, L Confalonieri, L Zetta, K G De Kruif, S Mammi, E Peggion, R Longhi, and H Molinari. 1999. “Studies of Bovine Beta-Lactoglobulin and Its 14 – 52 Fragment at Acidic PH.” *Biopolymers* 49: 441–50.

Razafindrazoto, Chantelli Iamblaudiot, Behoavy Mahafaly Ralaizanaka, Jolivet Auguste Rakotomalala, Christiane Stern, Soloniaina Hélio Razafimahefa, Rado Manitrala Ramanampamonjy, and Pascal Lebray. 2023. “Low - Phospholipid Associated Cholelithiasis (LPAC) Syndrome : An Unusual Form in an Elderly and Overweight Woman.” *Egyptian Liver Journal*, 2–6. https://doi.org/10.1186/s43066-023-00234-2.

Reis, P., K. Holmberg, H. Watzke, M. E. Leser, and R. Miller. 2009. “Lipases at Interfaces: A Review.” *Advances in Colloid and Interface Science* 147–148 (C): 237–50. https://doi.org/10.1016/j.cis.2008.06.001.

Reshetnyak, Vasiliy Ivanovich. 2013. “Physiological and Molecular Biochemical Mechanisms of Bile Formation.” *World Journal of Gastroenterology* 19 (42): 7341–60. https://doi.org/10.3748/wjg.v19.i42.7341.

Riethorst, Danny, Peter Baatsen, Caroline Remijn, Amitava Mitra, Jan Tack, Joachim Brouwers, and Patrick Augustijns. 2016. “An In-Depth View into Human Intestinal Fluid Colloids: Intersubject Variability in Relation to Composition.” *Molecular Pharmaceutics* 13 (10): 3484–93. https://doi.org/10.1021/acs.molpharmaceut.6b00496.

Riethorst, Danny, Raf Mols, Guus Duchateau, Jan Tack, Joachim Brouwers, and Patrick Augustijns. 2016. “Characterization of Human Duodenal Fluids in Fasted and Fed State Conditions.” *Journal of Pharmaceutical Sciences* 105 (2): 673–81. https://doi.org/10.1002/jps.24603.

Robic, Srebrenka, Kristin B. Linscott, Madiha Aseem, Ellen A. Humphreys, and Shannon R. McCartha. 2011. “Bile Acids as Modulators of Enzyme Activity and Stability.” *Protein Journal* 30 (8): 539–45. https://doi.org/10.1007/s10930-011-9360-y.

Rustan, Arild C, and Christian A Drevon. 2005. “Fatty Acids: Structures and Properties.” *Encyclopedia of Life Sciences*, 1–7. https://doi.org/10.1038/npg.els.0003894.

Rutherfurd-markwick, Kay J. 2012. “Food Proteins as a Source of Bioactive Peptides with Diverse Functions,” 149–57. https://doi.org/10.1017/S000711451200253X.

Sadaruddin, A, R Hassan, and S J Zuberi. 1980. “Bile Salt, Phospholipids and Cholesterol in Bile of Patients with Cholelithiasis.” *JPMA. The Journal of the Pakistan Medical Association* 30 (3): 60–62.

Saitoh, Tohru, Teruyuki Fukuda, Hirofumi Tani, Tamio Kamidate, and Hiroto Watanabe. 1996. “Equilibrium Study on Interactions between Proteins and Bile-Salt Micelles by Micellar Electrokinetic Chromatography.” *Analytical Sciences* 12 (4): 569–73. https://doi.org/10.2116/analsci.12.569.

Samsom, Melvin, and Mark A. M. T. Verhagen. 2004. “Intestinal Function.” *Gastrointestinal Function in Diabetes Mellitus*, 177–217. https://doi.org/10.1002/0470013877.ch5.

Sanchón, J., S. Fernández-Tomé, B. Miralles, B. Hernández-Ledesma, D. Tomé, C. Gaudichon, and I. Recio. 2018. “Protein Degradation and Peptide Release from Milk Proteins in Human Jejunum. Comparison with in Vitro Gastrointestinal Simulation.” *Food Chemistry* 239: 486–94. https://doi.org/10.1016/j.foodchem.2017.06.134.

Sangaraju, Dewakar, Yao Shi, Michael Van Parys, Adam Ray, Abigail Walker, Rachel Caminiti, Dennis Milanowski, Allan Jaochico, Brian Dean, and Xiaorong Liang. 2021. “Robust and Comprehensive Targeted Metabolomics Method for Quantification of 50 Different Primary, Secondary, and Sulfated Bile Acids in Multiple Biological Species (Human, Monkey, Rabbit, Dog, and Rat) and Matrices (Plasma and Urine) Using Liquid Chromato.” *Journal of the American Society for Mass Spectrometry* 32 (8): 2033–49. https://doi.org/10.1021/jasms.0c00435.

Sareen S. Gropper, Jack L. Smith, Timothy P. Carr. 2022. *Advanced Nutrition and Human Metabolism.* CENGAGE Learning Custom Publishing ISBN:9781305627857.

Schrodinger LLC. 2010. “The PyMOL Molecular Graphics System, Version 4.6.”

Schwartz-Narbonne, Heather, Chen Wang, Shouming Zhou, Jonathan P.D. Abbatt, and Jennifer Faust. 2019. “Heterogeneous Chlorination of Squalene and Oleic Acid.”

Environmental Science and Technology 53 (3): 1217–24. https://doi.org/10.1021/acs.est.8b04248.

Sélo, I., G. Clément, H. Bernard, J. M. Chatel, C. Créminon, G. Peltre, and J. M. Wal. 1999. “Allergy to Bovine β-Lactoglobulin: Specificity of Human IgE to Tryptic Peptides.” *Clinical and Experimental Allergy* 29 (8): 1055–63. https://doi.org/10.1046/j.1365-2222.1999.00612.x.

Sharma, Nupur, Manisha Yadav, Gaurav Tripathi, Babu Mathew, Vasundhra Bindal, Sanyam Falari, Viniyendra Pamecha, and Jaswinder Singh Maras. 2022. “Bile Multi-Omics Analysis Classifies Lipid Species and Microbial Peptides Predictive of Carcinoma of Gallbladder.” *Hepatology* 76 (4): 920–35. https://doi.org/10.1002/hep.32496.

Shewry, P. R. 1995. “Plant Storage Proteins.” *Biological Reviews* 70 (3): 375–426. https://doi.org/10.1111/j.1469-185X.1995.tb01195.x.

Shuken, Steven R. 2023. “An Introduction to Mass Spectrometry-Based Proteomics.” *Journal of Proteome Research* 22 (7): 2151–71. https://doi.org/10.1021/acs.jproteome.2c00838.

Silva, Raquel, Helena Ferreira, Collin Little, and Artur Cavaco-Paulo. 2010. “Effect of Ultrasound Parameters for Unilamellar Liposome Preparation.” *Ultrasonics Sonochemistry* 17 (3): 628–32. https://doi.org/10.1016/j.ultsonch.2009.10.010.

Silveira, Silvana T., Daniel Martínez-Maqueda, Isidra Recio, and Blanca Hernández-Ledesma. 2013. “Dipeptidyl Peptidase-IV Inhibitory Peptides Generated by Tryptic Hydrolysis of a Whey Protein Concentrate Rich in β-Lactoglobulin.” *Food Chemistry* 141 (2): 1072–77. https://doi.org/10.1016/j.foodchem.2013.03.056.

Sina Vahdatpour Mehdi Soleymani-Goloujeh Naser Maheri-Sis Hamid Mahmoodpour Tohid Vahdatpour, Aniseh Pourrasmi-Mamaghani. 2016. “The Systematic Review of Proteins Digestion and New Strategies for Delivery of Small Peptides.” *Electronic Journal of Biology*, no. May. http://ejbio.imedpub.com/the-systematic-review-of-proteins-digestion-and-newstrategies-for-delivery-of-small-peptides.php?aid=9725.

Smith, Margaret. 2019. *The Digestive System. Basic Science and Clinical Conditions*. Elsevier Limited. ISBN:9781119130536.

Sobott, Frank, Stephen J. Watt, Julia Smith, Mariola J. Edelmann, Holger B. Kramer, and Benedikt M. Kessler. 2009. “Comparison of CID Versus ETD Based MS/MS Fragmentation for the Analysis of Protein Ubiquitination.” *Journal of the American Society for Mass Spectrometry* 20 (9): 1652–59. https://doi.org/10.1016/j.jasms.2009.04.023.

Sousa, Raquel, Reto Portmann, Sébastien Dubois, Isidra Recio, and Lotti Egger. 2020. “Protein Digestion of Different Protein Sources Using the INFOGEST Static Digestion Model.” *Food Research International* 130 (September 2019): 108996. https://doi.org/10.1016/j.foodres.2020.108996.

Stappaerts, Jef, Benjamin Wuyts, Jan Tack, Pieter Annaert, and Patrick Augustijns. 2014. “Human and Simulated Intestinal Fluids as Solvent Systems to Explore Food Effects on Intestinal Solubility and Permeability.” *European Journal of Pharmaceutical Sciences* 63: 178–86. https://doi.org/10.1016/j.ejps.2014.07.009.

Stojadinovic, Marija, Jelena Radosavljevic, Jana Ognjenovic, Jelena Vesic, Ivana Prodic, Dragana Stanic-Vucinic, and Tanja Cirkovic Velickovic. 2013. “Binding Affinity between Dietary Polyphenols and β-Lactoglobulin Negatively Correlates with the Protein Susceptibility to Digestion and Total Antioxidant Activity of Complexes

Formed." *Food Chemistry* 136 (3): 1263–71. https://doi.org/https://doi.org/10.1016/j.foodchem.2012.09.040.

Sun, Tong, Xincen Wang, Peixu Cong, Jie Xu, and Changhu Xue. 2020. "Mass Spectrometry-Based Lipidomics in Food Science and Nutritional Health: A Comprehensive Review." *Comprehensive Reviews in Food Science and Food Safety* 19 (5): 2530–58. https://doi.org/10.1111/1541-4337.12603.

"SureCast ™ Handcast System, MAN0014073, Thermo Fisher Scientific." 2021. 2021. https://manuals.plus/m/db7bdf1da1f94421bf0b5cb0e39d9b4cc1ddcd4e8559b8f9da71f6e5e60e6656.

Sutantawong, Suwimon, Bum Jin Kim, Yunyao Qu, and David C. Dallas. 2025. "Survival of Intact Bovine Whey Proteins across in Vivo and Simulated Static in Vitro Models of the Adult Gastrointestinal Tract." *Food Chemistry* 465 (P1): 142013. https://doi.org/10.1016/j.foodchem.2024.142013.

Swell, L., C. C. Bell, and Z. R. Vlahcevic. 1971. "Relationship of Bile Acid Pool Size to Biliary Lipid Excretion and the Formation of Lithogenic Bile in Man." *Gastroenterology* 61 (5): 716–22. https://doi.org/10.1016/s0016-5085(19)33435-3.

Takkella, Dineshbabu, Sudhanshu Sharma, Jyoti Vishwakarma, and Krishna Gavvala. 2025. "Bile Salt Induced Aggregation and Nanostructure Formation of β-Lactoglobulin in Gastrointestinal Environments." *Food Hydrocolloids* 162: 110944. https://doi.org/https://doi.org/10.1016/j.foodhyd.2024.110944.

Tan, Yunbing, Hualu Zhou, and David Julian McClements. 2022. "Application of Static in Vitro Digestion Models for Assessing the Bioaccessibility of Hydrophobic Bioactives: A Review." *Trends in Food Science & Technology* 122: 314–27. https://doi.org/https://doi.org/10.1016/j.tifs.2022.02.028.

Tanaka, Kazuko, Kenji Matsumoto, Akira Akasawa, Toshiharu Nakajima, Takeshi Nagasu, Yoji Iikura, and Hirohisa Saito. 2002. "Pepsin-Resistant 16-KD Buckwheat Protein Is Associated with Immediate Hypersensitivity Reaction in Patients with Buckwheat Allergy." *International Archives of Allergy and Immunology* 129 (1): 49–56. https://doi.org/10.1159/000065173.

Tavares, Tânia, Maria Del Mar Contreras, Manuela Amorim, Manuela Pintado, Isidra Recio, and F. Xavier Malcata. 2011. "Novel Whey-Derived Peptides with Inhibitory Effect against Angiotensin-Converting Enzyme: In Vitro Effect and Stability to Gastrointestinal Enzymes." *Peptides* 32 (5): 1013–19. https://doi.org/10.1016/j.peptides.2011.02.005.

Tazuma, Susumu; 2017. *Bile Acids in Gastroenterology*. https://doi.org/10.1007/978-4-431-56062-3.

Tietel, Zipora, Simon Hammann, Sven W. Meckelmann, Carmit Ziv, Josch K. Pauling, Michele Wölk, Vivian Würf, Eliana Alves, Bruna Neves, and M. Rosário Domingues. 2023. "An Overview of Food Lipids toward Food Lipidomics." *Comprehensive Reviews in Food Science and Food Safety* 22 (6): 4302–54. https://doi.org/10.1111/1541-4337.13225.

Torcello-Gómez, A., A.B. Jódar-Reyes, J. Maldonado-Valderrama, and A. Martín-Rodríguez. 2012. "Effect of Emulsifier Type against the Action of Bile Salts at Oil–Water Interfaces." *Food Research International* 48 (1): 140–47. https://doi.org/10.1016/j.foodres.2012.03.007.

Torcello-Gómez, A., J. Maldonado-Valderrama, J. de Vicente, M. A. Cabrerizo-Vílchez, M. J. Gálvez-Ruiz, and A. Martín-Rodríguez. 2011. "Investigating the Effect of

Surfactants on Lipase Interfacial Behaviour in the Presence of Bile Salts." *Food Hydrocolloids* 25 (4): 809–16. https://doi.org/10.1016/j.foodhyd.2010.09.007.

Tsuzuki, Wakako, Akemi Ue, Akihiko Nagao, Miyuki Endo, and Masahiko Abe. 2004. "Inhibitory Effect of Lysophosphatidylcholine on Pancreatic Lipase-Mediated Hydrolysis in Lipid Emulsion." *Biochimica et Biophysica Acta - Molecular and Cell Biology of Lipids* 1684 (1–3): 1–7. https://doi.org/10.1016/j.bbalip.2004.05.002.

Turgeon, Sylvie L., Sylvie F. Gauthier, Daniel Mollé, and Joëlle Léonil. 1992. "Interfacial Properties of Tryptic Peptides of β-Lactoglobulin." *Journal of Agricultural and Food Chemistry* 40 (4): 669–75. https://doi.org/10.1021/jf00016a030.

Vance, J. E., and Dennis E. Vance. 2008. *Biochemistry Of Lipids, Lipoproteins And Membranes*. *Biochemistry of Lipids, Lipoproteins and Membranes*. https://doi.org/10.1016/B978-0-444-53219-0.X5001-6.

Venuti, Elena, Dmitry Shishmarev, Philip W. Kuchel, Shoma Dutt, Caron S. Blumenthal, and Kevin J. Gaskin. 2017. "Bile Salt Stimulated Lipase: Inhibition by Phospholipids and Relief by Phospholipase A2." *Journal of Cystic Fibrosis* 16 (6): 763–70. https://doi.org/10.1016/j.jcf.2017.07.005.

Verhoeckx, Kitty, Paul Cotter, Iván López-Expósito, Charlotte Kleiveland, Tor Lea, Alan Mackie, Teresa Requena, Dominika Swiatecka, and Harry Wichers. 2015. *The Impact of Food Bioactives on Health: In Vitro and Ex Vivo Models*. *The Impact of Food Bioactives on Health: In Vitro and Ex Vivo Models*. https://doi.org/10.1007/978-3-319-16104-4.

Verma, Santosh Kumar, Kallol K. Ghosh, Rameshwari Verma, Wanchun Xiang, Neng Li, and Xiujian Zhao. 2015. "Surface, Conformational and Catalytic Activity Approach of α-Chymotrypsin and Trypsin in Micellar Media." *Colloids and Surfaces A: Physicochemical and Engineering Aspects* 470: 188–93. https://doi.org/10.1016/j.colsurfa.2015.01.070.

Villa, Caterina, Joana Costa, Maria Beatriz P.P. Oliveira, and Isabel Mafra. 2018. "Bovine Milk Allergens: A Comprehensive Review." *Comprehensive Reviews in Food Science and Food Safety* 17 (1): 137–64. https://doi.org/10.1111/1541-4337.12318.

Vita, Randi, Swapnil Mahajan, James A Overton, Sandeep Kumar Dhanda, Sheridan Martini, Jason R Cantrell, Daniel K Wheeler, Alessandro Sette, and Bjoern Peters. 2018. "The Immune Epitope Database (IEDB): 2018 Update." *Nucleic Acids Research* 47 (D1): D339–43. https://doi.org/10.1093/nar/gky1006.

Vlahcevic, Z. R., C. C. Bell, D. H. Gregory, G. Buker, P. Juttijudata, and L. Swell. 1972. "Relationship of Bile Acid Pool Size to the Formation of Lithogenic Bile in Female Indians of the Southwest." *Gastroenterology* 62 (1): 73–83. https://doi.org/10.1016/S0016-5085(72)80011-8.

Vlahcevic, Z. R., C. Bell, and L. Swell. 1970. "Significance of the Liver in the Production of Lithogenic Bile in Man." *Gastroenterology* 59 (1): 62–69. https://doi.org/10.1016/s0016-5085(19)33804-1.

Vleeschauwer, Dries De, and Paul Van der Meeren. 1999. "Colloid Chemical Stability and Interfacial Properties of Mixed Phospholipid–Non-Ionic Surfactant Stabilised Oil-in-Water Emulsions." *Colloids and Surfaces A: Physicochemical and Engineering Aspects* 152 (1–2): 59–66. https://doi.org/10.1016/S0927-7757(98)00617-7.

Wal, J. M. 2001. "Structure and Function of Milk Allergens." *Allergy: European Journal of*

Allergy and Clinical Immunology, Supplement 56 (67): 35–38. https://doi.org/10.1034/j.1398-9995.2001.00911.x.

Wang, Mengxun, Shixiang Xu, Ling Zhi Cheong, Xuebing Xu, Yanlan Bi, and Hong Zhang. 2022. “Development of a Reliable PH-STAT in-Vitro Model for Gastrointestinal Digestion of Lipids and Application for Infant Formula.” *Food Science and Technology (Brazil)* 42. https://doi.org/10.1590/fst.115221.

Wang, Rong, Thomas C. Edrington, S. Bradley Storrs, Kathleen S. Crowley, Jason M. Ward, Thomas C. Lee, Zi L. Liu, Bin Li, and Kevin C. Glenn. 2017. “Analyzing Pepsin Degradation Assay Conditions Used for Allergenicity Assessments to Ensure That Pepsin Susceptible and Pepsin Resistant Dietary Proteins Are Distinguishable.” *PLoS ONE* 12 (2): 1–15. https://doi.org/10.1371/journal.pone.0171926.

Wang, Xin, Aiqian Ye, Quanquan Lin, Jianzhong Han, and Harjinder Singh. 2018. “Gastric Digestion of Milk Protein Ingredients: Study Using an in Vitro Dynamic Model.” *Journal of Dairy Science* 101 (8): 6842–52. https://doi.org/10.3168/jds.2017-14284.

Warren, Dallas B., David K. Chalmers, Keith Hutchison, Wenbin Dang, and Colin W. Pouton. 2006. “Molecular Dynamics Simulations of Spontaneous Bile Salt Aggregation.” *Colloids and Surfaces A: Physicochemical and Engineering Aspects* 280 (1–3): 182–93. https://doi.org/10.1016/j.colsurfa.2006.02.009.

Whitcomb, David C., and Mark E. Lowe. 2007. “Human Pancreatic Digestive Enzymes.” *Digestive Diseases and Sciences* 52 (1): 1–17. https://doi.org/10.1007/s10620-006-9589-z.

Whiting, M. J., R. H.L. Down, and J. Mc K. Watts. 1981. “Precision and Accuracy in the Measurement of the Cholesterol Saturation Index of Duodenal Bile. Lack of Variation Due to the Menstrual Cycle.” *Gastroenterology* 80 (3): 533–38. https://doi.org/10.1016/0016-5085(81)90016-0.

Wickham, Martin, Martin Garrood, John Leney, Peter D.G. Wilson, and Annette Fillery-Travis. 1998. “Modification of a Phospholipid Stabilized Emulsion Interface by Bile Salt: Effect on Pancreatic Lipase Activity.” *Journal of Lipid Research* 39 (3): 623–32. https://doi.org/10.1016/S0022-2275(20)33300-9.

Wickham, Martin, Peter Wilde, and Annette Fillery-Travis. 2002. “A Physicochemical Investigation of Two Phosphatidylcholine/Bile Salt Interfaces: Implications for Lipase Activation.” *Biochimica et Biophysica Acta - Molecular and Cell Biology of Lipids* 1580 (2–3): 110–22. https://doi.org/10.1016/S1388-1981(01)00196-2.

Wilde, P. J., and B. S. Chu. 2011. “Interfacial & Colloidal Aspects of Lipid Digestion.” *Advances in Colloid and Interface Science* 165 (1): 14–22. https://doi.org/10.1016/j.cis.2011.02.004.

Wolf-Yadlin, Alejandro, Alex Hu, and William S. Noble. 2016. “Technical Advances in Proteomics: New Developments in Data-Independent Acquisition.” *F1000Research* 5 (0): 1–12. https://doi.org/10.12688/f1000research.7042.1.

Wu, Guoyao. 2016. “Dietary Protein Intake and Human Health.” *Food and Function* 7 (3): 1251–65. https://doi.org/10.1039/c5fo01530h.

Wuyts, Benjamin, Danny Riethorst, Joachim Brouwers, Jan Tack, Pieter Annaert, and Patrick Augustijns. 2015. “Evaluation of Fasted and Fed State Simulated and Human Intestinal Fluids as Solvent System in the Ussing Chambers Model to Explore Food Effects on Intestinal Permeability.” *International Journal of*

Pharmaceutics 478 (2): 736–44. https://doi.org/10.1016/j.ijpharm.2014.12.021.

Xavier, Ana A O, and Lilian R B Mariutti. 2021. “ScienceDirect Static and Semi-Dynamic in Vitro Digestion Methods : State of the Art and Recent Achievements towards Standardization.” *Current Opinion in Food Science* 41: 260–73. https://doi.org/10.1016/j.cofs.2021.08.002.

Xu, Suowen, Zhiping Liu, and Peiqing Liu. 2013. “HDL Cholesterol in Cardiovascular Diseases: The Good, the Bad, and the Ugly?” *International Journal of Cardiology* 168 (4): 3157–59. https://doi.org/10.1016/j.ijcard.2013.07.210.

Xuemei Han, Aaron Aslanian, and John R. Yates. 2008. “Mass Spectrometry for Proteomics.” *Bone* 23 (1): 1–7. https://doi.org/10.1016/j.cbpa.2008.07.024.Mass.

Yang, Tom. 2023. “PEAKS Studio 11 User Manual.”

Yates, John R. 2004. “Mass Spectral Analysis in Proteomics.” *Annual Review of Biophysics and Biomolecular Structure* 33: 297–316. https://doi.org/10.1146/annurev.biophys.33.111502.082538.

Zajac, Ian T., Danielle Herreen, Kathryn Bastiaans, Varinderpal S. Dhillon, and Michael Fenech. 2019. “The Effect of Whey and Soy Protein Isolates on Cognitive Function in Older Australians with Low Vitamin B 12 : A Randomised Controlled Crossover Trial.” *Nutrients* 11 (1): 1–13. https://doi.org/10.3390/nu11010019.

Zhao, Changhui, and Tolulope Joshua. 2020. “Bioactivity and Safety of Whey Peptides.” *LWT* 134 (June): 109935. https://doi.org/10.1016/j.lwt.2020.109935.

Zhao, Qianru, Yuwei Wang, Zhengming Zhu, Quanyu Zhao, Liying Zhu, and Ling Jiang. 2023. “Food Science and Human Wellness Effi Cient Reduction of β -Lactoglobulin Allergenicity in Milk Using Clostridium Tyrobutyricum Z816.” *Food Science and Human Wellness* 12 (3): 809–16. https://doi.org/10.1016/j.fshw.2022.09.017.

Zhou, Houjiang, Ruijun Tian, Mingliang Ye, Songyun Xu, Shun Feng, Chensong Pan, Xiaogang Jiang, Xin Li, and Hanfa Zou. 2007. “Highly Specific Enrichment of Phosphopeptides by Zirconium Dioxide Nanoparticles for Phosphoproteome Analysis.” *Electrophoresis* 28 (13): 2201–15. https://doi.org/10.1002/elps.200600718.

Zhou, Hualu, Yunbing Tan, and David Julian McClements. 2023. “Applications of the INFOGEST In Vitro Digestion Model to Foods: A Review.” *Annual Review of Food Science and Technology* 14 (1): 135–56. https://doi.org/10.1146/annurev-food-060721-012235.

7 Appendix

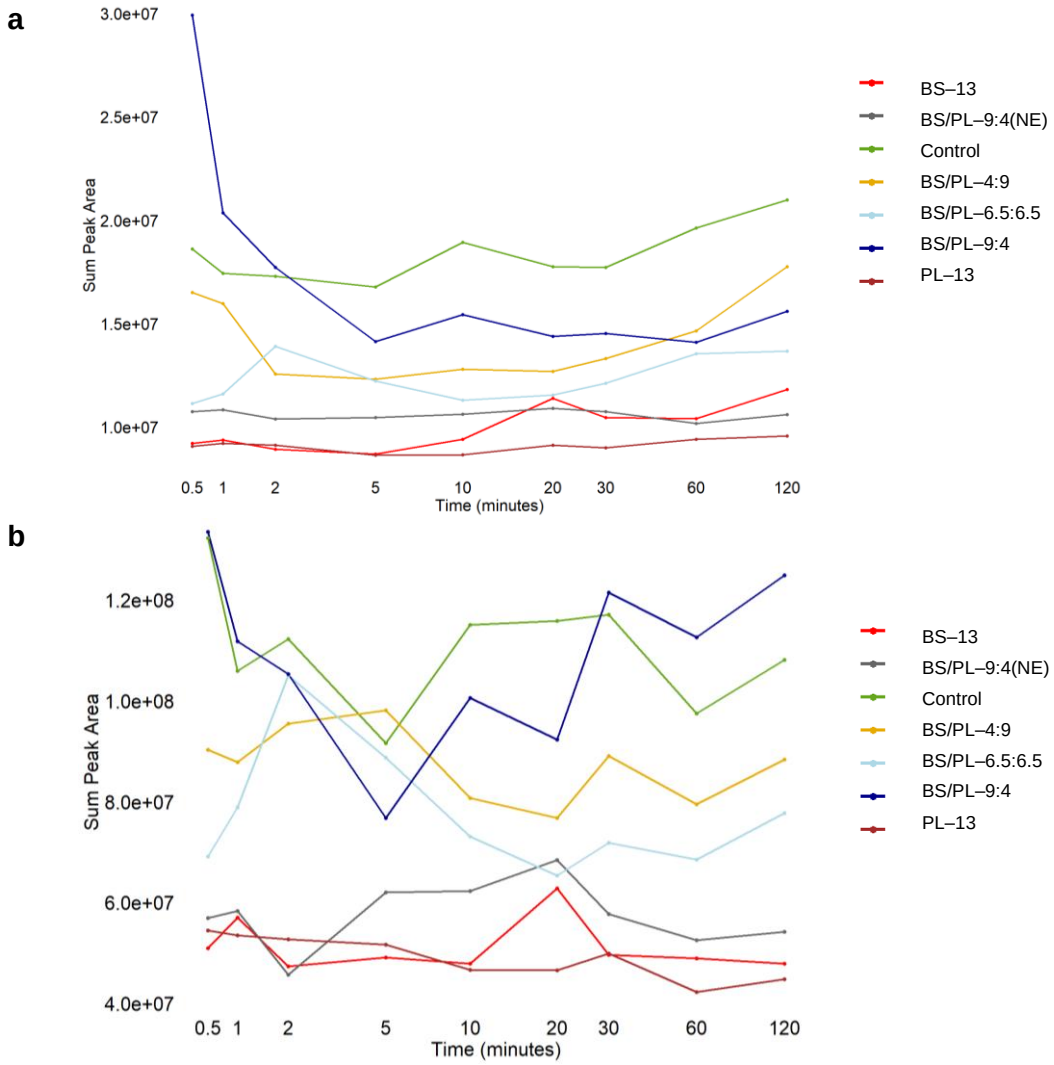

Figure 7.1 The sum peak area over time during 2-hour intestinal digestion of WPI proteins under various conditions (Table 13); a) bovine serum albumin (BSA); b) α-lactalbumin (α-La).

Table 17. Sequence coverage of WPI proteins during intestinal digestion, obtained from LFQ analysis in PEAKS 11.

Protein	BS/PL-9:4(NE)	BS/PL-4:9	BS/PL-9:4	Control	BS-13	PL-13	BS/PL-6.5:6.5
P00711|LALBA_BOVIN	90.1	85.9	86.6	95.8	93.7	90.1	86.6
P02769|ALBU_BOVIN	83.0	84.8	84.8	85.7	89.6	82.0	82.9
P02754|LACB_BOVIN	100.0	100.0	100.0	97.2	96.6	91.6	91.6

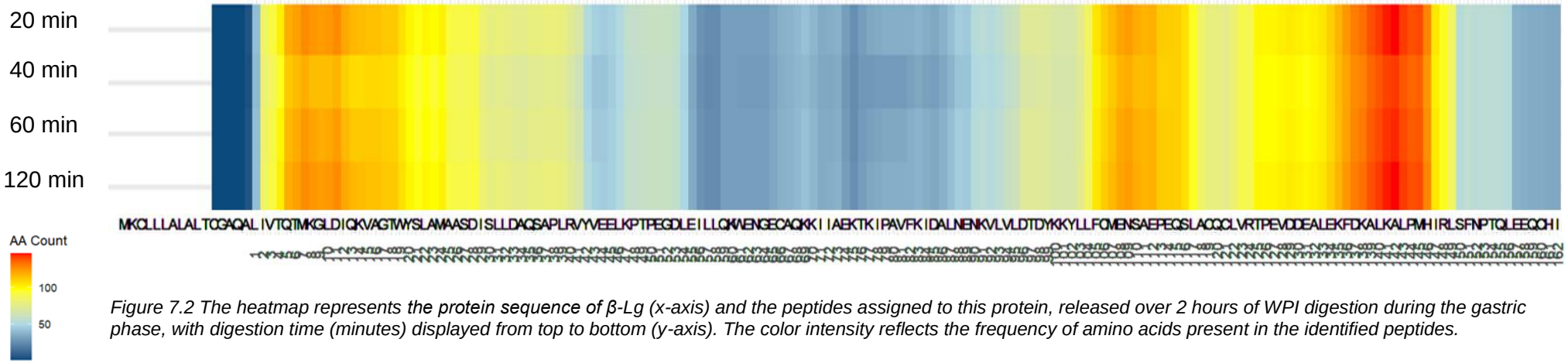

Figure 7.2 The heatmap represents the protein sequence of β-Lg (x-axis) and the peptides assigned to this protein, released over 2 hours of WPI digestion during the gastric phase, with digestion time (minutes) displayed from top to bottom (y-axis). The color intensity reflects the frequency of amino acids present in the identified peptides.

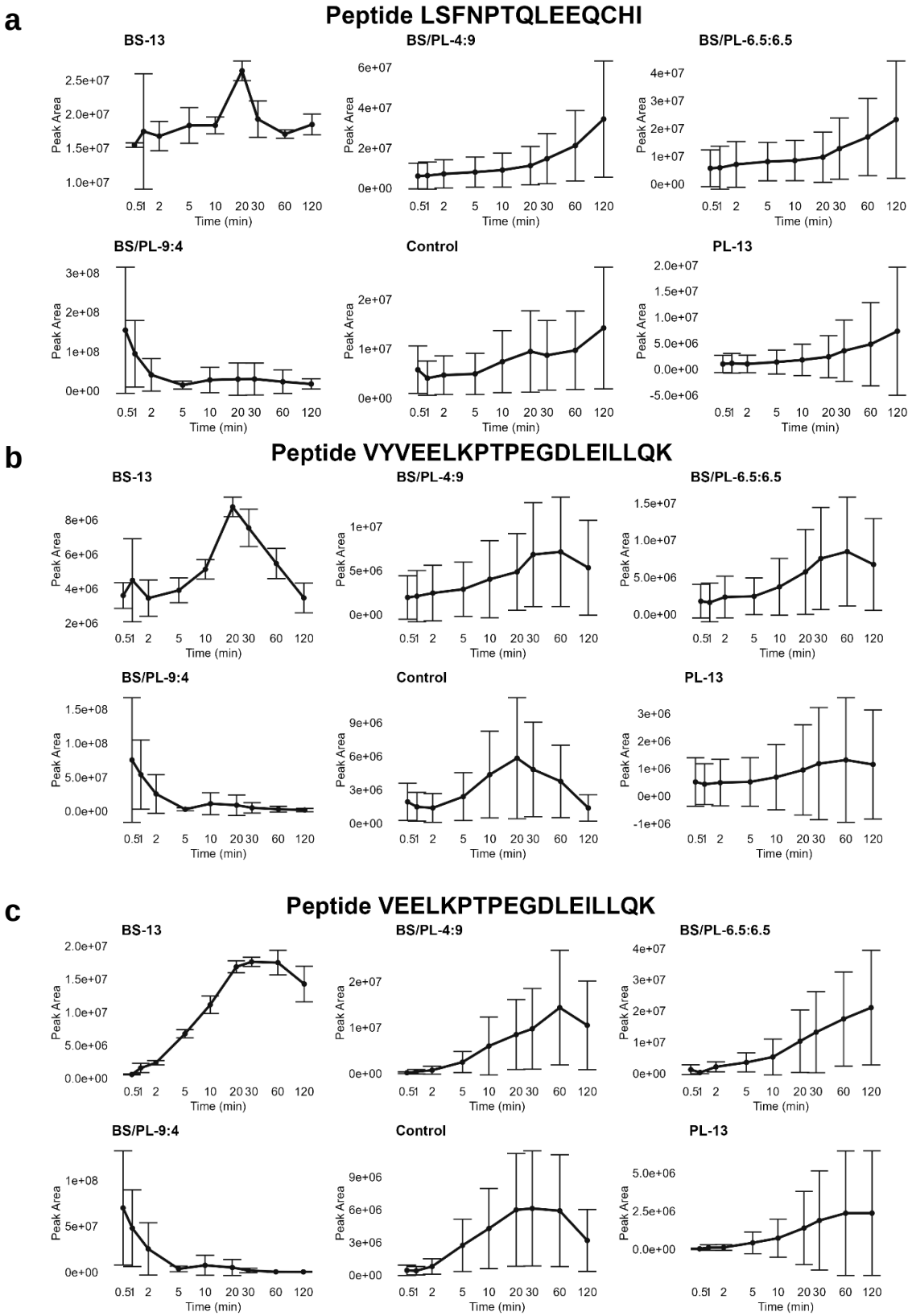
a
Peptide LSFNPTQLEEQCHI
BS-13
BS/PL-4:9
BS/PL-6.5:6.5
BS/PL-9:4
Control
PL-13
b
Peptide VYVEELKPTPEGDLEILLQK
BS-13
BS/PL-4:9
BS/PL-6.5:6.5
BS/PL-9:4
Control
PL-13
c
Peptide VEELKPTPEGDLEILLQK
BS-13
BS/PL-4:9
BS/PL-6.5:6.5
BS/PL-9:4
Control
PL-13
Peak Area
Time (min)
0.5 1 2 5 10 20 30 60 120

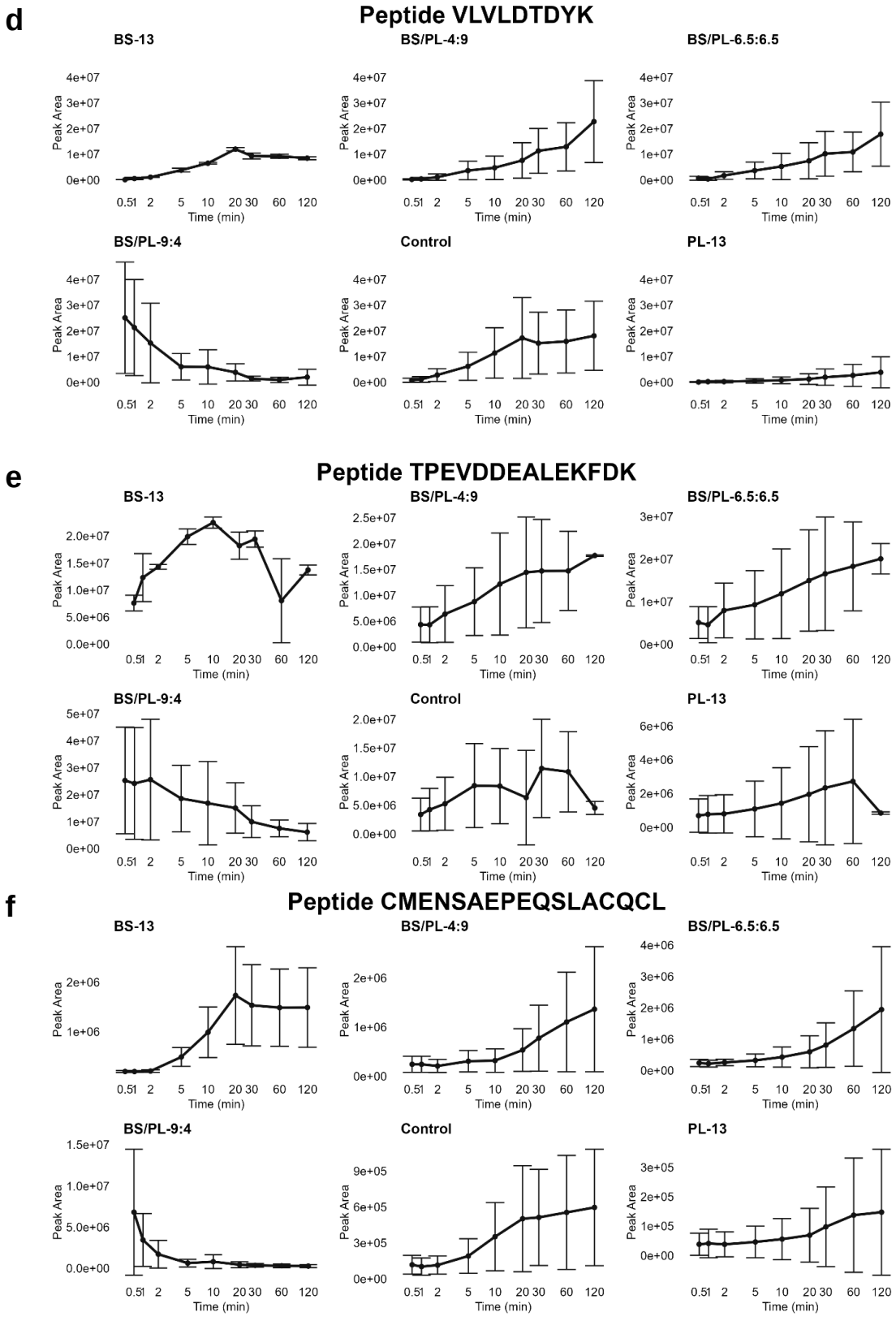
d
Peptide VLVLDTDYK
BS-13
BS/PL-4:9
BS/PL-6.5:6.5
BS/PL-9:4
Control
PL-13
Peak Area
Time (min)
0.51 2 5 10 20 30 60 120
e
Peptide TPEVDDEALEKFDK
BS-13
BS/PL-4:9
BS/PL-6.5:6.5
BS/PL-9:4
Control
PL-13
f
Peptide CMENSAEPEQSLACQCL
BS-13
BS/PL-4:9
BS/PL-6.5:6.5
BS/PL-9:4
Control
PL-13

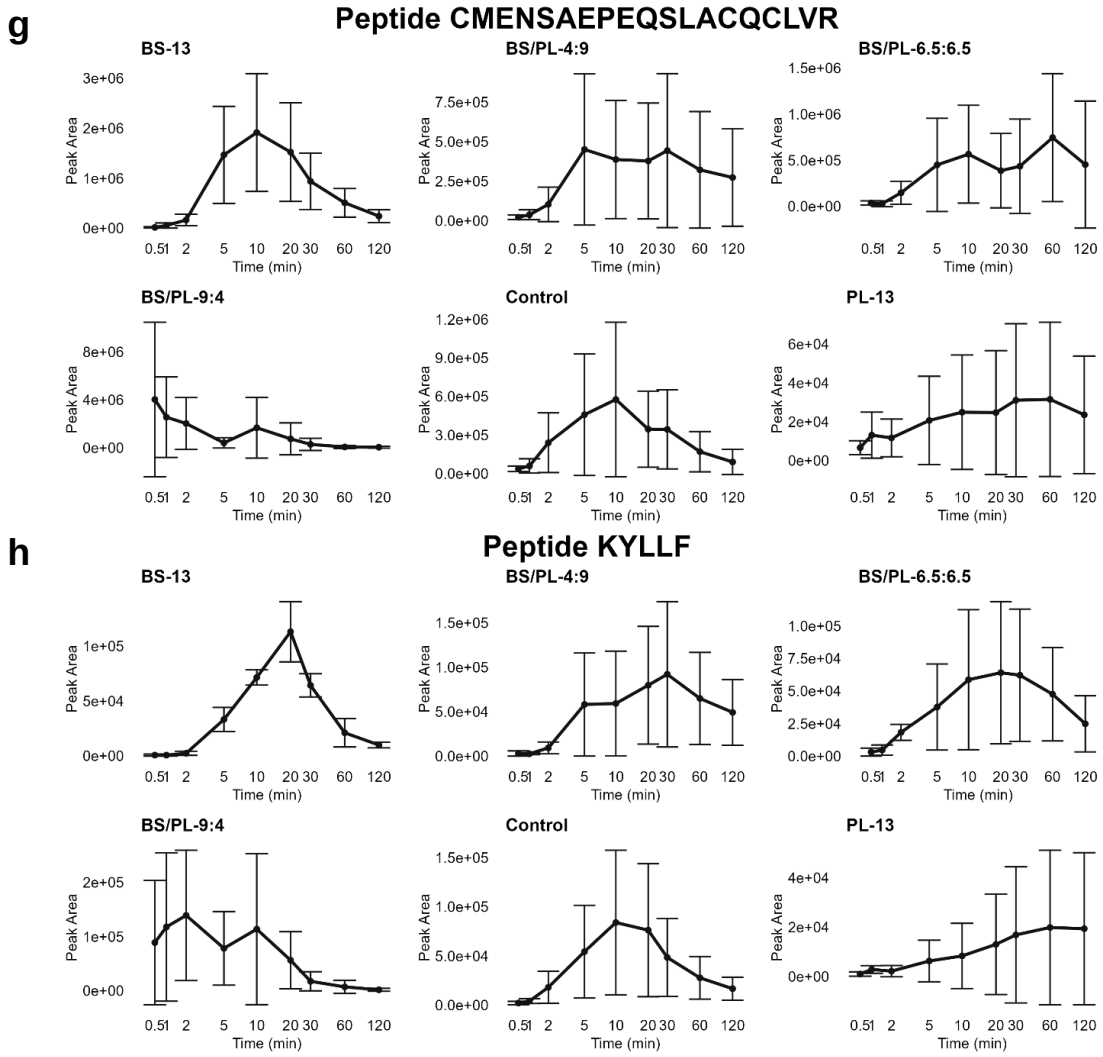

Figure 7.3. Peptide kinetics with outstanding signal intensity during the initial stage of intestinal digestion under BS/PL-9:4 conditions. The graphs show the kinetics of these peptides for various digestion conditions (Table 13), including standard deviations (SD).

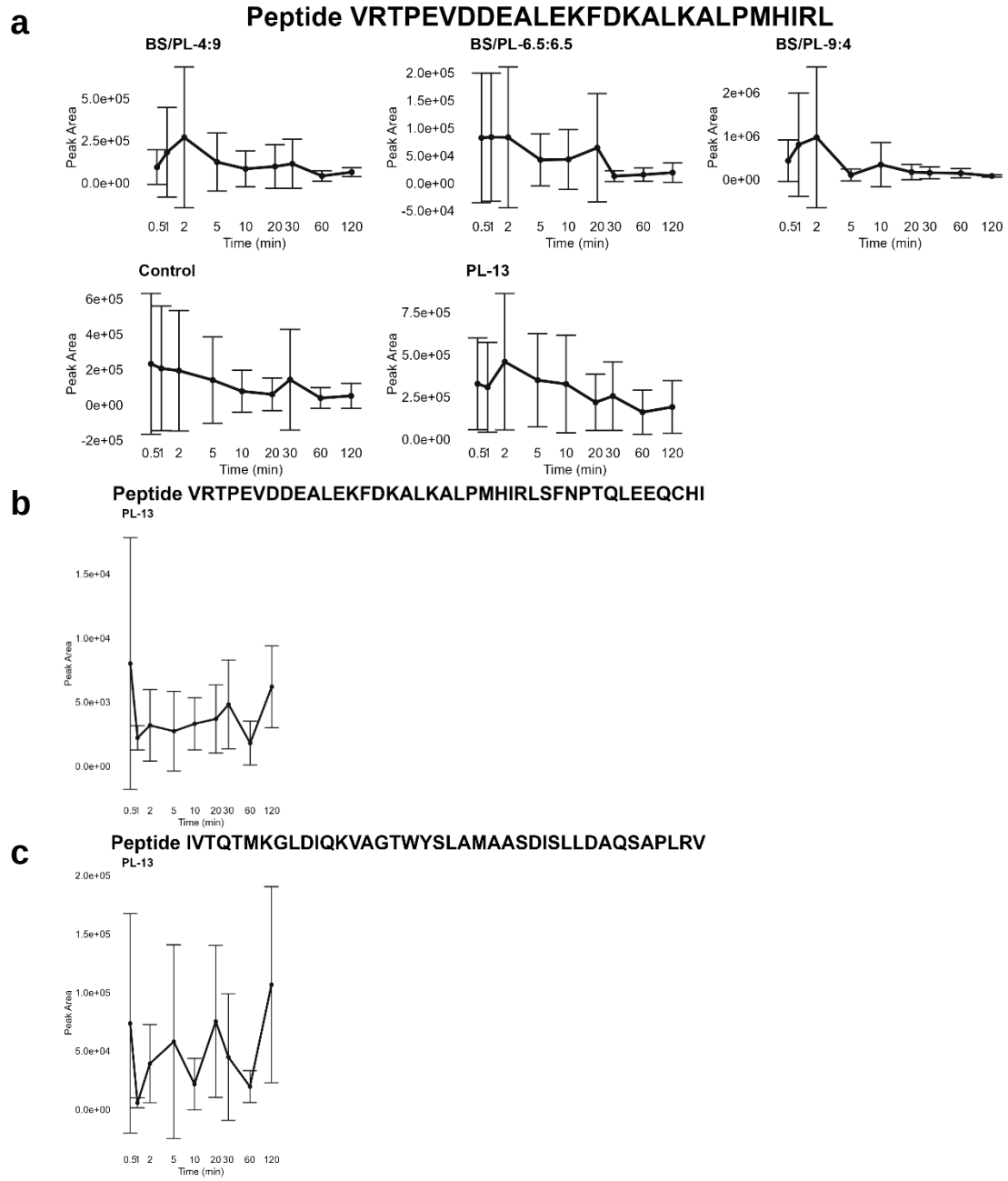

Figure 7.4 The examples of long peptides originating from gastric phase and its kinetics in the intestinal phase under various conditions.

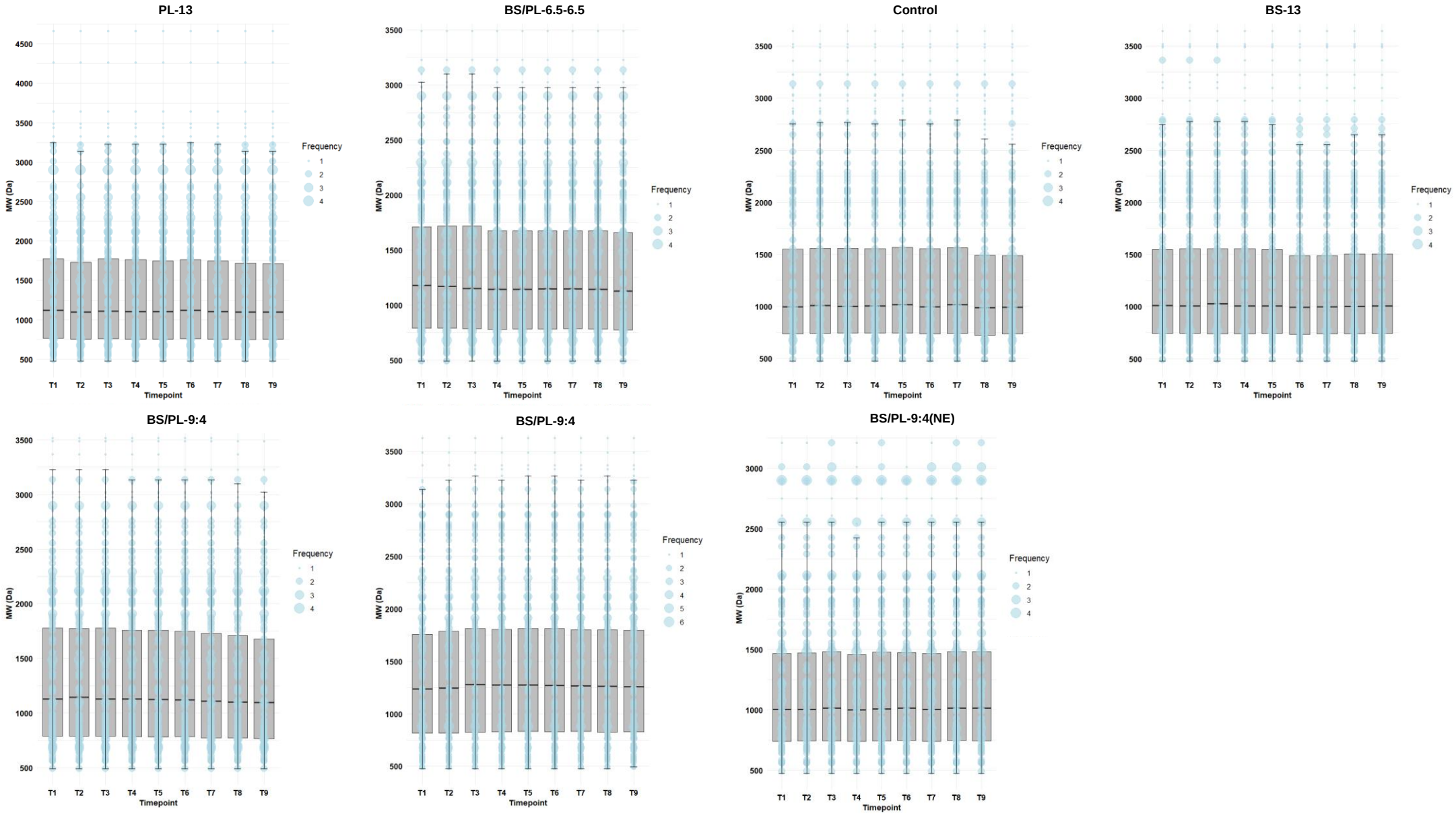

Figure 7.5 Size distribution (Molecular Weight, MW (Da)) over time at various conditions (Table 13) of intestinal phase. T1-T9 represents time-points of sample uptake in the intestinal phase (Table 3).

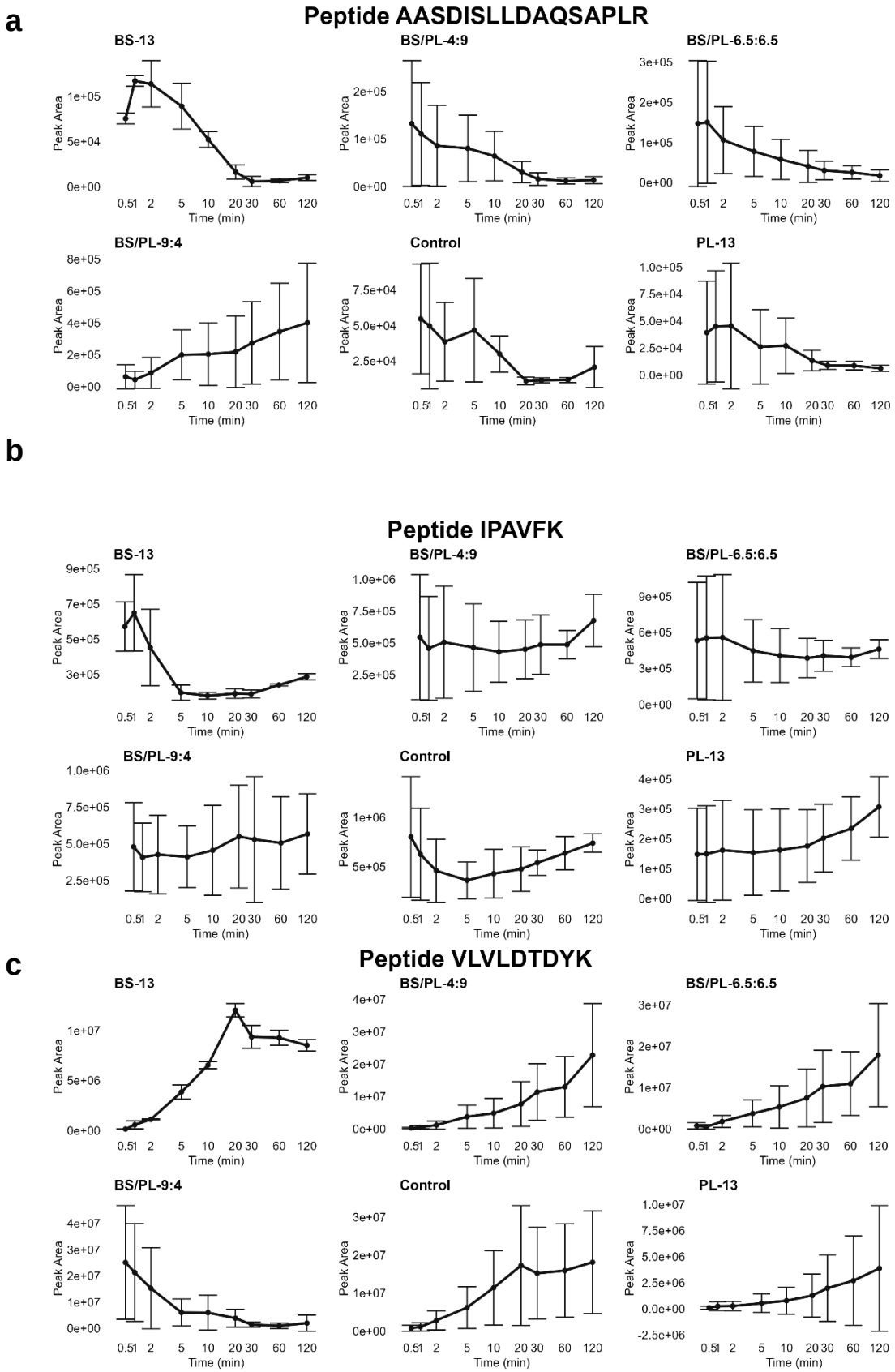
a
Peptide AASDISLLDAQSAPLR
BS-13
BS/PL-4:9
BS/PL-6.5:6.5
BS/PL-9:4
Control
PL-13
Peak Area
Time (min)
0.5 1 2 5 10 20 30 60 120
b
Peptide IPAVFK
BS-13
BS/PL-4:9
BS/PL-6.5:6.5
BS/PL-9:4
Control
PL-13
Peak Area
Time (min)
c
Peptide VLVLDTDYK
BS-13
BS/PL-4:9
BS/PL-6.5:6.5
BS/PL-9:4
Control
PL-13
Peak Area
Time (min)

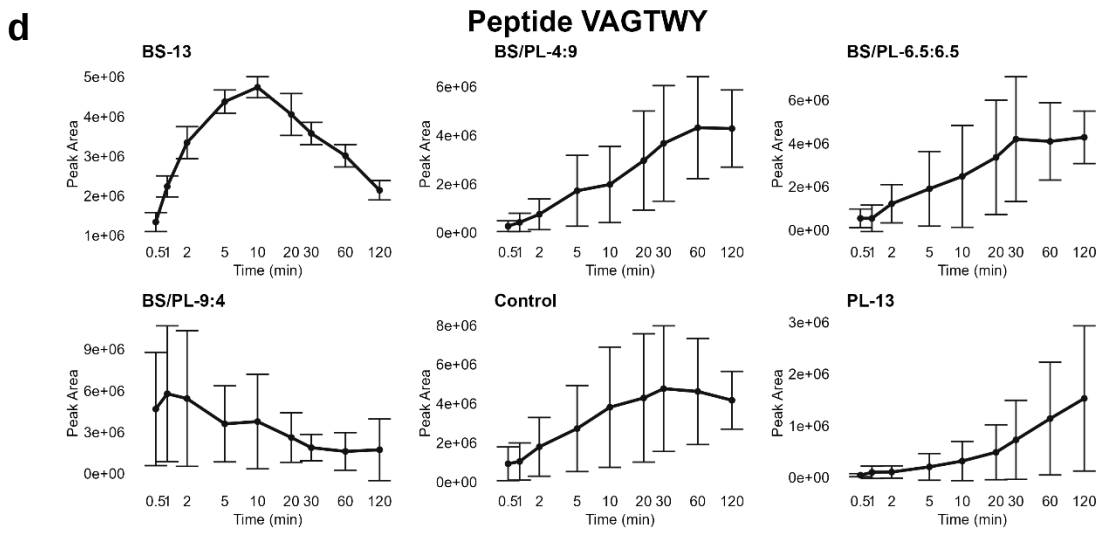

Figure 7.6 The kinetics of bioactive peptides (a-d) assigned for β-Lg found during 2-hour WPI intestinal digestion under various biliary surfactant concentrations (only BSs: BS-13; BS/PL mixtures: BS/PL-9:4, BS/PL-6.5:6.5, BS/PL-4:9; only PLs: PL-13; and Control, without biosurfactants).

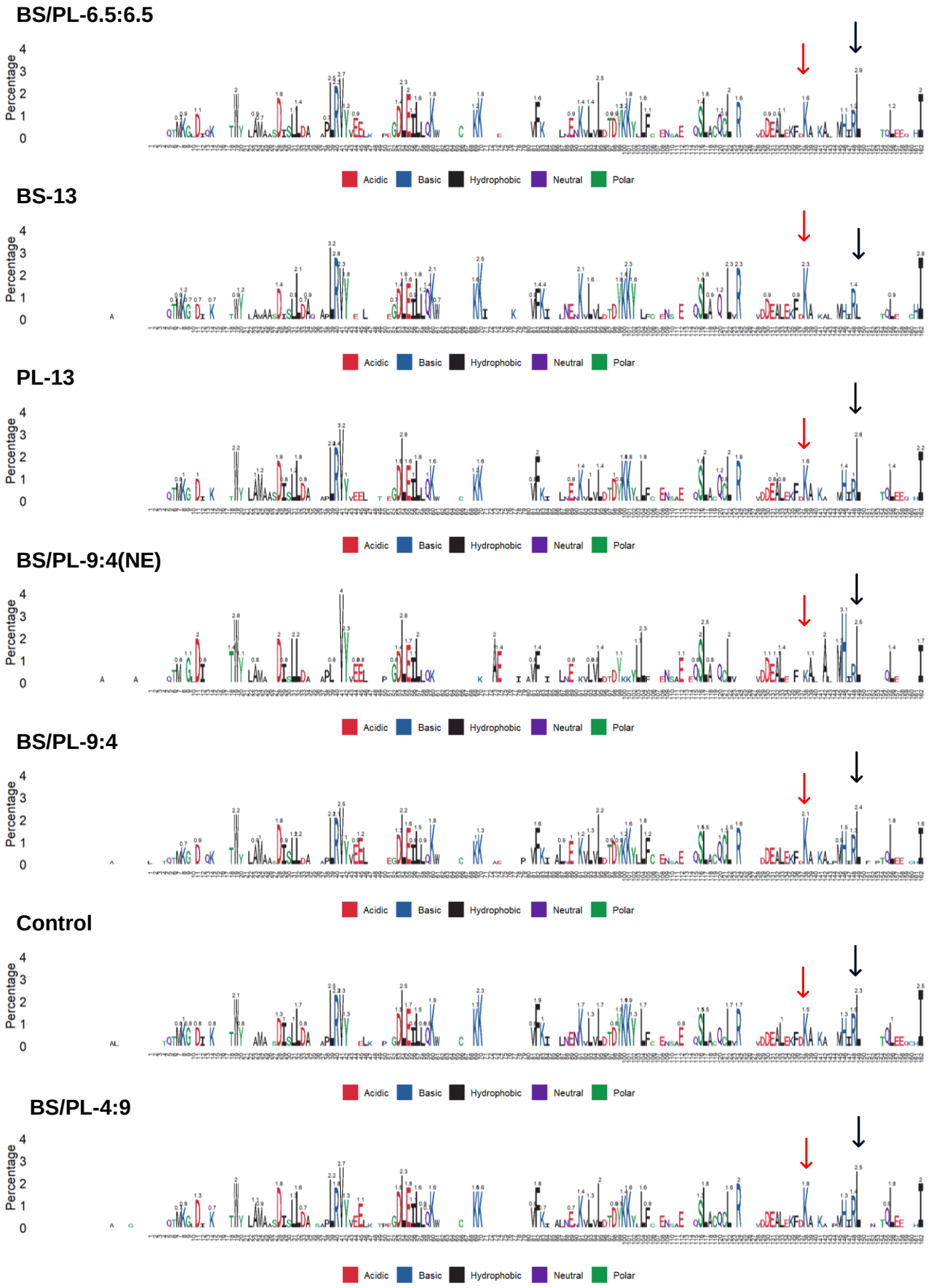

Figure 7.7. The enzyme cleavage sites are displayed as the percentage occurrence of specific amino acids at the ends of peptides generated during a 2-hour digestion under various intestinal conditions. Amino acid symbols are aligned with positions in the protein sequence, and the labels indicate the percentage frequency of peptides with a particular terminal amino acid under the experimental conditions. Red arrow indicates Lys138, black arrow indicates Leu149.

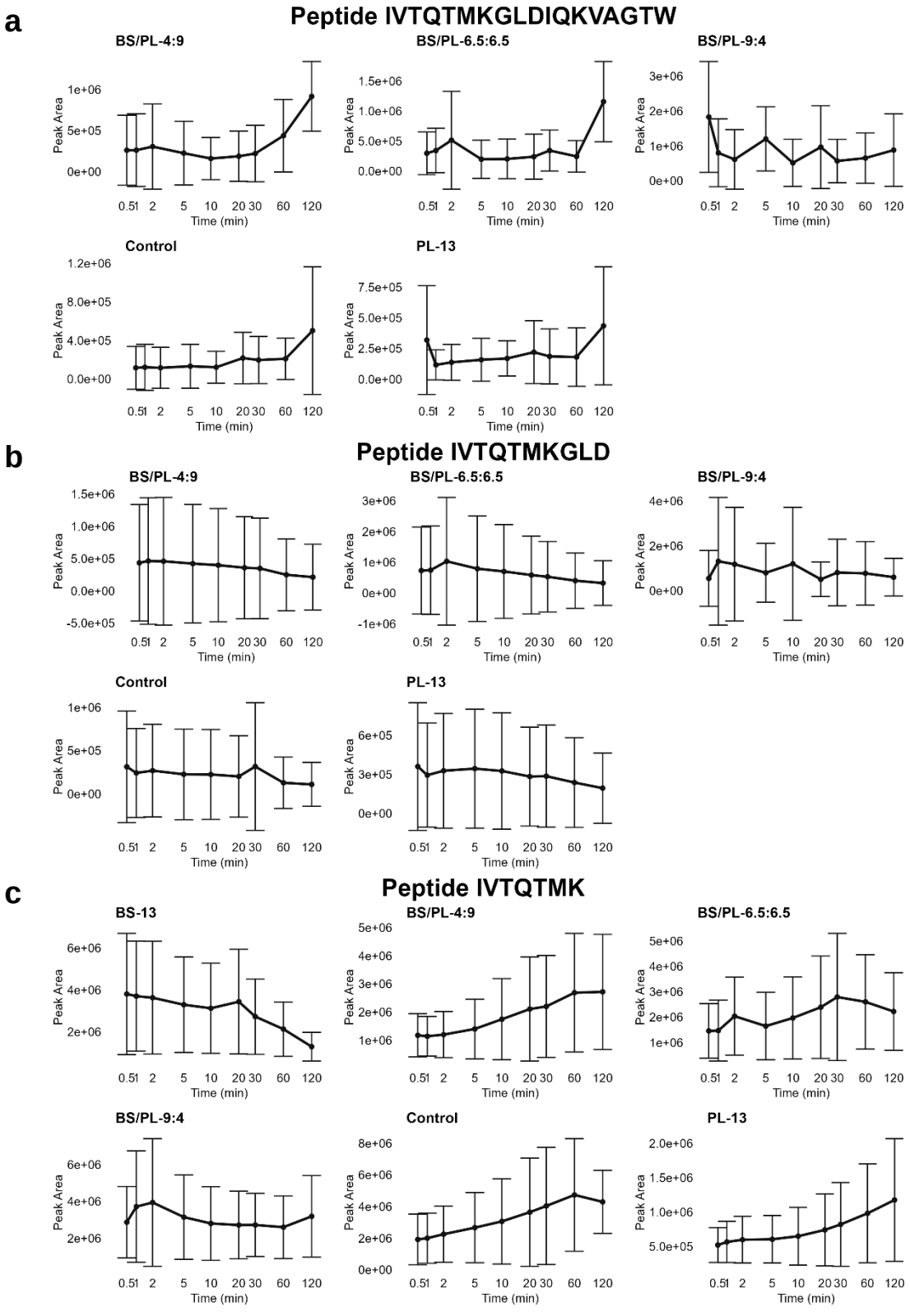
a
Peptide IVTQTMKGLDIQKVAGTW
BS/PL-4:9
BS/PL-6.5:6.5
BS/PL-9:4
Control
PL-13
b
Peptide IVTQTMKGLD
BS/PL-4:9
BS/PL-6.5:6.5
BS/PL-9:4
Control
PL-13
c
Peptide IVTQTMK
BS-13
BS/PL-4:9
BS/PL-6.5:6.5
BS/PL-9:4
Control
PL-13
Peak Area
Time (min)
0.5 1 2 5 10 20 30 60 120

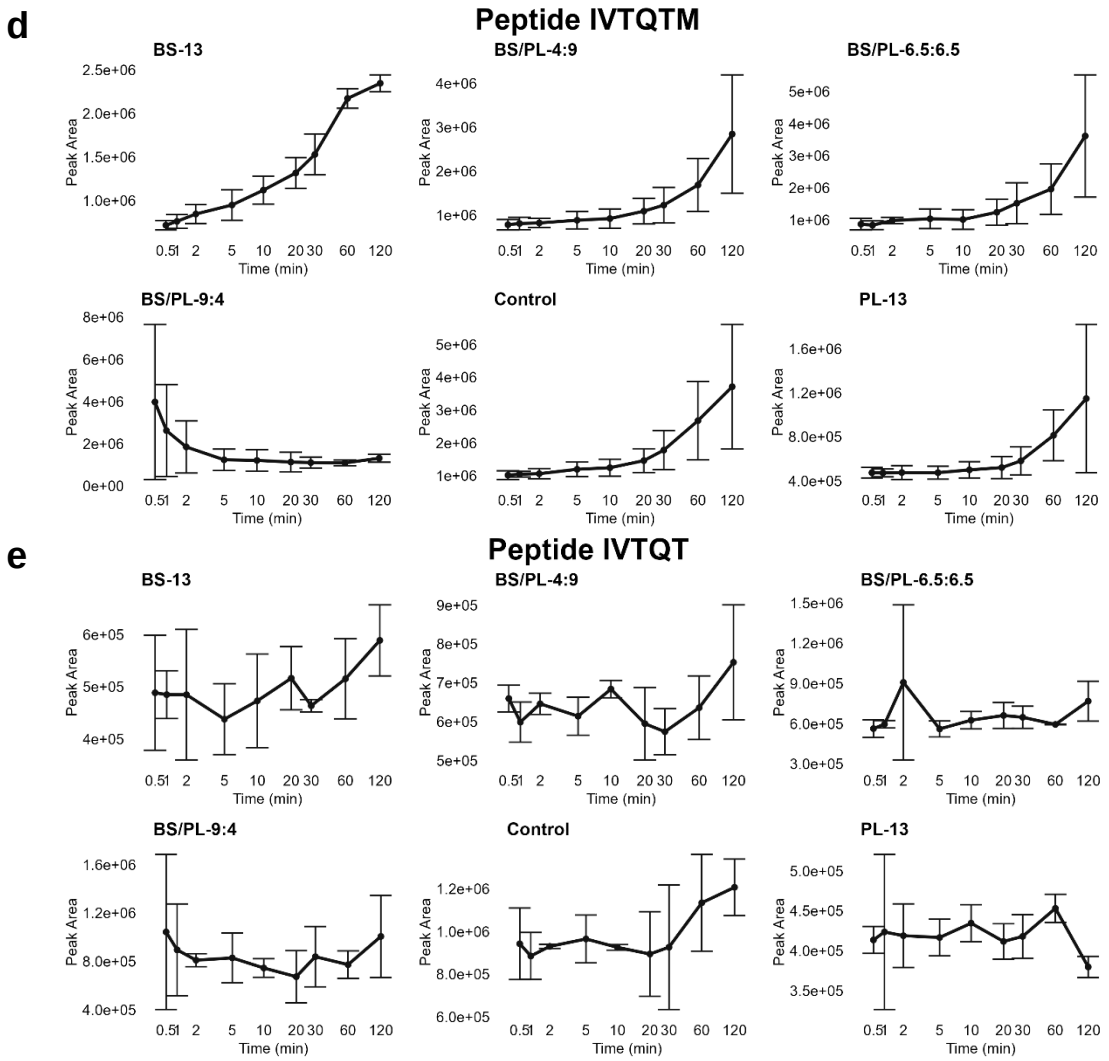

Figure 7.8 The kinetics of peptides from the β-Lg sequence range 2-19 found during WPI digestion under various intestinal conditions. The absence of a graph for a specific condition indicates the non-detection of that peptide under these conditions.

a

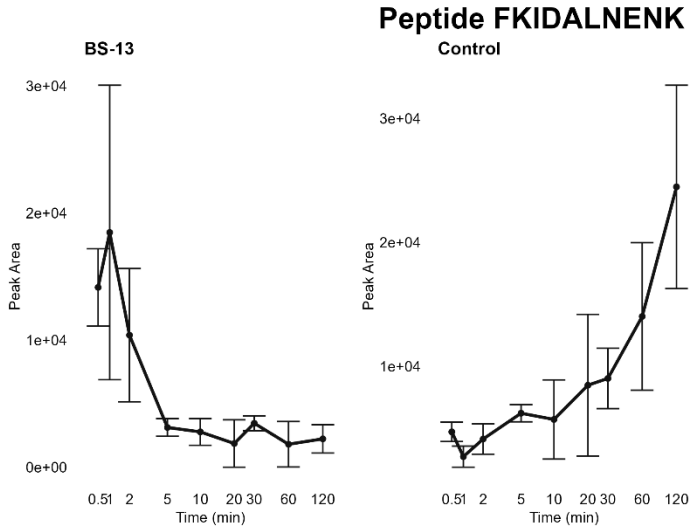
Peptide FKIDALNENK
BS-13
Control
Peak Area
Time (min)
0.5 1 2 5 10 20 30 60 120
3e+04
2e+04
1e+04
0e+00

b

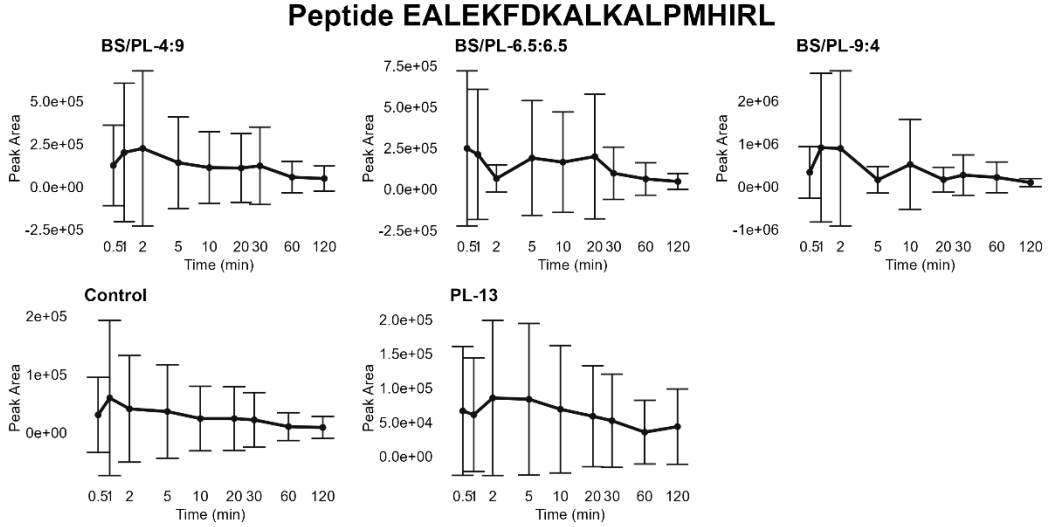
Peptide EALEKFDKALKALPMHIRL
BS/PL-4:9
BS/PL-6.5:6.5
BS/PL-9:4
Control
PL-13
Peak Area
Time (min)
0.5 1 2 5 10 20 30 60 120

c

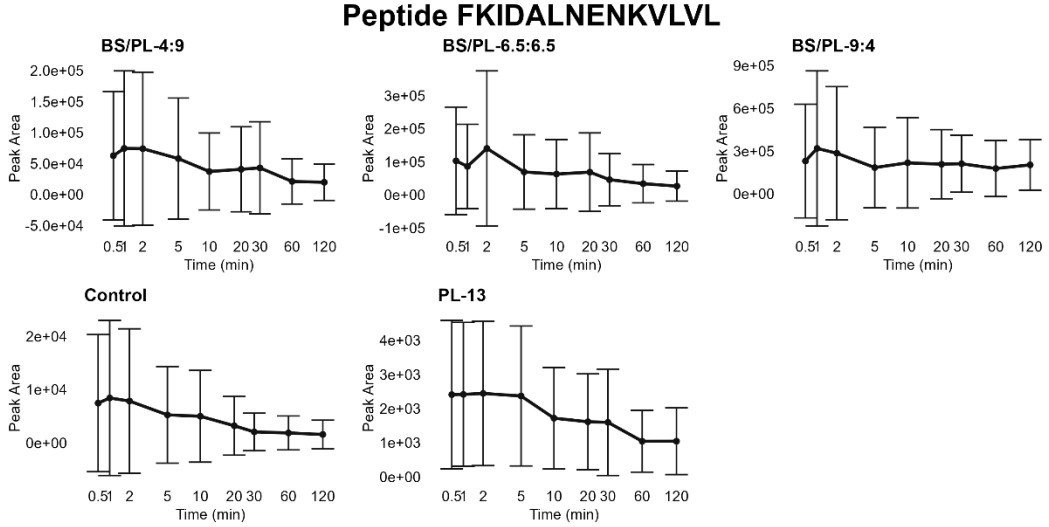
Peptide FKIDALNENKVLVL
BS/PL-4:9
BS/PL-6.5:6.5
BS/PL-9:4
Control
PL-13
Peak Area
Time (min)
0.5 1 2 5 10 20 30 60 120

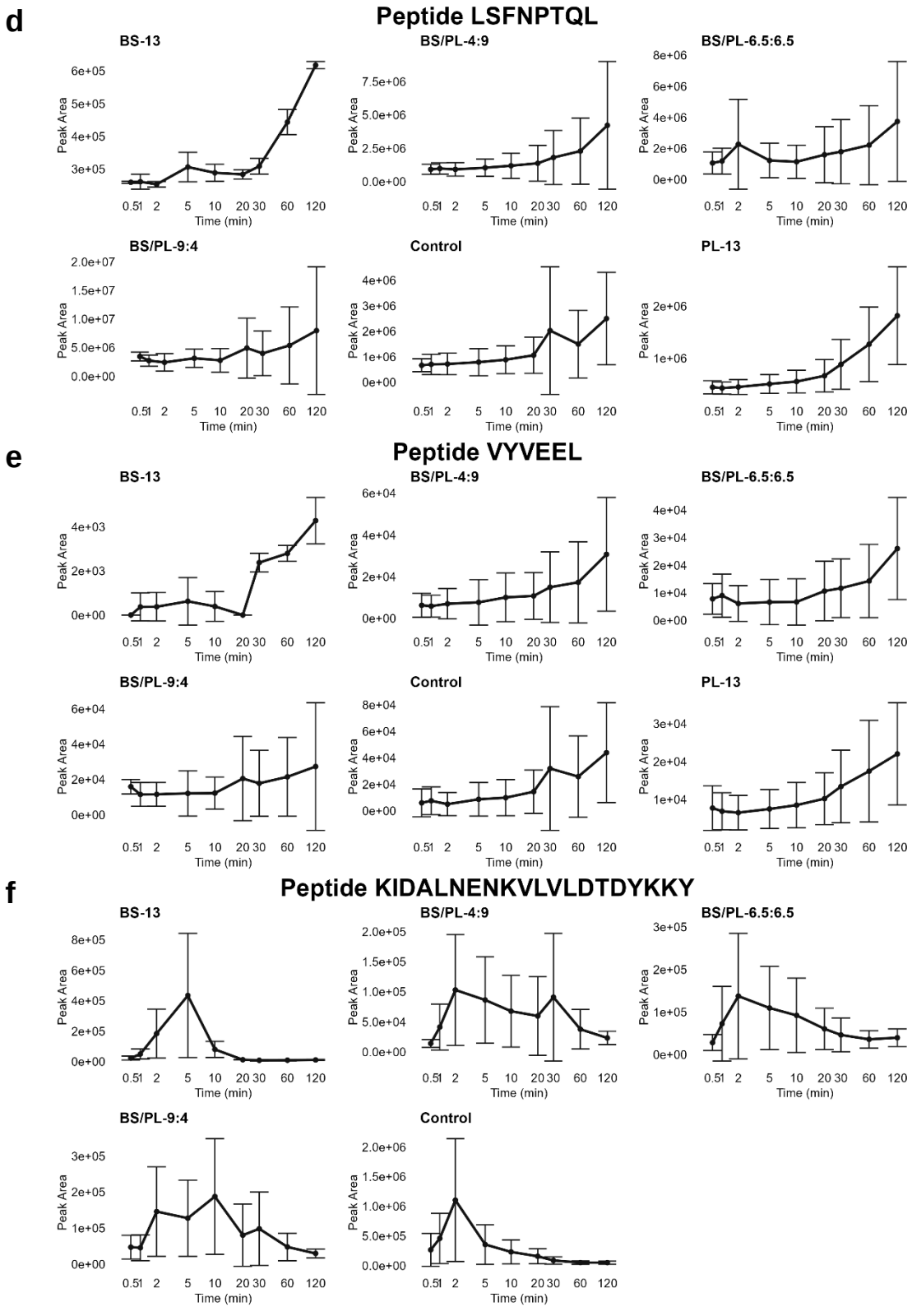
d
Peptide LSFNPTQL
BS-13
BS/PL-4:9
BS/PL-6.5:6.5
BS/PL-9:4
Control
PL-13
e
Peptide VYVEEL
BS-13
BS/PL-4:9
BS/PL-6.5:6.5
BS/PL-9:4
Control
PL-13
f
Peptide KIDALNENKVLVLDTDYKKY
BS-13
BS/PL-4:9
BS/PL-6.5:6.5
BS/PL-9:4
Control
Peak Area
Time (min)
0.5 1 2 5 10 20 30 60 120

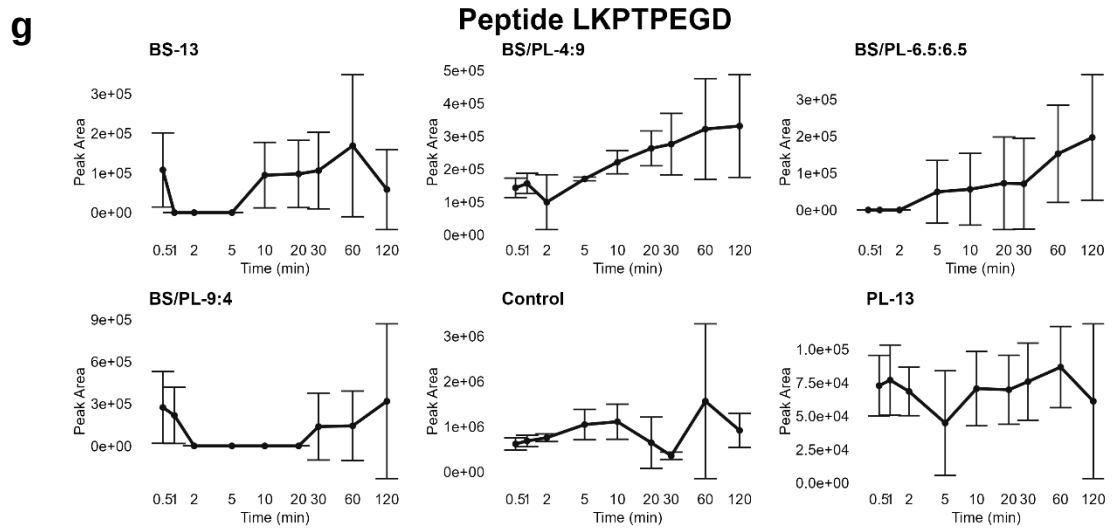

Figure 7.9 Examples of peptides showing disparities and similarities in their kinetics between conditions during intestinal digestion of WPI. The absence of a graph for a specific condition indicates the non-detection of that peptide under these conditions.

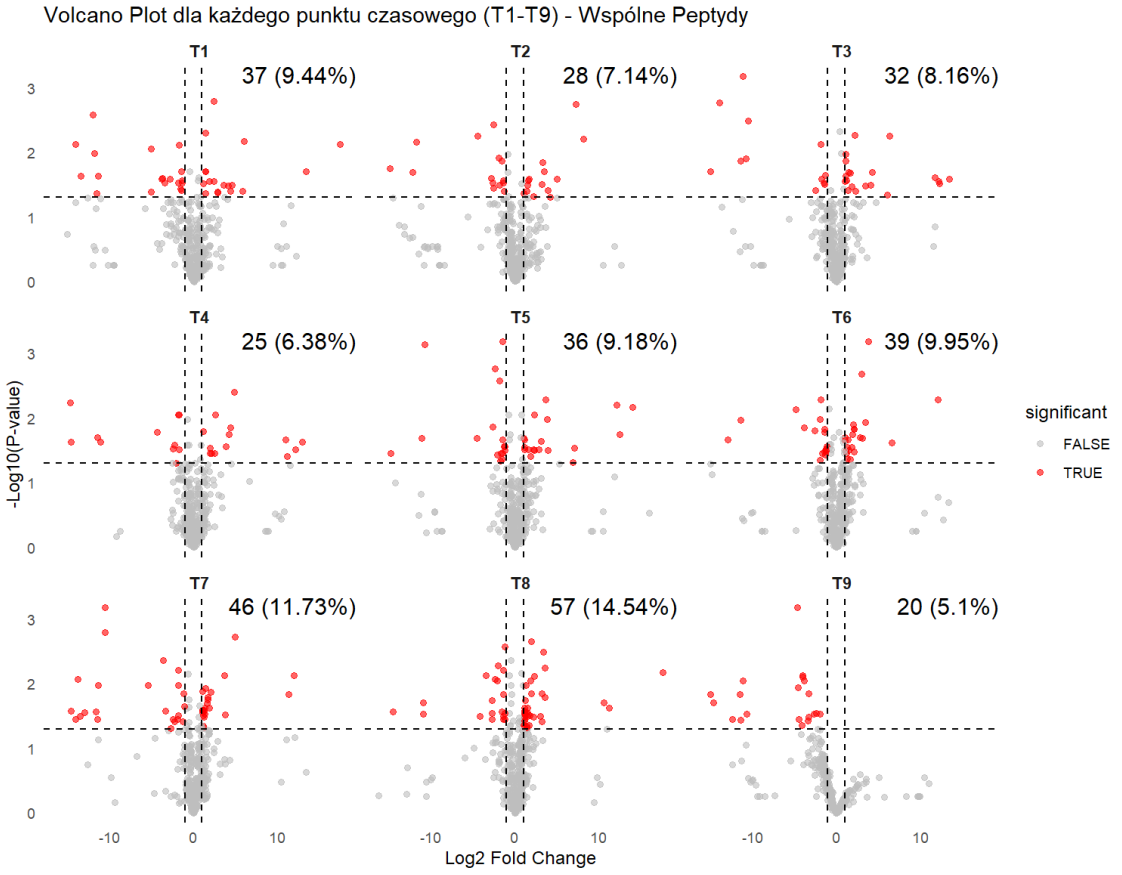

Figure 7.10 Volcano plots for each intestinal digestion time point present the differences in peak area of peptides between the physiologically relevant condition (β-Lg-BS/PL-9:4) and control (β-Lg-Control). The x axis shows the Log2 Fold Change with a cut-off Fold Change of <0.5 and >2, and the y-axis shows -log10(p-value) with a cut-off p-value of <0.05 after FDR correction. Gray dots indicate peptides that do not reach the cutoffs, red dots indicate peptides with statistical relevance. Values in the top left corners indicate numbers of statistically relevant peptides and their percentage contribution of total number of peptides taken to the analysis, n = 392.

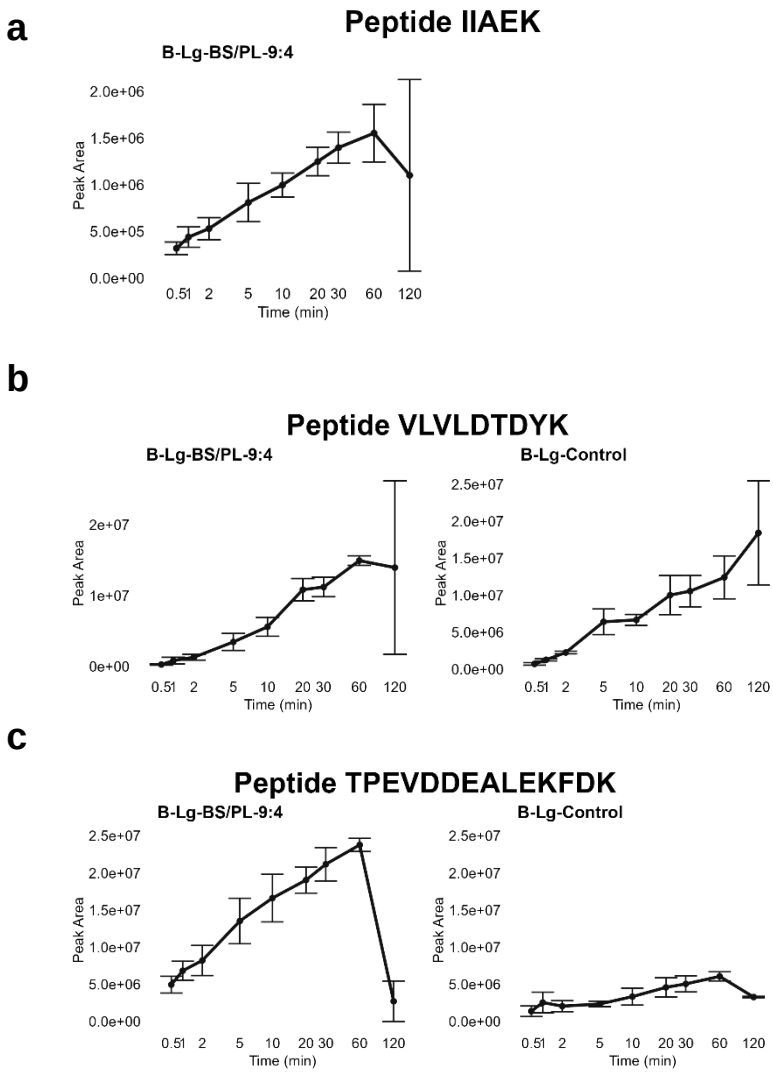

Figure 7.11 Peptides released during pure β-Lg intestinal digestion under physiologically relevant conditions (β-Lg-BS/PL-9:4) and control (β-Lg-Control). The absence of a graph for a specific condition indicates the non-detection of that peptide under these conditions.